ENVIRONMENTAL ASPECTS OF STORM RUNOFF DISCHARGE FROM A TIMBER PORT, TAURANGA, NEW ZEALAND

A thesis submitted in fulfilment of the requirements

for the Degree of

Doctor of Philosophy

in Earth Sciences

at the University of Waikato

by

Fengming Tian

April 1997
Hamilton, New Zealand

To my parents

who did not teach me any scientific knowledge because they have never been in school, but they did tell me how to be an upright person.

ABSTRACT

An investigation was undertaken into storm runoff water quantity and quality, contaminant input to the receiving tidal waters from the Mt. Maunganui wharf, accumulation of potentially toxic resin acids in adjacent sediments, and the dilution of the wharf runoff in the receiving tidal waters, in order to assess the possible adverse environmental impact associated with the log operation at the Port of Tauranga Ltd.

Based upon field data and rainfall records, about a half of the annual precipitation over the log handling areas is converted to surface runoff (117,000 m^3a^{-1}). Annual runoff volume per hectare of wharf surface is estimated as 7,500 $m^3ha^{-1}a^{-1}$ for the sealed area and 3,700 $m^3ha^{-1}a^{-1}$ for the gravelled area.

The optical quality of the wharf runoff is degraded due to addition of bark and soil particles. The black disk visual clarity (0.01-0.02 m) was only 0.5-1.0% of that in the receiving tidal waters. The wharf runoff appears very dark gray to yellowish brown in apparent colour (10YR1/3 to 10YR5/6 Munsell colour chart) and has a soluble yellow substance concentration of about 25 m^{-1}. Power relationships between the traditionally used parameters, for example, suspended solids and turbidity, were identified. The wharf surface pavement types had a significant influence on visual clarity, but little influence on yellow substance concentration.

The potentially toxic resin acids in the wharf runoff have been determined with SIM GC-MS. The average total resin acid level (1,030 ppb) is comparable to that of 1,000 ppb reported at which acute toxicity is likely to be exhibited. A relationship of resin acids against volatile suspended solids was established. Tests undertaken suggest that conventional treatment methods of natural sedimentation and flocculation-sedimentation are able to remove the resin acids effectively.

The levels of biological oxygen demand (BOD), total phosphorus and nitrogen in the wharf runoff are considerably higher than those of common urban runoff. However, the wharf runoff contributes little nitrate nitrogen and oil and grease to the receiving environment.

About 87,500 kg of suspended solids, 43,000 kg of volatile suspended solids, 14,200 kg of BOD, 500 kg of phosphorus, and 103 kg of resin acids are discharged to the Tauranga Harbour annually from runoff from the Mt. Maunganui wharf.

Analyses show that the impact on adjacent sediments from the storm runoff is limited to a distance of about 100 m from the discharge points and the resin acid levels in the sediments within this distance are not significantly higher compared to that of the storm runoff. The net resin acid accumulation rate in the shipping channel (Stella Passage) beside the log handling areas was estimated to be in the range of 300 to 370 ppb per year.

Based on field investigation and numerical simulations, the findings on dispersion and dilution of the wharf runoff in the receiving tidal waters are as follows: (i) the sea water around Stella Passage experiences an obvious natural salinity stratification, the extent of which depends greatly on the weather conditions; (ii) the wind drag stress and the pressure gradient caused by the addition of runoff had the greatest influence on the plume dynamics during the flood tide. The plumes basically remain within the top 2-3 m of the water column under different winds; (iii) the plume is unlikely to advect to the Whareroa Marae under strong (30-40 knots) easterly or northeasterly winds for a storm with a 5-year return period. However, there is an obvious influence on the Whareroa Marae under 30-40 knot northerly winds; and (iv) the short duration and restricted region of the low dilution pulse of effluent around slack water may explain why there has been no reports of acute toxic events.

Sealing the gravel covered wharf area, improving the sweeping efficiency, and extending the present outfalls to the sea floor might be potential options for mitigating the environmental impact associated with discharge of the wharf runoff.

ACKNOWLEDGEMENTS

I wish to take the opportunity to thank people who have aided me to complete this thesis.

My most sincere thanks go to my chief supervisor Professor Terry Healy for initiating the project, organising the scholarship to undertake this study, and for his continued support and editing.

I would like to thank Professor Kerry Black for generously allowing me to use his 3DD numerical model and giving me lots of help for field investigation design, modelling skills and thesis editing.

Many thanks go to Professor Alistair Wilkins in the Chemistry Department for helping me with identification and quantification of the organic substance in the runoff and sediment samples, and thesis editing.

Dr. Robert Davies-Colley, my second supervisor in NIWA, thanks for the help on investigation of optical water quality of the wharf runoff and the critical comments for the thesis outline at the initial stage of this study.

I am indebted to John Palmer and Geoffrey Thompson for their generous support for this study (That was too true. Yes, they offered financial support for this project). Thanks must be also given to Lance Wood, Owen Maynard, Alan Holst, Rex Riddler, and Mike Petherick, the other technical officers from the Port of Tauranga Ltd, for their help with field investigation and other assistant.

Thanks also should go to Mike Wilson and the other friends in the Watch Office at the Port of Tauranga, for offering me accommodation and the lovely tea, in particular the friendly chat when I was waiting for the coming of heavy rains with great anxiety.

I am grateful to Dr. Robert Bell in NIWA for offering me the model grids with the latest bathymetric survey results and other helps. A very special thank you to Dr. Richard Gorman for allowing and helping me to use his PLOT3DD.

Sincere thanks to Prof. C. S. Nelson and Associate Prof. R. Briggs for encouragement and partial financial support to attend international and national conferences.

Dirk Immenga and John Radford - thanks for all you have done for me. The field work for my project was really very hard.

Many thanks to Mike Vennard, Laurence Gaylor, Steve Bergin, Heather Windsor, Greg Foster and Qi Ma (although Heather, Greg and Qi had left our Department), for their assistance both in the field and laboratory.

To Jannine Sims, the technician in the Chemistry Department , Middy Wang and Dawei Deng, DPhil students in the Chemistry Department, many thanks for their help with identification of organic acids.

The Earth Sciences secretaries, Sydney Wright and Elaine Norton, are thanked for their general assistance over the past 4 years.

Joseph Matthew, my roommate in Coastal Marine Group, is thanked for his assistance and help for the past 4 years. Nenad Domijan, Scott Stephen, Tony Dolphin, Brett, Sohail, James Hutt, thanks for the helps for field work and other occasions.

Special thanks to David McLean and Dulcie McLean, my friends in Putaruru, for their encouragement, kindness and lots of help.

To my all other friends inside and outside the university, thanks for showing me that there was more to life than this thesis.

Last but not least, I would like to thank my wife, Xiaobing Dong, and my daughter, Tina Fang Tian, who encouraged me all the way during my university years.

TABLE OF CONTENTS

CHAPTER FOUR - STORM RUNOFF WATER QUALITY: II. OPTICAL QUALITY

CHAPTER FIVE - STORM RUNOFF WATER QUALITY: III. EXTRACTABLE ORGANIC ACIDS

LIST OF FIGURES

LIST OF TABLES

CHAPTER ONE

INTRODUCTION

CHAPTER ONE

INTRODUCTION

1.1 NATURE OF THE PROBLEM

Over the last few decades, secondary treatment plants have become more widespread and industrial discharge has been reduced significantly. As a result, the relative pollutant load contribution of nonpoint source discharges has gradually increased. Storm runoff from urban areas is one such nonpoint discharge (Anon, 1986; Browne, 1990).

At the Port of Tauranga (Figure 1.1), New Zealand's largest timber export port, there is a potential environmental problem associated with the discharge of storm runoff from the wharf log handling areas. During the log storing, shifting, and loading, a significant amount of bark and soil material is unavoidably stripped from the logs and accumulates on the wharf surface (Figure 1.2). Even after mechanical cleaning, a substantial quantity of bark and soil material is still left behind on the ground (Figure 1.3). With the continual trafficking by the log handling machinery, some bark becomes crushed, and eventually decomposes, especially on the gravel surfaced wharf areas. When it rains, the crushed bark and other material adhering to the bark are carried into the receiving water body - Tauranga Harbour - by surface runoff (Figure 1.4). Thus the seawater near the discharge points becomes discoloured, the turbidity of the seawater increases, and some organic substances which are potentially toxic to aquatic life, such as dehydroabietic acid, may be washed into the harbour (Tian *et al.*, 1995). It is likely that additional contaminants, such as nutrients, oxygen demanding substances, and oil and grease from the soil materials or the fuel leakage, get into the storm runoff and are discharged into the harbour.

After the mid 1980s, log exports at the Port of Tauranga increased greatly. In recent years, annual log exports exceeded 2 million tonnes. According to the trade forecast from the Port of Tauranga Ltd, the annual log export is expected to be maintained at about 2 million tonnes during the period from 1995 to 2000 (Port of Tauranga Ltd, 1990). Accordingly, any contamination associated with the log handling will potentially be maintained over a long period if an effective storm runoff treatment facility is not implemented.

Apart from the Port of Tauranga, logs are also exported through other New Zealand ports. The above mentioned problems are also an issue facing these timber export ports. However, to date, no comprehensive studies on environmental impact related the storm runoff discharge from the log handling areas at these timber ports have been undertaken.

For Port of Tauranga three investigations concerning wharf runoff water quality have been undertaken:

McCabe (1991) analysed suspended solid concentration and particle size distribution of four runoff samples collected from the Mount Maunganui wharf.

Kingett Mitchell and Associates (1993) analysed for pH, suspended solids, volatile suspended solids, turbidity, conductivity, dissolved reactive phosphorus, total Kjeldahl nitrogen, ammonia nitrogen, biological oxygen demand, and extractable natural organic compounds (mainly resin and fatty acids) of the runoff samples from the Mount Maunganui wharf in another study, but only nine runoff samples were collected for the entire investigation.

Because both of these studies were restricted to a few samples, the results do not adequately represent the highly variable runoff characteristics.

Tian *et al.*, (1993) collected more runoff samples (36) than the above two studies from 7 sampling sites around the log handling areas at the Sulphur Point wharf during 5 storm episodes. One aim was to understand the characteristics of light absorption by yellow substance in the runoff samples (Tian *et al.*, 1994). Also, natural extractable organic substance, some of which are toxic to aquatic life in concentrated form, were identified. However, this study focused on only a few aspects of runoff water quality, namely, suspended solids, volatile suspended solids, turbidity, yellow substance and natural extractable organic substance. Some other important aspects for runoff water quality, such as colour, visual clarity, oxygen demand material, nutrients, oil and grease, were not investigated. Furthermore, the relationships between different parameters and the influence on runoff water quality from wharf surface pavement types and rainfall history were not investigated.

1.2 AIM OF THE STUDY

The aim of this study is to advance understanding of aspects of storm runoff from the log handling area at the Port of Tauranga, by investigating:

1. hydrology of the wharf catchment for the log handling area;

2. water quality of storm runoff;

3. contaminant load to the receiving environment;

4. accumulation of toxic resin acids in the sediment adjacent to the discharge points, and

5. mixing and dispersion of the storm runoff in the receiving tidal waters.

This investigation focuses mainly on water quality, particularly optical quality and organic extractives of wharf runoff. Biological impact is also a very important aspect but this has been preliminarily investigated by Grace (1993) and further investigation is planned to be conducted separately by the Port of Tauranga. It is necessary to examine a wide range of issues in the above five categories and this thesis does not attempt to address the biological issues in any detail.

1.3 STUDY AREA

This investigation primarily relates to the Mount Maunganui timber wharf at the Port of Tauranga and Tauranga Harbour (Figure 1.5a, b).

1.3.1 Tauranga Harbour

Tauranga Harbour is a large barrier enclosed estuarine lagoon covering a total area of 218 km^2 in the northern Bay of Plenty, New Zealand (Figure 1.5a). The harbour catchment covers an area of 1275 km^2 and is well developed with extensive horticultural and agricultural land use. At the southern end of the harbour, the city of Tauranga supports a large residential population of about 67,000 (McIntosh, 1994).

Geomorphically, Tauranga Harbour is a micro-tidal estuarine lagoon impounded by a barrier island (Matakana Island) and two barrier tombolos, Mount Maunganui at the southern entrance and Bowentown to the north (McIntosh, 1994). The harbour is predominantly shallow with 62% of its total area being intertidal.

Based on a full tidal cycle gauging, total inflows to the harbour were estimated as 260,200,000 m^3, with outflows of 271,500,000 m^3 (McIntosh, 1994). The difference between inflows and outflows is presumably due to measurement

error and freshwater input. In total 66 surface streams were identified as flowing into Tauranga Harbour (McIntosh, 1994). Due to a lack of data, total stream input of freshwater into Tauranga Harbour has been estimated to total of order of 37 m^3/s for mean annual flows and 20 m^3/s for dry flow estimates (McIntosh, 1994). Among the streams entering the harbour, the Wairoa River is the main freshwater source which accounts for approximately 45% of the total dry weather flow.

The residence time of water in various parts of the harbour is still poorly known (McIntosh, 1994). For the harbour as a whole, the theoretical residence times were calculated by Heath (1985, cited by McIntosh, 1994) and presented in table form along with estimates for other harbours and estuaries in New Zealand.

Dye studies in the upper reaches of the harbour show that flushing of water from the upper reaches of the sub-estuaries is very poor. Water entering via streams may oscillate for four or more tidal cycles before mixing with the large water bodies of the main harbour basins (McIntosh, 1994). To date, no studies have been undertaken on salinity oscillation, vertical distribution, the relationship between horizontal and vertical salinity variation and freshwater input around the shipping channel near the log handling area. Salinity structure was assessed as "well mixed" by the Tauranga Harbour Study (Barnet, 1985). This classification is shown to be inadequate as stratification was observed and found to be important during this study.

The first comprehensive study of Tauranga Harbour was carried out during the Tauranga Harbour Study of 1983-1985, commissioned to undertake a major investigation into the hydrodynamics and sediment transport patterns of the inner harbour (Black, 1983 and Barnett, 1985). Barnett (1985) reports on the findings of the S21 2-dimensional hydrodynamic model concentrating primarily on the calibration and verification of the model. In connection with

the capital dredging programme of 1991-1992 of the Port of Tauranga and the extensions of the Sulphur Point wharf in 1994, Bell (1991, 1994) re-ran the S21 model using the updated bathymetry. Figure 1.6 shows Bell's (1994) model results of mean tide velocity pattern at peak flood, peak ebb, and full tidal cycle residual velocity vector pattern in the harbour next to the port area.

The current speed around the log handling area is relatively low. The maximum mean tide current speed in the shipping channel (Stella Passage) between the Sulphur Point and Mount Maunganui wharves is around 0.4 m/s at peak ebb and 0.3 m/s at peak flood.

1.3.2 Port Area

Port of Tauranga is located near the southern entrance of Tauranga Harbour (Figure 1.5a). It consists of two wharves, Mount Maunganui and Sulphur Point. The Mount Maunganui wharf is the main one for export of logs, woodchip, forest products, and bulk cargoes, and was the only one prior to April 1, 1992. The Sulphur Point wharf was commissioned on April 1, 1992 and was initially designed as a container wharf. Presently, a small amount of logs are also exported through the Sulphur Point wharf.

The log storage and handling area at the Mount Maunganui wharf covers about 20 ha. There are two types of surface pavement: sealed and gravelled. Field observation showed that suspended solid level of storm runoff from these two types of wharf surface are different (Figure 1.4).

1.3.3 Drainage Systems Around the Port and Harbour Outfalls

There are around 20 outfalls along the Mount Maunganui wharf. These outfalls can be divided into three different types: industrial stormwater only, industrial plus port stormwater, and port stormwater only. Because these drainage

systems receive runoff from different sub-catchments, the runoff water quality from these systems are different. This investigation focuses on environmental impact related to the storm runoff discharge from the log handling area only.

There are two drainage systems around the log handling area (see Figure 3.1, page 36). The outfalls of both drainage systems are located between low and high waters (Figure 1.7).

The wharf face at Maunganui has a RL of approximately 4.6 m (Port datum 0.0 = approximately spring tide low water). Typically, the land behind the wharf rises for a distance of approximately 30 - 50 m to an RL of 5.0 m. The fall is then back towards the rear of the storage area at a general grade of approximately 1:100. The distance back to the *"low point"* in the land area can be as much as 150 - 200 m, and some of the storage area therefore has an RL between 3.0 and 3.5 m. This means that at High Water Spring Tide (HWST, approximately RL 2.0 m) the head available from surface level to tide level to create flow is only 1 to 1.5m. Tide levels therefore control the capacity of the lines.

The drainage systems were designed to be able to drain runoff formed with a storm with a five year return period at a tidal level of RL 1.5 m. Examination of tide curves shows that there is about 20% of probability that at any point in time the tidal level will be above RL 1.5 m. Therefore, that is in effect designing for a return period of 25 years when a rainfall with five year return period occurs at a tidal level above RL 1.5 m.

1.4 STRUCTURE OF THE THESIS

In order to achieve the objectives established, the following structure is used in the study:

Chapter 2 presents the investigation of hydrology for the Mount Maunganui wharf.

Chapters 3-6 outline the storm runoff water quality, and focus on degraded optical quality, extractable organic substances, oxygen demanding substances, nutrients, and oil and grease in the runoff.

In Chapter 7 contaminant load to the receiving water relating to the log operation is calculated.

Chapter 8 analyses the possible accumulation of the potentially toxic resin acids in the sediment adjacent to the runoff discharge points.

Chapter 9 presents field measurements of runoff dilution and dispersion in the receiving tidal waters and plume characteristics under various scenarios of numerical model simulation. The model was applied primarily to specify dilution and dispersal distances. It was found that 3-dimensional hydrodynamics and salinity structure played an important roll on plume characteristics.

Chapter 10 outlines the main findings and recommendations for further study.

Although this project was established in response to an environment impact assessment required by the Port of Tauranga related to the runoff discharge from the timber wharf, the project focuses on a number of fundamental scientific problems. Briefly the project is involved with the nature of runoff from a timber port, - a topic which has rarely been reported in the scientific and engineering literature. There are a number of intrinsic scientific challenges, for example, the nature of the deteriorated optical quality and concentration of organic extractives in the discharged water from the timber export wharves.

Figure 1.1 Aerial photo of the Port of Tauranga and the Tauranga Harbour, showing the Sulphur Point wharf and the log handling areas at the Mount Maunganui wharf.

Figure 1.2 Bark and soil-like material left on the wharf surface after the logs were shifted from the log storage area at the Mount Maunganui wharf.

(A)

(B)

Figure 1.3 Bark and soil-like material left on the sealed wharf area (A) and gravel surfaced area (B) after mechanical cleaning.

(A)

(B)

Figure 1.4 The sealed wharf surface (A) and gravel covered surface (B) at the Mount Maunganui wharf after heavy rain.

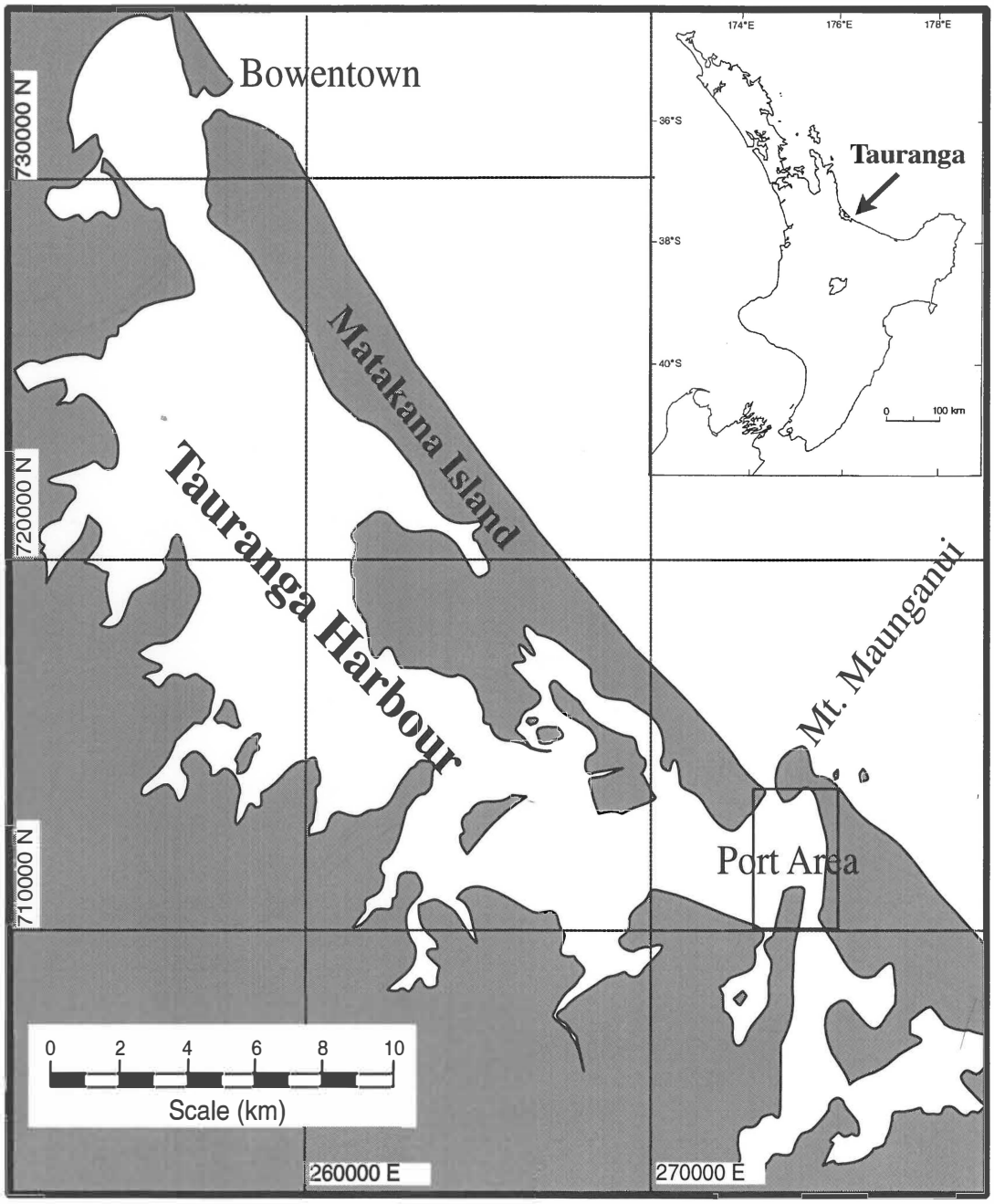

Figure 1.5a Map of Tauranga Harbour and location of the Port of Tauranga.

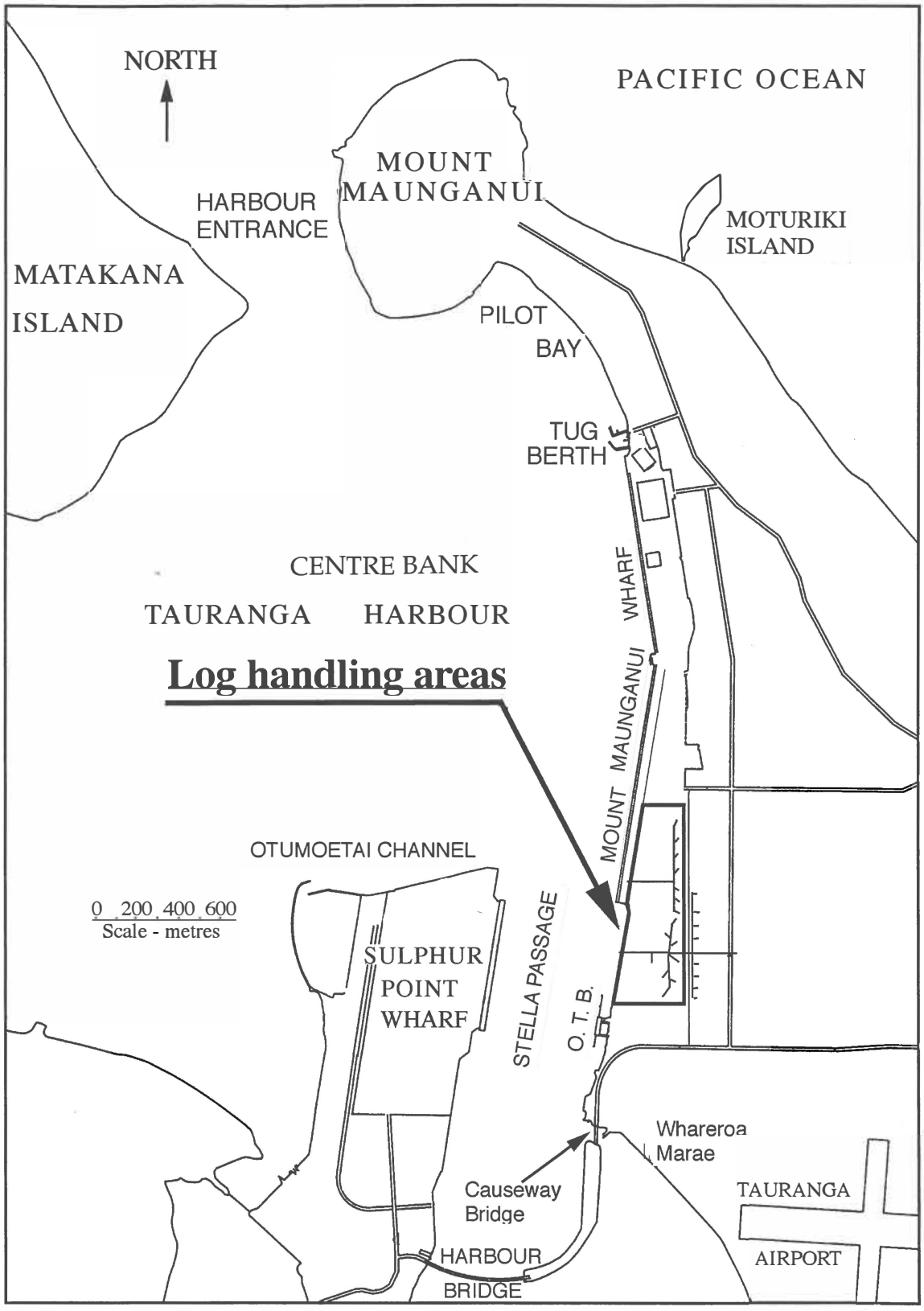

Figure 1.5b Port of Tauranga showing the log handling areas and the Tauranga Harbour around the port.

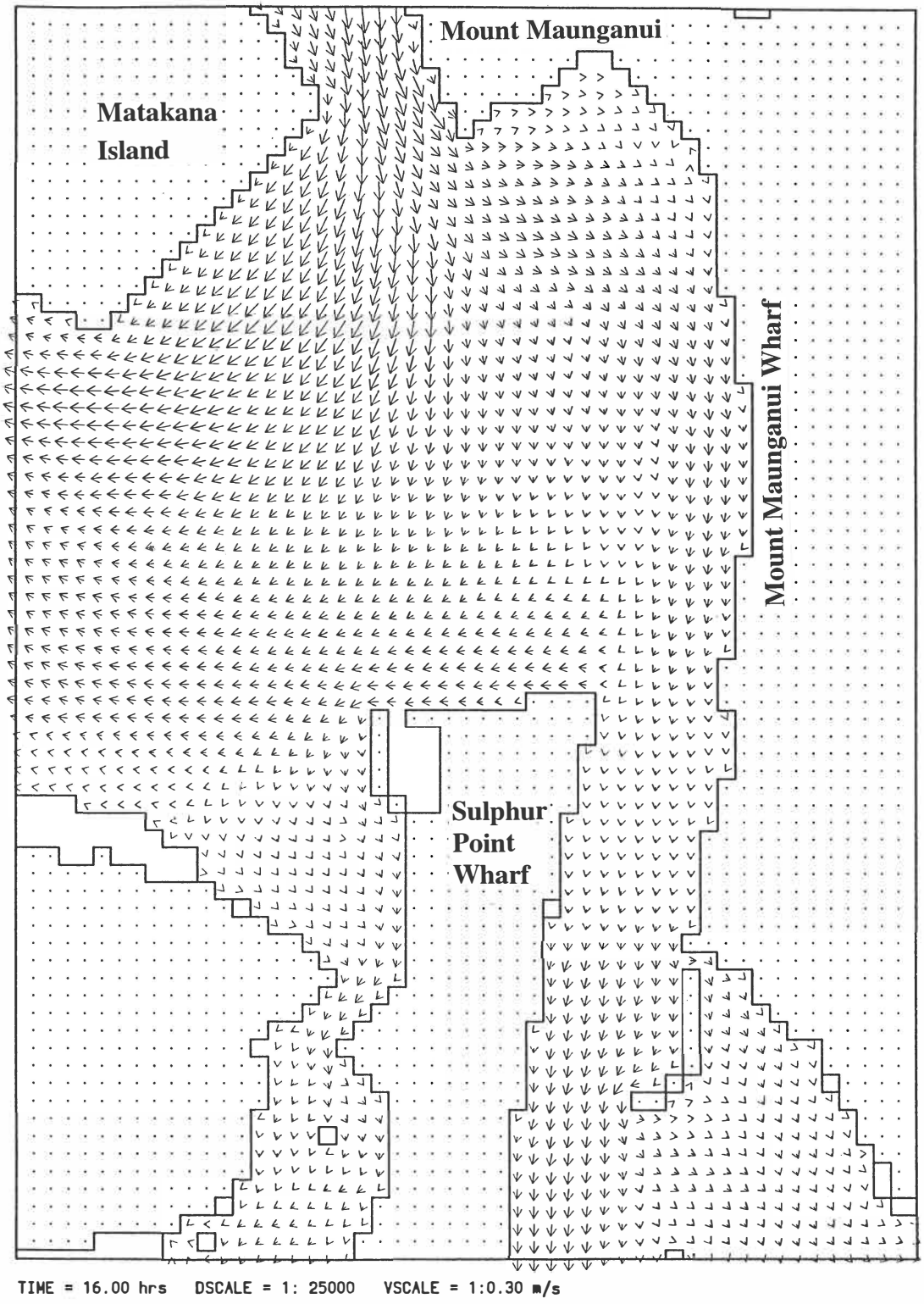

Figure 1.6a Mean tide velocity pattern at peak flood in Tauranga Harbour around the Port area (After Bell, 1994).

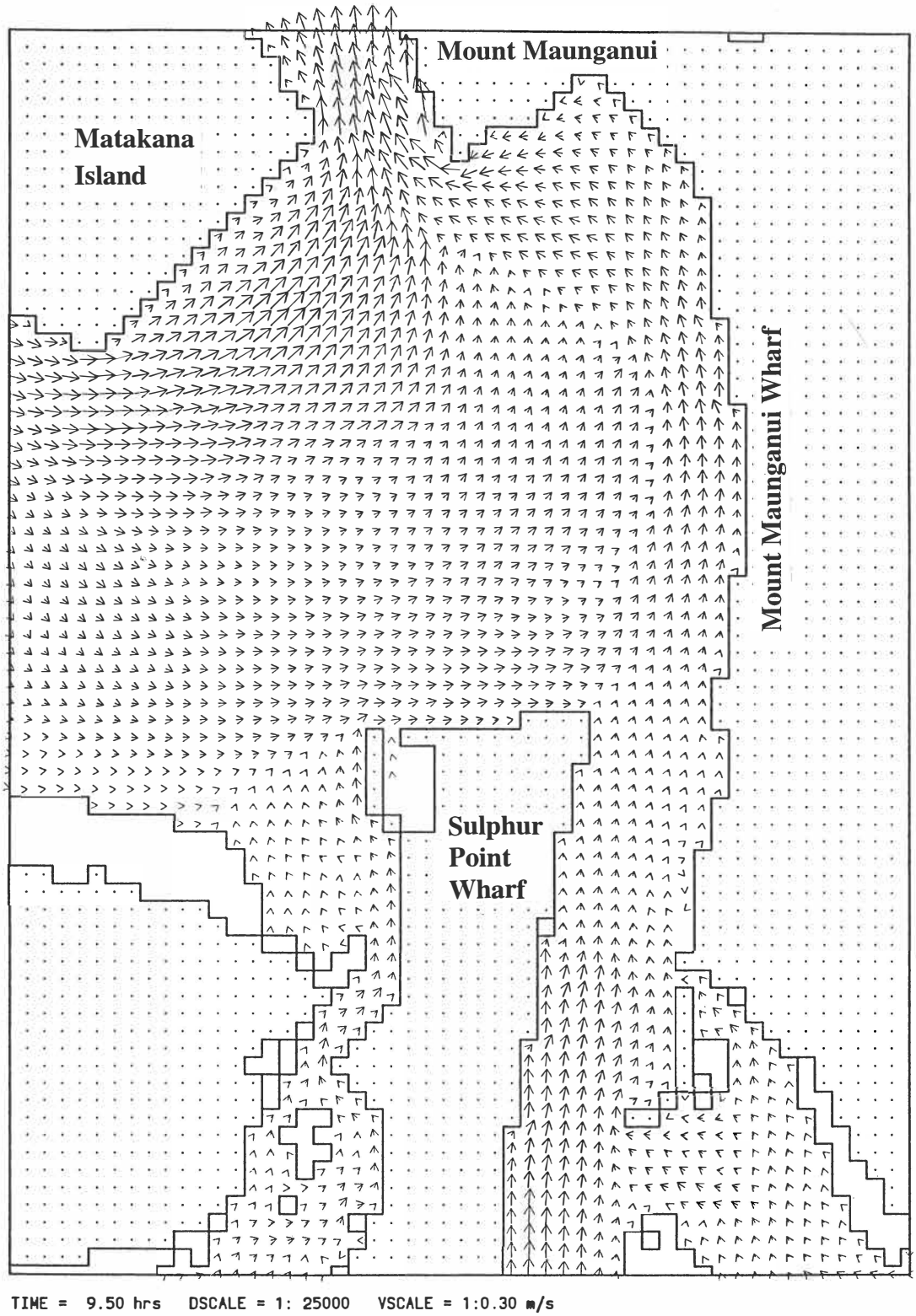

Figure 1.6b Mean tide velocity pattern at peak ebb in Tauranga Harbour around the Port area (After Bell, 1994).

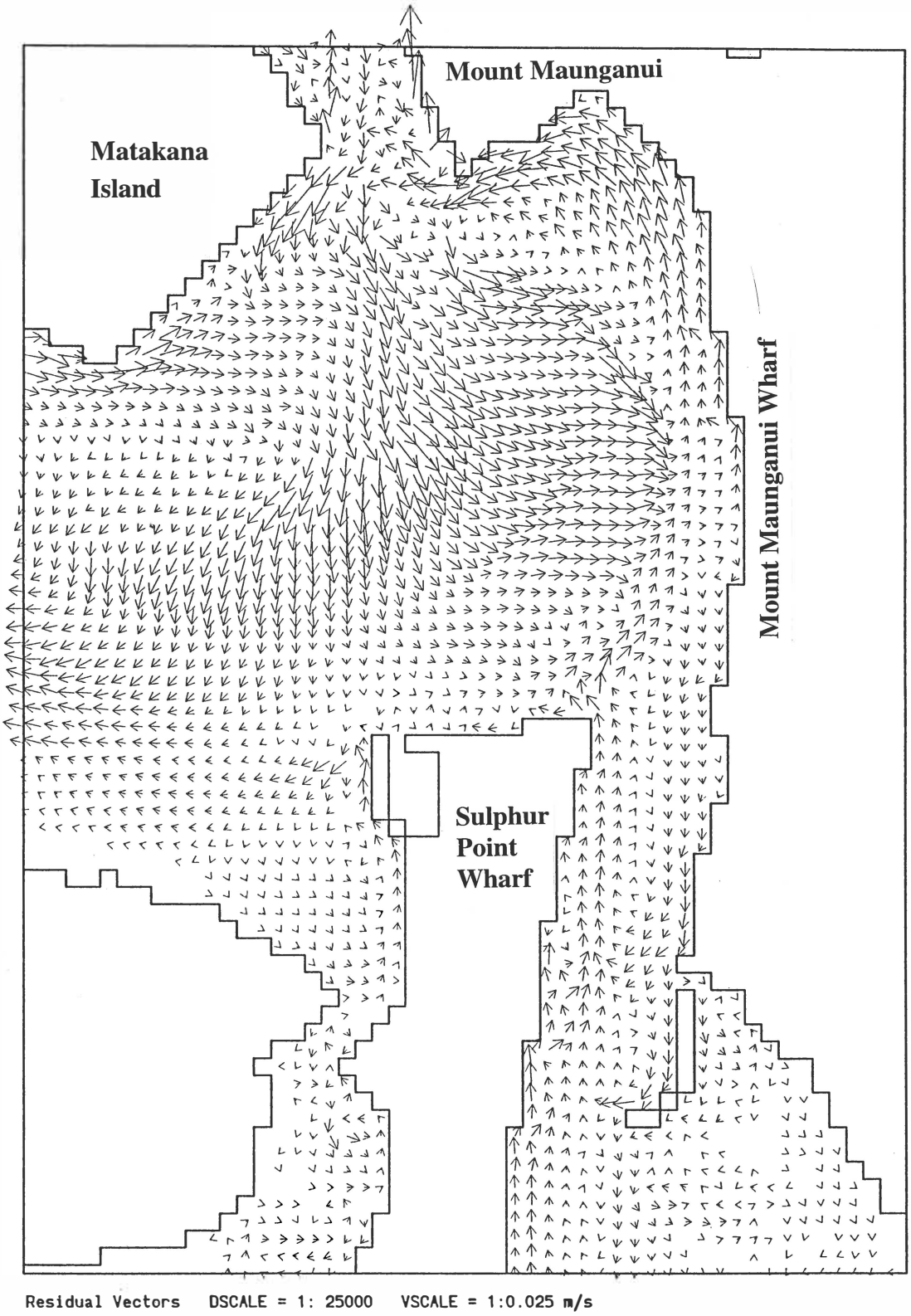

Figure 1.6c Full tidal cycle residual velocity vector pattern in Tauranga Harbour around the port area (After Bell, 1994).

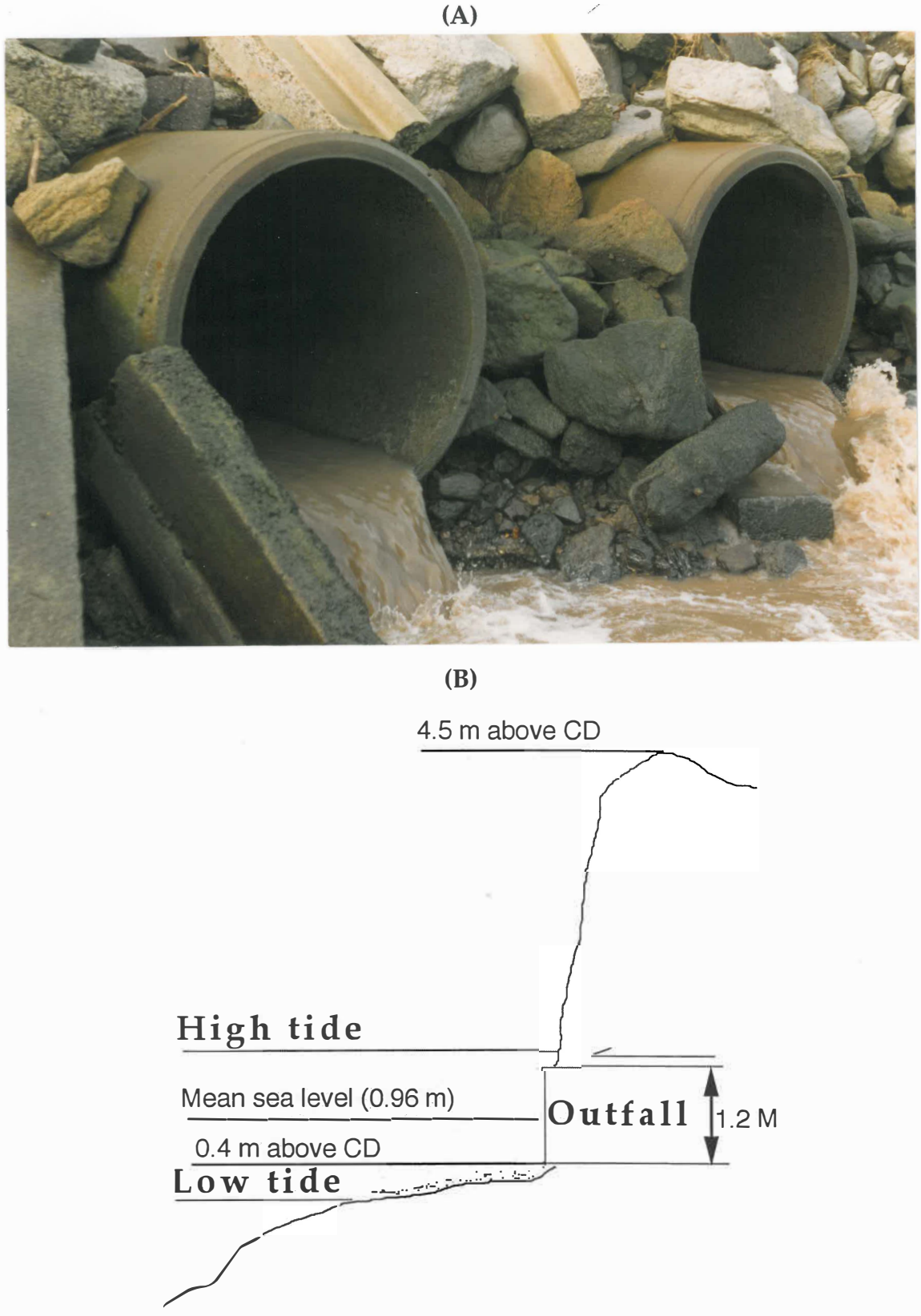

Figure 1.7 Photo of the southern outfalls around the log handling area at the Port of Tauranga (A) and its dimension and elevation relative to mean sea level (B). CD: Port datum.

CHAPTER TWO

WHARF HYDROLOGY

CHAPTER TWO

WHARF HYDROLOGY

2.1 INTRODUCTION

Little is known about the specific characteristics of the hydrology of a large log export wharf, which is essentially the hydrology of a large flat surface with storage buildings and thousands of logs on its surface. It is necessary to investigate the nature of the runoff from the wharf surface in order to address the general objectives of determining the annual contaminant load to the receiving tidal waters from the log handling areas, and if necessary, consider the alternatives if the runoff water quality cannot meet the discharge criteria set by the local environmental management authorities

Accordingly, the objectives of this chapter are to:

i) review and analyse the available rainfall data for the Mount Maunganui log export wharf;

ii) calculate annual runoff volume; and

iii) assess frequency of surface flooding around the log operation area.

2.2 RAINFALL DATA

For recording rainfall at the log handling area during this study period, two Lambrecht 1509H rain-gauges were set up at and near the log handling areas (Figure 2.1).

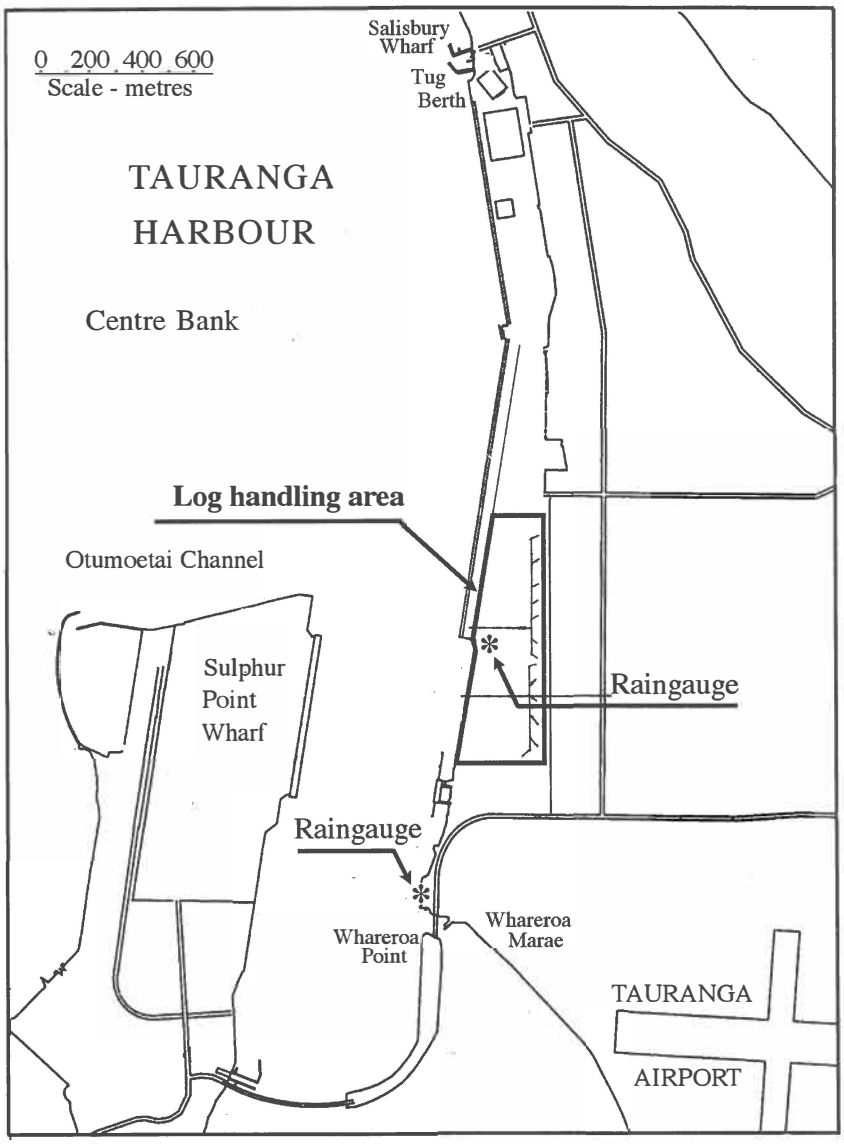

Figure 2.1 Locations of the two Lambrecht 1509H rain-gauges established around the wharf log handling area.

The long-term daily rainfall records (1985-1995) from the Meteorological Station at Tauranga Airport (which is about 1.0-1.5 km away from the two rain-gauges set in this study and at the same elevation with the rain-gauges) were obtained from the Meteorological Database held by NIWA.

2.3 LONG-TERM SEQUENCE OF RAINFALL EVENTS

Long-term sequences of rainfall events of the study area were analysed to estimate annual runoff from the wharf log handling area. Ideally, long term records of discrete rainfall events, for example, more than 10 years, should be obtained. However, only daily rainfall records from January 1, 1980, to December 31, 1995, at the Tauranga Airport Meteorological Station were available for this study. Fortunately, there would not be a great error if we assume that the rainfall for each day comes from a single rainfall event over a long period, that is, we treat each daily rainfall as a discrete rainfall event. When the daily *cumulative* rainfall is low, it is not apparent whether the total daily rainfall comes from one, or several rainfall episodes, because no appreciable runoff will be produced. When the total daily rainfall is high, it is also not apparent whether the total daily rainfall comes from one or a few rainfall events. After the soil becomes saturated, there is not a significant difference, in terms of the runoff volume, whether the rainfall derives from one episode or several discrete events within 24 hours.

Figure 2.2 shows the long term sequence of daily rainfall from January 1, 1980, to December 31, 1995, at the Tauranga Airport Meteorological Station. The average annual rainfall for this period was 1214 mm, 135 mm less than that during the period of 1898 - 1980 (Quayle, 1984).

From Figure 2.2, it is evident that:

i) the fine days (here defined as daily rainfall < 1.0 mm) accounted for 70.9% of the period between 1980-1995. The days with a rainfall less than 6.0 mm accounted for 85.7 %. Only 0.62% of the days had a rainfall more than 50 mm;

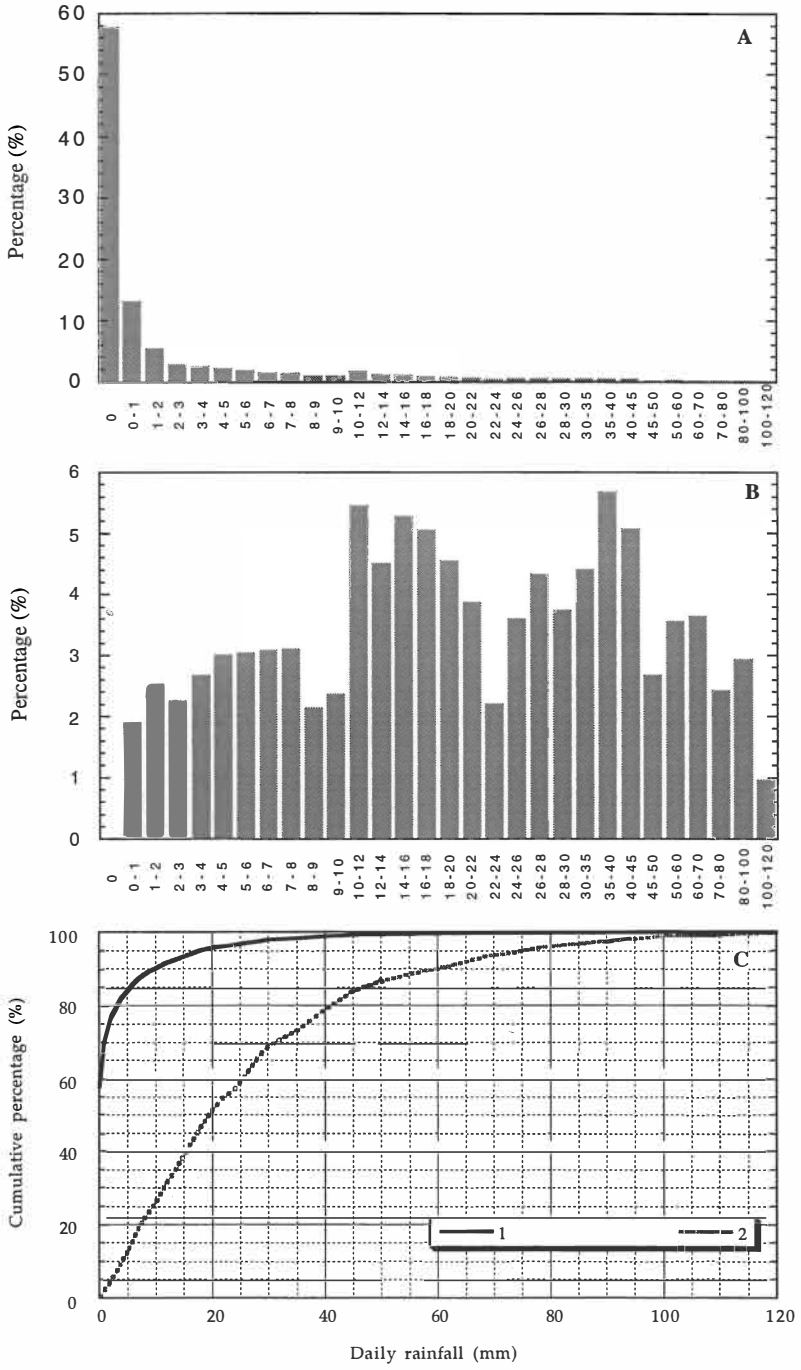

Figure 2.2 Frequency distribution of daily rainfall from January 1, 1985, to December 31, 1995, at the Tauranga Airport. (A) Frequency distribution based on days with a certain daily rainfall. (B) Frequency distribution based on daily rainfall. (C) Cumulative frequency distribution based on days (curve 1) and based on daily rainfall (curve 2).

ii) the days with a rainfall less than 6.0 mm, which accounted for 85.7% of this period, contributed only 15.5% of the total precipitation during the period of 1980 - 1995. The days with a rainfall more than 50 mm, which accounted for only 0.62% of the study period, contributed 13.5% of the total precipitation during the same period.

2.4 ANNUAL RUNOFF VOLUME

Due to the complexity of converting rainfall into runoff at a known location, the high variability in the measured results in the field, as well as the practical difficulties of measuring runoff flow rates for the log handling area, the following simple formula is used in the present investigation of wharf hydrology, instead of using complex hydrological and hydraulic models.

According to Nix (1994), Li and Adams (1993), and ARC (1992b), the following formula is commonly used to calculate runoff volume per unit area for a single storm event if the difference of saturation levels of soils at the commencement of each storm is neglected:

$$V_r = K\,(S - C) \qquad (2.1)$$

where V_r -- runoff volume (m^3).
S -- accumulative rainfall of a storm event (m)
C -- depression storage (m)
K -- runoff coefficient

The key to calculating runoff volume from equation 2.1 is to determine depression storage, C, and runoff coefficient, K, properly.

Different values of depression storage, C, were used for pervious and impervious areas by previous researchers. The popular Storm Water Management Model Level 1 (Nix, 1994) assumes 0.25 and 0.0625 inch (6.4 and 1.6 mm) are the maximum depression storage for pervious and impervious

areas. Auckland Regional Council (1992) assigned a value of 0.015 m and 0.002 m for pervious and impervious areas.

No data is available for the sealed or gravelled log handling areas which are the focus of this study.

In this study, the sealed and gravel surfaced wharf areas were not treated simply as impervious and pervious areas. Firstly, the huge amount of logs and bark around the log handling area (see Chapter 4) can absorb a significant amount of water, thereby increasing the depression fraction. Secondly, there are a considerable number of "potholes" on the wharf surface because of a long period of log operations, particularly on the gravel surfaced area. These potholes also increase the depression storage.

For estimating the depression storage, *C*, the necessary rainfall required to produce appreciable runoff for the sealed and gravelled wharf areas was investigated by the author during six storm events. "Appreciable runoff" is defined in this study as the runoff flow rate at a cesspit exceeded 1 l/s (Table 2.1).

Although further investigation may be required to predict precisely how much rainfall is needed to produce appreciable runoff from the wharf area, these results can still be used for estimating the approximate annual runoff. From these results (Table 2.1), 6 and 11 mm could be used for initial approximation for the depression storage parameter, *C*, for the sealed and gravel surfaced wharf area.

The Storm Water Management Model (Level 1) uses 0.9 and 0.15 as runoff coefficients for the impervious and pervious areas (Nix, 1994). ARC (1992) recommended values for the runoff coefficient $K = 1.0$ and 0.5 for impervious and pervious areas. At the Mount Maunganui wharf, the sealed area is impervious and the infiltration can be considered as 0. However, field observations in this study showed that, for a bark pile, 30 - 45 cm of the top

bark layer became wet only after 20 mm of rainfall yet the underlayer was still dry. Likewise, some bottom logs of a log stack with a height of 5 m were dry until after 20 mm of rainfall. Therefore, a value of 0.9 is reasonable to be used as runoff coefficient K for the sealed wharf area. For the gravel surfaced area, the field observations showed that it seems K = 0.5 (as recommended by ARC, 1992) is low because the pores among the gravel were blocked by the crushed bark and the soil particles after long periods of log operation. This decreased the infiltration rate of water through the gravel layer. A value of 0.6 is believed suitable as runoff coefficient K for the gravelled area.

Table 2.1 Cumulative rainfall (mm) when appreciable runoff formed at the gravel surface and sealed wharf areas.

Date	Lapse time from last rain (Days)	Sealed area	Gravel surfaced area
10/11/1993	4 (10.5)[1]	5.2	10.0
18/3/1995	3 (15.7)	3.9	7.6
24/5/1994	26(12.0)	5.0	--[3]
24/7/1995	5(20.4)	10.3[2]	12.7[2]
28/5/1995	8(12)	5.5	10.7
12/7/1995	7(15.7)	7.7	13.4
Mean		6.3	10.9

[1] the number in the bracket is the cumulative rainfall since the last rainfall.

[2] drizzled for 17. 7 hours and had a total rainfall of 9 mm.

[3] no runoff entered the cesspit from this area when the rain stopped (cumulative rainfall was 5.0 mm).

Accordingly, the runoff volume from the sealed (V_{rs}) and gravel surfaced (V_{rg}) areas were calculated with equations 2.2 and 2.3 for a given storm,

$$V_{rs} = 0.9\, A_s(S - 0.006) \qquad (2.2)$$

$$V_{rg} = 0.6\, A_g\, (S - 0.011) \qquad (2.3)$$

where A_s is the sealed area (124,000 m^2) and A_g the gravel surfaced area (68,000 m^2).

The total runoff volume, V_{rt}, from the whole log handling area for a given storm can then be calculated by,

$$V_{rt} = V_{rs} + V_{rg} \qquad (2.4)$$

An equation similar to 2.1 may be used to calculate annual runoff volume, V_{ar} (m^3a^{-1}), for a given catchment,

$$V_{ar} = K\,(S - S_i) \qquad (2.5)$$

where S - annual precipitation (m),
S_i - "ineffective annual precipitation" (m).

"Ineffective annual precipitation" is defined as the sum of precipitation within a year which cannot produce runoff for a given land surface. Nix (1994) called it "annual effect of depression storage". It consists of two parts, namely the sum of rainfall events ≤depression storage and the sum of the initial rainfall which falls in the depressions from rainfall events >storage depression.

"Ineffective annual precipitation" depends on the land surface types and distribution of long-term rainfall events. Nix (1994) indicated that the impact on annual runoff from depression storage for Minneapolis, USA, fits a power equation,

$$\text{"annual effect (in inches)} = 5.234\,(DS)^{0.5857} \qquad (2.6)$$

where DS - depression storage, in inches.

For the sealed log handling area at the Port of Tauranga, only the rainfall events with a rainfall >6 mm could produce appreciable runoff. From Figure 2.2, 15.5% of annual precipitation came from rainfall events with a rainfall <6 mm. This part of annual precipitation should be subtracted from the total annual precipitation. For the rainfall events >6 mm (52 events annually), the first 6 mm of rainfall would not produce significant runoff. Accordingly, "ineffective annual precipitation" for the sealed area, S_{is}, was calculated as,

$$S_{is} = (S \times 15.5\%) + (52 \times 0.006) \quad (2.7)$$
$$= 0.209 + 0.312$$
$$= 0.520\ (ma^{-1})$$

The annual runoff volume entering the receiving tidal waters from the sealed log handling area, V_{rs}, was calculated as,

$$V_{rs} = 0.9 \times (S - S_u) \times A_s \quad (2.8)$$
$$= 0.9 \times 0.828 \times 124{,}000$$
$$= 92{,}000\ (m^3a^{-1})$$

Dividing this result by the sealed log handling area (12.4 ha), the annual runoff per hectare of sealed area is 7500 $m^3ha^{-1}a^{-1}$.

Similarly, the "ineffective annual rainfall" for the gravel surfaced log handling area, S_{ig} was calculated based on the following statistics (Figure 2.2): 29.0% of total annual precipitation came from rainfall events <11 mm and there were 34 rainfall events with cumulative rainfall >11 mm annually,

$$S_{ig} = S \times 29.0\% + 34 \times 0.010 \quad (2.9)$$
$$= 0.390 + 0.34$$
$$= 0.730\ (ma^{-1})$$

The annual runoff volume entered the receiving tidal water from the entire gravel covered log handling area, V_{rg}, was,

$$V_{rg} = 0.6 \times (S - S_u) \times A_g \qquad (2.10)$$
$$= 0.6 \times 0.618 \times 68{,}000$$
$$= 25{,}000 (m^3 a^{-1})$$

The annual runoff per hectare of gravel surfaced wharf area (25,000/6.80 = 3700 $m^3 ha^{-1} a^{-1}$) was only a half of that from the sealed wharf area.

The total annual runoff volume from the entire log handling areas at the Mount Maunganui wharves are:

$$V_{rt} = V_{rs} + V_{rg} \qquad (2.11)$$
$$= 92{,}000 + 25{,}000$$
$$= 117{,}000 (m^3 a^{-1})$$

Figure 2.3 illustrates "ineffective annual rainfall", S_u (mm), against depression storage, DS (mm). The relationship, $S_i = 76 + 87DS - 2.3DS^2$ (R=1.0, obtained by least squares curve fitting), may be able to be used for other ports with similar a distribution of annual precipitation, but different land surface pavement types.

2.5 SURFACE FLOODING

According to the initial design, the design return period of the two storm drainage systems around the log handling areas at Mount Maunganui wharf is 4 years (personal communication: J. Palmer, Engineering Manager, Port of Tauranga Ltd).

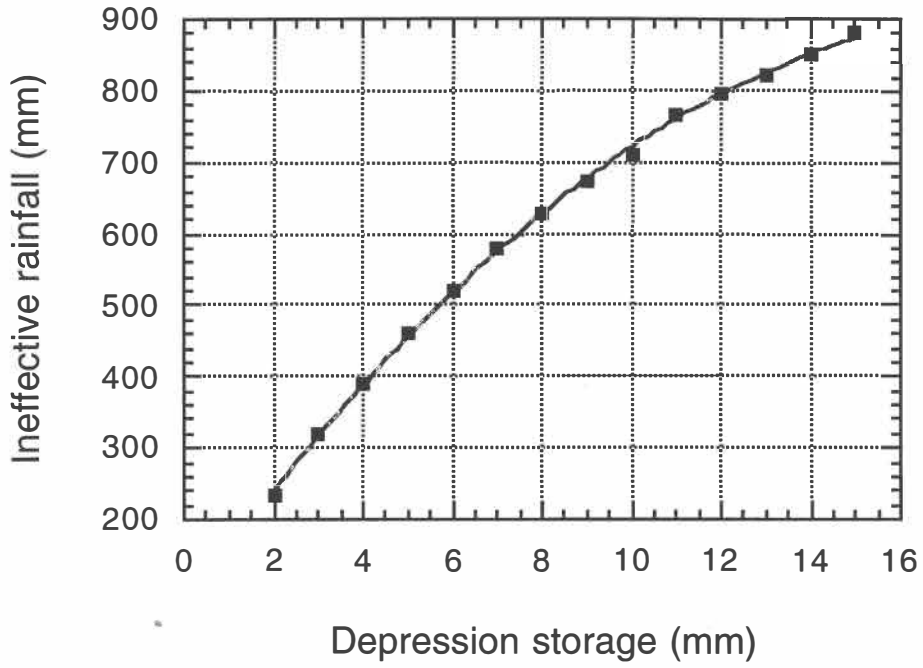

Figure 2.3 Plot of "ineffective annual rainfall" against depression storage for the log handling areas at the Port of Tauranga.

During the field observations of this study, it was found that the actual surface flooding frequency around the log handling area was considerably higher than the designed frequency. On average, surface flooding occurred around the log handling area a few times per year. Figure 2.4 illustrates four floods monitored during this study.

Statistical data from the Tauranga Airport Meteorological Station showed that for a storm with a return period of 2 years, rainfall duration of 10 minutes, 20 minutes, and 30 minutes realised 12 mm, 19 mm, and 23 mm rainfall, respectively (Quayle, 1984). From Figure 2.4, the most intensive rainfall with a period of 10 minutes, 20 minutes, and 30 minutes during the four rainfall episodes which caused surface flooding, was less than 12 mm, 19 mm, and 23 mm. In other words, the rainfall events which caused surface flooding were less intensive than the design ones.

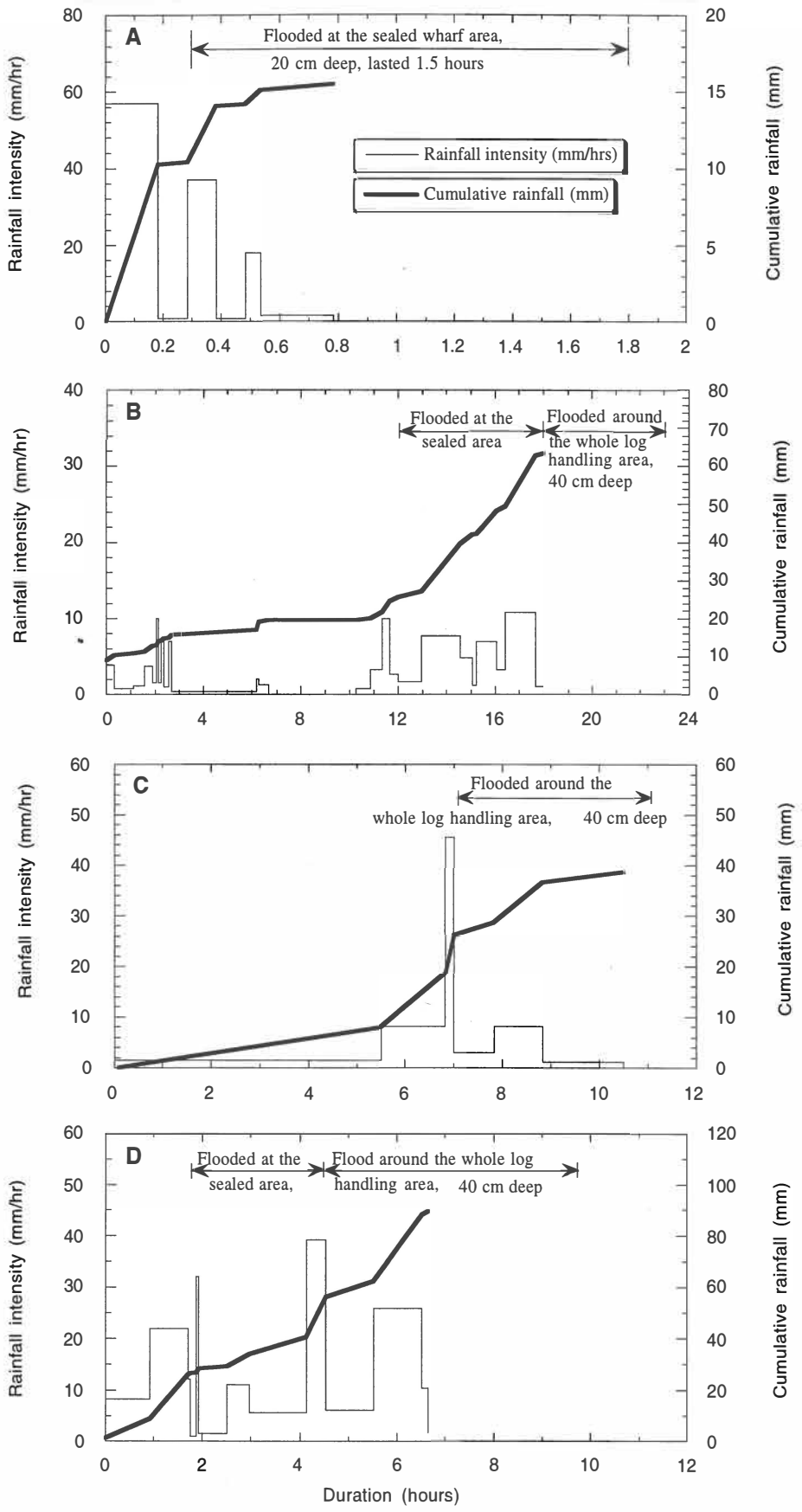

Figure 2.4 Rainfall intensity, cumulative rainfall, and occurrence of floods during four storm episodes in 1994-1995. A: 18/3/1994; B: 25/7/1994; C: 3/4/1995; and D: 28/5/95.

Observation at the outfalls showed that the main discharge pipes were only half full before and during the floods during three rainfall events. The reasons for the unexpectedly high incidence of surface flooding are explained below:

i) Unlike the common urban area, where most of the cesspits of a storm drainage system are available during a rainfall, a number of cesspits of the drainage systems around the log handling areas were always covered by logs. Seven random on-site investigations showed that, on average, only 7 out of 17 cesspits were available around the log handling area (Table 2.2). Practically, it is very difficult to avoid not covering the cesspits with logs during log stacking operations.

Table 2.2 Available cesspits out of the 17 cesspits of the southern and northern drainage systems around the log handling area for the seven random on-site investigations. AC: available cesspits

Date	11/11/93	16/3/94	18/3/94	24/7/94	3/4/95	28/5/95	12/7/95	Average
AC	6	3	6	5	7	8	7	7

ii) From Figure 2.4, it is evident that almost all surface flooding occurred during and after a period of intensive rainfall. The overland flow produced by the intensive rainfall could carry large pieces of bark chunks to the cesspits. These bark pieces could not pass through the cesspit grill and thus deposited on the cesspits covers, impeding the flow of water. On-site observation by the author during 4 surface flooding events showed that all the available cesspits were impeded by large pieces of bark. Sometimes, the bark and the covers of the cesspits had to be removed manually in order to accelerate draining the runoff. Surface flooding would not occur without a period of intensive rainfall which could carry bark chunks during a storm event, even though the rainfall may last a long time and the cumulative rainfall be relatively high.

2.6 CONCLUSIONS

Based on the analyses of a 10 year sequence of rainfall records, field observations of a major export port log handling area in this study, and assessment of "ineffective annual precipitation", the following can be concluded:

1. About 45% of the annual precipitation from the log handling areas at the Mount Maunganui wharves is converted to runoff (117,000 m^3) and enters the receiving tidal waters.

2. Annual volume of runoff per hectare of wharf surface is calculated as about 7,500 $m^3 ha^{-1} a^{-1}$ for the sealed area and about 3,700 $m^3 ha^{-1} a^{-1}$ for the gravelled area.

3. Surface flooding around the log handling areas occurred more frequently than designed for because of the coverage of cesspits by stored logs, and the blockage of available cesspits by bark chunks carried by overland flow during periods of high intensive rainfall.

CHAPTER THREE

WHARF RUNOFF WATER QUALITY

I. INTRODUCTION

CHAPTER THREE

STORM RUNOFF WATER QUALITY I. INTRODUCTION

3.1 STUDY OBJECTIVE

Chapter 2 discussed quantity of storm runoff from the log handling areas at the Mount Maunganui wharves. Chapters 3-6 present the results investigated into storm runoff water quality, including:

1. selected physical, chemical and biological characteristics of storm runoff from the wharf log handling areas of concern to local environmental management authorities; and

2. the influence on storm runoff water quality from rainfall processes and wharf surface pavement types.

3.2 LITERATURE REVIEW AND RESEARCH BACKGROUND

Concern about storm runoff water quality is not new. In England, as early as 1893, Wardle stated "the first storm washings contain quantities of putrescible organic matter, they are very foul and often contain as much as the sewage itself" (Lindholm and Balmer, 1978). Wilkinson (1956, cited by Mance and Harman, 1978) demonstrated that stormwater runoff from a separately sewered housing estate was of much poorer quality than the original rainwater. In the United States, Benzie *et al.* (1966) and Burm *et al.* (1968) indicated that separate storm sewer discharges had a definite pollution effect on receiving water. Even so, only after the early 1970s, urban storm runoff has been increasingly recognised as the primary source of surface water degradation and more attention has been paid to this problem

(Sartor *et al.*, 1974; Whipple *et al.*, 1974; Overton and Meadows, 1976; Roesner, 1982; Rogers and Rosenthal, 1988).

From the early 1970s, there have been many studies concerned with the effects of urbanisation on water quality over the world. For example, Cordery (1977) in Sydney, Australia; Goettle and Krauth (1981) in Munich, Germany; Mealanen and Laukkanen (1981), in Finland; Quresh and Dutka (1979, cited by Ishaq and Khararjian, 1988) in Ontario, Canada. They reported their research results concerning storm runoff quality and quantity from highways, parking lots, commercial areas, residential areas, and so on. In the USA, a number of major works on storm runoff water quality and its environmental impact have been undertaken and a variety of storm water management models have been developed, for example, the United States Environmental Protection Agency (EPA)'s Storm Water Management Model (SWMM) and SWMM Level 1 (Metcalf, *et al.*, 1971, cited by Browne, 1990), the Corps of Engineers STORM (Hydrologic Engineering Centre, 1976, cited by Browne, 1990) and the Hydrologic Simulation Program-Fortran (HSPF) (Hydrocomp, 1976, cited by Browne, 1990).

In addition to the study of stormwater from urban areas, there have also been a considerable number of studies about effects of logging on water quality, for example, Hornbeck, *et al.* (1970); Patric and Reinhart (1971); Brown, *et al.* (1971, 1973); and Harr and Fredriksen (1988). These studies reported the effects of logging, road construction in bush areas, and slash burning on storm runoff quality and quantity. In the United States, many states are organising different programs to control nonpoint pollution from forest lands (Brown *et al.*, 1993).

In New Zealand, it seems the study of storm runoff water quality and its effects on receiving environment began from the early 1980s (Leersnyder, 1992). Williamson (1985, 1986) investigated the stormwater quality from three urban areas. Auckland Regional Water Board (ARWB, 1988) assessed the urban and industrial storm runoff which flows into Manukau Harbour.

Under the Resource Management Act (1991), which aims to promote the sustainable management of natural and physical resources, a "resource consent" is required from the regional council for any discharge to the natural environment. Accordingly, greater attention has been paid to potential environmental impacts related to the discharge of stormwater. Auckland Regional Council undertook an investigation on urban stormwater quality in Auckland Region (ARC, 1992a) and developed a "Design guideline manual of stormwater treatment devices" based on the monitoring results (1992b). Some industrial companies, for example, the Port of Tauranga Ltd (Tian, 1993) and the Port Marlborough New Zealand Ltd (Kingett Mitchell and Associates, 1993), have undertaken some preliminary investigation on stormwater quality related to their port operations.

Although great progress in understanding the stormwater quality from different land uses and its impacts on receiving environment has been made, storm runoff water quality from some special watersheds, for instance, from a timber port or a log storage yard in paper mills, has not been well understood.

At the Port of Tauranga, some preliminary investigations have been undertaken on storm runoff water quality from its wharves (McCabe, 1991; and Kingett Mitchell and Associates, 1993; Tian *et al.*, 1994, 1995). However, these studies focused on only some aspects of storm runoff water quality and no relationships between contaminant concentrations and other factors, such as rainfall processes and wharf surface pavement types, were established because of insufficient number of samples collected in their studies. Accordingly, a comprehensive investigation of storm runoff water quality was attempted.

3.3 SAMPLING AND INVESTIGATION TERMS

3.3.1 Sampling

The log handling areas at the Mount Maunganui wharf covers an area of about 20 hectares and have two types of wharf surface pavements: sealed and gravel covered. There are two main storm drainage systems around the log handling areas (Figure 3.1). The details of these two drainage system, for example, their dimensions and elevation relative to mean sea level, are presented in Figure 1.7.

Six sampling sites were selected, five around the log handling area and one at the adjacent urban area (Figure 3.1). Sites 1 and 2 are two cesspits located at the gravel surfaced and sealed wharf areas, which were suitable for investigating the effect of wharf surface pavement types on runoff water quality. Site 3 is at the outfall of the northern storm drainage system around the log handling area. This system receives storm runoff from the gravelled and sealed wharf areas only. Sites 4 and 5 are the outfalls of the southern storm drainage system. This system has two parallel pipes and receives runoff from both the wharf log handling area and the adjacent urban area. Sites 3, 4, and 5 were able to be sampled only at low tide because these outfalls were inundated during high tide. Site 6 was at the point where the urban runoff enters the southern wharf drainage system from an open channel.

The samples were collected in 1 or 2 litre polypropylene bottles and stored chilled in the dark immediately after sampling. In total 123 samples were collected from seven significant rainfall events between November, 1993 and July, 1995. Samples were not able to be collected from all the sampling sites during each storm because of logistic difficulties.

Two Lambrecht 1509H recording raingauges were established at and near the log handling area to record the rainfall.

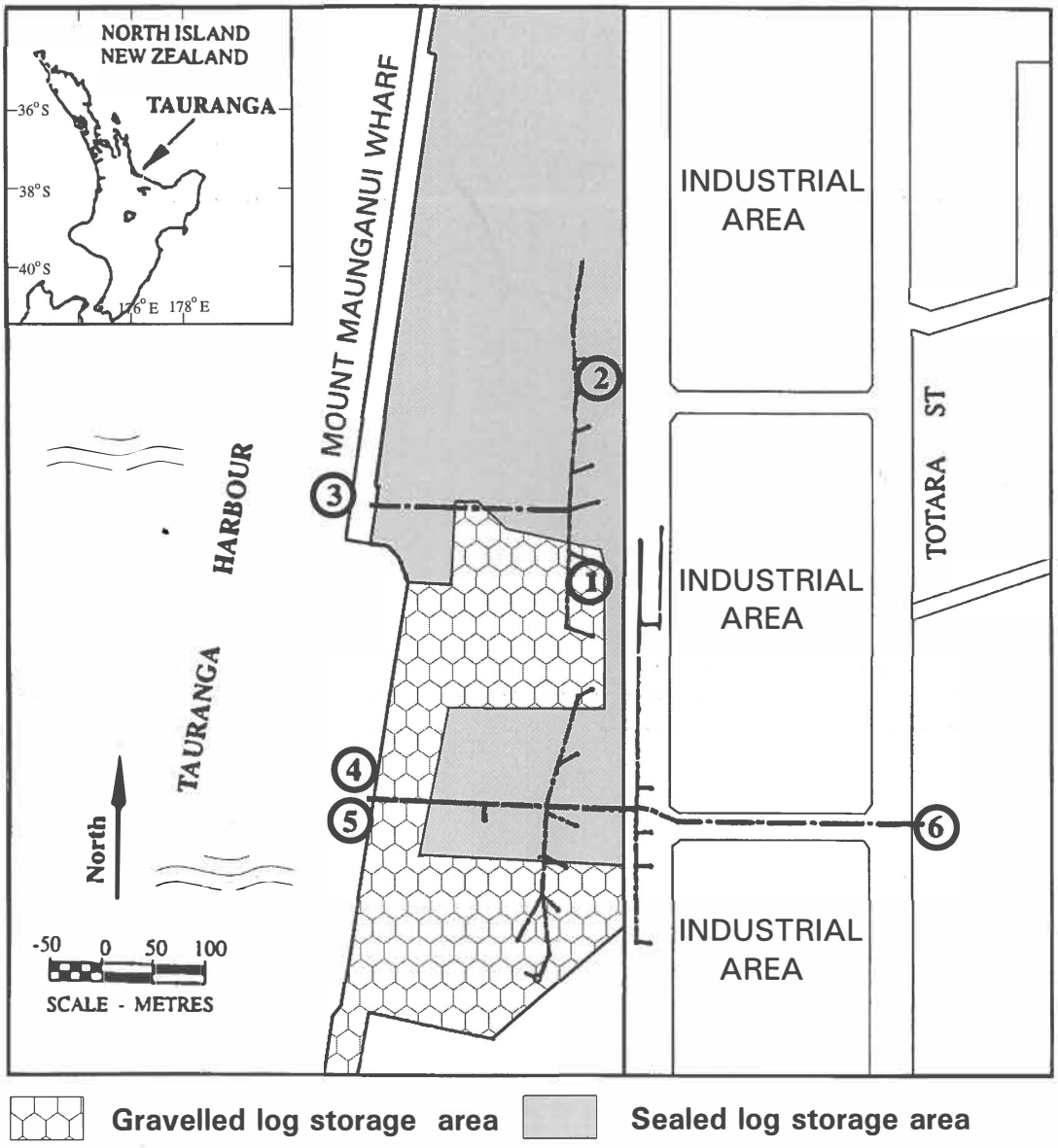

Figure 3.1 The log handling area at the Port of Tauranga, New Zealand, showing the types of wharf surface pavements, storm drainage systems and the sampling sites.

3.3.2 Investigation Terms

It is practically difficult to measure all contaminants in the wharf runoff. The investigation had to be focused on the main concerns associated with the discharge of the wharf storm runoff from the log handling areas.

McFarlane (1993) summarised 5 potential problems related to the discharge of log yard runoff:

- Deposition of suspended or settleable solids
- Foam
- Colour
- Toxicity
- Oxygen demand

Kingett Mitchell and Associates (1993) examined five groups of water quality parameters of runoff from wharf log handling areas. They were:

- Suspended solids
- Oxygen demanding substances
- Nutrients
- General constituents such as pH and conductivity
- Natural organic compounds

NCASI (1992) reviewed water quality of storm runoff from log storage yards or log decks of paper and pulp mills in the USA. The review focused on the following aspects:

- Suspended solid and volatile suspended solids
- Oxygen demanding substances
- Nutrients

- General constituents such as pH and conductivity
- Natural organic compounds
- Toxicity

Tian *et al.*'s (1995) study on stormwater quality from the Sulphur Point wharf at the Port of Tauranga reported:

- the suspended solid concentration was relatively high and remained at high level during a storm episode;

- the runoff was highly discoloured. The mean concentration of soluble yellow substance (g_{440}) is 17.9 m^{-1}; and

- there were indeed some natural organic substance present in the stormwater, for example, dehydroabietic acid (DHAA), which is potentially toxic to marine life.

Optical water quality of natural waters, domestic and industrial effluent has been receiving greater attention since the 1980s (see Section 4 of this Chapter). Accordingly, optical properties of the wharf runoff should be investigated as an important aspect of water quality in this investigation. In summary, the following five aspects of storm runoff water quality were investigated in this present study:

1) Optical properties,
2) Extractable organic substance, mainly focus on resin and fatty acids,
3) Nutrients,
4) Oxygen demanding substances, and
5) Oil and grease.

Field observations by the author during a few storm events indicated that there was some foam in the storm runoff, but little on the sea surface near the outfall, hence it was not regarded as a serious problem.

CHAPTER FOUR

WHARF RUNOFF WATER QUALITY
II. OPTICAL QUALITY

CHAPTER FOUR

STORM RUNOFF WATER QUALITY
II. OPTICAL QUALITY

4.1 INTRODUCTION

Optical quality of natural waters, primarily their visual clarity and colour, can strongly affect their recreational value, aesthetic appeal, and aquatic life (Davies-Colley and Close, 1990) and may be of most concern to environmental authorities because any conspicuous change in optical quality to receiving water is visible. However, such quality has received little attention in previous studies concerning domestic and industrial effluents, although suspended solid concentration and turbidity of the effluent are normally determined. This is probably because "optical water quality" is a relatively new concept (Kirk, 1988). Likewise the optical water quality of storm runoff from a timber port or log storage yards of paper mills is deteriorated significantly due to the addition of a substantial amount of fine bark and soil particles (Tian *et al.*, 1995), but few studies appear to have been conducted. Accordingly, a comprehensive study on optical properties of the storm runoff from the log handling area was undertaken as part of this environmental investigation, including:

* visual clarity,
* colour, and
* contribution of soluble and particulate substance to light attenuation.

4.2 VISUAL CLARITY

4.2.1 Research background and rationale

Clarity refers to the transparency of water (Davies-Colley *et al.*, 1993). There are two different aspects of clarity which are required to protect: visual clarity and light penetration. Visual clarity is the maximum distance at which an objective can be viewed through water. It is measured as the maximum sighting distance of a standard visual target. Light penetration refers to the penetration of sunlight into water (Kirk, 1983). This diffused sunlight in water is the basis for all aquatic ecosystems. It is measured by lowering a light sensor into different depth of water and recording the lighting from the surface downwards. Smith *et al.* (1991) indicated that visual clarity was the best single predictor for rating the suitability of freshwater for bathing through on site user interview.

Traditionally, suspended solid concentration and turbidity are the parameters that have been used to express the optical properties, primarily visual clarity, of natural waters, domestic effluent and industrial wastewater. Suspended solids and turbidity of urban storm runoff have been well documented, for example, Cordery (1977); Mance and Harman (1978); Black (1980); Roesner (1982); and Williamson (1985 and 1986). However, the impact of suspended solids on aquatic environment depends not only on their mass concentration, but also on their composition and particle size distribution. Likewise the nephelometric turbidity of a water sample depends not only on the water sample itself, but also on the instruments used for the measurement. Therefore, both suspended solid concentration and turbidity are not substitutes for visual clarity measurement. McCluney (1975) advocated measurement of beam attenuation coefficient instead of turbidity. However, this measurement involves expensive instrumentation.

Using a black disk as a target rather than the traditionally used Secchi disk to measure visual clarity of waters possesses significant theoretical and practical advantages (Davies-Colley, 1988). Firstly, the black disk sighting range, y_{BD}, is inversely proportional only to the beam attenuation coefficient, c (units: m^{-1}), one of inherent optical properties of water, i.e., $y_{BD} = \psi/c$. As ψ is independent of optical properties of the water and depends

only on the threshold contrast of the eye, a black disk can be used for measuring visual clarity of water samples offsite in a trough when it is inconvenient or unlikely to undertake the measurement *in situ* (Davies-Colley and Smith, 1992). Secondly, the beam attenuation coefficient, c, is additive (Kirk, 1983). This suggests that the black disk visual clarity of very turbid water samples, whose visual clarity is difficult to measure precisely, can be measured after dilution using a clear water with known beam attenuation coefficient (Davies-Colley and Smith, 1992). Following the "mass balance", the balance on attenuation cross-section of water sample, dilution water, and mixture is as follows:

$$C_m V_m = C_s V_s + C_d V_d \qquad (4.1)$$

Where, C and V are light attenuation coefficient and the volume; the subscripts denote the mixture (m), dilution water (d), and water sample (s). Rearranging equation 4.1 and letting dilution rate R = Vm/Vs, we obtain:

$$C_s = C_m R - C_d(R - 1) \qquad (4.2)$$

Theoretically, as ψ depends only on the threshold contrast of the eye, which is a constant under sufficient light (Blackwell, 1946), then ψ should be a constant. Measurement of visual clarity by black disk method over a wide range of lake and river waters in New Zealand resulted in ψ, averaging 4.8, as basically constant (Davies-Colley, 1988). Thus we obtain:

$$y_{BDs} = \frac{1}{R/y_{BDm} - (R-1)/y_{BDd}} \qquad (4.3)$$

In equation 4.3, dilution rate R, black disk visual clarity of the mixture, y_{BDm}, and black disk visual clarity of the dilution water, y_{BDd}, are known, hence y_{BDs} can be obtained. Since y_{BDm} in this study is relatively small (y_{BDm} was adjusted between 0.15 to 0.3 m during the visual clarity

measurement through controlling dilution rates, which ensured that the angular size of the disk remained within 7.6 - 3.8° range of arc when a 20 mm black disk was used) and y_{BDd} is significantly larger (local tap water, y_{BDd} = 10 m, SD = 0.14 m, Davies-Colley and Smith, 1992), the ratio of R/y_{BDm} varies from 133 to 67 (R = 20) and from 267 to 133 (R = 40). Furthermore, the values of $(R - 1)/y_{BDd}$ are only 1.9 (R = 20) and 3.9 (R = 40). Accordingly, the error should not be greater than 3% if the ratio of $(R - 1)/y_{BDt}$ in equation 4.3 is neglected, namely:

$$y_{BDs} = \frac{y_{BDm}}{R} \qquad (4.4)$$

In particular when the dilution rate was 40 and y_{BDm} was about 0.2 m, which were the most common situations during the measurement, the error would be less than 2% when the visual clarity of the samples was calculated from equation 4.4.

4.2.2 Methods

4.2.2.1 Measurement of visual clarity

A 20 mm black disk was used to measure the visual clarity in a 600 mm long white PVC trough. The top and bottom widths of the trough are 120 and 85 mm, and with a height of 70 mm. The bright nature of the white PVC surface ensured that the light field in the trough was uniform along the path of sight. A glass window with a diameter of 45 mm was installed at one end of the trough to undertake observations. During the measurement, the trough was levelled on a table. The following methods were used for the measurements:

i) The mean distance for disappearance and reappearance of the black disk was taken as the measure of black disk visual clarity. For minimising

possible bias (the author had already known some physical features of the samples, for example, suspended solid concentration and turbidity when the measurement was undertaken), another person with little knowledge of environmental science, made independent observations. The visual clarity presented in this paper is the mean of observations from the two observers.

ii) The water samples in the trough were agitated with a glass rod to minimise the particle settling just before taking readings because most of the samples still had relatively high suspended solid concentration even though the samples were diluted in advance.

iii) A frustum of a cone shaped viewer, which was made with thick black plate, was stuck on the class window to minimise the light reflection from the window glass.

4.2.2.2 Measurement of beam attenuation coefficient

A Pye-Unicam PU8800 spectrophotometer with the samples held in two different positions was employed in this study to measure the beam attenuation coefficient, c (units; m^{-1}). The principle and procedures of the measurement are shown in Section 4.4. Beam attenuation coefficient of 35 wharf runoff samples and 13 adjacent urban runoff samples were determined.

4.2.2.3 Measurement of other parameters

The measurement of suspended solid concentration and volatile suspended solid concentration follows the *Standard Method for the Examination of Water and Wastewater* (APHA *at al.*, 1992). Turbidity was measured with a Hach Model 16800 Turbidimeter.

The water samples were stored chilled in the dark immediately after sampling and were analysed within 48 hours of collection for all terms

analysed in this study with exception of organic extractives. The analyses of organic extractives are shown in Chapter 5.

4.2.3 Results and discussion

4.2.3.1 Overall Average Visual Clarity

Table 4.1 gives the average visual clarity, as well as suspended solid concentration, volatile suspended solid concentration, and turbidity of the samples collected from the 6 sampling sites during seven storms from November, 1993 to July, 1995.

There are significant differences of average black disk visual clarity, as well as suspended solid concentration, volatile suspended solid concentration and turbidity between the runoff from the gravel covered (site 1) and sealed (site 2) areas. The average visual clarity of the samples from site 1 is only 38% of that from site 2. The suspended solid concentration and turbidity of the site 1 samples are about 3 times that of the site 2 samples. During a rainfall episode, the visual clarity of the site 2 samples was nearly always lower and suspended solid concentration and turbidity were always higher than those of the site 2 samples. Figure 4.1 presents the visual clarity, suspended solid concentration, and turbidity of the samples collected from sites 1 and 2 during the rainfall episode of March 17, 1994.

The lower visual clarity for the site 1 samples could be attributed to much greater fine bark and soil material being available within the gravel surfaced wharf area. At the log handling area, the wharf ground is mechanically cleaned regularly for mitigating the potential contaminant source. However, the mechanical cleaning efficiency for the gravel surfaced area is lower than that for the sealed area, firstly because the gravel surfaced area is rougher than the sealed area, and secondly, there are more potholes around the gravel covered area than at the sealed area after a long period of log handling operation.

Table 4.1 The arithmetic average black disk visual clarity, suspended solid (SS) concentration, volatile suspended solid (VSS) concentration, and turbidity of the runoff samples from sites 1 - 6 at the Mount Maunganui wharf during seven storms from November, 1993 to July, 1995.

Sampling sites	Storm events (n)	Sample numbers (n)	Visual clarity (m)	SS (mg/l)	VSS (mg/l)	Turbidity (NTU)
Gravelled area (site 1)	3	23	0.009	1529	549	1038
Sealed area (site 2)	5	40	0.024	529	318	303
Northern outfall (site 3)	2	15	0.012	895	350	542
Southern outfall (site 4)	2	16	0.017	537	163	316
Southern outfall (site 5)	2	16	0.019	471	148	292
Adjacent urban area (site 6)	2	13	0.042	329	82	246

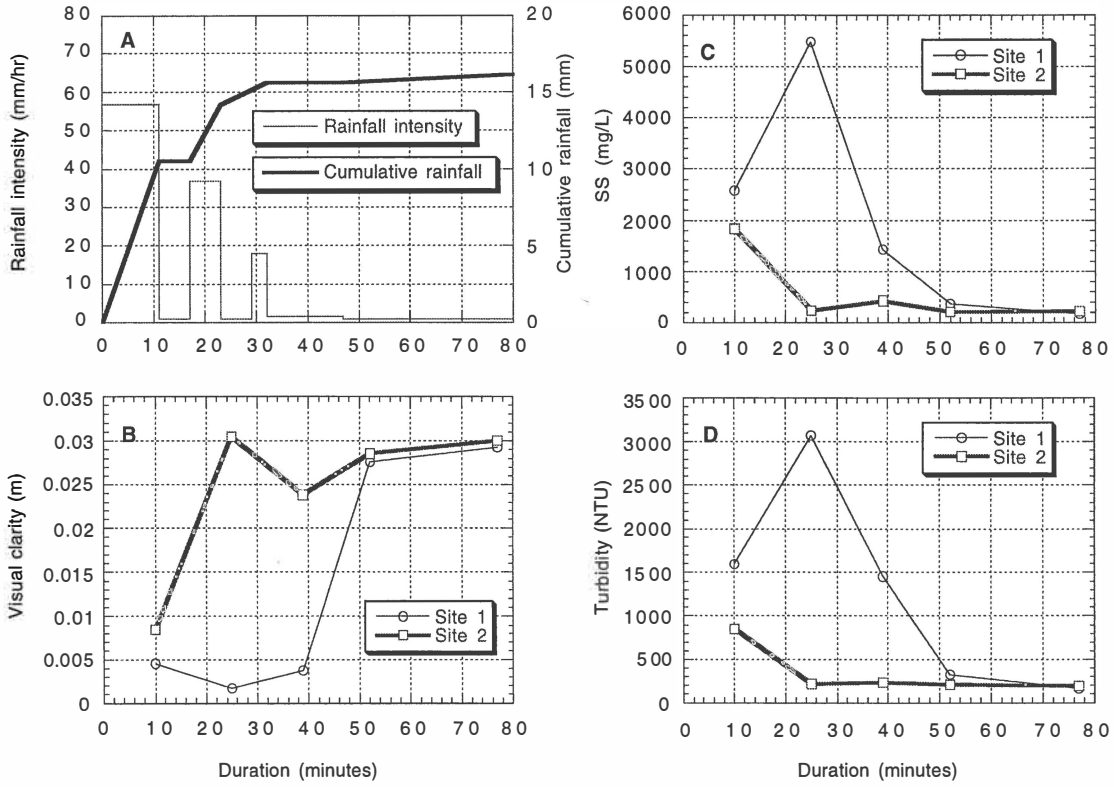

Figure 4.1 Black disk visual clarity (B), suspended solid concentration (C), and turbidity (D) of the runoff samples collected from the gravel surfaced (site 1) and sealed area (site 2) at Mount Maunganui wharf during the rainfall of March 17, 1994.

The samples collected at Site 3 came from both the sealed and gravel surfaced areas. The average visual clarity, suspended solid concentration and turbidity were between those values of site 1 and site 2 samples.

The adjacent urban runoff (site 6), which entered the southern wharf storm drainage system, had significant higher visual clarity values and lower suspended solid concentrations compared to those of the wharf runoff samples.

Because of the addition of the urban runoff, the runoff samples collected from the two outfalls of southern drainage system (sites 4 and 5) had higher visual clarity values and lower suspended solid concentrations than those of the site 3 samples .

Investigation of water quality in Tauranga Harbour from 1990 to 1991 showed that the average black disk visual clarity of 52 seawater samples from 4 sampling sites along the Mount Maunganui wharf was about 2.1 m (McIntosh, 1994).

From the *Guidelines for the Management of Water Colour and Clarity* (The Ministry for the Environment of New Zealand, 1994), the black disk visual clarity of receiving waters should not be changed by more than 20% for Class A waters (where visual clarity is an important characteristic of the water body) and 33% - 50% for other waters after reasonable mixing (depending on site conditions). As the receiving tidal water next to the wharf log handling area is a busy shipping channel and cannot be used for recreation, it is reasonable to consider the receiving water as "other water" in which the black disk visual clarity should not be changed by more than 33%-50%.

According to the "mass balance" equation (4.1), the dilution rates of the runoff from the wharf log handling area, which will meet the requirements from the Guidelines, can be calculated. The dilution rates which can meet the criteria for the runoff from the sealed area is 175 to 87. For the runoff

from the gravelled surfaces at present, the required dilution is higher. The Port company is planning to seal all the log handling areas at the Mount Maunganui wharves in the next few years.

4.2.3.2 Visual clarity and rainfall processes

Apart from the influence of the wharf surface pavement types, the rainfall intensity and cumulative rainfall also have a significant impact on visual clarity, suspended solid concentration, and turbidity of the runoff. Figure 4.2 presents these parameters of the runoff samples from the gravel surfaced (site 1) and sealed (site 2) areas during the storm of July 25, 1994, which was one of the heaviest rainfall events during the three year period of this investigation at Tauranga.

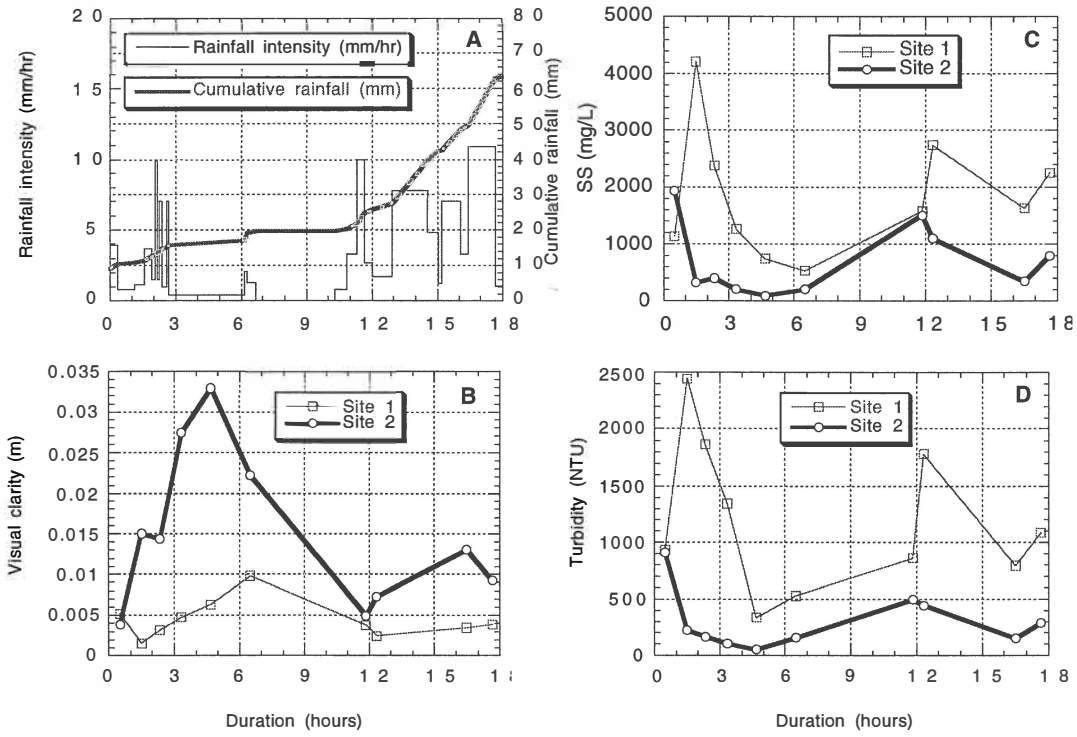

Figure 4.2 Black disk visual clarity (B), suspended solid concentration (C), and turbidity (D) of the runoff samples collected from the gravel surfaced area (site 1) and sealed area (site 2) at Mount Maunganui wharf during the rainfall event of July 25, 1994.

From Figure 4.2, it can be deduced that:

(i) As in Figure 4.1, the black disk visual clarity of the samples from gravelled area (site 1) was always lower than that from the sealed areas, and suspended solid concentration and turbidity were always higher.

(ii) When the cumulative rainfall increased from 9 mm to 18 mm (the 9 mm cumulative rainfall came from the rainfall which stopped a few hours previously), the visual clarity, suspended solid concentration and turbidity varied in the similar way shown in Figure 4.1, namely, visual clarity of the samples from both sites 1 and 2 became higher with increasing cumulative rainfall (suspended solid concentration and turbidity decreased).

Evidently the available fine particles which could be carried by the runoff at the log handling area had been washed away. However, when the rain restarted about 6 hours later, the visual clarity of the runoff from both sampling sites 1 and 2 dropped and suspended solid concentration rose again. Even after 50 mm rainfall, when the rainfall intensity increased, the visual clarity of site 1 samples dropped and the visual clarity of site 2 samples still remained at a considerably low level. The suspended solid concentration and turbidity of samples from both sites 1 and 2 increased again.

Many studies concerning different aspects of urban runoff quality were summarised by Ishaq and Khararjian (1988) who concluded that suspended solids are highly concentrated in the "first flush" at the commencement of urban runoff and the suspended solid concentration falls rapidly to quite low levels during the passage of a storm episode. Indeed, in this present study, the black disk visual clarity, suspended solid concentration, and turbidity of the adjacent urban runoff (site 6) showed a similar variation pattern (Figure 4.3). However, the results for wharf runoff presented in Figures 3 and 4 are different to the variation pattern of those parameters commonly obtained for the urban runoff. The variation of visual clarity and

suspended solid concentration after the peak values passed would depend on the consequent rainfall intensity and cumulative rainfall. If the consequent rainfall intensity remained at a similar level or decreased, the visual clarity of the runoff from both sites 1 and 2 would increase, and suspended solid concentration would decrease gradually. There would be only one "first flush" as shown in Figure 4.1. However, if the rainfall intensity significantly increased after the "first flush", the visual clarity might decrease and suspended solid concentration might increase again even after 50 mm of rainfall. It was more evident for the gravelled surfaced wharf area.

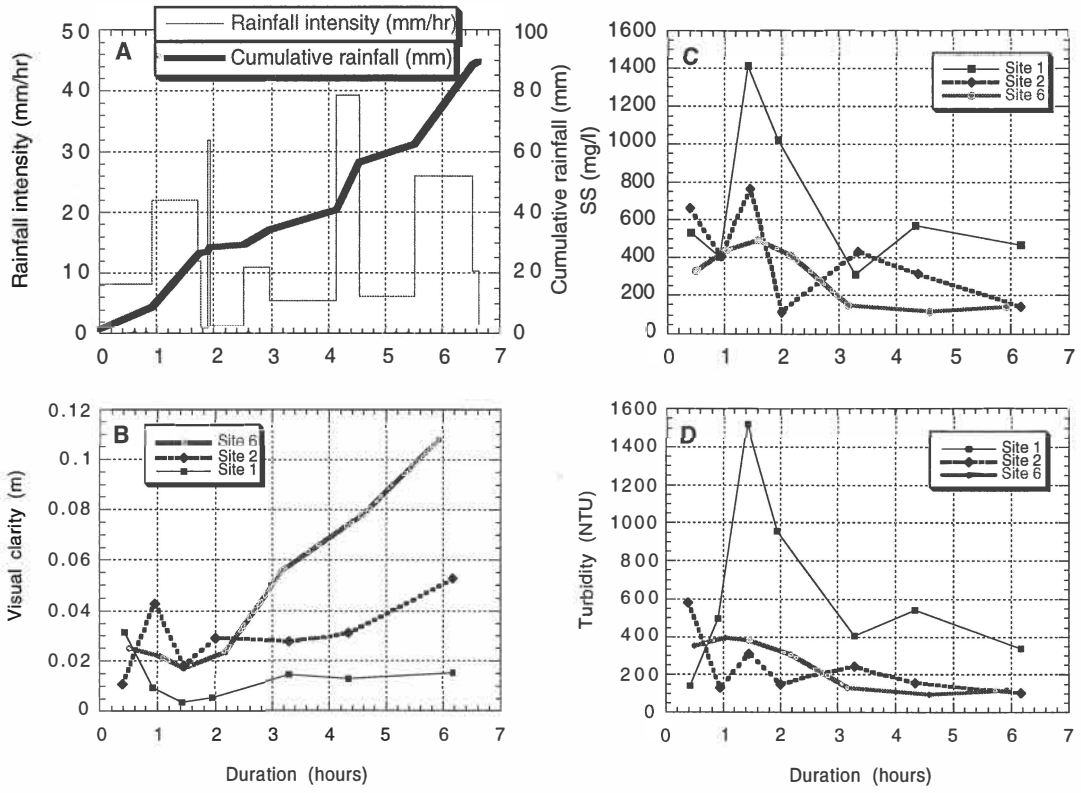

Figure 4.3 Black disk visual clarity (B), suspended solid concentration (C), and turbidity (D) of the runoff samples collected from the gravel covered area (site 1), sealed area (site 2), and urban area in the vicinity to the wharf (site 6) during the rainfall event of May 28, 1995.

The following factors are likely responsible for the difference between wharf runoff and common urban runoff.

i) The daily supply of fine bark and soil particles is great. This comes from the huge amounts of logs, about 6,000 tonnes per day, shifted around the log handling area at the Port of Tauranga. On average, 0.37 kg of bark and soil material with a particle size < 4.0 mm, which are easier to be carried by the runoff, were left on the wharf surface per cubic metre of logs shifted (see Chapter 7). This suggests that at least 2,200 kg of fine bark and soil material with particle size < 4.0 mm are left on the log handling area daily. During a rainfall episode the log handling continuously adds "fresh" bark and soil particles to the runoff.

ii) A considerable amount of fine bark and soil material accumulates around the log handling area. It is difficult to remove the bark and soil material thoroughly, especially for the gravel covered area due to the potholes. In some potholes, the accumulated bark and soil material are up to 10 cm.

iii) The release of the fine bark and soil material from the log stacking and bark piling sub-areas is slow. For example, when the rainfall intensity was not high, only the fine bark and soil material on the top layer of a bark pile could get into the runoff . Measurement during three storms in this study showed that only 35 - 50 cm of top bark layer of a bark pile got wet after 20 mm rainfall. Underneath this wet layer, the bark and soil material were still dry. After the fine bark and soil material in the top layer were washed off, less fine bark and soil material were available to enter the runoff if the rainfall intensity remained at a similar level or decreased. As a result, the visual clarity of the runoff would become higher gradually with increasing rainfall duration. However, when the rainfall intensity increased to a certain level at which the runoff produced by the rainfall could move some large piece of bark or surface flooding formed at the wharf log handling area, some fine bark and soil material in the underlayer could get into the runoff.

Therefore, the visual clarity of the runoff might decrease and the suspended solid concentration might increase again. As most of the fine bark and soil particles have been washed off at some sub-areas where have been mechanically cleaned, the runoff visual clarity in "second flush" was higher than that in the "first flush".

4.2.3.3 Visual clarity, suspended solid concentration and turbidity

Power relationships of black disk visual clarity against suspended solid concentration of the runoff samples from the 6 sites were identified (Figure 4.4).

As the sub-catchments were different for the 6 sampling sites, the coefficient, m, and power index, n, in the regression equation $y_{BD} = m\ SS^n$ [y_{BD} = black disk visual clarity (metre); SS = suspended solid concentration (mg/l); m = constant) were different.

From the regression equations shown in Figures 4.4, the same suspended solid concentration in the samples from the gravel surfaced area (site 1) always produces lower visual clarity than those in the samples from the sealed area (site 2). This is probably due to two reasons: the availability of (a) finer and (b) inorganic particles, in the runoff from the gravel surfaced wharf area.

Comparatively, there are more finer particles within the gravelled wharf area because the rougher surface in this area is harder to be cleaned mechanically. The average ratio of fixed suspended solids, which can be considered approximately as a measure of inorganic substance, to total suspended solids of the samples from the gravelled area (0.64) is significantly higher than that (0.40) of the samples from the sealed areas. According to Davies-Colley *et al.* (1993), inorganic substance with a particle size $< 2\ \mu$ has a stronger ability to attenuate light than organic substance.

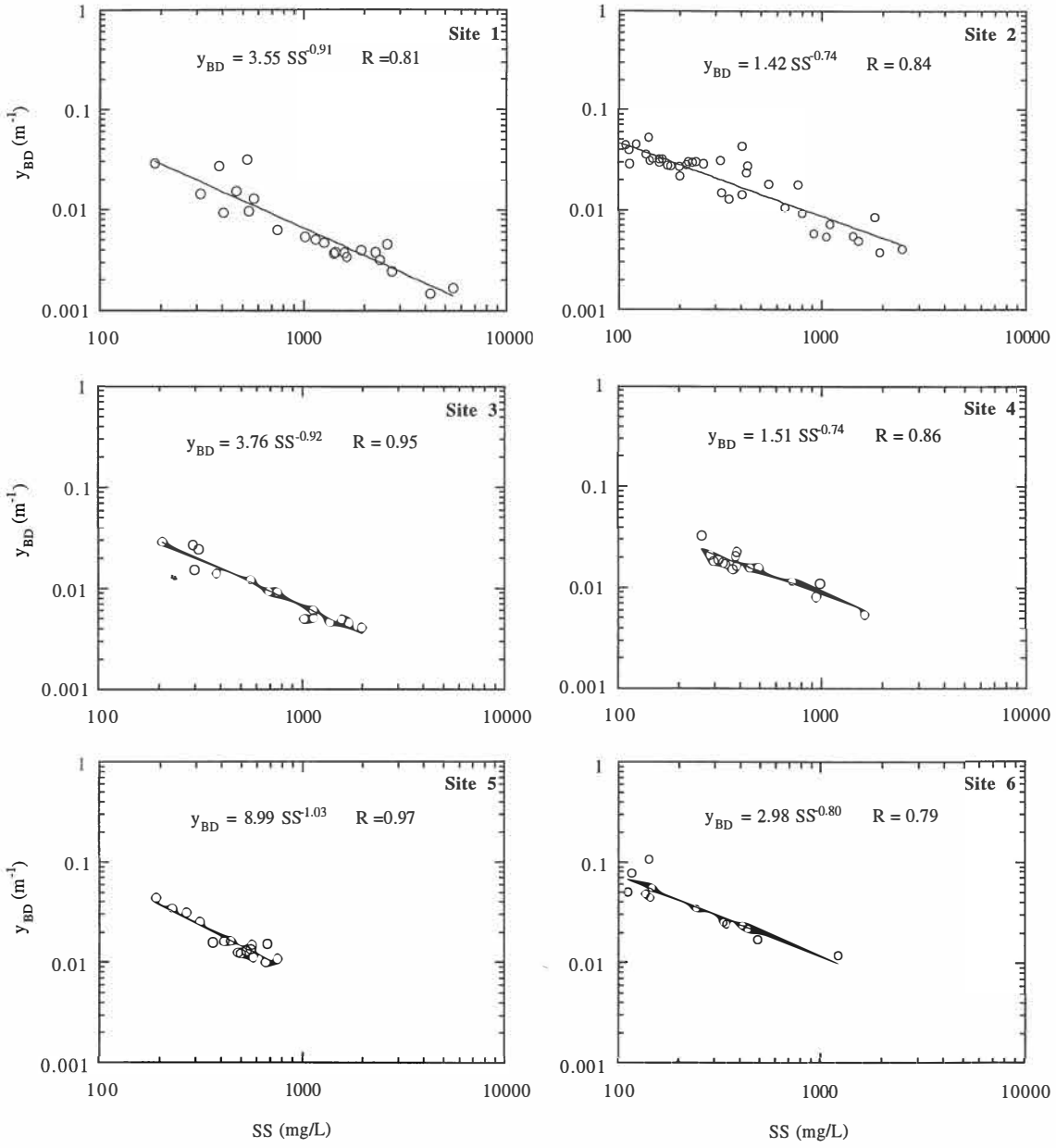

Figure 4.4 Relationships between black disk visual clarity (y_{BD}) and suspended solid (SS) concentration of the runoff samples collected from the 6 sampling sites during the seven storms from November, 1993 to July, 1995.

There are also power relationships of black disk visual clarity against turbidity of the runoff samples (Figure 4.5).

It is of significance to establish relationships of black disk visual clarity against suspended solid concentration and turbidity of the runoff. Black disk visual clarity can be estimated from historical records of suspended solid concentration or turbidity for the runoff from the log handling areas at a timber port or from log storage yards of paper mills.

4.2.3.4 Visual clarity and beam attenuation coefficient

Beam attenuation coefficient, c (m^{-1}), at 555 nm, which is the peak sensitivity of the human being eye, of 35 typical wharf runoff samples with visual clarity ranging from 0.002 to 0.053 m, and 13 adjacent urban runoff samples with visual clarity varying from 0.012 to 0.108 m, were determined (see Section 4.4). Based on the measured beam attenuation coefficient, the dimensionless proportional factor, ψ, in equation $c = \psi/y_{BD}$ was calculated for these samples. The average value of ψ for the wharf and adjacent urban runoff samples was 4.67 (standard deviation = 0.90) and 4.23 (standard deviation = 0.69). It is similar to the average ψ value (4.8) obtained through investigation of y_{BD} and c on diverse New Zealand lake and river waters (Davies-Colley, 1988). This result suggests that the beam attenuation coefficient, c, of the storm runoff from the log handling areas can be obtained through simply measuring the black disk visual clarity though the runoff has a much shorter visual range than most of the natural waters.

A slight but significant trend in which ψ slightly decreased (log-linear) with increasing visual range of the water samples because the angle subtended by the disk at the eye decreased with increased visual range was noted by Davies-Colley (1988). However, no such trend was found in this study probably because that the angle subtended by the disk at the eye did not vary greatly for the samples with different visual ranges because different

dilution rates were used to make the visual range of the mixers similar (Figure 4.6).

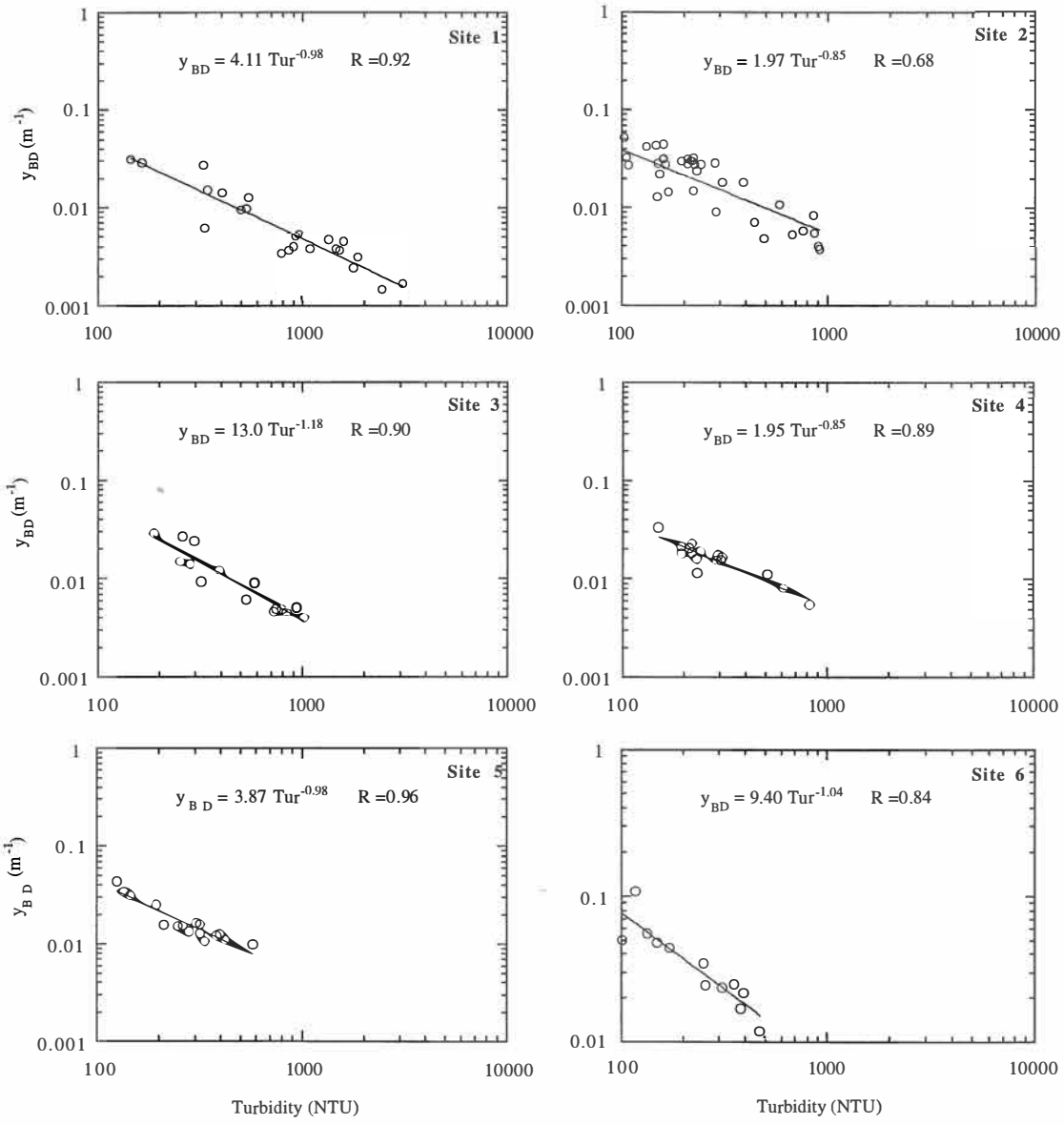

Figure 4.5 Relationships between black disk visual clarity (y_{BD}) and turbidity of the runoff samples from the 6 sampling sites during the seven storms in November, 1993 - July, 1995.

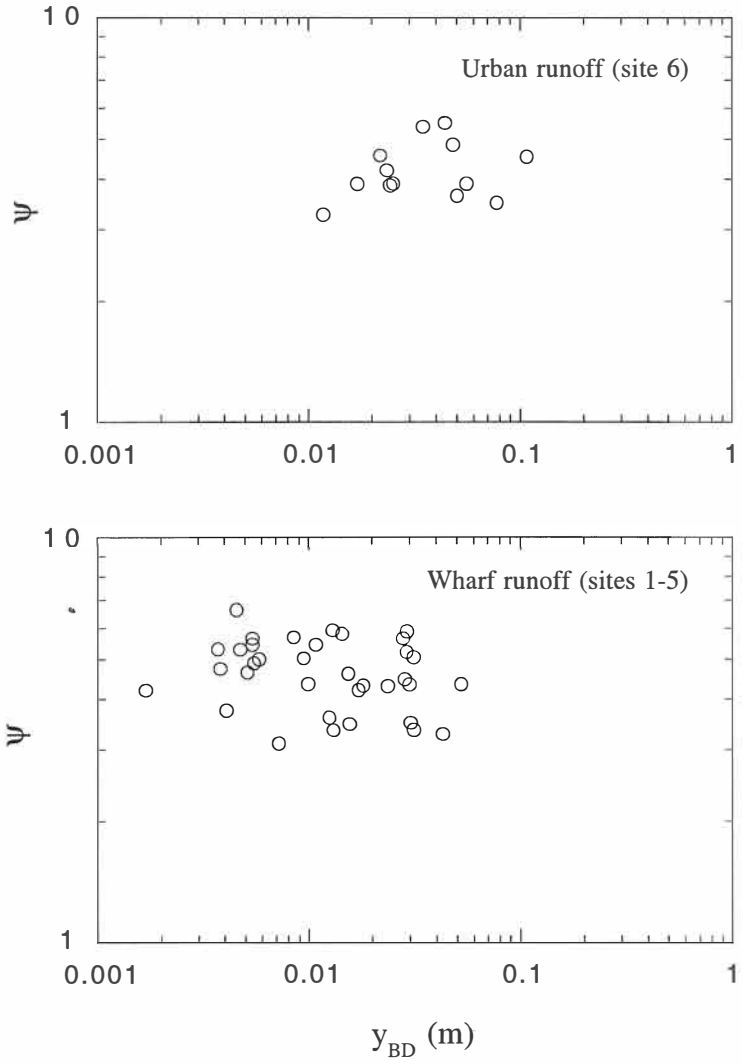

Figure 4.6 Black disk visual clarity (y_{BD}), plotted against the dimensional proportional factor, y, in $c = \psi / y_{BD}$, of the 13 runoff samples collected from the urban area in the wharf vicinity (site 6) and the 35 wharf runoff samples taken from sites 1 - 5 at Mount Maunganui wharf from March, 1994 to May, 1995.

4.2.4 Conclusions

1 A simple short trough can be used for off-site measurement of black disk visual clarity of storm runoff samples from the log handling areas. As only a small volume of samples is required (dilution is needed before measurement), it is convenient for investigating the variation of visual clarity of the runoff during a storm episode.

2 The storm runoff from the gravelled and sealed wharf log handling areas at the Port of Tauranga, with a suspended solid concentration from 96 mg/l to 5480 mg/l, had a black disk visual clarity ranging from 0.05 m to 0.002 m, with a mean value of 0.019 m.

3 The wharf surface pavement types have a significant influence on black disk visual clarity of the storm runoff. The visual clarity of the runoff samples from the gravel surfaced area is only 38% of that from the sealed wharf area. This might be attributed to accumulations of fine bark and soil material within the gravelled area, because of the lower mechanical cleaning efficiency and potholes.

4 Unlike the common urban runoff, the variation pattern concerning black disk visual clarity, suspended solids, and turbidity during a storm depended on the rainfall history. There might be second or more "flushes" concerning visual clarity, suspended solids and turbidity of the runoff during a storm episode.

5. Power relationships of black disk visual clarity against suspended solid concentration and turbidity of the runoff from the log handling area were identified. Based on these relationships, the black disk visual clarity can be derived from the historical records of suspended solid concentration or turbidity for the runoff from the log handling area at a timber port or from the log storage yard of a paper mill

6. The relationship between black disk visual clarity, y_{BD}, and beam attenuation coefficient, c, of the wharf runoff, is ascertained as: $c = 4.67/y_{BD}$.

4.3 COLOUR

4.3.1 Introduction

Like visual clarity, the *colour* of water is another important optical property of natural waters and also has impact on aesthetics and aquatic life. It seems blue and green are the proper colours of unpolluted natural waters and they are aesthetically attractive (Wilcock *et al.*, 1983). Other colours (technically "*hues*"), for example, yellow or brown, visually imply contamination of a water body to some extent. Significant colour change of a water body will substantially decrease its recreation value and will have potential adverse impacts on aquatic habitats. For example, the spectral sensitivity of some fish's eyes is well-matched to the colour of their typical aquatic living environment (Lythgoe, 1979) and these fish are sensitive to colour change of their underwater illumination.

Although the colour of water is of great importance, little attention has been paid to the colour of storm runoff in previous studies. Makepeace *et al.*, (1995) summarised 140 articles containing water quality analysis of urban storm water through the use of international computer databases and environmental bibliographies. None of these papers quantified the colour of storm water. Among the few previous investigations on water quality of storm runoff from log handling areas at a timber port, or log storage yards from pulp and paper mills (Kingett Mitchell and Associates, 1993; Tian *et al.*, 1995 and NCASI, 1992), none of these studies paid enough attention to water colour although the storm runoff is usually highly discoloured. An investigation on light absorption by soluble yellow substance in the runoff from the log handling area at the Sulphur Point wharf, Tauranga, New Zealand, was conducted by Tian *et al.* (1994), but the study focused only on

light absorption spectral properties of yellow substance. Accordingly, a comprehensive investigation of the storm runoff colour from the log handling area at Mount Maunganui wharf was undertaken as part of the entire investigation, including:

1) measurement of apparent colour of the runoff samples using Munsell colour charts;

2) yellow substance (taking light absorption coefficient at 440 nm wavelength, g_{440}, as an index) in the runoff samples; and

3) the main factors affecting the apparent colour and yellow substance of the runoff, such as wharf surface pavement types, black disk visual clarity, ratios of volatile suspended solids to total suspended solids, and rainfall processes.

4.3.2 Research background and rationale

Water colour refers to the light emanating from within the water volume due to the scattering process. *Guidelines for the Management of Water Colour and Clarity* (Ministry for the Environment of New Zealand, 1994) defines water colour as: "the perception of light backscattered from within the water mass as observed when viewing downwards at a near-vertical angle".

The colour of water can be divided into two categories: true colour and apparent colour. The former is “the colour of water from which turbidity has been removed” and the latter “includes not only colour due to substances in solution, but also that due to suspended matter” (APHA *et al.*, 1992). When the concentration of suspended solids or phytoplankton in a water body is significantly high, there will be an appreciable difference between apparent and true colour. In this study, both apparent colour and

yellow substance, which is responsible for imparting the true yellow colour, of the runoff samples were determined.

It is evidently significant to investigate the apparent colour of the storm runoff because it reflects the real appearance of the runoff and has a direct visual impact on receiving water. But why is it also necessary to investigate the yellow substance in the runoff samples?

For most natural waters, the true colour appears yellow to brown because of the existence of "yellow substance". Yellow substance, the filter-passing organic substance known as "aquatic humus" (Thurman, 1985), "Gelbstoff" (Kalle, 1938, cited by Bricaud *et al.*, 1981) or "Gilvin" (Kirk, 1976), is the only single category of components responsible for imparting the true yellow colour of water (Kirk, 1983) and is typically the largest single category of components of the dissolved organic carbon (DOC) in natural waters. There is an overall correlation of DOC and light absorption (Moore, 1985 and Grieve, 1985). As yellow substance amounts to direct competition with phytoplankton for capture of photosynthetically available radiation and also changes the colour of natural waters by shifting the energy of maximum transmission to longer wavelengths, it is of great interest to determine the yellow substance of a water sample. For the storm runoff samples from a timber wharf, they showed yellow after the suspended substance was removed with a membrane, no matter what colour the samples appeared before filtration. The concentration of yellow substance in the wharf runoff was fairly high (Tian *et al.*, 1994). The storm runoff will still have a potential environmental impact to the receiving aquatic environment even though the suspended solids in the runoff are removed. Therefore, it is of significance to investigate the yellow substance in the runoff.

The *Standard Methods for the Examination of Water and Wastewater* does not offer an effective method to determine the apparent colour although it suggests making such measurements for highly coloured industrial or other wastewaters (APHA, 1992).

The Munsell standard colour chart was used to describe the apparent colour of some New Zealand lake and river waters by Davies-Colley *et al.* (1988 and 1990). It was found that this method was convenient and the water hues matched to Munsell standard colour chart agreed well with the spectrophotometric measurements of the water colour.

The Munsell colour system has three attributes known as *hue* (symbol H), *value* (V) and *chroma* (C) (Anon., 1954). The *hue* notation of a colour refers to its relation to yellow, green and red and are arranged on a closed circle divided into 100 *hue* units. The Munsell *hue* can be described either as a number from 0 - 100 or a number less than 10 plus one or two capital letters (the letters are the first letters of the words for the colours, for example, R for red and Y for yellow). The Munsell *value* indicates the apparent brightness of a colour and ranges from 0 (black) to 10 (white). The Munsell *chroma* relates to colour saturation and ranges from 0 (neutral grey) to 10 for most saturated colours. For a given colour, a notation in the form of H V/C is used to describe it. Unlike the chloro-platinate standard colour solution, Munsell standard colour charts are available in a convenient book.
For the filtered wharf runoff samples, it seems much simpler to determine yellow substance concentration of the runoff than to determine the dominant wavelength, purity, and saturation recommended by the *Standard Handbook for the Examination of Water and Wastewater* (APHA, 1992) for determining the true colour.

4.3.3 Methods

4.3.3.1 Apparent colour

Four litres of samples, which were enough to ensure no background reflection could penetrate to the viewer through the samples, were placed into a beaker and compared to the Munsell colour charts. The samples were viewed horizontally from the side. According to the definition of colour, the observers should view the samples and the Munsell colour charts

downwards at a near-vertical angle. However, this made the colour comparison difficult because some foam were always on the surface of the samples.

Special attention was paid to the colour comparison. Two independent observers undertook the colour comparison, and results showed no appreciable difference between the two observers. The results presented in this section are the average from the two observers. In addition, the colour comparison was made out of the direct sunlight to minimise the reflection from the glass wall of the beaker.

4.3.3.2 Yellow substance

A Pye-Unicam PU8800 spectrophotometer was used to determine light absorption coefficient at 440 nm, g_{440} (units: m^{-1}), as an index of yellow substance concentration. The determination of g_{440} is shown in Section 4.4.

4.3.4 Results and discussion

4.3.4.1 Apparent colour

Munsell hue

The Munsell *hue* was the same for most of the runoff samples including those from the adjacent urban area (site 6) although the black disk visual clarity of these samples varied greatly (Table 4.2). Among the 123 samples examined, 87% of the samples classified as 20 (10YR) in Munsell *hue* scale, 8.1% as 18.8 [8.8YR, the average of 17.5 (7.5YR) and 20 (10YR) from the two observers], and 4.9% as 17.5 (7.5YR). This differs to the Munsell *hues* of 92 New Zealand rivers under baseflow conditions (Davies-Colley and Close, 1990). There was a weak (r=0.38), but highly significant ($p<<0.0001$) linear relationship between Munsell *hue* and black disk visual clarity of the river waters. As clarity increased from low values of a few 100 mm towards high

values around 10 m or more, there was a tendency for Munsell *hue* to change from orange or yellow towards blue-green or blue. Two factors are believed responsible for the difference of Munsell *hues* of the river waters and the storm runoff samples in this present study. Firstly, there was a significant difference of visual clarity between the river waters and the wharf runoff samples. The visual clarity of the wharf runoff (0.002 m to 0.05 m) was substantially lower than that of the river waters. Secondly, there is likely a diverse composition of suspended solids in the river waters due to the different river catchments, whereas the composition of suspended solids in the wharf runoff was relatively simple.

Munsell value

Figure 4.7 shows the Munsell *value* of the runoff samples from each site plotted against the black disk visual clarity. The relationships for these two parameters are slightly scattered. However, as a first approach, linear regressions were fit.

Munsell *value* indicates the apparent brightness of the water colour and depends on the reflectance coefficient, the ratio of upwelling to downwelling light in the water. Within the runoff samples with lower black disk visual clarity, as there are more fine particles in these samples, the path length for the backwards scattered light to reach the water surface is increased due to multiple scattering. Therefore, the opportunity for the photons being absorbed by either soluble or particulate matter is increased. As a result, the ratio of upwelling to downwelling light at the water surface decreases, thus these samples have lower Munsell *values*. In contrast, within the samples with higher black disk visual clarity, the path length for the backwards scattered light to reach the water surface is shorter due to less suspended solids, thus there is less chance for the photons to be absorbed. The ratio of upwelling to downwelling light at the water surface is higher, hence the Munsell *value* is higher.

Table 4.2 Arithmetic mean Munsell *hue*, *value*, *chroma*, and other relevant parameters of the runoff samples collected from the 6 sampling sites at the Port of Tauranga during the seven storms from November, 1993 to July, 1995. site 1: gravel surfaced; site 2: sealed; site 3: outfall of the northern drainage system; sites 4 and 5: the outfalls of the southern drainage system; and site 6: the urban area in the vicinity of the wharf.

Sites	1	2	3	4	5	6
Sample number (n)	23	40	15	16	16	13
Munsell *hue*	19.7	18.2	19.8	20	17.9	20
Munsell *value*	3.3	4.2	3.2	3.8	4.1	4.9
Munsell *chroma*	2.4	3.5	2.3	2.1	2.2	2.4
yBD (m)	0.009	0.024	0.012	0.017	0.019	0.042
SS (mg/l)	1529	529	895	537	471	329
VSS/SS	0.36	0.60	0.39	0.30	0.31	0.25

Munsell chroma

The average Munsell *chroma* of the runoff samples from site 1 and sites 3-6 was similar (2.1-2.4), and was appreciably lower than that of the site 2 samples (3.5).

Within the runoff samples from each site, only the Munsell *chroma* of the site 2 samples increased significantly with black disk visual clarity (Figure 4.8). For the sites 3-6 samples, the Munsell *chroma* basically remained independence of visual clarity.

Munsell *chroma* is the measurement of the energy distribution of the backwards scattered light and the energy distribution depends on the composition of the suspended solids when the mass concentration and particle size distribution remain the same or similar. From Table 4.1, the ratio of volatile suspended solids to total suspended solids (VSS/SS) of the site 2 samples (0.60) is significantly higher than those of the other site samples (0.25 - 0.39). Most of volatile suspended solids in the wharf runoff possibly consist of fine bark particles. As the composition of suspended

solids in the site 2 sample is relatively "pure", the backwards scattered light from within the site 2 samples have a narrow energy distribution.

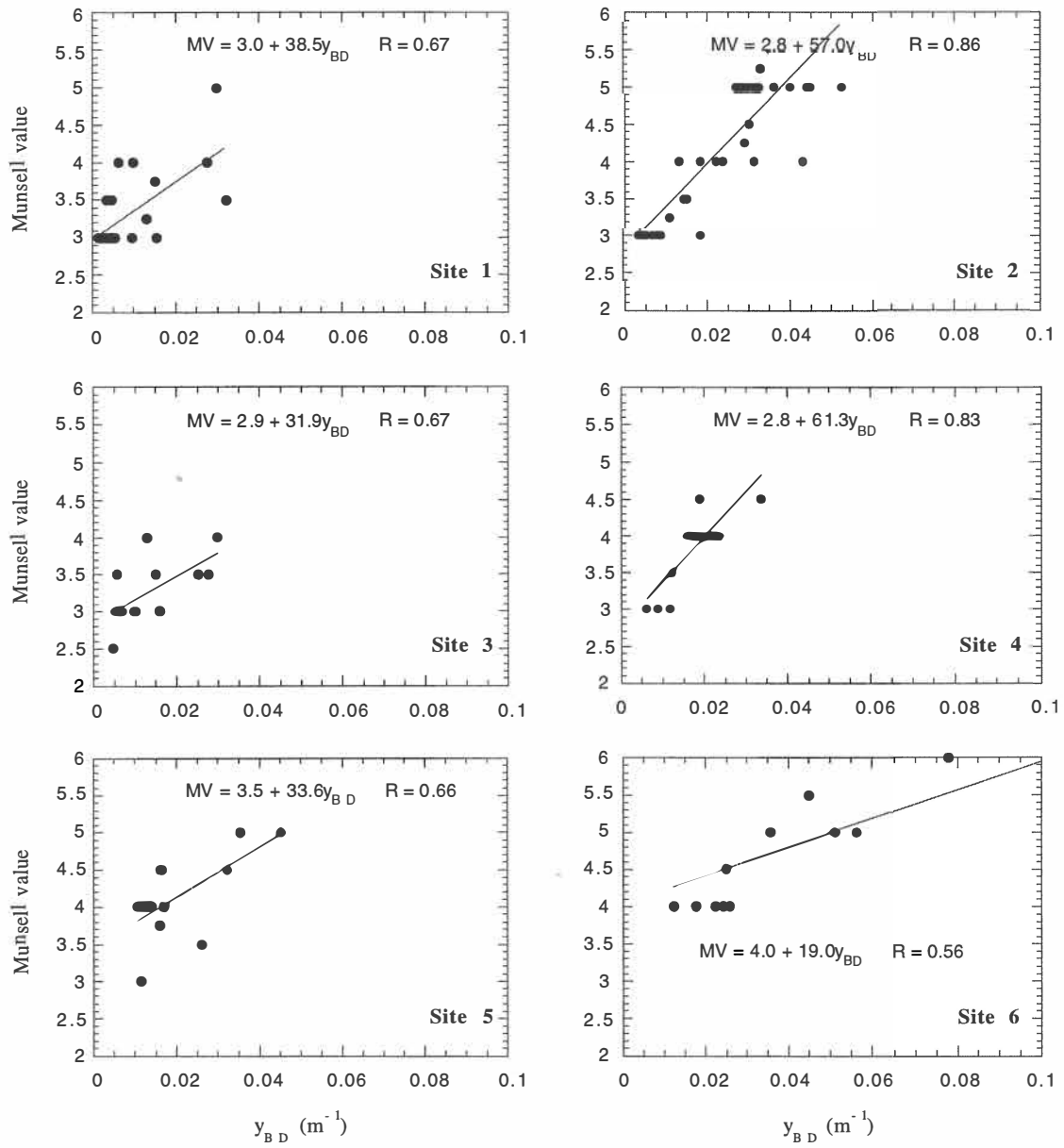

Figure 4.7 Munsell *value* (MV) plotted against black disk visual clarity (y_{BD}) of the runoff samples collected from the six sampling sites around the Mount Maunganui wharf and at the adjacent urban area during the seven storm events from November, 1993 to July, 1995.

The VSS/SS ratios of the site 2 samples slightly increased with visual clarity (Figure 4.9). The samples with higher visual clarity had higher VSS/SS ratios. The suspended solids of these samples were "purer", thus a narrower energy distribution of the backwards scattered light was observed. This might explain why the Munsell *chroma* of the site 2 samples increased significantly with increasing visual clarity. In contrast, the site 3-6 samples had lower VSS/SS ratios (0.25 - 0.39). That means most of suspended solids are inorganic particles which may consist of different constituents. Accordingly, the backwards scattered light from within these samples had a wide energy distribution (lower Munsell chroma). As the VSS/SS ratios of the site 3-6 samples were basically independence of visual clarity, the Munsell *chroma* did not vary with visual clarity.

Figure 4.10 shows the variation of Munsell *value* and *chroma* of the samples from the gravel surfaced (site 1) and sealed (site 2) areas, the main two wharf pavement types around the log handling area, during the storm on July 25, 1994. Evidently, the Munsell *value* and Munsell *chroma* of the site 2 samples varied greater than that of site 1 samples and the variation was basically in accord with that of visual clarity and VSS/SS ratio of the samples during the storm.

4.3.4.2 Yellow substance

Overall yellow substance concentration

The runoff samples from the wharf log handling area had considerably higher average yellow substance concentrations, 26.70 m^{-1} for site 1, 23.24 m^{-1} for site 2, and 25.03 m^{-1} for site 3, compared to that, 1.77 m^{-1}, of the adjacent urban runoff from site 6 (Table 4.3). Due to the addition of the urban runoff, runoff samples collected at sites 4 and 5 were "diluted", with average yellow substance concentrations of 5.0 m^{-1} for site 4 and 5.65 m^{-1} for site 5.

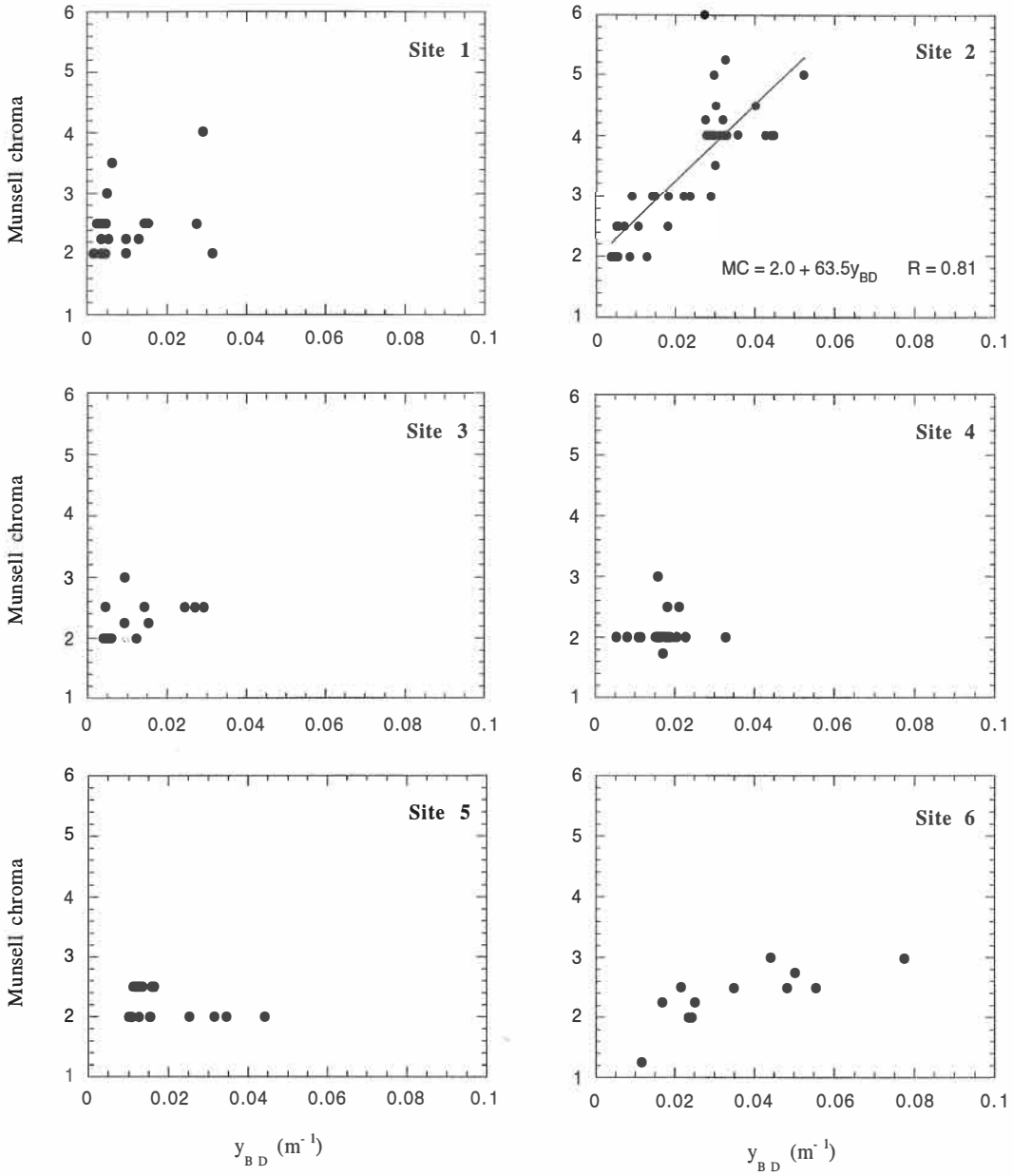

Figure 4.8 The relationships between Munsell *chroma* (MC) and black disk visual clarity (y_{BD}) of the runoff samples collected from the six sampling sites around the Mount Maunganui wharf and at the adjacent urban area during the seven storm events from November, 1993 to July, 1995.

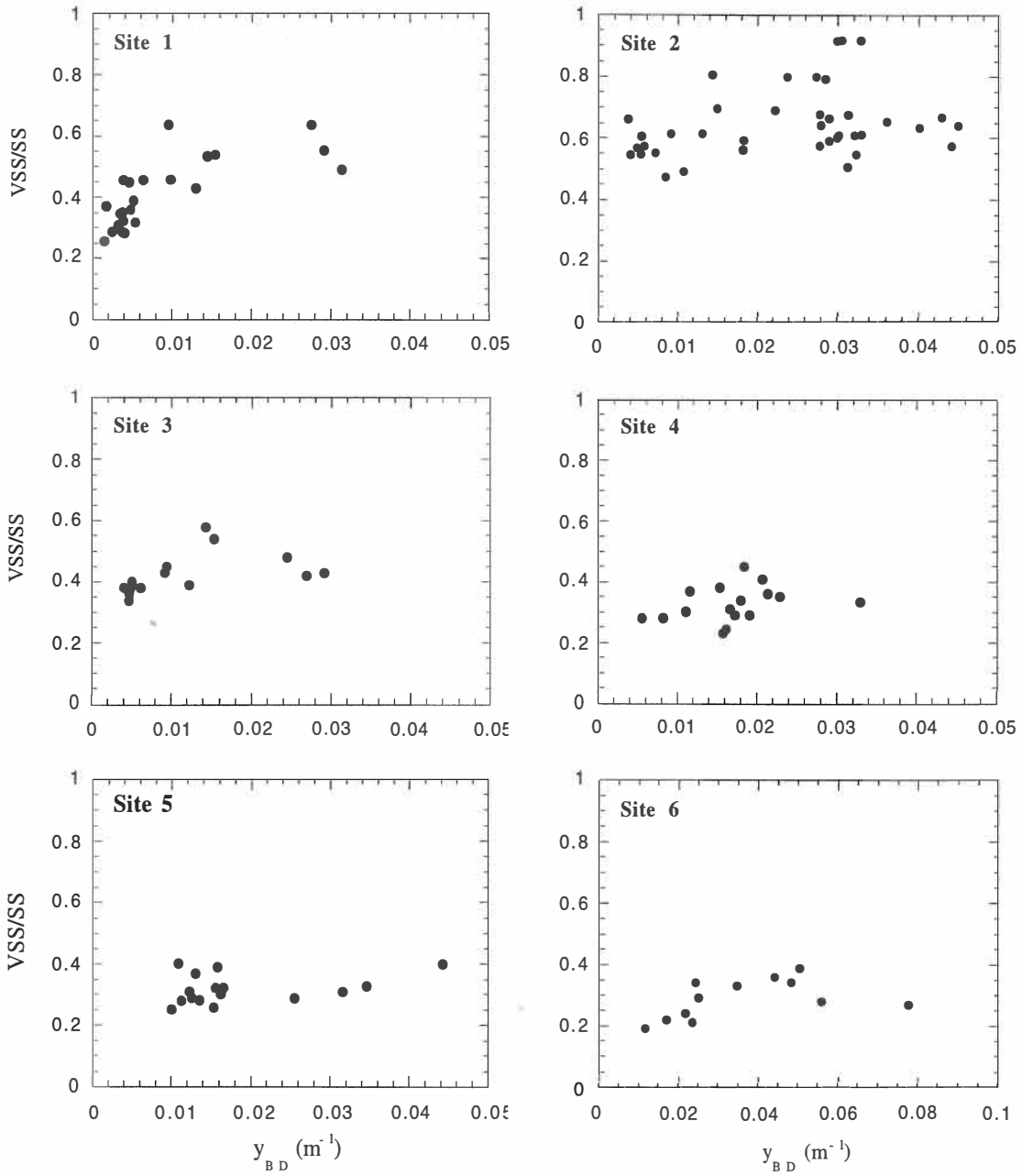

Figure 4.9 The ratios of volatile suspended solids to total suspended solids (VSS/SS) against black disk visual clarity (y_{BD}) of the runoff samples from the six sampling sites around the Mount Maunganui wharf and at the adjacent urban area during the seven storm events from November, 1993 to July, 1995.

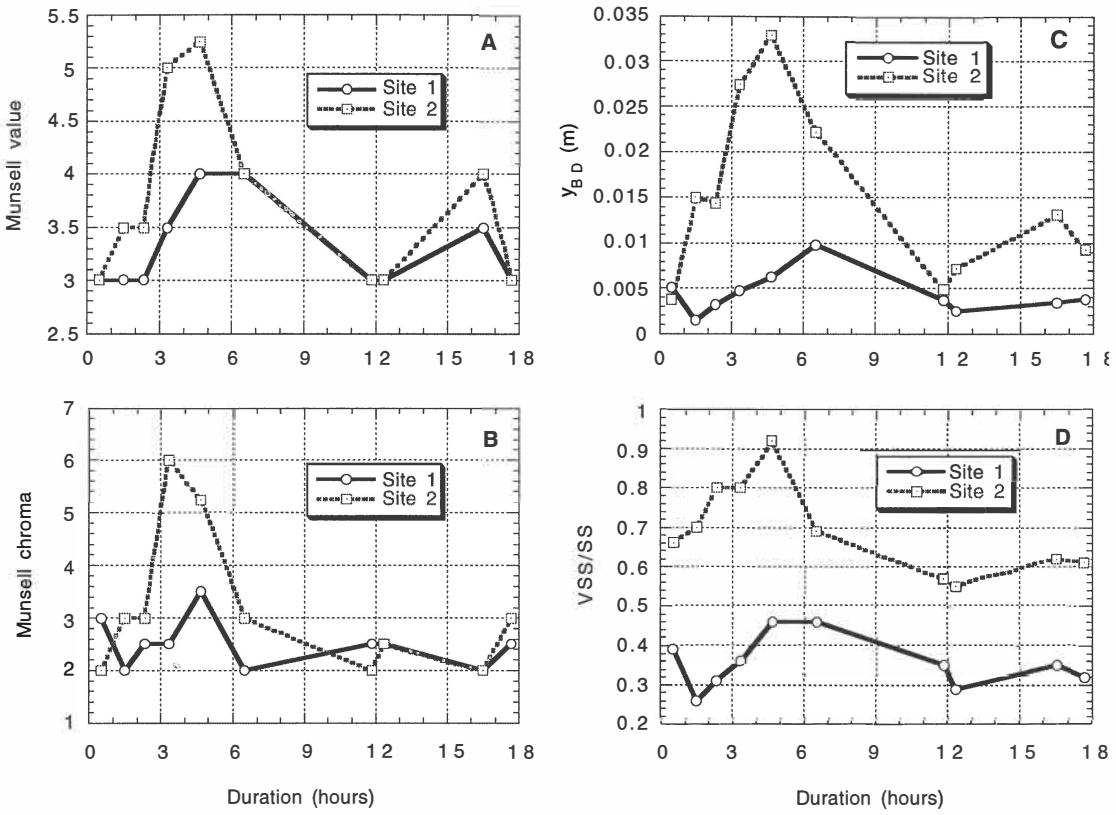

Figure 4.10 Munsell *value* (A), *chroma* (B), black disk visual clarity (y_{BD}, C) and ratios of volatile suspended solids to total suspended solids (VSS/SS, D) of the runoff samples taken from gravelled (site 1) and sealed (site 2) areas at the Port of Tauranga during the storm episode of July 25, 1994.

Table 4.3 The range (minimum and maximum), arithmetic mean, and coefficient of variation of suspended solids (SS), black disk visual clarity (y_{BD}), and yellow substance concentration (g440) of the runoff samples from the 6 sampling sites during the 7 storms examined from November, 1993 to July 1995. Storm 1: November 11, 1993; Storm 2: March 17, 1994; Storm 3: May 24, 1994; Storm 4: June 21, 1994; Storm 5: July 25, 1994; Storm 6: May 28, 1995; and Storm 7: July 12, 1995. site 1: gravel surfaced; site 2: sealed; site 3: outfall of the northern drainage system; sites 4 and 5: the outfalls of the southern drainage system; and site 6: the urban area in the vicinity of the wharf.

	SS			y_{BD}			g440		
	Range (mg/l)	Mean (mg/l)	C.V. (%)	Range (m)	Mean (m)	C.V. (%)	Range (m^{-1})	Mean (m^{-1})	C.V. (%)
Site 1	185-5480	1529	85.7	0.002-0.032	0.009	100.0	10.4-43.5	26.7	30.6
Storm 2	185-5480	2012	107.4	0.002-0.030	0.013	103.0	19.3-43.5	30.3	33.6
Storm 5	535-4210	1849	59.1	0.002-0.010	0.004	52.3	15.7-32.5	25.0	20.0
Storm 6	310-1410	672	58.9	0.004-0.032	0.013	69.2	10.4-42.6	26.6	41.7
Site 2	96-2464	529	109.3	0.004-0.053	0.024	54.2	8.8-50.0	23.2	45.1
Storm 1	108-548	188	59.0	0.018-0.045	0.033	21.4	8.8-25.6	17.9	29.7
Storm 2	215-1840	590	119.3	0.009-0.031	0.024	37.9	26.5-50.0	39.2	23.2
Storm 3	912-2464	1461	48.0	0.004-0.006	0.005	14.4	30.9-35.0	32.5	5.5
Storm 5	96-1940	691	91.2	0.004-0.033	0.015	66.7	11.5-26.7	18.0	28.9
Storm 6	113-765	404	60.4	0.011-0.053	0.030	46.7	9.9-44.2	24.9	52.4
Site 3	206-1980	895	64.4	0.004-0.029	0.012	72.5	20.3-31.6	25.0	11.0
Storm 4	206-1980	734	84.9	0.004-0.029	0.016	67.3	20.3-26.0	23.7	10.5
Storm 5	295-1705	1037	51.2	0.005-0.015	0.008	54.3	23.3-31.6	26.2	9.6
Site 4	258-1645	537	69.5	0.011-0.044	0.017	35.3	2.5-7.3	5.0	26.8
Storm 4	284-446	346	15.3	0.015-0.021	0.018	11.3	3.5-6.9	4.7	24.3
Storm 5	258-1645	728	63.0	0.006-0.033	0.016	50.2	2.5-7.3	5.3	28.8
Site 5	190-760	471	35.2	0.010-0.044	0.019	52.6	3.5-7.1	5.7	21.1
Storm 4	364-664	497	19.1	0.010-0.017	0.013	17.9	3.5-7.1	5.6	22.4
Storm 5	190-760	446	49.6	0.011-0.044	0.024	50.2	3.7-7.1	5.7	21.3
Site 6	112-1216	329	90.1	0.012-0.108	0.042	64.3	1.4-2.3	1.8	16.4
Storm 6	117-490	296	53.4	0.017-0.108	0.047	74.5	1.4-2.3	1.9	15.2
Storm 7	112-1216	366	116.1	0.012-0.051	0.036	56.4	1.4-1.8	1.6	13.0

Compared to the yellow substance of a considerable number of inland and marine waters summarised by Kirk (1983), the yellow substance concentration of the wharf runoff samples was fairly high.

The average yellow substance concentration of 35 seawater samples from the Tauranga Harbour collected at different water depths and different tide conditions was 0.21 m^{-1} (Tian *et al.*, 1995), less than 1% of those in the wharf runoff samples.

From Tian *et al.* (1995), the average yellow substance concentration in the runoff from the log handling area at the Sulphur Point wharf, Tauranga, was 17.9 m^{-1}, about 70 % of the Mount Maunganui wharf samples. In explanation, the Mount Maunganui wharf has been used for log exporting for many years and there are numerous potholes at the log handling area due to the long term effects of the log operation, especially at the gravel surfaced area. As it is difficult to mechanically clean these potholes, some broken bark fragments may have been present within these potholes for a considerable period. In contrast, the Sulphur Point wharf had been used for log handling for only one month when sampled in the previous study (Tian *et al.*, 1994) and there were no potholes on the well sealed wharf surface. The mechanical cleaning efficiency of the wharf surface was higher at the Sulphur Point wharf. Therefore, the bark left on the Sulphur Point wharf surface was much "fresher" than that on Mount Maunganui wharf. According to Kirk (1983), the humic material is formed in the course of plant tissue decomposition. It comes from either oxidation and polymerisation directly from the existing phenolic compounds (particularly lignin) in the decomposing plant tissue, or from the phenolic substance excreted by some saprophytic fungi when grown on carbohydrate. No matter how the humic material is formed, a certain period is needed for the oxidation and polymerisation. More humic substance is likely formed due to longer presence of bark at the wharf surface. Accordingly, the yellow substance concentration in the Mount Maunganui wharf samples is higher.

Yellow substance and wharf pavement types

Wharf pavement types had a significant influence on black disk visual clarity and suspended solids of the runoff samples. For instance, the average visual clarity of the runoff samples from the gravel surfaced area (site 1) was only 38% of that from the sealed area (site 2). However, the yellow substance concentration of the site 1 samples (26.7 m^{-1}) was only slightly higher than that of the site 2 samples (23.2 m^{-1}). This suggests that the yellow substance concentration was basically independent of black disk visual clarity, and no significant relationships between these two parameters were found (Figure 4.11).

Although yellow substance is the middle products in the course of plant tissue decomposition (Kirk, 1983), no significant relationships between yellow substance and volatile suspended solids, which is an approximate measurement of organic substance, were found for the runoff samples from all the sampling sites (Figure 4.12).

Variation of yellow substance during storms

Table 4.3 presents the ranges, mean, and coefficient of variation (C.V.) of suspended solids, black disk visual clarity, and yellow substance concentration of the runoff samples from each site during the storms sampled.

Coefficients of variation (CV) for SS and yellow substance can be used to compare the variation of these two parameters during a storm and from storm to storm. From Table 4.3, the yellow substance concentration did not vary as greatly as suspended solids during most of the storm events. For example, during storm 2, the CV value of suspended solid concentration of the site 1 samples is 107%. However, the CV value of yellow substance is only 33.6%. This trend was more evident for the site 3 samples which contain runoff from both gravel surfaced and sealed areas. For example,

during storm 4, the CV value for suspended solid concentration of the site 3 samples is 84.9%. However, the CV value for yellow substance is 10.5%. Figure 4.13 illustrates typical variation of yellow substance, suspended solids and visual clarity of the samples from sites 1-5 during the rainfall of July 25, 1994.

The average yellow substance concentration did not vary as greatly as average suspended solid concentration from storm to storm. For site 1 samples the CV values for suspended solid concentration ranged 59% to 107%, with a mean CV of 85.7% during the three storms examined, whereas the CV values for yellow substance concentration ranged only from 20.0% to 41.2%, with a mean of 30.6% during the same three storms. Likewise, the CV values for average suspended solid concentration of the site 3 samples were 51.2% and 84.9% during the 2 storms examined, but the CV values for average yellow substance concentration were only 9.6% and 10.5% during the same two storm events.

It is of significance that the yellow substance concentration in the wharf runoff was considerably higher than that of the receiving tidal water and adjacent urban runoff, and remained relatively stable compared to suspended solids and visual clarity during a storm episode and from storm to storm.

As will be discussed in Section 6.1.3, there is a close relationship between BOD and yellow substance. That means yellow substance is chemically active. However, as the water samples were stored chilled in the dark and analysed within 48 hours after collection, the possible variation of colour with time within 48 hours was not investigated. Further investigation is required to identify the variation of colour with time.

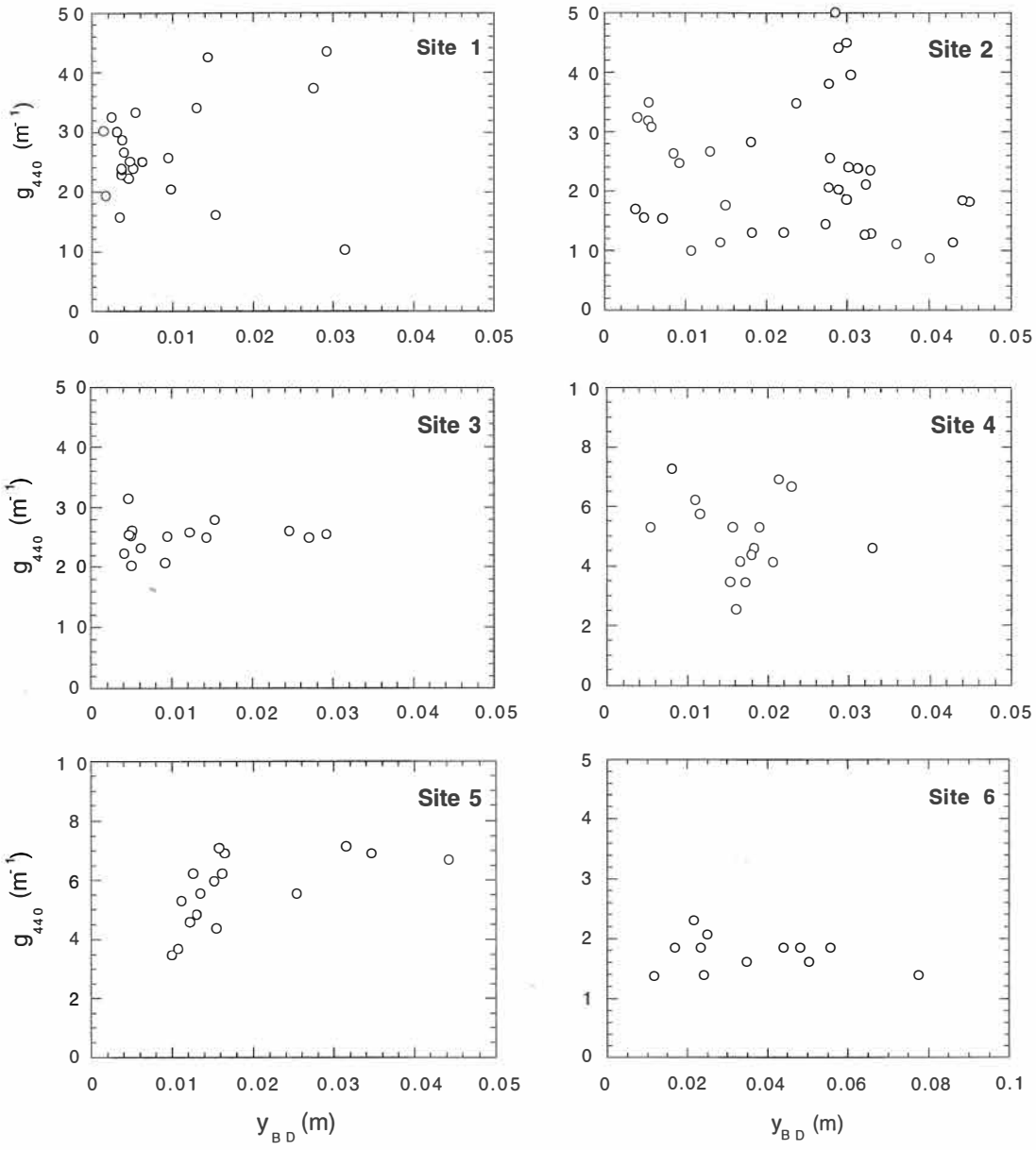

Figure 4.11 Plots of yellow substance concentration (g440) against black disk visual clarity (y_{BD}) of the runoff samples collected from the six sampling sites at the Mount Maunganui wharf and the adjacent urban area during seven storms from November, 1993 to July, 1995.

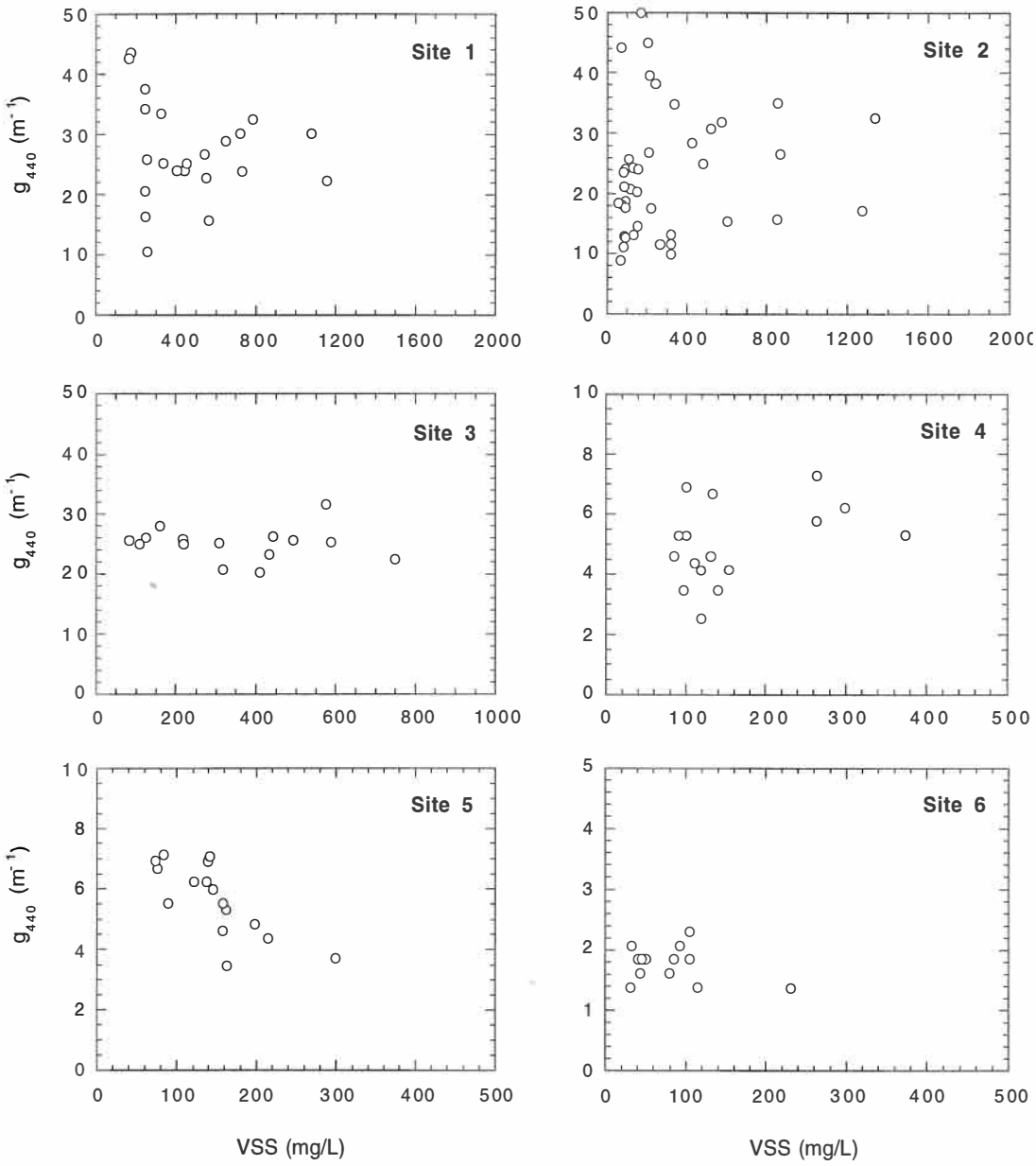

Figure 4.12 Plots of yellow substance concentration (g_{440}) against volatile suspended solid concentration (VSS) of the runoff samples collected from the six sampling sites at the Mount Maunganui wharf and the adjacent urban area during seven storms from November, 1993 to July, 1995.

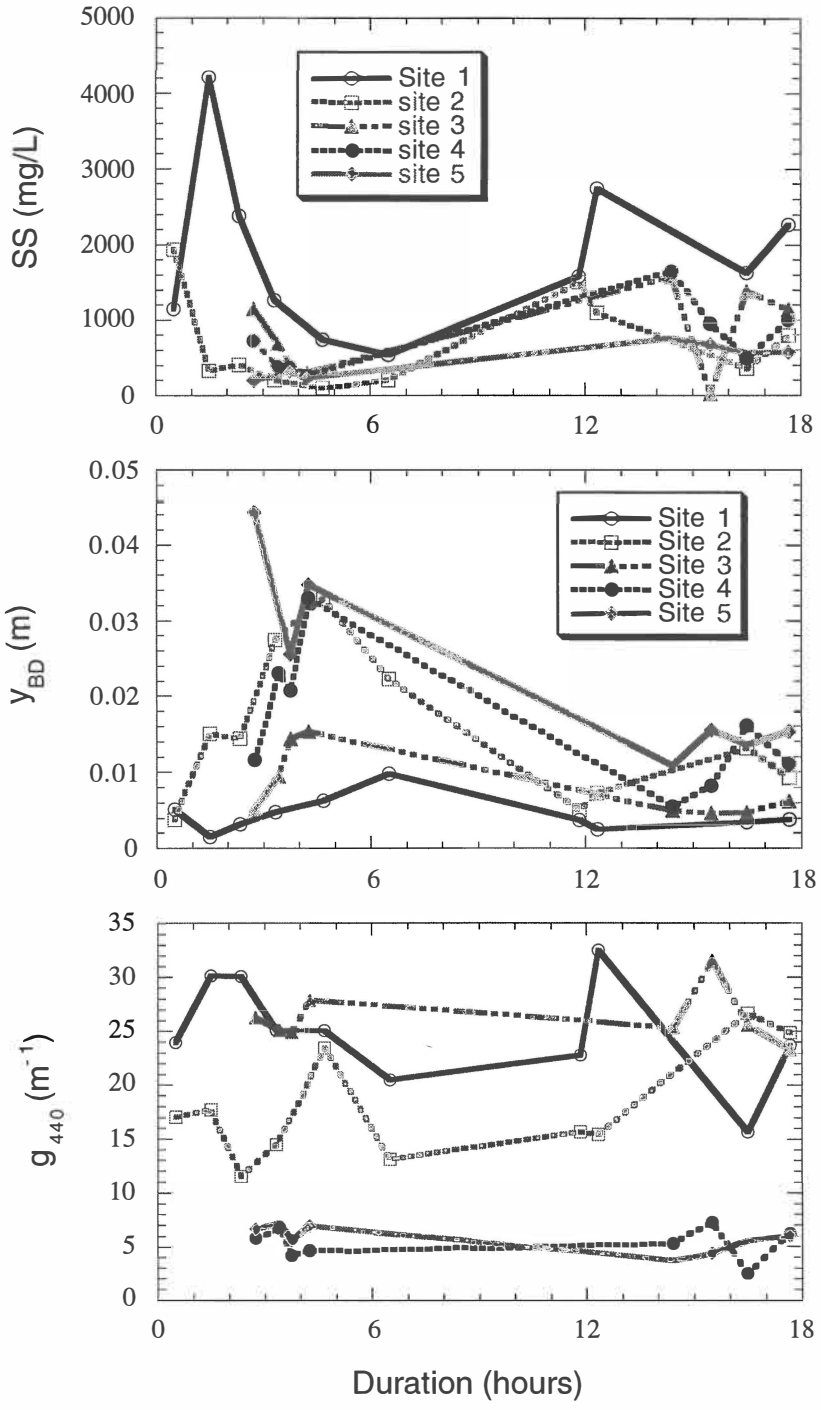

Figure 4.13 Yellow substance concentration of the runoff samples from sampling sites 1-5 around the Mount Maunganui wharf, Tauranga, during the storm episode of July 25, 1994.

4.3.5 Conclusions

Based upon analysis of 123 samples collected from various wharf and urban sub-catchments around a log export port:

1. Apparent colour of unfiltered samples, ranged from 10YR 3/1.5 (very dark gray) to 10YR 6/5 (yellowish brown), which is quite different to the true colour (yellow, dominant wavelength = 576 nm) due to high suspended solids in the runoff samples.

2. Munsell *hue* of the runoff samples in this study remained similar at 20 (10YR) in Munsell *hue* scale although the black disk visual clarity of the samples varied greatly (30 fold). This differs to the Munsell *hue* values of 92 New Zealand rivers under base flow conditions (Davies-Colley and Close, 1990), which is proportional to black disk visual clarity,

3. Munsell *value* is linearly proportional to black disk visual clarity of the runoff samples from the wharf areas and the adjacent urban area.

4. The wharf pavement types, which had a significant impact on suspended solids and black disk visual clarity, did not have an appreciable influence on yellow substance concentration. The yellow substance concentration of the runoff samples from different wharf sub-catchments, around 25 m^{-1}, was 120 and 14 times that of the receiving tidal water and the adjacent urban runoff.

5. The yellow substance in the wharf runoff remained relatively stable compared to suspended solids and visual clarity during a storm episode and from storm to storm. This finding provides a useful means to trace dispersion of the wharf runoff in receiving tidal waters which may be subject to additional runoff from the adjacent urban areas.

4.4 CONTRIBUTION OF SOLUBLE AND PARTICULATE SUBSTANCE TO OPTICAL PROPERTIES OF THE RUNOFF

4.4.1 Introduction

Understanding how much the soluble and particulate substance contribute to the optical properties of the storm runoff is of considerable interest for the design of storm runoff treatment facilities, or for environmental managers to assess an appropriate treatment method, or to assess the potential environmental impact on the receiving aquatic environment. Unfortunately, there has been a lack of such understanding. Accordingly, the contribution of soluble and particulate substance to the optical properties of the runoff samples collected from the log handling areas and the adjacent urban area at the Port of Tauranga, and the removal of soluble yellow substance by conventional flocculation/sedimentation treatment, were studied as part of the storm runoff environmental investigations.

4.4.2 Research background and rationale

Three intrinsic optical quantities determine the light behaviour in water , namely, absorption coefficient, a (m^{-1}), scattering coefficient, b (m^{-1}), and volume scattering function, β, all functions of wavelength (Jerlov, 1976). The sum of absorption and scattering coefficient is the beam attenuation coefficient, c , also with units m^{-1}.

As light photons can be absorbed by either soluble or particulate substance, light absorption coefficient, a (m^{-1}), can be written as $g + p$ (m^{-1}). The parameter g is the light absorption coefficient by soluble substance, and p is light absorption coefficient by particulate fraction. Because the soluble substance are responsible for imparting yellow colour of most natural waters, they are called yellow substance (Kirk, 1976; Bricaud *et al.*, 1981). Then, we have:

$$c = a + b = g + p + b \qquad (4.5)$$

As the existence of particulate substance, the actually measured apparent absorption coefficient of a water sample using spectrophotometric method, χ, can be expressed by (Davies-Colley, 1993):

$$\chi = a + (1-\varepsilon)b \qquad (4.6)$$

where ε is the fraction of scattered light collected by the photon detector. Using a spectrophotometer with a diffuse reflectance accessory (DRA) or with the samples held in two different positions with respect to the light detector, two similar equations can be obtained:

$$\chi_1 = a + (1-\varepsilon_1)b \qquad (4.7)$$

$$\chi_2 = a + (1-\varepsilon_2)b \qquad (4.8)$$

where ε_1 and ε_2 are the fractions of scattered light collected by the detector when a water sample is held in the first (normal) and a second position. For a given water sample and a spectrophotometer, ε_1 and ε_2 are constant (Davies-Colley, 1993). Subtracting equation 4.8 from equation 4.7, we have:

$$\chi_1 - \chi_2 = (\varepsilon_2-\varepsilon_1)b \qquad (4.9)$$

then, scattering coefficient, b, can be calculated by:

$$b = (\chi_1 - \chi_2)/(\varepsilon_2-\varepsilon_1) \qquad (4.10)$$

As a = g+p, equation 4.8 can be written as:

$$\chi_2 = g + p - (1-\varepsilon_2)b \qquad (4.11)$$

thus, absorption coefficient, p, can be calculated by:

$$p = \chi_2 - (1-\varepsilon_2)b - g \qquad (4.12)$$

When ε_2 and ε_1 are known, b and p can be obtained.

4.4.3 Methods

A Pye-Unicam PU8800 spectrophotometer with the samples held in two different positions was employed to determine g, p, and b in this study. About 40% and 90% of scattered light by the particles in a water sample can be collected by the light detector when the sample was held in the first (normal) and second position (Davies-Colley *et al.*, 1993).

The absorption coefficient by soluble substance, g, was determined by:

$$g = 230.3D/r \qquad (4.13)$$

where, D was absorbance, r was the cuvette path length (10 mm). For minimising the impact of scattering, absorption spectrum was run with the samples, which were filtered with a 0.2 μ Sartorius membrane, held in the second position.

From equation 4.10, b approximately equals to $2(\chi_1 - \chi_2)$, and p can be calculated by:

$$p = \chi_2 - 0.1b - g \qquad (4.14)$$

For avoiding multiple scattering in the runoff samples, all samples were diluted with distilled water to 30 - 50 NTU before the measurement was undertaken.

Standard jar tests were conducted to estimate the removal of suspended solids and soluble yellow substance (ASTM, 1987). A locally available commercial liquid aluminium sulphate, containing 40% of $Al_2(SO_4)_3$, was used as coagulant.

In total, 32 typical wharf storm runoff samples with a wide range of suspended solid concentration and black disk visual clarity and 13 adjacent urban runoff samples were examined. Table 4.4 summarises the optical properties of these samples.

4.4.4 Results and discussion

Figure 4.14 shows the ratios of absorption coefficient of the runoff samples from sites 1-5 and site 6 by soluble yellow substance, *g*, to beam attenuation coefficient, c, at 555 nm, the peak of the sensibility of the human eye.

Table 4.4 Summary of optical properties of the runoff samples collected from the log handling areas at Mount Maunganui wharf (sites 1-5, 32 samples) and adjacent urban area (site 6, 13 samples) during the study period from November, 1993 to June, 1995. SS: suspended solid concentration; BDVC: black disk visual clarity; and YS: yellow substance.

	Wharf runoff			Adjacent urban runoff		
	Min	Max.	Mean	Min	Max.	Mean
SS (mg/l)	113	5480	970	112	1216	329
Turbidity (NTU)	102	3068	662	96	473	246
BDVC (m)	0.002	0.053	0.015	0.012	0.108	0.042
YS (m^{-1})	3.45	50	25.1	1.38	2.30	1.77
Munsell value	3	5	3.6	4	7	4.9
Munsell chroma	1.8	5	2.5	1.3	3	2.4

Overall, yellow substance contributed only a very small percentage to light attenuation in the wharf runoff ranging from 0.2% to 13.6%, with a mean of 3.6%, although the yellow substance concentration in the wharf runoff was considerably higher compared to diverse inland and marine waters.

The contribution of yellow substance to light attenuation was inversely proportional to light attenuation coefficient of the wharf runoff samples (Figure 4.14). Yellow substance played an appreciable roll for light attenuation only for the samples with a lower suspended solid concentration.

For the adjacent urban runoff, because of the low concentration of yellow substance, particulate substance dominated the light attenuation (98.4%-99.8%, with a mean of 99.3%) although suspended solid concentration was significantly lower than that of the wharf runoff samples.

On average, particulate substance contributed 87% (with lowest contribution of 58%) of light attenuation for 96 New Zealand rivers under baseflow (Davies-Colley and Close, 1990). Although the yellow substance concentration in the wharf runoff is nearly 50 times that of the river waters, the contribution of yellow substance to light attenuation was still substantially lower than that of the river samples because the average black disk visual clarity of the river samples (3.2 m) was some 200 times that of wharf runoff samples.

There was an appreciable difference between apparent colour and true colour for almost all runoff samples examined in this present study. The apparent colour depended greatly on suspended solids and ratios of volatile suspended solids to total suspended solids (VSS/SS) although the average yellow substance of the wharf runoff was considerably higher.

For the samples with higher suspended solid concentration (lower visual clarity), the samples appeared "very dark gray" (10YR 3/1), "very dark

grayish brown" (10YR 3/2), "dark brown" (10YR 3/3), and "dark grayish brown" (10YR 4/2). The influence from yellow substance was not appreciable for these samples. For the samples with lower suspended solid concentration (higher visual clarity) and higher VSS/SS, for instance, suspended solid concentration <200 mg/l and VSS/SS ratio >0.7, the samples appeared "yellowish brown" (10YR 5/4 or 10YR 5/5). For these samples, the soluble yellow substance played a relatively important role for imparting the apparent colour.

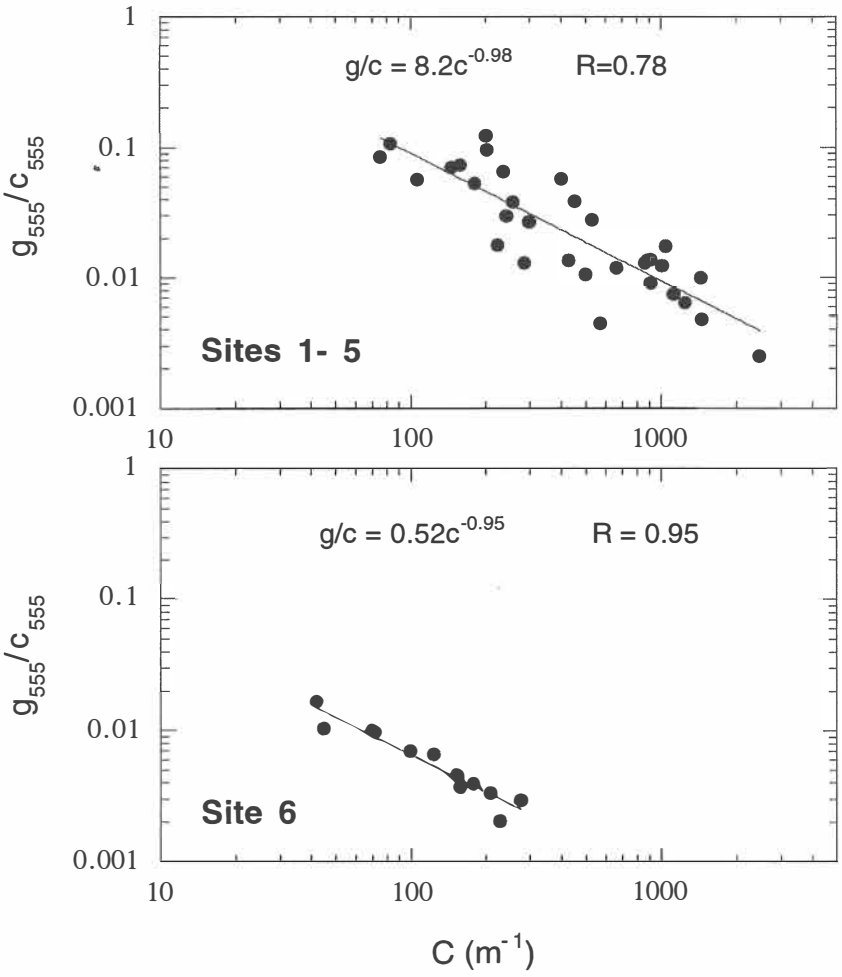

Figure 4.14 Ratios of light absorption coefficients by soluble yellow substance at wavelength = 555 nm, g_{555} (m^{-1}), to beam attenuation coefficient at 555 nm, C_{555} (m^{-1}) of the 32 wharf runoff samples (sites 1-5) and 13 adjacent urban runoff samples (site 6) at the Mount Maunganui wharf, Tauranga.

As particulate substance dominated the light attenuation in the wharf runoff, removal of these particulate substance is of major concern for improving their optical quality. According to the author's unpublished data, it is unlikely to improve the optical quality of the runoff significantly with natural sedimentation because of the presence of fine silt and clay particles in the runoff which played a key roll for attenuating light. It seems flocculation is necessary to aggregate the fine particles, hence to accelerate the sedimentation velocity of the particles.

A few standard jar flocculation/sedimentation tests were conducted for the runoff samples from the wharf gravel covered area with turbidity ranging between 700 NTU to 1000 NTU. Results showed that most of the fine particles in the samples could be removed when the alum dosage reached 70 mg/l. With removal of suspended solids, a great fraction of soluble yellow substance was also removed (Figure 4.15). This could be due to the adsorption of soluble yellow substances by the large amount of flocculates. With the removal of these flocculates, the adsorbed soluble substance was removed as well.

4.4.5 Conclusions

Based on measurement of absorption coefficient by soluble substance, g, absorption coefficient by particulate substance, p, and scattering coefficient, b, of 32 wharf runoff samples and 13 adjacent urban runoff samples, and flocculation/sedimentation jar tests:

1. suspended solids in the wharf runoff with a concentration ranging from 113 mg/l to 5480 mg/l contributed 87.8% to 99.7%, with a mean of 96.4%, to light attenuation, although the average soluble yellow substance concentration (25.1 m^{-1}) was considerably higher compared to that in the inland and marine waters;

2. because of low concentration (1.77 m^{-1}) in the adjacent urban runoff, which had suspended solid concentration ranging from 112 mg/l to 1216 mg/l, yellow substance contributed only 1.6% to 0.2% to the light attenuation;

3. the apparent colour depended primly on the concentration of suspended solids. The role of soluble yellow substance became appreciable only when the suspended solid concentration was lower and the ratio of volatile suspended solids to total suspended solids was higher; and

4. the conventional flocculation/sedimentation treatment could significantly remove yellow substance.

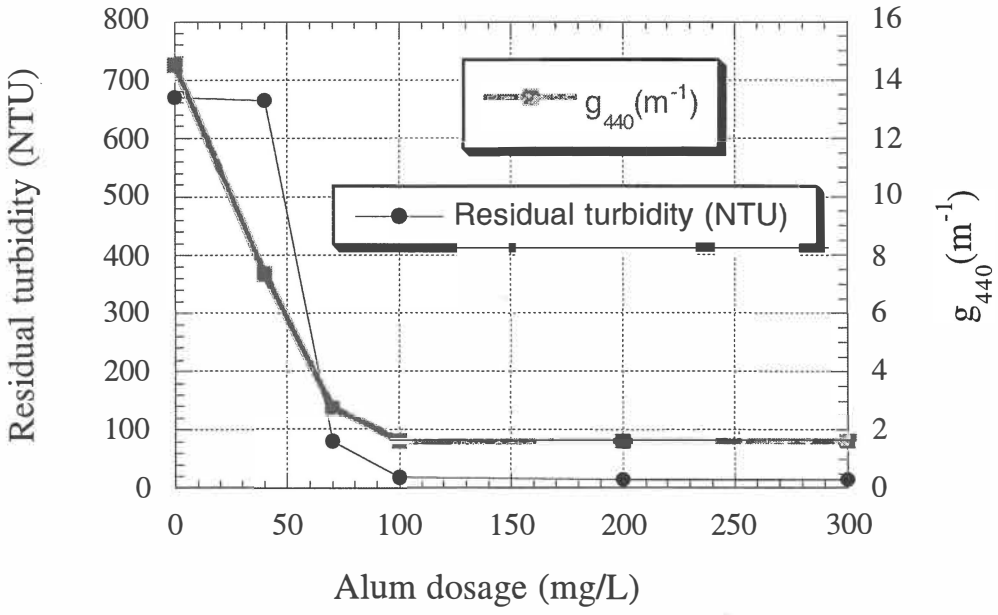

Figure 4.15 Residual turbidity and yellow substance concentration (g_{440}) of the supernatants in jar tests with different alum dosages for a wharf runoff sample from the gravel covered area at the Mount Maunganui wharf during the rainfall of June 28, 1995.

CHAPTER FIVE

WHARF RUNOFF WATER QUALITY
III. EXTRACTABLE ORGANIC ACIDS

CHAPTER FIVE

STORM RUNOFF WATER QUALITY III. EXTRACTABLE ORGANIC ACIDS

5.1 BACKGROUND AND OBJECTIVE

Radiata pine (*Pinus radiata*) is the main species of timber for export and the prime raw material for the pulp and paper industry in New Zealand. The softwood and bark of radiata pine possess a variety of resin and fatty acids in their cell tissue (Harman *et al.*, 1967; Porter, 1969; McDonald and Porter, 1969; and Lloyd, 1978). It is well documented that resin and fatty acids, either in their original or chlorinated forms, can be released into the effluent during pulping and bleaching processes (Kinae *et al.*, 1981; Wilkins, *et al.*, 1989; Morales, 1992; and Dell, 1993). Resin acids and unsaturated fatty acids are potentially toxic to aquatic life (Leach *et al.*, 1978; Chung *et al.*, 1979; Oikari *et al.*, 1980, 1985; Naohide, 1981; Wilkins, *et al.*, 1987; Tana, 1988; and Sandstrom, 1988; McCarthy *et al.*, 1990; Owens, 1991). Whilst much is known about the resin and fatty acids in the effluent from pulp and paper mills, little information is available concerning storm runoff from a timber port or log storage yards of paper and pulp mills.

The few previous studies of storm runoff from log handling areas at a timber port or paper mills focused on the resin and fatty acids themselves only. Little attention was paid to the variation of resin and fatty acids in the runoff during a storm, the influence of wharf pavement types, and the relationships between resin and fatty acids and other parameters, probably due to the inadequate amount of samples collected in the studies (NCASI, 1992; Kingett Mitchell and Associates, 1993; and Tian *et al.*, 1995). Furthermore, if the runoff water quality cannot meet the discharge criteria set by the local environmental authorities, treatment of the runoff is

necessary. It is unknown whether conventional treatment designed for the removal of suspended solids, such as plain sedimentation or flocculation-sedimentation, could remove resin and fatty acids. Accordingly, a comprehensive investigation of resin and fatty acids in the wharf storm runoff was undertaken. The objectives of the study are to investigate:

- the resin and fatty acid concentrations in the runoff from the wharf log handling area, the adjacent urban area, and in the receiving tidal waters;

- the variation of resin and fatty acid levels in the runoff during a storm;

- the influence of wharf surface pavement types, rainfall processes, volatile suspended solid concentration and yellow substance on resin and fatty acid levels; and

- the reduction of resin and fatty acid concentrations with the removal of particulate substance by centrifugation or flocculation-sedimentation.

5.2 METHODS

5.2.1 Sample Selection and Pre-treatment

It is difficult to identify the organic constituents in all the 123 water samples as the time and funding restraints. Therefore, only a selection of wharf runoff samples were extracted [8 samples from the gravel surfaced wharf area (site 1) during two storm events, 8 samples from the sealed area (site 2) during the same two storm episodes]. In addition, 2 runoff samples from the adjacent urban area (site 6) and 2 seawater samples, collected from the Tauranga Harbour during low and high tide conditions on August 21, 1995, were also extracted.

The water samples were extracted without any pre-treatment because "total recoverable" resin and fatty acid levels were wanted. However, for estimating the possible removal of resin and fatty acids by conventional treatments, a further four extractions of the supernatant of two wharf runoff samples (T2 and T10), after most of the suspended solids were removed by centrifugation and flocculation-sedimentation, were also undertaken.

One litre of distilled water was also extracted as a blank extraction. Identical procedures were applied in the blank experiment. In total 25 water samples were extracted and the organic species were identified. Details and some selected physical parameters of these samples are given in Table 5.1.

A GS-4100 centrifuge was used to separate the particulate substance from the runoff. 600 ml of sub-samples from T2 and T10 were centrifugalised for 10 minutes at 2500 rpm, separately. More than 96% of suspended solids (SS) and volatile suspended solids (VSS) were removed after centrifugation.

Standard flocculation/sedimentation jar tests were conducted to remove the suspended solids as well. A locally available commercial liquid aluminium sulphate, containing 40% of $Al_2(SO_4)_3$, was used as coagulant. 225 mg/l of $Al_2(SO_4)_3$ were added to the samples T2 and T10. The pH of these samples were adjusted with 0.1 M NaOH to 6.7-7.0 after addition of the coagulant. The procedures of the jar test followed the *Annual Book of ASTM Standards. Section II: Water and Environmental Technology* (ASTM, 1987). Not only were SS and VSS greatly reduced, but also yellow substance concentration decreased significantly after flocculation-sedimentation.

5.2.2 Extraction Techniques

Water samples (1 l for the distilled water, seawater and urban runoff samples; 400 ml for the pre-treated wharf runoff samples, and 100 ml for the untreated wharf samples) were extracted for 16 hours with AR chloroform using liquid-liquid extractors. *O*-methylpodocarpic acid (PDA) was added to

the runoff samples as surrogate (recovery) standard immediately before extraction commenced. PDA, prepared as a 0.12 mg/ml solution in chloroform, was typically added at the rates of 240 µg/l (wharf runoff), 12 µg/l (distilled water and seawater), 24 µg/l (urban runoff), and 60 µg/l (pre-treated wharf runoff). After extraction, *O*-methylpodocarpic acid ethyl ester (PDA-Et) was added to the chloroform extract as quantification standard. PDA-Et, prepared as a 0.105 mg/ml solution in chloroform, was typically added at the rates of 210 µg/l (wharf runoff), 10.5 µg/l (distilled water and seawater), 21 µg/l (urban runoff), and 52.5 µg/l (pre-treated wharf runoff). The sample volumes used for extraction and PDA-Et addition rates were derived from the estimated resin acid levels in different samples from the two trial extractions, performed in advance.

The chloroform extract was concentrated to 1-2 ml under reduced pressure using a rotary evaporator. The concentrated extract was then derivatised using an ethereal solution of diazomethane (CH_2N_2) (**CARE**, diazomethane is explosive and carcinogenic, Vogel, 1978). For fully converting the acids to methyl esters, the concentrated extracts with added diazomethane were allowed to stand at room temperature for 30 minutes and left in a refrigerator (1-3^{o}C) for 24 hours. Excess diazomethane was blown off under a stream of oxygen free nitrogen.

5.2.3 GC Acquisition Parameters

Typical parameters used for GC-FID analyses are given in Table 5.2. Resin and fatty acids were identified according to their retention times. Identification was confirmed by GC-MS analyses

Figures 5.1a-f are typical GC-FID profiles of a wharf runoff sample, a adjacent urban runoff sample, a seawater sample, a wharf runoff sample with pre-treatment of centrifugation, a wharf runoff sample with pre-treatment of flocculation-sedimentation, and the reference mixture.

Table 5.1 Details and selected features of the water samples extracted and identified in this study. Abbreviations used in this table: SS: suspended solid concentration; VSS/SS: ratios of volatile suspended solids to total suspended solids; g_{440}: light absorption coefficient at 440 nm. site 1: gravel surfaced wharf area; site 2: sealed area; site 6: adjacent urban area; site 7: Tauranga Harbour; CR: cumulative rainfall.

Sample code	Sites	Date	CR (mm)	Pre-treatment	SS (mg/l)	VSS/SS	g_{440} (m^{-1})
T1	1	28/5/95	4.0	No	530	0.49	10.36
T2	1	28/5/95	17.0	No	1410	0.29	23.95
T3	1	28/5/95	34.0	No	310	0.53	42.60
T4	1	28/5/95	75.0	No	465	0.54	16.12
T5	1	25/7/95	10.0	No	4210	0.26	30.17
T6	1	25/7/95	20.0	No	535	0.46	20.5
T7	1	25/7/95	27.0	No	2740	0.29	32.47
T8	1	25/7/95	50.0	No	1630	0.35	15.68
T9	2	28/5/95	4.0	No	660	0.49	9.90
T10	2	28/5/95	17.0	No	765	0.56	28.32
T11	2	28/5/95	34.0	No	430	0.58	38.22
T12	2	28/5/95	75.0	No	140	0.69	17.73
T13	2	25/7/95	10.0	No	1940	0.66	17.04
T14	2	25/7/95	20.0	No	200	0.69	13.13
T15	2	25/7/95	27.0	No	1095	0.55	15.43
T16	2	25/7/95	50.0	No	348	0.62	26.71
T2C	1	28/5/95	17.0	centrifugation	9	0.35	23.95
T10C	2	28/5/95	17.0	centrifugation	29	0.64	28.32
T2F	1	28/5/95	17.0	flocculation	38	0.37	1.38
T10F	2	28/5/95	17.0	flocculation	6	0.60	1.84
T21	7	21/8/95	low tide	No	19	0.22	0.46
T22	7	21/8/95	high tide	No	12	0.18	0.23
T23	6	28/5/95	4.7	No	330	0.29	2.07
T24	6	28/5/95	68.5	No	142	0.23	2.07

Table 5.2 parameters used for GC-FID.

Parameters used	GC-FID
Column internal diameter (mm)	0.22
Column length (m)	25
Purge on time (min)	0.25
Initial time (min)	4
Initial temperature (°C)	140
Rate (°C/min)	4
Final temperature (°C)	295
Hold time (min)	2

For the distilled water, urban runoff, seawater, and treated samples, the resin acid concentration were too low to be reliably identified using GC-FID detection. Even for the wharf samples, the levels of some minor compounds were also too low to be reliably identified using GC-FID detection. Quantification was therefore routinely performed using selected ion mode (SIM) GC/MS detection (See Section 5.2.5).

5.2.4 Total ion GC-MS

Fatty acids were routinely quantified using total ion (TIC) GC-MS detection. The detected limited of TIC GC-MS in this study was 0.5 μg/l. Typical parameters used for the acquisition of total ion GC/MS are given in Table 5.3.

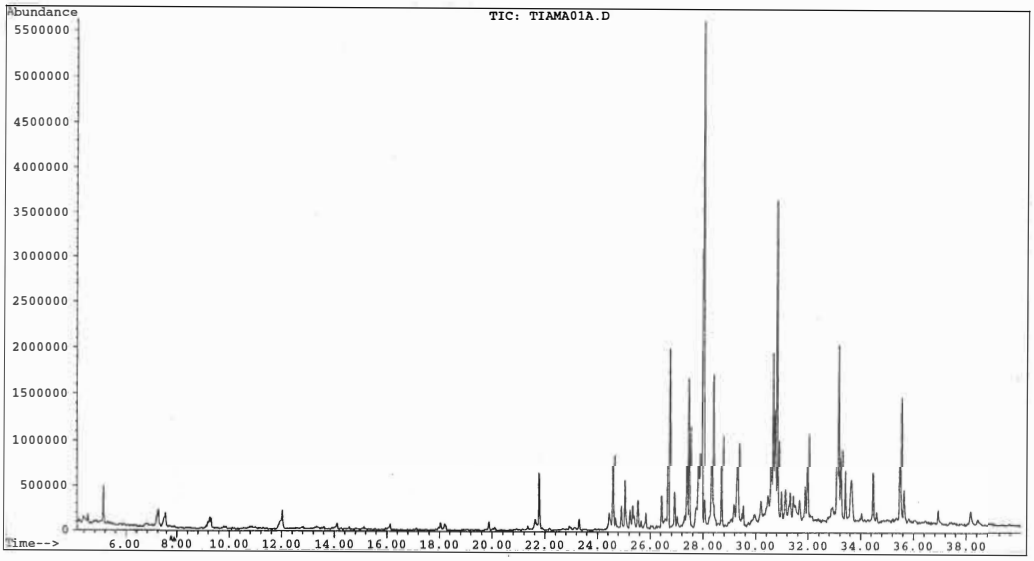

Figure 5.1a GC-FID chromatogram of a wharf runoff sample (T1).

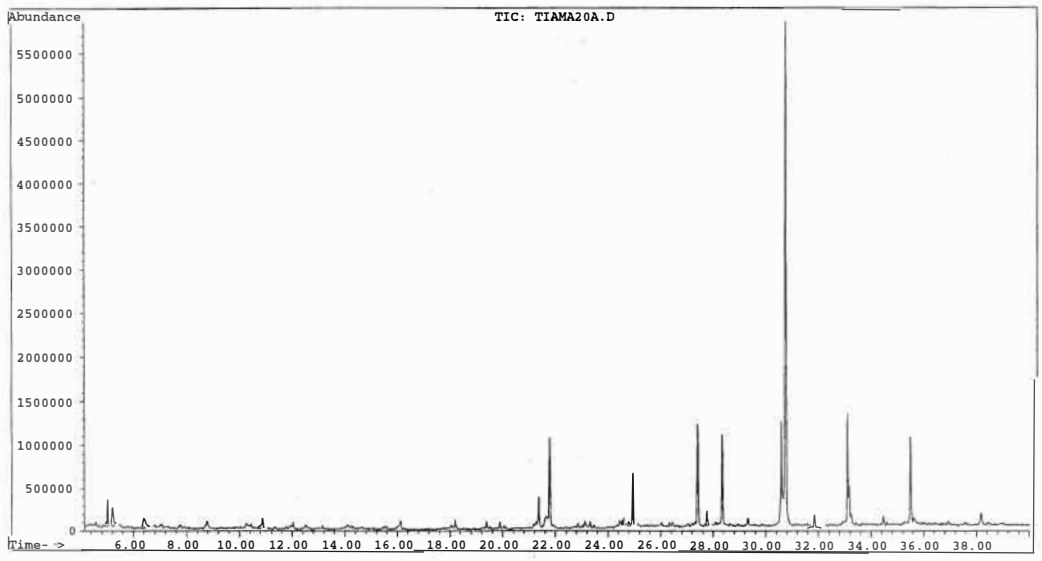

Figure 5.1b GC-FID chromatogram of a adjacent urban runoff sample (T23).

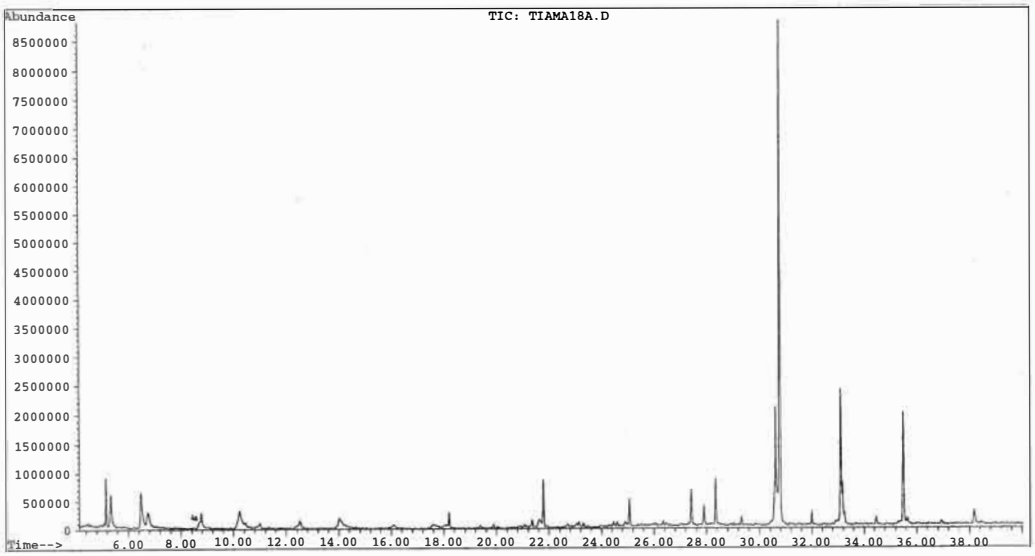

Figure 5.1c GC-FID chromatogram of a seawater sample (T21).

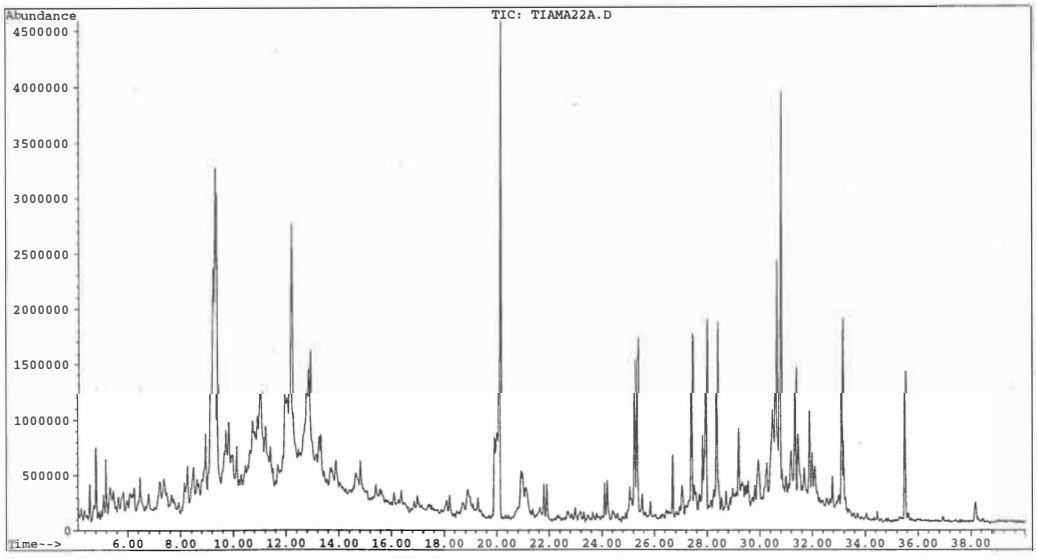

Figure 5.1d GC-FID chromatogram of a wharf runoff sample with pre-treatment of centrifugation (T2C).

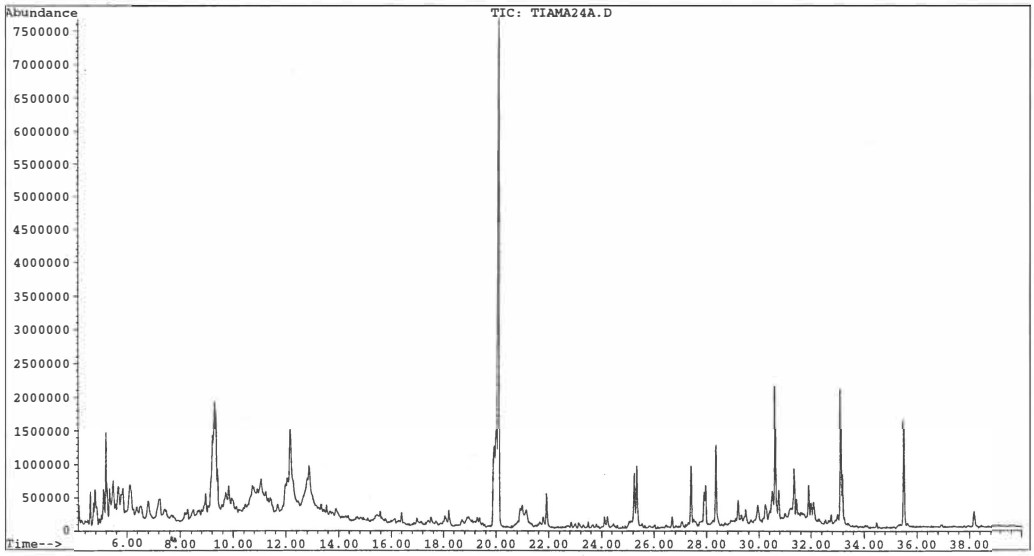

Figure 5.1e GC-FID chromatogram of a wharf runoff sample with pre-treatment of flocculation-sedimentation (T2F).

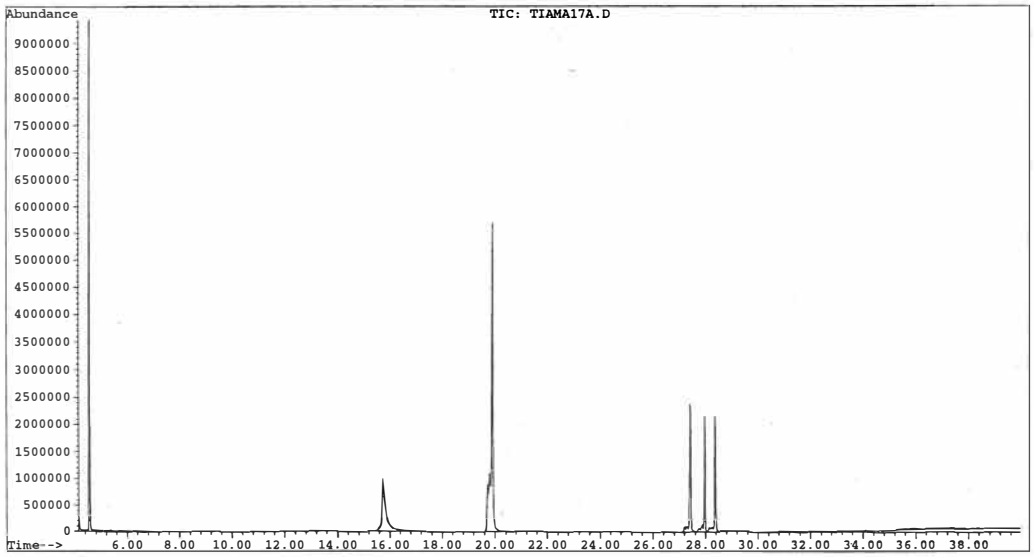

Figure 5.1f GC-FID chromatogram of a reference mixture (T17).

Table 5.3 parameters used for total ion GC-MS analyses

Parameters used	GC-MS (TIC)
Column length (m)	25
Column internal diameter (mm)	0.22
Purge on time (min)	0.2
Initial temperature (°C)	140
Rate (°C/min)	4.0
Final temperature (°C)	295
Hold time (min)	2
Ion range (*m/z*)	40 - 400

5.2.5 Selected Ion GC-MS

Resin acids were routinely quantified using selected ion mode (SIM) GC/MS detection. The detected limit of SIM GC-MS in this study was 0.05 µg/l.

The ions used in SIM GC-MS analyses are shown in Table 5.4.

Table 5.4 Ions used for SIM GC-MS analyses. de-DHAA: dehydro dehydroabietic acid; 7-OH DHAA: 7-hydroxy dehydroabietic acid. Ions shown in bold were used for quantification, the others were utilised as confirmation ions.

Compounds	Ions used (*m/z*)	Compounds	Ions used (*m/z*)
PDA-Me and PDA-Et	**227**	de-DHAA	**237**
pimaric acid	**121**, 316	7-OH DHAA	**237**
sandaracopimaric acid	**121**, 316	dehydroabietic acid	**239**, 299, 314
secodehydroabietic acid-1	**146**, 316, 187	isopimaric acid	**241**, 256
secodehydroabietic acid-2	**146**, 316	abietic acid	**256**, 241, 316

5.2.6 Detector Linearity

A set of solutions, with a fixed amount of PDA-Et (300 µl of 105 µg/l solution) and variable amounts of a reference mixture (50, 100, 150, 200, 300, 400, and 600 µl) containing the methyl esters of C_{18} (114 µg/ml), PDA (119 µg/ml), and DHAA (100 µg/ml) were analysed by SIM GC-MS to demonstrate the detector linearity.

Detector linearity can be illustrated by plotting the ratios of the target compound peak area to that of PDA-Et, against the ratios of target compound to PDA-Et added. The resulting detector linearity profile for DHAA in the mixture is shown in Figure 5.2.

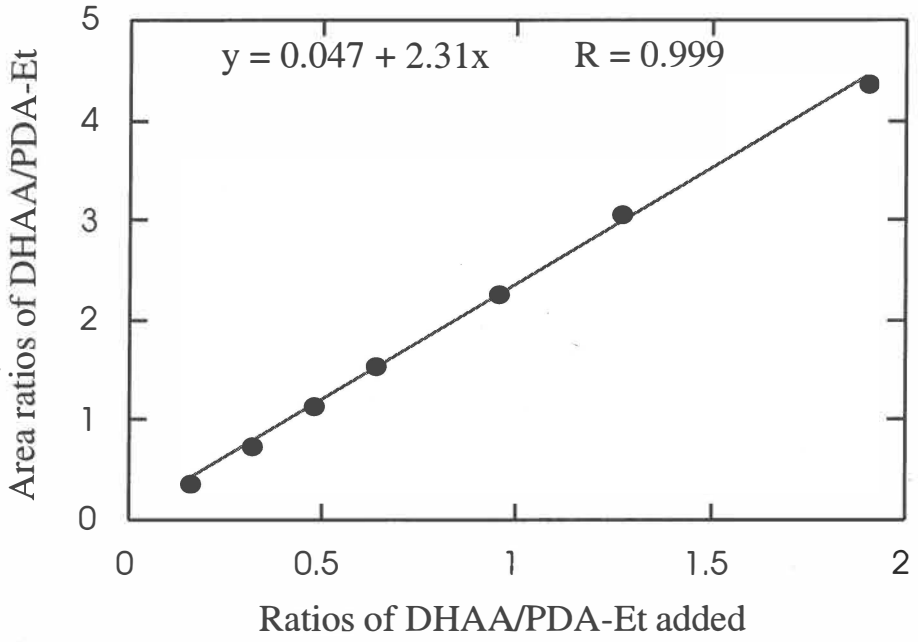

Figure 5.2 Detector linearity of DHAA.

5.2.7 Response Factors and Quantification

The response factors (RF) vary with type of compounds and the techniques used. Normally, similar compounds have similar response factors.

In this study, response factors for total ion (TIC) GC-MS were calculated relative to PDA-Et. A mixture of methylated (with CH_2N_2) PDA, PDA-ET, *n*-octadecane (C_{18}), and DHAA, was used for obtaining the response factors. Response factors were 0.921 for resin acids (dehydroabietic acid) and 2.71 for fatty acids (C_{18}, *n*-octadecane acid).

SIM GC-MS response factors were determined using 7 samples containing known, GC-FID determined concentration of resin acids (Wilkins *et al.*, 1996). It is more preferable to determine SIM GC-MS response factors using a reference solution containing weighed target compounds. However, not all the target resin acids were available commercially (nine individual resin acids were identified in this study, but only three of them were commercially available when the identification was undertaken). All the SIM GC-MS response factors determined from the reference solutions had coefficient of variation (CV) in the range of 2.4% - 15.9%, which is acceptable for environmental analyses (Table 5.5).

Compound concentrations were calculated by the following equation:

$$\text{Concentration of compound } (\mu g/l) = \frac{peak\ area\ of\ compound \times concentration\ of\ standard}{peak\ area\ of\ standard \times respons\ factor\ for\ compound}$$

5.2.8 Reproducibility and Extraction Recovery Tests

Five 200 ml quantities of well mixed wharf runoff sample T7 (taped T7-1, T7-2, T7-3, T7-4 and T7-5) were extracted in five extractors by the liquid-liquid extraction method. The same procedures were applied to all the five samples. Quantification was performed using SIM GC-MS (Table 5.6).

The results of 5 replicate extractions showed that the liquid/liquid extraction and SIM GC-MS analyses are reproducible for having coefficient of variation in the range of 6.8% - 14.2%.

The percentage recovery of PDA, added to the water phase as a surrogate standard, was also determined for the five replicate extractions (Table 5.7).

Table 5.5 Mean response factors for selected ion mode (SIM) GC-MS analysis determined using 7 samples containing known, GC-FID determined, concentration of resin acids, relative to PDA-Et. SD: standard deviation; CV: coefficient of variance.

Compounds	Mean response factors	SD	CV (%)
PDA	1.207	0.156	12.9
pimaric acid	1.087	0.105	9.7
abietic acid	0.348	0.042	12.2
dehydroabietic acid	1.217	0.193	15.9
isopimaric acid	0.299	0.047	15.9
sandaracopimaric acid	1.061	0.108	10.2
secodehydroabietic acid-1	0.475	0.011	2.4
secodehydroabietic acid-2	0.727	0.059	8.1
7-OH dehydroabietic acid	0.837	0.737	8.8
de-DHAA	0.442	0.057	12.3

The percentage extraction recovery of PDA in the 24 extractions (excluding the distilled water) varied from 65.2%-83.2%, with a mean percentage of 74.7% (CV = 8.2%). The mean recovery percentage is slightly lower than that from the five replicate extractions (85.6%), which is possibly because the samples were filtered before the extraction, thereby the interference of suspended solids was minimised.

Table 5.6 Mean concentrations (µg/l) of some selected resin acids determined by SIM GC-MS for the five replicate extractions of the wharf runoff sample T7[a]. Pim: pimaric acid; Ab: abietic acid; DHAA: dehydroabietic acid; 7-OH DHAA: 7-hydroxy-dehydroabietic acid; SD = standard deviation, CV = coefficient of variation.

Compounds	T7-1	T7-2	T7-3	T7-4	T7-5	Mean	SD	CV(%)
Pim	34.5	31.4	30.3	30.9	25.7	30.6	3.2	10.4
Ab	46.5	40.7	52.4	NR[b]	56.7	49.1	7.0	14.2
DHAA	219	211	245	214	190	216	19.7	9.1
7-OH DHAA	95.6	76.0	75.3	96.8	75.7	83.9	11.2	13.4
de-DHAA	62.5	63.4	62.9	53.5	59.5	60.4	4.1	6.8

[a] The results given in this table are different to those in Table 5.8 because the sample T7 was filtered with cotton wool before the five replicate extractions, whereas the sample T7 was extracted without any pre-treatment.

[b] NR: not recorded.

Table 5.7 Recovery of PDA in the five replicate extractions of the cotton wool filtered wharf runoff sample T7.

	T7-1	T7-2	T7-3	T7-4	T7-5	mean	SD	CV(%)
PDA added (µg)	24.0	24.0	24.0	24.0	24.0	24.0		
PDA recovered (µg)	21.3	20.3	20.7	20.2	20.2	20.6	0.46	2.3
% recovery	88.8	84.6	86.3	84.2	84.2	85.6	2.0	2.3

5.2.9 Measurement of other Terms

Determination of suspended solids (SS), volatile suspended solids (VSS), black disk visual clarity, and yellow substance is given in Chapter 4.

5.3 RESULTS AND DISCUSSION

The levels of resin acids identified by SIM GC-MS and fatty acids determined by TIC GC-MS in the 25 water samples are given in Table 5.8. Figure 5.3 shows the chemical structures of these resin and fatty acids.

5.3.1 Overall Levels of Resin and Fatty acids

The total resin acid concentrations of the 16 untreated wharf runoff samples from the log handling areas ranged from 72 to 2260 μg/l, with a mean concentration of 1035 μg/l.

The total resin acid levels of the two adjacent urban runoff samples, 1.3 and 4.1 μg/l, were only 0.1-0.4% of the mean total resin acid concentration (1035 μg/l) of the untreated wharf runoff samples, although the VSS concentrations of these two urban runoff samples (33 and 96 mg/l) were 7.4 and 21.6% of the mean VSS concentration of the wharf runoff samples (445 mg/l). This is probably because most of the VSS in the wharf runoff samples originates from crushed bark particles, whereas the VSS in the urban runoff samples does not. Visual examination of the urban runoff flow revealed the presence of dried grass, tree leaves, and other organic debris in the adjacent urban runoff. The extracts of the two urban runoff samples appeared green in colour. The green colour might come from chlorophylls in the grass and/or tree leaves.

No resin acids were detected in the seawater sample collected during high tide which came from the open ocean outside the Harbour. 0.2 μg/l of DHAA were identified in the seawater sample collected during low tide. As a few steams enter the southern end of the Tauranga Harbour, such as Rocky Stream, Waitao Stream, Ngapeke Stream, Waikite Stream, Kaitemako Stream, and Waimapu Stream, the seawater sample collected during low tide contained some freshwater. The DHAA might have come

from the freshwater inputs. Since the DHAA level (0.2 µg/l) is only marginally above the detective limit (0.05 µg/l), the single low tide seawater result must be interpreted with caution.

The toxicity of resin acids to aquatic life has been well documented. As early as the 1970s, Leach *et al*. (1978) indicated that when bio-treatment was adequate to reduce the concentration of total resin acids to less than 1000 µg/l, the resulting effluents from paper and pulp mills exhibited no acute toxicity. More recently, Tavendale (1994) summarised the toxicity of some resin acids. The 96-h LC50 (the concentration required to kill 50% of population in 96 hour period) of abietic acid, DHAA, isopimaric acid, pimaric acid and sandaracopimaric acid for trout are 700-1500, 800-1740, 400-1000, 700-1200, and 360 µg/l, respectively. The potential impact on marine life, particularly the benthic biota, is beyond the scope of this study and will be investigate separately. To date, there have been no reports of acute toxic events among harbour fish, probably because the quick and massive dilution of the wharf runoff in the receiving tidal waters (see Chapter 9).

Among the nine individual resin acids identified in the wharf runoff samples in this study, dehydroabietic acid (DHAA) was always dominant (Figure 5.4). On average, DHAA accounts for about 45% of the total resin acids and did not vary significantly among the 16 untreated wharf runoff samples (mean ratio of DHAA to total resin acids is 0.45, with a coefficient of variance of 17.3%), although the total resin acid concentration of these samples varied greatly (72 to 2260 µg/l). 7-OH dehydroabietic and pimaric acids are the second and third largest individual resin acids, respectively. The sum of secodehydroabietic acid-1, secodehydroabietic acid-2, and sandaracopimaric acid typically accounted for only 6% of total resin acids.

Kingett Mitchell and Associates (1993) detected a large amount of oxygenated resin acids (3,300 µg/l) possessing molecular weights in the range of 328 - 350

amu, which accounted for 46% of total resin acids, in the eight runoff samples collected around the log handling areas at the Mount Maunganui wharf in 1992. GC-MS analyses indicated these oxygenated resin acids to be monohydroxylated or dihydroxylated resin acids possessing abietic or dehydroabietic acid-like skeletons. About 2,000 µg/l of oxygenated resin acids were also detected in the runoff sample collected at the log handling area at the Sulphur Point wharf (Tian *et al.*, 1995).

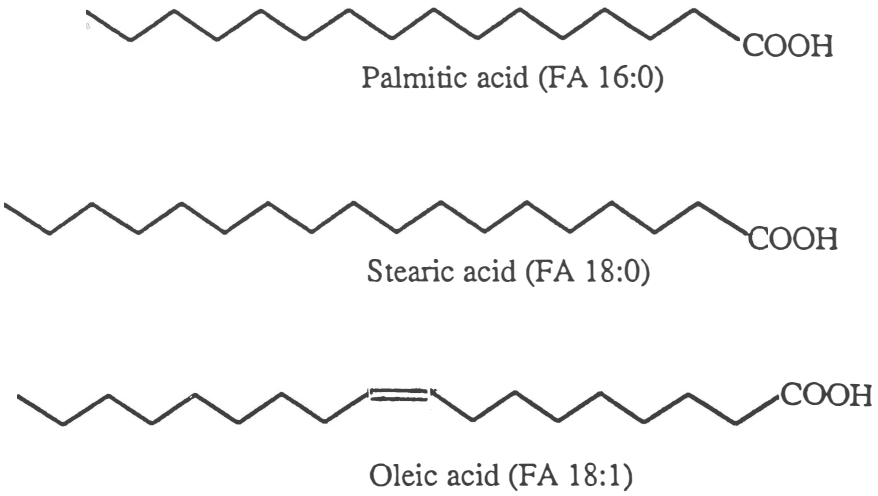

Figure 5.3a Chemical structures of fatty acids identified by TIC GC-MS in the 24 water samples extracted in this study.

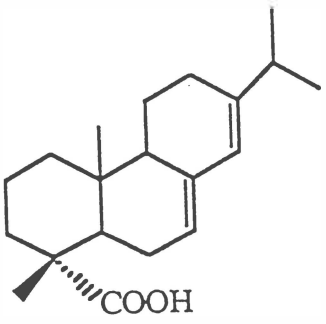

Abietic acid

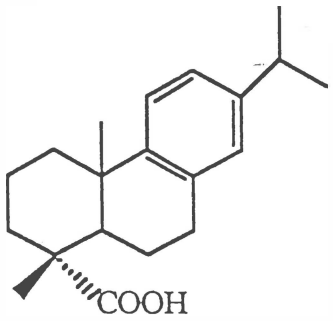

Dehydroabietic acid

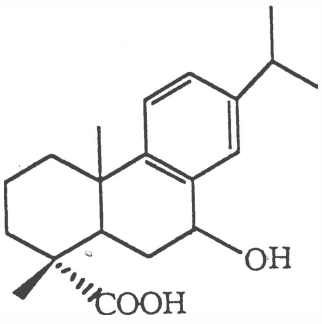

7-OH dehydroabietic acid

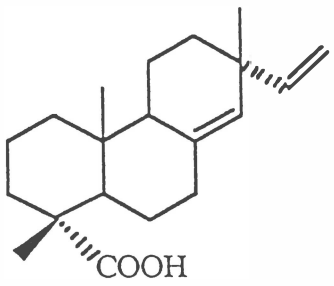

Sandaracopimaric acid

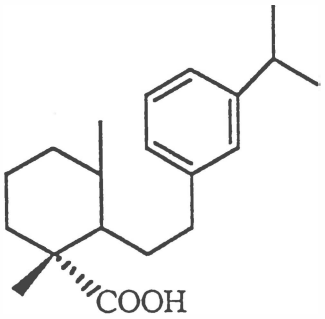

Secodehydroabietic acid-1

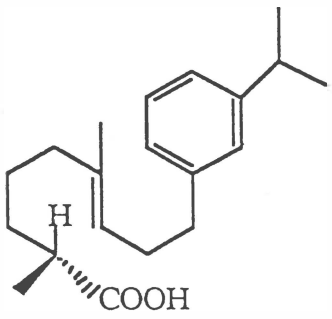

Secodehydroabietic acid-2

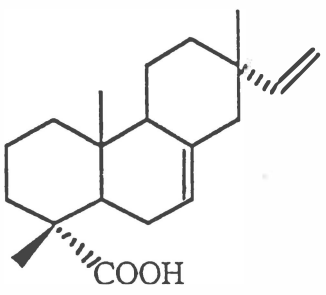

Isopimaric acid

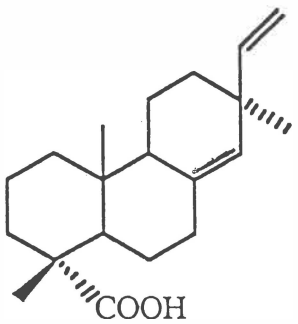

Pimaric acid

Figure 5.3b Chemical structures of resin acids identified by SIM GC-MS in the 24 water samples extracted in this study.

Table 5.8 Resin acid levels (µg/l) determined by SIM GC-MS and fatty acid levels (µg/l) determined by TIC GC-MS in the 24 water samples collected in this investigation. The details and selected features of these samples are shown in table 1. Abbreviations used in this table: HDAA: dehydroabietic acid; Ab: abietic acid; Pim: pimaric acid; Iso: isopimaric acid; de-D: dehydro-DHAA; 7-OH: 7-hydroxydehydroabietic acid; Seco1: secodehydroabietic acid-1; Seco2: secodehydroabietic acid-2; sand: sandaracopimaric acid; TRA: total resin acids; F16:0: palmitic acid; F18:0: stearic acid; F18:1: oleic acid; TFA: total fatty acids; Re: percentage of recovery of PDA.

Code	Type*	DHAA	Ab	Pim	Iso	de-D	7-OH	Seco1	Seco2	Sand	TRA	F16:0	F18:1	F18:0	TFA	Re (%)
T1	WG	760	87	180	110	99	120	56	25	39	1480	17	41	18	76	65.2
T2	WG	210	23	94	39	32	370	24	11	12	820	47	84	20	150	77.8
T3	WG	130	7.9	15	8.4	56	140	2.5	1.1	5.4	370	37	87	19	140	74.1
T4	WG	350	37	74	43	70	150	12	7.2	15	760	51	130	18	200	72.3
T5	WG	580	76	110	73	74	100	20	9.5	28	1070	46	93	42	180	78.2
T6	WG	250	13	40	23	41	82	7.0	3.3	10	470	24	33	24	82	80.6
T7	WG	1100	210	320	230	72	180	57	26	69	2260	95	350	56	500	81.2
T8	WG	360	24	58	32	45	110	9.7	4.9	13	660	25	22	20	68	78.3
T9	WS	32	ND	8.2	12	8.3	ND	6.8	3.3	1.2	72	25	50	15	90	83.2
T10	WS	880	180	270	200	130	240	52	26	50	2030	90	180	36	300	74.0
T11	WS	510	110	150	85	96	170	20	9.2	27	1180	56	110	22	190	74.7
T12	WS	140	35	70	33	56	43	11	4.7	11	400	44	120	17	180	78.4
T13	WS	990	110	250	240	140	190	45	20	59	2040	50	150	35	240	80.7
T14	WS	490	51	100	86	110	170	14	7.3	26	1050	53	180	18	250	75.4
T15	WS	460	55	100	75	93	130	15	7.2	20	960	36	130	17	180	74.4
T16	WS	420	69	93	68	94	170	13	5.5	21	950	47	150	16	210	74.0
T2C	WC	66	4.0	15	4.2	29	14	8.2	3.7	3.5	150	6.2	ND	5.7	12	72.2
T10C	WC	78	6.1	16	9.1	99	64	5.0	2.3	6.0	290	9.4	6.7	11	27	67.5
T2F	WF	39	ND	7.2	1.9	4.5	9.10	3.6	1.7	1.5	69	2.1	ND	ND	2.1	55.5
T10F	WF	83	3.4	10	3.8	20	43	3.9	1.9	3.9	170	3.6	ND	3.0	6.6	67.0
T21	SL	0.2	ND	ND	ND	ND	ND	ND	ND	ND	0.2	4.0	ND	2.4	6.4	66.3
T22	SH	ND	ND	ND	ND	ND	ND	ND	ND	ND	ND	2.8	ND	2.6	5.4	65.4
T23	AU	0.7	ND	ND	0.6	ND	ND	ND	ND	ND	1.3	12	ND	4.7	17	84.5
T24	AU	1.9	ND	0.5	0.7	1.0	ND	ND	ND	ND	4.1	6.8	ND	4.3	11	82.8

* WG - wharf runoff samples from the gravelled area (site 1); WS - wharf runoff samples from the sealed area (site 2); WC - wharf runoff samples after most of the suspended solids were removed with centrifugation; WF - wharf runoff samples after most of the suspended solids were removed with flocculation-sedimantation; SL - seawater sample collected during low tide; SH - seawater sample collected during high tide; AU - adjacent urban runoff

Oxygenated resin acids are not usually detected in wood and bark effluents (Wilkins *et al.*, 1994). Their presence is suggestive of the anaerobic modification of dehydroabietic, abietic, pimaric and isopimaric acids in the environment existing on the surface around the log handling areas. As no data are available for how long the bark particles had existed on the wharf surface when the samples were collected, further investigation is required to find the main factors which influence the modification of resin acids.

Palmitic acid (F16:0), stearic acid (F18:0) and oleic acid (F18:1) were detected in all of the 16 untreated runoff samples. The total fatty acid levels (68 - 499 µg/l, with a mean of 190 µg/l) was significantly lower than the total resin acid levels (76-2260 µg/l, with a mean of 1035 µg/l).

The ratios of each individual fatty acids to total fatty acids is basically constant (Figure 5.5).

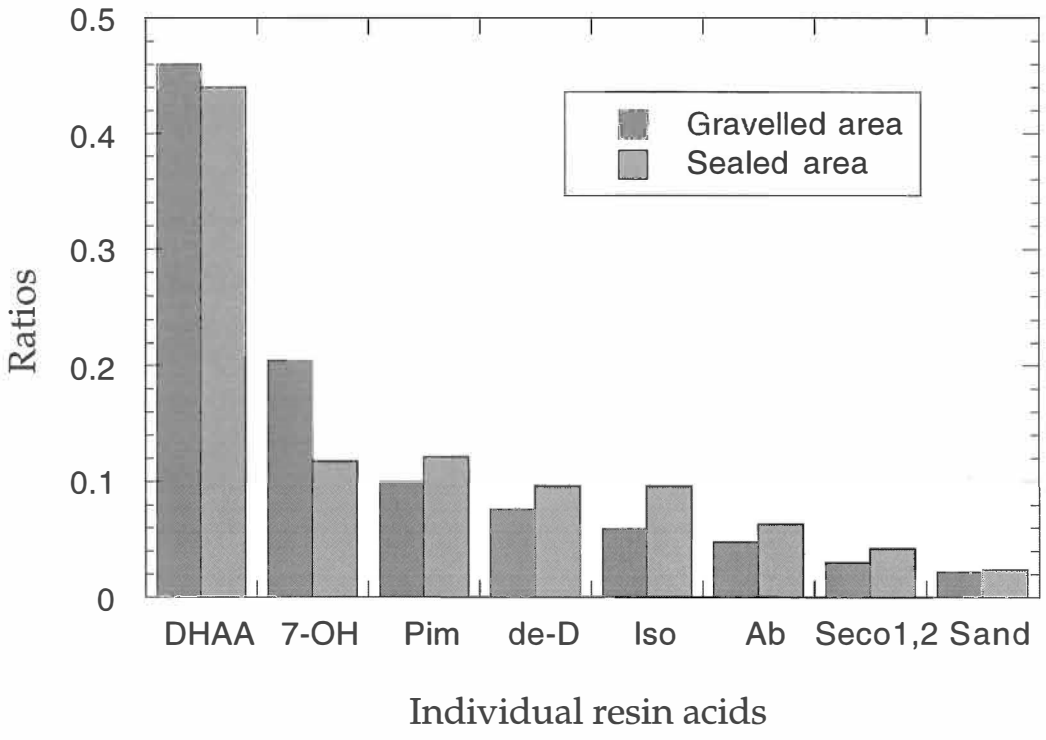

Figure 5.4 Ratios of individual resin acids to total resin acids identified in the runoff samples from gravelled and sealed wharf areas. The details of these samples are shown in Table 5.1.

The total fatty acid levels of the two adjacent urban runoff samples, 17 and 11 μg/l, were 5.8% and 8.9% of that in the untreated wharf runoff (190 μg/l). In the case of resin acid, the resin acid level of the adjacent urban runoff were 0.1% and 0.4% of the untreated wharf runoff samples (1035 μg/l). This suggests that the fatty acids come from multiple sources, instead of bark or wood only. On site observations showed that there were some dried grass, tree leaves, and other organic debris in the adjacent urban runoff. The VSS concentrations of these two urban runoff samples (33 and 96 mg/l) were 7.4 and 21.6% of the mean VSS of the wharf runoff samples (445 mg/l). These organic debris contributed appreciable fatty acids to the urban runoff, but little resin acids.

Only low levels of fatty acids (6.4 and 5.4) μg/l, were detected in the two seawater samples.

5.3.2 Organic Acids and Other Parameters

Probably because the VSS in the wharf runoff consist mostly of bark particles which are a source of resin acids, a weak, but significant linear relationship was identified between total resin acids and VSS (Figure 5.6). This means that reducing the VSS concentration of the runoff would effectively decrease the total resin acid level of the runoff. No significant relationship was found between yellow substance and total resin acid levels.

Similar weak linear relationships were also found between VSS and some individual resin acids, for instance, DHAA, isopimaric acid, abietic acid, secodehydroabietic acid isomers, sandaracopimaric acid and pimaric acid (Figure 5.7). There did not appear to be linear relationships between 7-OH dehydroabietic acid, de-DHAA and VSS.

There is also a linear relationship between total fatty acids and VSS in the wharf runoff (Figure 5.8), but the relationship is weaker compared to that between resin acids and VSS. This is probably because VSS is not the only source of fatty acids. These sources have not however been identified.

5.3.3 Variation of Resin Acids during a Storm

Figure 5.9 shows total resin acid levels in the wharf runoff from the sealed and gravelled areas during the two storm episodes. The total resin acid levels of the runoff from both sealed and gravelled wharf areas basically followed the variation of VSS during the two storms. From Chapter 4 we know, there might be "second" or more "flushes" after the "first flush" concerning SS and VSS which depended on the rainfall history. From this finding it can be deduced that there might be "second" or more "flushes" concerning total resin acid concentration as well.

As for the resin acids, the variation in levels of total fatty acids basically followed the VSS (Figure 5.10).

5.3.4 Removal of Organic Acids by Conventional Treatment

Comparing total resin and fatty acid levels of the T2, T2C, and T2F samples, as well as the T10, T10C, and T10F samples (Table 5.8), it is clear that the resin and fatty acid level decreased greatly with the removal of suspended solids by either centrifugation or flocculation-sedimentation. It seems that the flocculation-sedimentation treatment removes organic acids slightly more effectively than centrifugation (Figure 5.11). This is probably because some soluble organic acids were adsorbed by flocculates and removed with the settled flocculate.

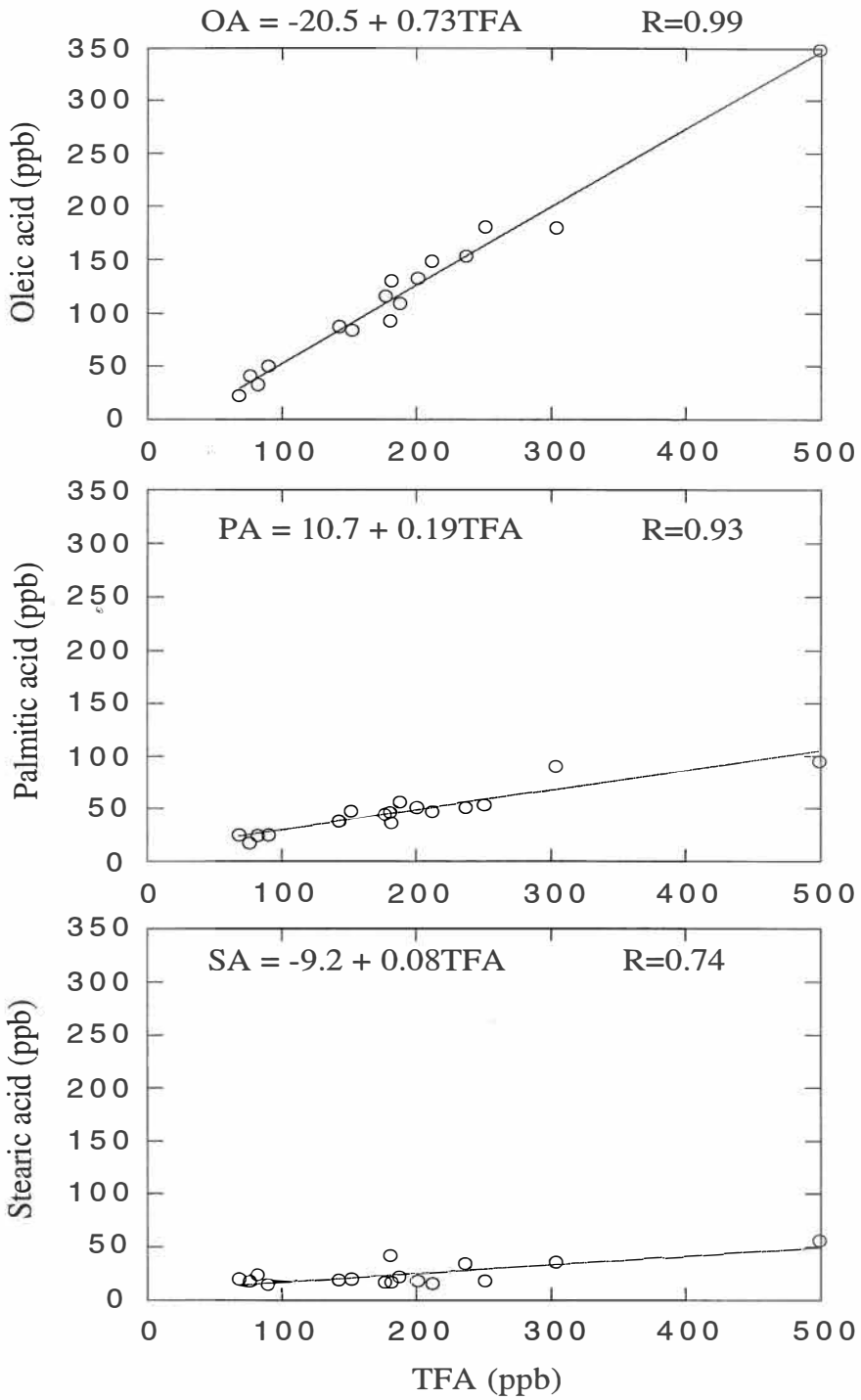

Figure 5.5 Ratios of individual fatty acid to total fatty acids identified in the runoff samples from wharf log handling areas. The details of these samples are shown in Table 5.1.

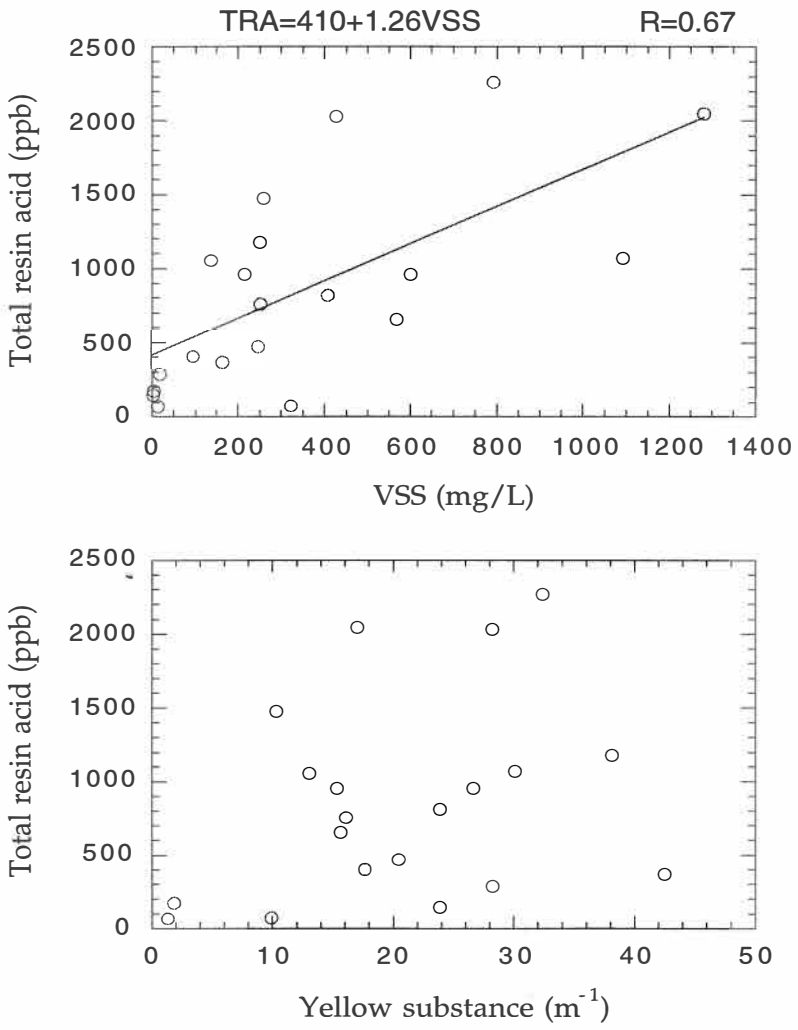

Figure 5.6 Plots of total resin acids against volatile suspended solids (VSS) and yellow substance in the wharf runoff samples, including the treated ones.

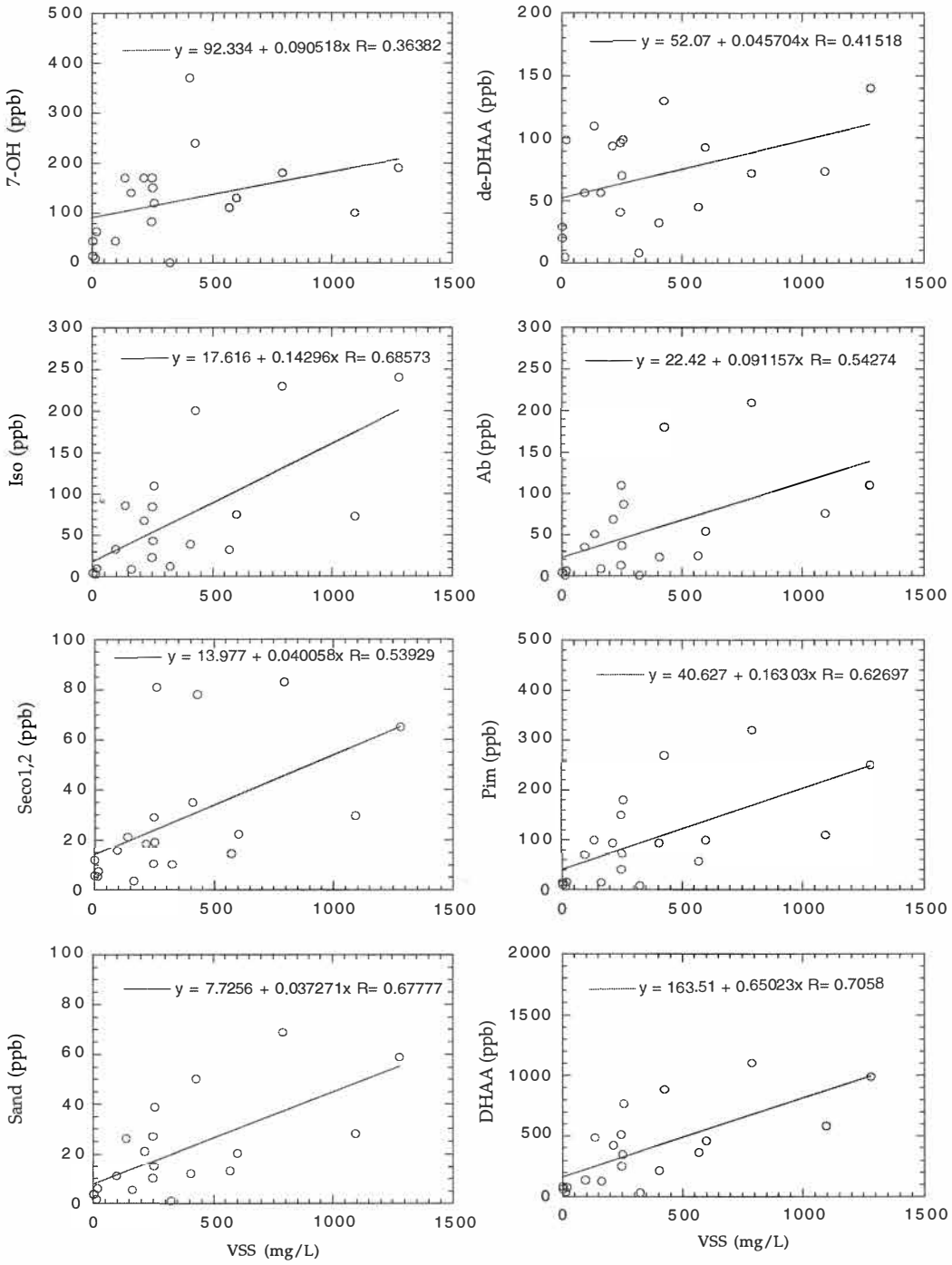

Figure 5.7 Plots of volatile suspended solids (VSS) against individual resin acids identified in the wharf runoff samples.

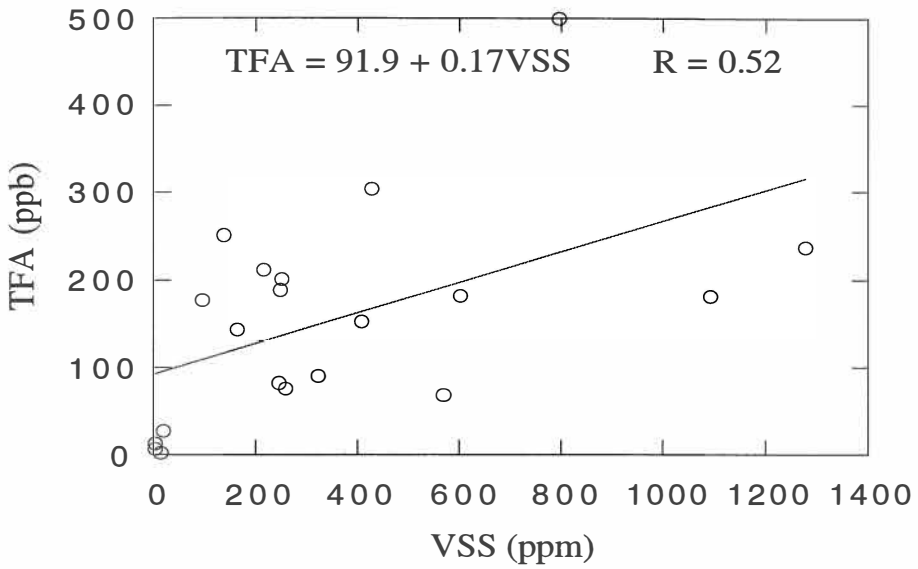

Figure 5.8 Plot of total fatty acids against volatile suspended solids (VSS) in the wharf runoff samples.

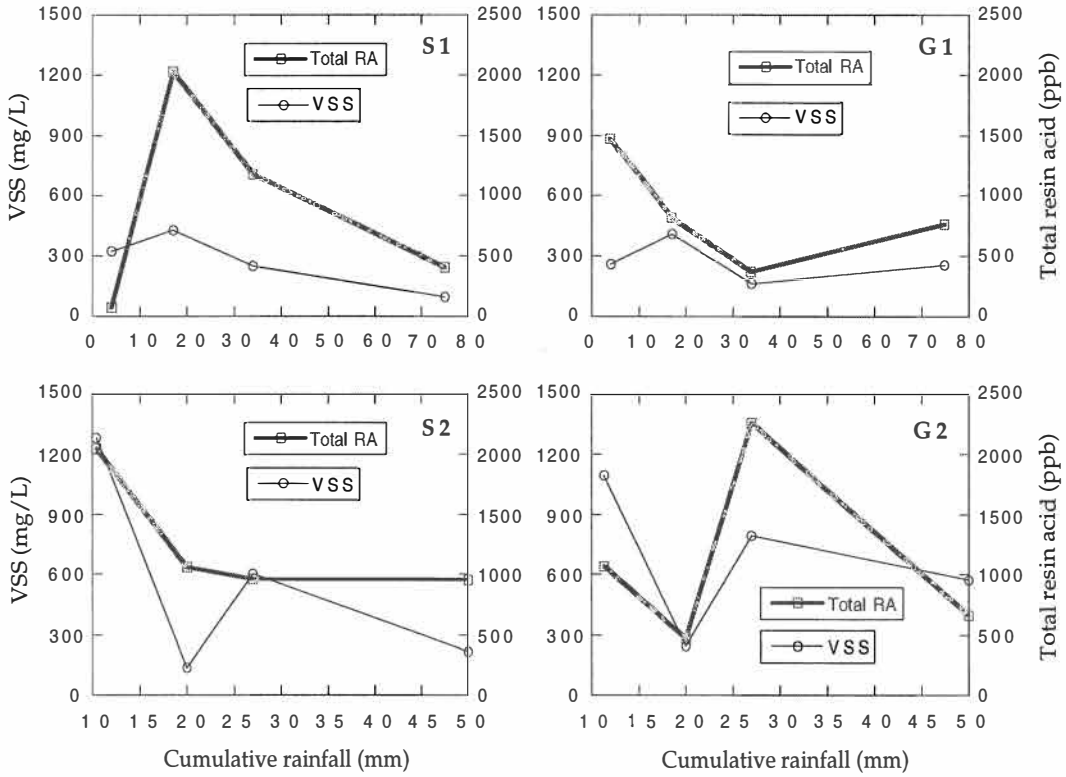

Figure 5.9 Volatile suspended solids (VSS) and total resin acid concentration of the runoff samples collected from the sealed and gravelled areas during storm on May 28, 1995 (S1, G1) and July 25, 1995 (S2, G2).

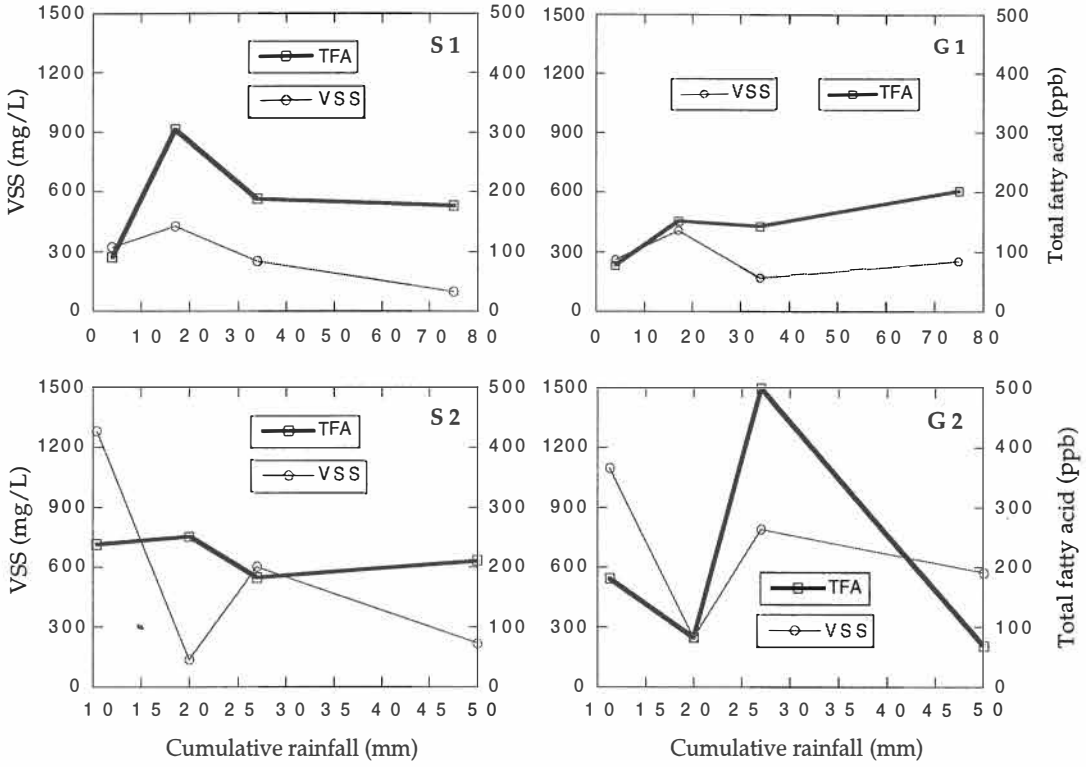

Figure 5.10 Volatile suspended solids (VSS) and total fatty acid concentration of the runoff samples collected from the sealed and gravelled areas during storm on May 28, 1995 (S1, G1) and July 25, 1995 (S2, G2).

5.4 CONCLUSIONS

Based on the GC-MS analyses of 16 untreated wharf runoff samples from both sealed and gravelled areas, 2 runoff samples from the adjacent urban area, 2 seawater samples from the receiving tidal waters, and 4 runoff samples, after removing most of the VSS by centrifugation and flocculation-sedimentation, the following can be concluded:

1. The mean total resin levels in the wharf runoff water samples was 1030 μg/l.

2. The mean resin acid level of 1030 µg/l is comparable to that of 1000 µg/l reported at which acute toxicity is likely to be exhibited. However, because of the quick and massive dilution of the wharf runoff in the receiving tidal waters (see Chapter 9), there have been no reports of acute toxicity among harbour fish.

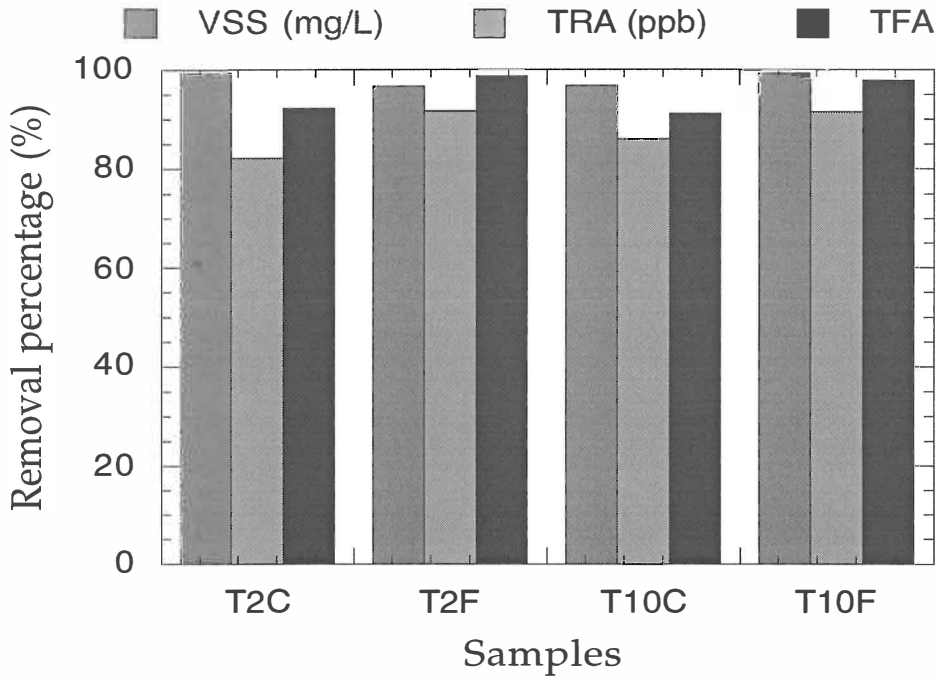

Figure 5.11 Removal efficiency of volatile suspended solids (VSS), fatty acids, and resin acids by centrifugation and flocculation-sedimentation for the samples T2 and T10.

3. Dehydroabietic acid was identified as the dominant individual resin acid in the extracts of wharf runoff samples, and typically represents 45% of total resin acids.

4. Palmitic, stearic and oleic acids were the dominant fatty acids in the wharf runoff samples. The mean total fatty acid level (190 µg/l) was lower than the total resin acid level (1030 µg/l).

5. Weak, but significant linear relationships between total resin acids, fatty acids and volatile suspended solids (VSS) were identified. As the mean VSS concentration of the wharf runoff from the sealed area is significantly lower than that of the runoff from the gravelled wharf, sealing the entire wharf surface will substantially decrease the wharf resin and fatty acid level of the runoff.

6. Conventional treatment, designed to remove volatile suspended solids, could effectively reduce the total resin and fatty acid level.

7. The variation of resin and fatty acid levels during storm events basically followed the time course of VSS.

CHAPTER SIX

WHARF RUNOFF WATER QUALITY
IV. BOD, NUTRIENTS, OIL AND GREASE

CHAPTER SIX

STORM RUNOFF WATER QUALITY IV. BOD, NUTRIENTS, OIL AND GREASE

6.1 BIOLOGICAL OXYGEN DEMAND

6.1.1 Introduction

The biological oxygen demand (BOD) determination is an empirical test in which standardised laboratory procedures are used to determine the relative oxygen requirement of wastewaters, effluents and polluted waters (APHA, 1992). The BOD level in any effluent is always of concern to environmental authorities because there is a potential depletion of dissolved oxygen in the receiving water after the effluent is discharged into a water body. Accordingly, the BOD levels in the storm runoff from the log handling areas at the Mount Maunganui wharf were investigated, with the objectives of investigating:

1. the BOD levels of the runoff from the log handling areas, and

2. the possible relationships between BOD level and other factors and parameters, such as land surface pavement types, rainfall history, volatile suspended solid concentrations, and yellow substance.

6.1.2 Methods

Due to time restraints, only 30 runoff samples were analysed for BOD. Details and some selected features of these samples are given in Table 6.1.

Five day BOD (hereafter BOD) was determined by the Waikato Regional Council Laboratory. Determination procedures followed the method (5210B) recommended by *Standard Methods for the Examination of Wastewater* (APHA, 1992).

6.1.3 Results and Discussion

Table 6.1 presents the BOD values, as well as the other parameters, which will be discussed in the following sections, of the 30 samples collected from the sealed and gravel surfaced wharf areas at the Mount Maunganui wharf during three storms from November, 1993 to July, 1994.

The BOD values of the wharf runoff determined in this study, 104 mg/l for the sealed area and 183 (mg/l) for the gravel surfaced area, were comparable to those obtained by previous researchers. Kingett Mitchell and Associates (1993) showed that the BOD values of 7 runoff samples collected from the log handling area at the Mount Maunganui wharf during 4 storm episodes ranged from 92 to 470 mg/l, with a mean of 140 mg/l. The BOD values of the runoff from log yard and dry deck in USA paper mills were 352 and 110-300 mg/l (NCASI, 1992).

Mean BOD values in urban storm runoff have a wide range of 9 to 31 mg/l (Makepeace, *et al.*, 1995). Compared to the urban runoff, the mean BOD value of the wharf runoff obtained in this present study was in the order of 5-15 times that of the urban runoff.

Typical BOD values of untreated domestic effluent range from 110 mg/l to 400 mg/l (Makepeace, *et al.*, 1995). In Tauranga, the typical BOD value of untreated municipal effluent is about 200 mg/l (BECD Steven, 1991), slightly higher than that of the wharf runoff.

Table 6.1 The concentrations (mg/l) of suspended solids (SS), volatile suspended solids (VSS), BOD, total Kjeldahl nitrogen (TKN), nitrate nitrogen (NO_3-N), total phosphorus (TP), dissolved reactive phosphorus (DRP), and oil and grease (OAG) of the runoff samples collected from the sealed and gravel surfaced log handling areas at the Mount Maunganui wharf during three storms from November, 1993 to July, 1994. C.R: cumulative rainfall (mm).

Sample No.*	C.R	SS	VSS	BOD	TKN	NO3-N	TP	DRP	OAG
G2-1	10.4	2580	1160	100	3.8	0.034	5.9	1.1	1.3
G2-2	14.2	5480	2030	75	3.1	0.028	3.9	1.0	0.6
G2-3	15.5	1430	650	280	6.6	0.041	4.4	1.2	0.8
G2-4	15.5	385	245	350	13.4	0.052	4.7	1.8	0.7
G2-5	15.5	185	175	330	9.5	0.060	4.1	2.0	0.6
G5-1	10.4	1145	445	110	4.2	0.036	6.4	2.6	1.6
G5-4	16.0	1260	455	160	3.7	0.040	5.2	2.4	1.2
G5-6	19.5	535	245	110	7.2	0.037	4.8	1.9	0.9
G5-8	26.3	2740	785	210	6.8	0.056	9.8	4.0	1.4
G5-9	50.3	1630	565	84	3.3	0.026	6.6	3.1	1.4
G5-10	63.0	2260	730	130	4.9	0.033	8.8	3.0	1.3
S1-1	2.0	159	96	28	1.2	ND	2.8	1.4	1.0
S1-3	3.0	136	89	24	1.0	ND	1.8	1.1	1.0
S1-5	4.6	112	71	12	0.7	ND	1.4	0.9	0.7
S1-7	6.2	174	112	120	2.9	ND	5.4	3.1	1.0
S1-9	7.2	122	78	73	2.1	ND	6.8	3.7	1.0
S1-11	11.1	164	90	80	2.8	ND	1.2	0.5	1.0
S1-12	20.2	260	154	64	2.7	ND	8.3	4.1	1.0
S1-13	20.2	548	324	90	4.8	ND	8.0	4.3	1.0
S2-1	10.4	1840	870	88	1.2	0.022	2.1	1.2	0.5
S2-2	15.1	240	220	190	2.8	0.052	3.4	2.6	1.1
S2-3	15.5	425	340	170	2.6	0.034	3.6	3.0	0.4
S2-4	15.5	215	170	220	3.8	0.063	4.4	2.9	1.4
S2-5	15.5	230	210	210	2.9	0.054	4.1	3.2	0.7
S5-1	10.4	1940	1280	65	1.7	0.027	2.2	0.8	0.7
S5-4	16.0	198	158	74	2.1	0.022	2.1	1.4	1.2
S5-6	19.5	200	138	99	2.5	0.037	4.8	2.1	0.9
S5-8	26.3	1095	605	80	1.6	0.031	3.7	2.2	0.9
S5-9	50.3	348	214	140	3.4	0.043	3.5	1.4	0.4
S5-10	63.0	796	488	140	2.9	0.047	3.4	1.4	0.8

* The first capital letter S or G of a sample number means the sample comes from the sealed or gravelled wharf areas; the number immediately after the capital letter refers to which storm event the sample was collected; and the number after the bar is the sequence number in the same storm episode.
ND: not determined.

Although the average suspended solid concentration and BOD value (1910 and 183 mg/l) of the runoff from the gravelled area were significantly higher than those (500 and 104 mg/l) of the runoff from the sealed area, no significant relationships between BOD and suspended solids or volatile suspended solids were found. Instead, there was a strong linear relationship

between BOD and soluble yellow substance (Figure 6.1). This relationship has not been reported from previous researchers. However, an overall correlation of dissolved organic carbon (DOC) and yellow substance was reported (Gjessing, 1976, cited by Davies-Colley *et al.*, 1987) and the yellow substance comprised typically 40-60% of the total DOC (Thurman, 1983).

Williamson's investigation (1985) on water duality of urban runoff indicated that all the parameters measured in his study, except nitrogen, were predominantly associated with particulate material and closely followed the variation pattern of suspended solids during a storm. However, the BOD values of the runoff from the sealed and gravelled areas during two storm episodes did not follow the variation pattern of suspended solids and always remained at a relatively high level (Figure 6.2). Further study is needed to understand how BOD values of the wharf runoff vary and which factors control the variation during a storm.

Care must be exercised in assessing the potential impact of BOD if toxins are one component of the BOD. From Chapter 5, the wharf runoff contains significant concentrations of resin and fatty acids which may be part of the BOD in the examined water samples. However, compared with the average BOD levels (133 mg/l), the contribution of resin acid (1000 μg/l) to the BOD in the runoff samples is negligible. Therefore, the main concern of BOD in the wharf runoff is the potential depletion of dissolved oxygen in the receiving tidal waters. The potential impact of resin acids on marine life is being investigated separately from this project.

6.1.4 Conclusions

Based on measurement of BOD of the 30 runoff samples collected from the sealed and gravelled wharf log handling areas during three storm events, the following conclusions can be made:

1. The overall BOD level of the wharf runoff (133 mg/l) is comparable to that of typical weak untreated domestic effluent.

2. The wharf surface pavement types had a significant influence on BOD levels of the wharf runoff.

3. A strong linear relationship between BOD and yellow substance was found.

4. The BOD levels did not follow the variation pattern of suspended solids or volatile suspended solids during a storm.

6.2 NUTRIENTS

6.2.1 Introduction

Nutrients (nitrogen and phosphorus) stimulate the growth of aquatic plants. The adverse impacts related to the discharge of excessive amount of nutrients to a water body lie in the accelerated enrichment which would result in dissolved oxygen depletion.

Most nutrients in urban runoff are leached from the atmosphere by rainwater, washed from soils, and from decaying plant material (Anon, 1996). As these possible sources exist around the log handling areas, it is likely that the runoff from the log handling areas has a relatively higher concentration of nutrients, and this hypothesis was investigated.

6.2.2 Methods

Four parameters, total Kjeldahl nitrogen, nitrate, total phosphorus, and dissolved reactive phosphorus, were determined by R. J. Hill Laboratory of Hamilton, a registered laboratory. Determination of these parameters

followed the methods recommended by *Standard methods for the examination of water and wastewater* (4500P-C, 4500-NO_3^{-1}-G, APHA, 1992).

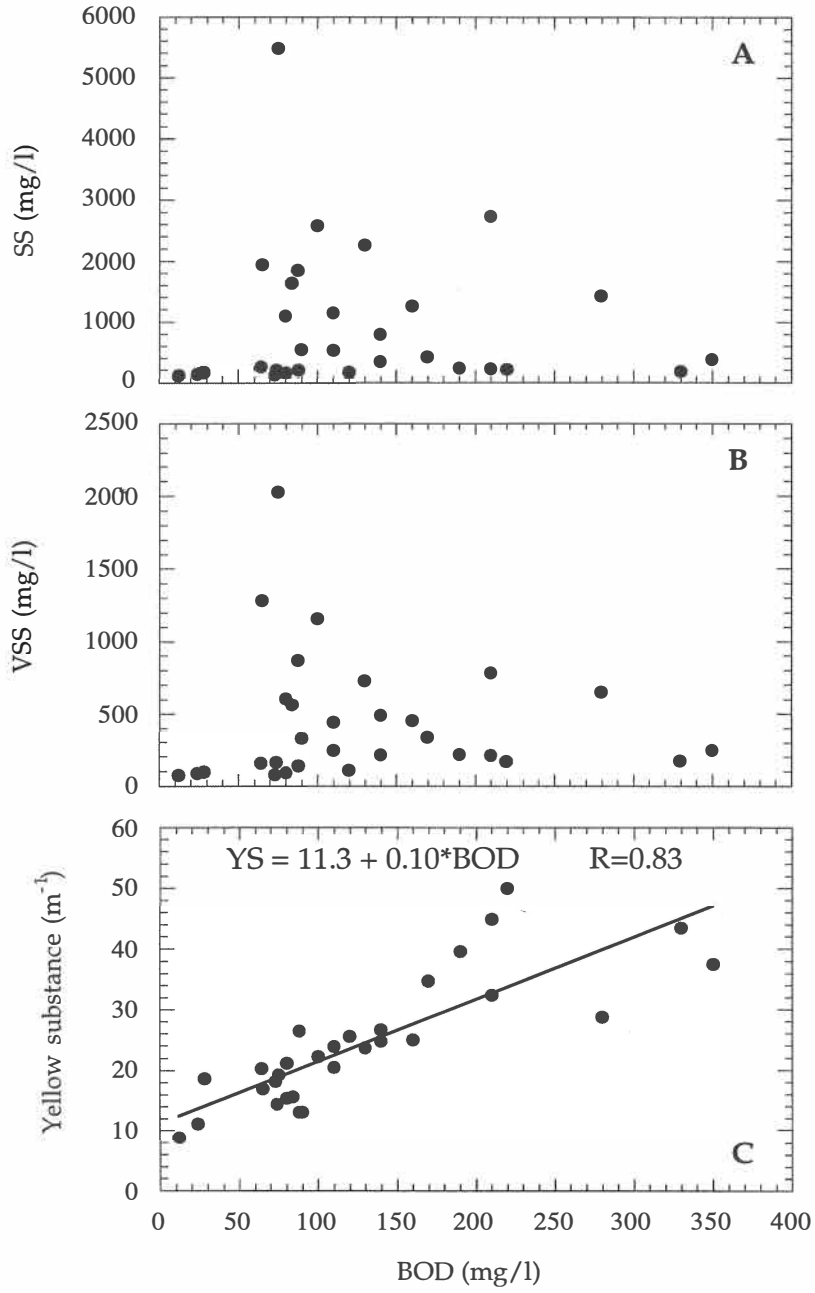

Figure 6.1 Plots of BOD against suspended solids (A), volatile suspended solids (B), and yellow substance (C) of the 30 runoff samples collected from the sealed and gravelled log handling areas at the Mount Maunganui wharf during three storms from November, 1993 to July, 1994.

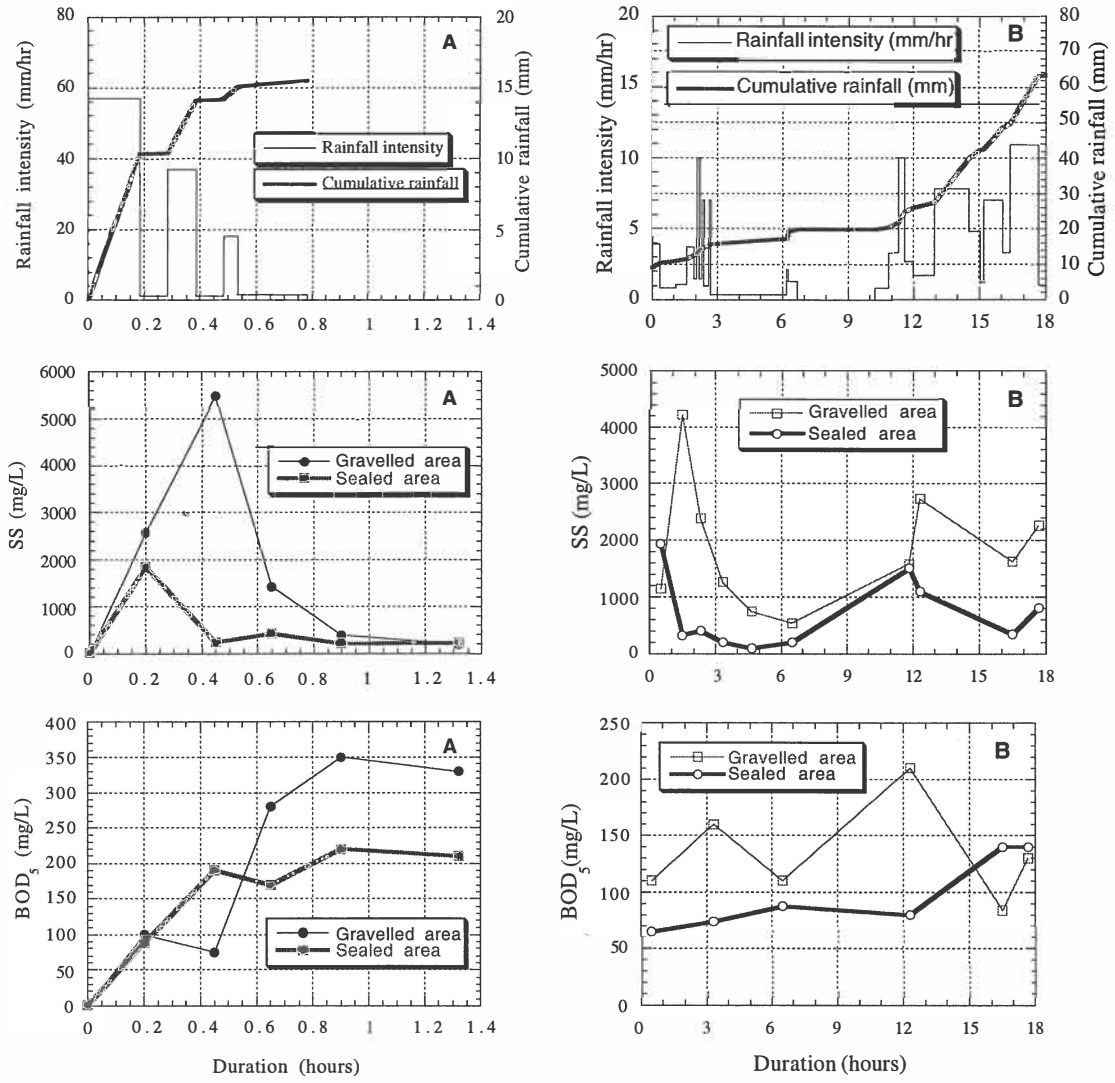

Figure 6.2 Suspended solid concentration and BOD values of storm runoff samples collected from the sealed and gravelled log handling areas at the Mount Maunganui wharf, during the storms of March 17, 1994 (A) and of July 25, 1994 (B).

For the same reasons mentioned in Chapter 5, only 30 samples were analysed. The details and selected features of these samples are shown in Table 6.1.

6.2.3 Results and Discussions

6.2.3.1 Phosphorus

From Table 6.1, the average total phosphorus (TP) concentration of the wharf runoff from the sealed and gravelled log handling areas was 3.8 and 5.8 mg/l. The dissolved reactive phosphorus concentration (DRP) was 2.1 and 2.2 mg/l for the runoff from the sealed and gravelled areas.

The TP level of the runoff from the gravelled wharf areas is significantly higher than that from the sealed wharf area, but little difference occurs for DRP. In other words, the difference of TP levels in the runoff from the gravelled and sealed areas comes from the particulate phosphorus or the soluble phosphorus adhering to the particulate substance. Although the TP level, suspended solids, and volatile suspended solid concentration of the runoff from the gravelled area are significantly higher than those in the runoff samples from the sealed wharf area, no significant relationships of suspended solid and volatile suspended solid concentration against TP were identified (Figure 6.3).

Linear relationships between DRP and TP were found for the runoff samples from both sealed and gravelled wharf areas (Figure 6.4).

The DRP concentrations of 7 runoff samples collected from the log handling area at the Mount Maunganui wharf during four storm events ranged from 0.76 to 2.80 mg/l, with a mean of 1.4 mg/l (Kingett Mitchell and Associates, 1993). The DRP level determined in this study was slightly higher than those of storm runoff from log handling areas obtained in previous studies.

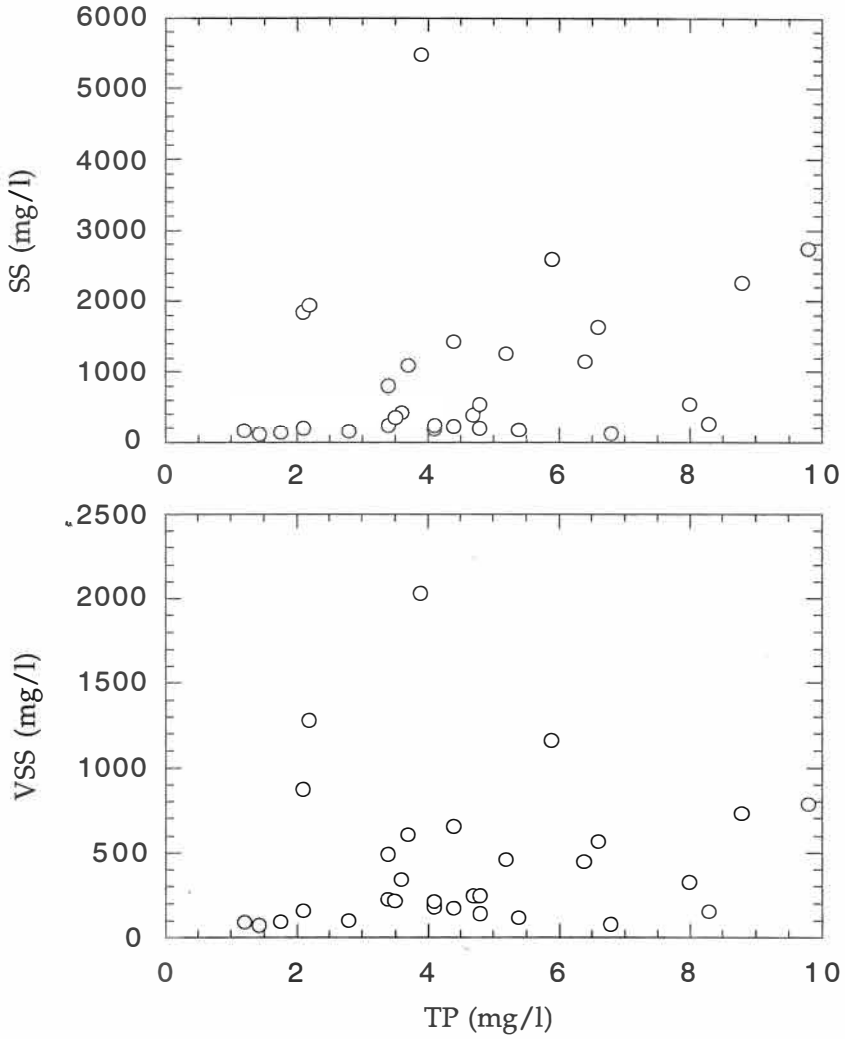

Figure 6.3 Plots of total phosphorus (TP) against suspended solids and volatile suspended solids of the storm runoff samples collected from the sealed and gravelled area at the Mount Maunganui wharf during three storms from November, 1993 to July, 1994.

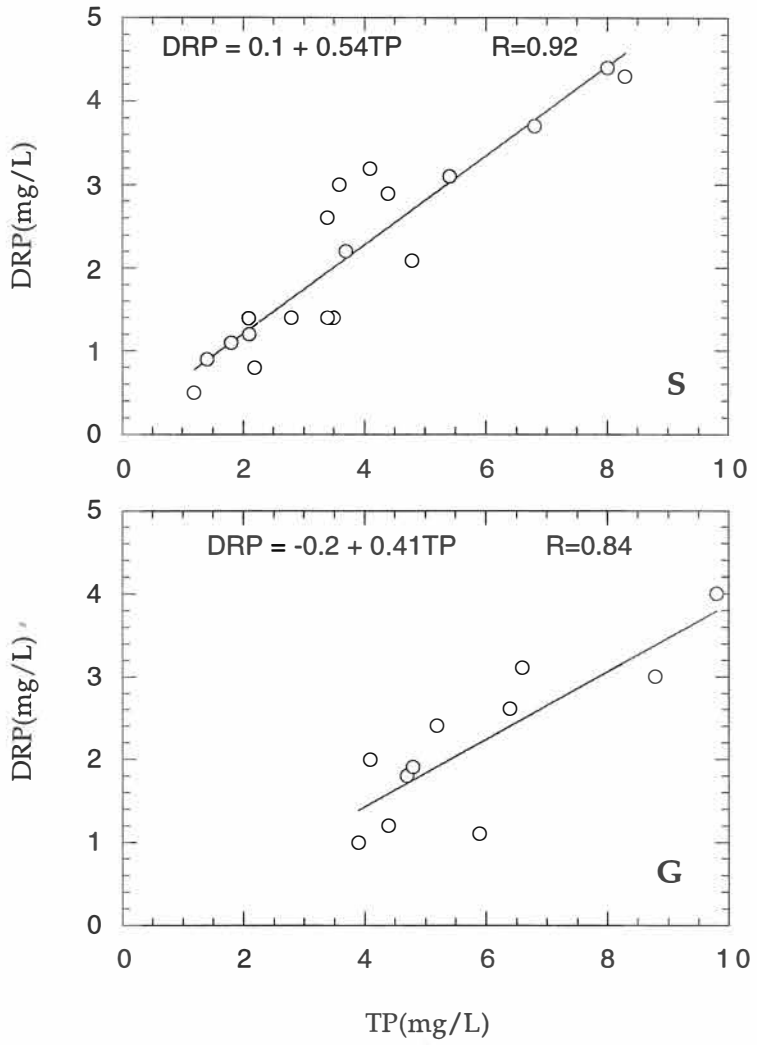

Figure 6.4 Plots of dissolved reactive phosphorus (DRP) against total phosphorus (TP) of the storm runoff samples collected from the sealed area (S) and gravelled area (G) at the Mount Maunganui wharf, Tauranga, during three storms from November, 1993 to July, 1994.

According to Makepeace (1995), TP concentration in urban storm runoff has been found ranging from 0.01 to 7.3 mg/l, with means of 0.015 to 0.82 mg/l. Soluble phosphorus concentrations in urban storm runoff range from 0.038 to 3.52 mg/l, and particulate phosphorus concentrations range from 0.014 to 2.85 mg/l. The mean TP level in the wharf runoff obtained in this study was substantially higher than that of urban runoff. This is probably due to the

availability of more tree leaves and fertilisers, which are two of the main phosphorus sources (Makepeace, 1995) around the log handling areas.
The average TP and DRP levels of the receiving water samples taken from three sampling sites along the Mount Maunganui wharf monthly from July, 1990 to July, 1991 by Environment BOP were 0.021 and 0.007 mg/l, respectively (McIntosh, 1993). The average TP and DRP levels of the wharf runoff were about 210 and 300 times more than those of the receiving tidal waters.

Compared to the average TP level (8 mg/l) of the domestic effluent in Tauranga after secondary treatment (Power, 1990), the TP concentration in the wharf runoff is lower.

Similar to the variation of BOD, the TP and DRP levels did not follow the variation pattern of SS during the two storms examined in this study (Figure 6.5). The TP and DRP concentration did not vary as greatly as SS during the two storms. Further study is required to identify the cause of the variation pattern of TP and DRP.

6.2.3.2 Nitrogen

From Table 6.1, the average total Kjeldahl nitrogen (TKN) concentration of the runoff from the gravelled log handling area (5.93 mg/l) was significantly higher than that from the sealed area (2.4 mg/l).

Although the TKN level of the wharf runoff samples from the gravelled area is considerably higher than that from the sealed wharf area, no significant relationships between suspended solids and TKN was identified (Figure 6.6).

Urban stormwater has a wide range of TKN concentrations from 0.32 to 16.0 mg/l (Makepeace, 1995). The mean total nitrogen of urban runoff ranges from 3 to 10 mg/l (Browne, 1990). The average TKN concentration of the

wharf runoff either from the sealed or gravelled areas was at a similar level compared to that of the urban runoff. In other words, the nitrogen should not be of special concern to local environmental authorities compared to that of common urban runoff.

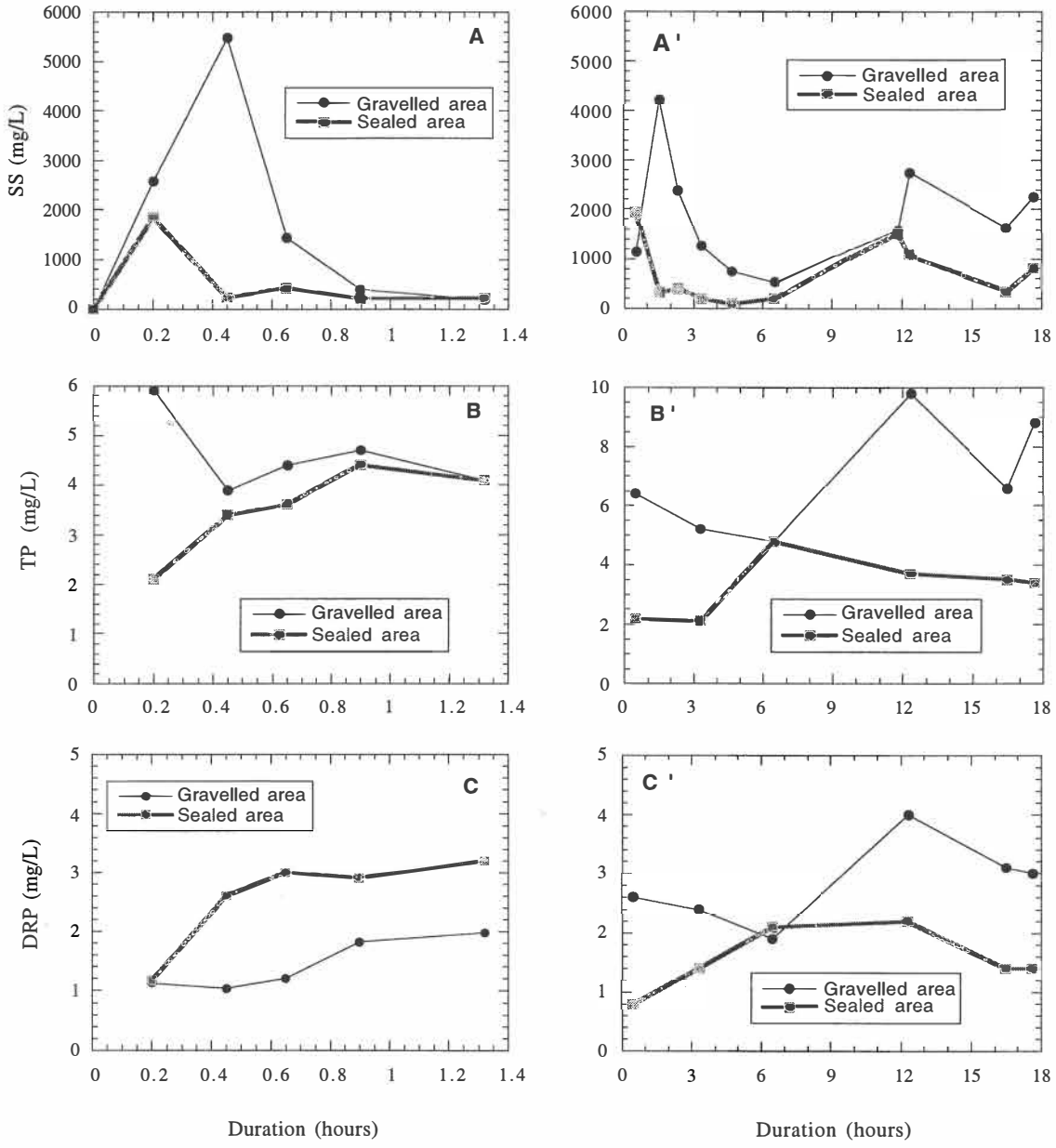

Figure 6.5 Suspended solid concentration, total phosphorus (TP), and dissolved reactive phosphorus (DRP) of the storm runoff samples collected from the sealed and gravelled log handling areas at the Mount Maunganui wharf, during the storms of March 17,, 1994 (A, B, and C) and of July 25, 1994 (A', B', and C').

Unlike BOD levels of the wharf runoff which is comparable to the domestic effluent, the TKN level in the wharf runoff is significantly lower compared to that of domestic effluent. For example, the typical average TKN concentrations of the USA domestic effluent is 40 mg/l, much higher than that of the wharf runoff.

Similar to the variation of BOD, TP, and DRP, TKN did not follow the pattern of suspended solids during a storm (Figure 6.7). TKN did not vary as greatly as suspended solids. This result is in accord with that obtained by Williamson (1985).

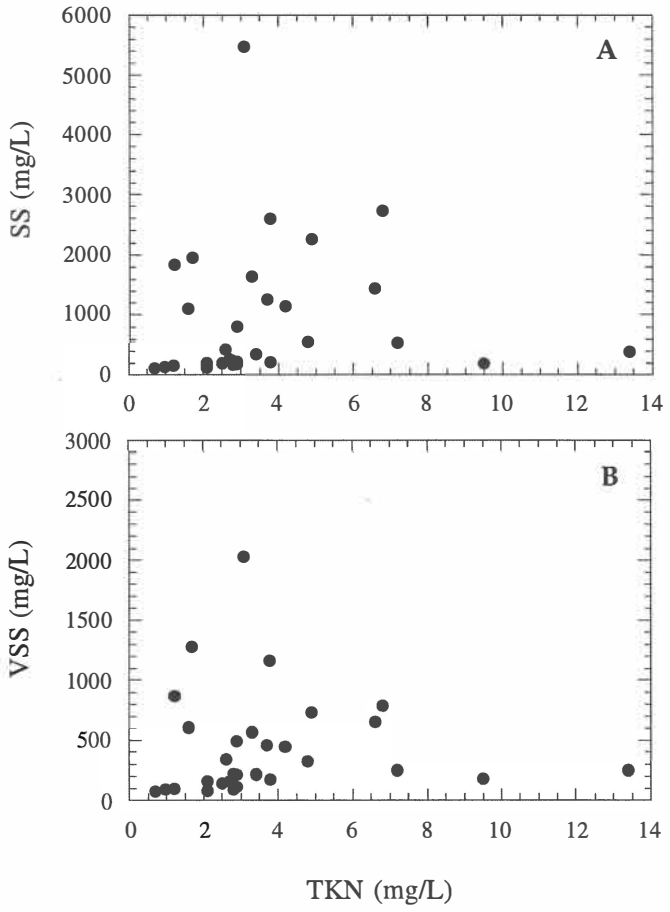

Figure 6.6 Plots of BOD against suspended solids (A), volatile suspended solids (B), and yellow substance (C) of the 30 runoff samples collected from the sealed and gravelled log handling areas at the Mount Maunganui wharf, Tauranga, during three storms from November, 1993 to July, 1994.

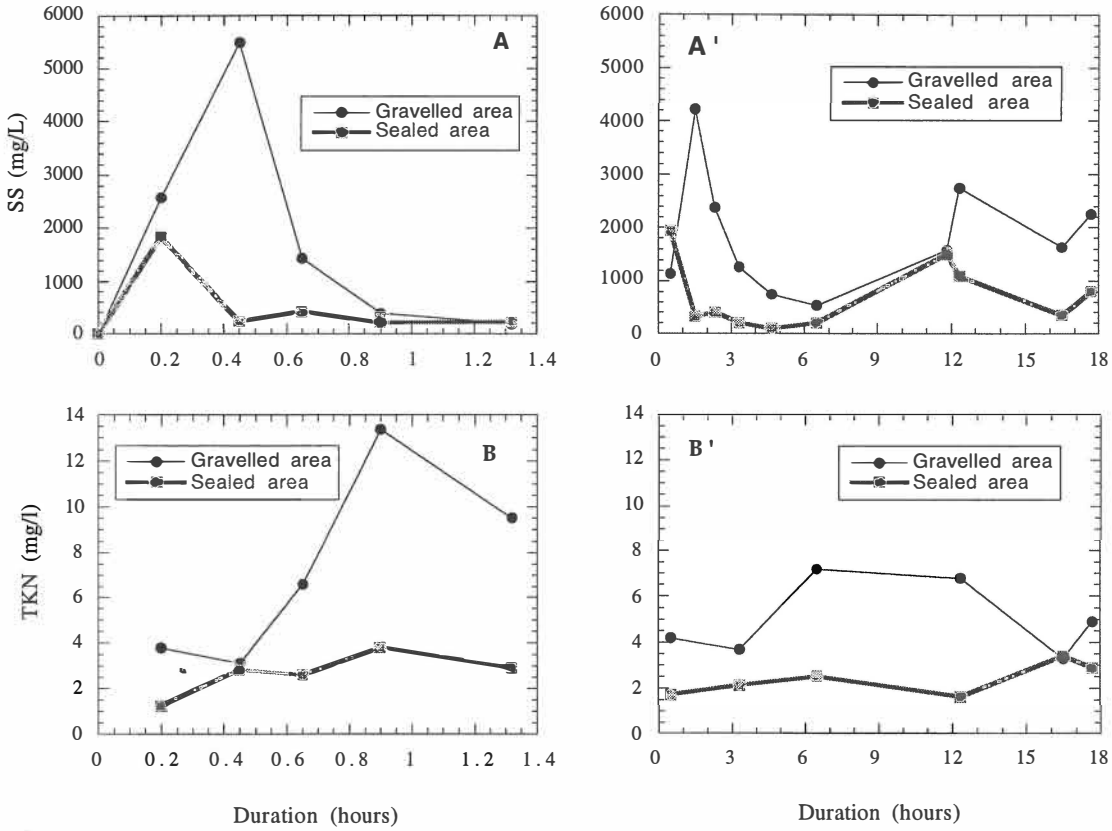

Figure 6.7 Suspended solid concentration and BOD values of storm runoff samples collected from the sealed and gravelled log handling areas at the Mount Maunganui wharf, Tauranga, during the storms of March 17,, 1994 (A) and of July 25, 1994.

Average nitrate concentration was 0.041 and 0.040 mg/l respectively. According to Makepeace (1995), the nitrate level of urban runoff ranged from 0.01 to 12 mg/l. The average nitrate concentration of the receiving tidal water at Tauranga was 0.098 mg/l (McIntosh, 1993). Accordingly, the nitrate nitrogen of the wharf runoff from the log handling area should not be of concern because it contributes little nitrate to the receiving water.

6.2.4 Conclusions

1. The average concentration of total phosphorus was substantially higher than that of urban runoff.

2. There is linear relationship between dissolved reactive phosphorus and total phosphorus in the wharf runoff.

3. The total Kjeldahl nitrogen was at the similar level compared to typical urban runoff and the nitrate concentration was significantly lower than that of urban runoff.

4. The levels of total phosphorus, dissolved reactive phosphorus, and total Kjeldahl nitrogen did not follow the variation pattern of suspended solids during a storm. These three parameters did not vary as greatly as the suspended solids during a storm.

6.3 OIL AND GREASE

6.3.1 Introduction

Oil and grease, which may cause surface film and shoreline deposits if present in excessive amounts, is one of the main contaminants contributing to the environment from urban storm runoff. The oil and grease contribution from urban runoff to the ocean was estimated at approximately 5% of total input (Anon, 1975, cited by Stenstrom *et al.*, 1984) or even more (Eganhouse *et al.*, 1981a and 1981b).

Oil and grease emissions from vehicles, most notably from crankcase oil emission, are the main hydrocarbon sources to urban storm runoff (Wakeham, 1977; Hunter *et al.*, 1979; and MacKenzie *et al.*, 1979) although there are many other sources. As trucks, graders, and loaders work around the log handling areas 24 hours a day, there is a possibility that oil leakage occurs from these vehicles, hence some oil and grease get into the receiving water with the runoff during a rainfall event. This author was unable to find any information on oil and grease levels in the stormwater runoff from a log handling area. Even for urban runoff, the information on oil and grease and hydrocarbon pollution is much less intensive than other aspects

related to urban runoff pollution. The following presents the oil and grease levels determined in this study of the stormwater runoff from the log handling area at Mount Maunganui wharf.

6.3.2 Methods

The partition-infrared method (5520C) recommended by *Standard methods for the examination of water and wastewater* (APHA, 1992) was used to determine oil and grease in the runoff samples. Analyses were carried out by R. J. Hill Laboratory of Hamilton.

6.3.3 Results and Discussion

The average oil and grease level in the wharf runoff from the sealed and gravel surfaced wharf areas were 0.9 and 1.1 mg/l (Table 6.1).

The oil and grease level in urban storm runoff have a wide range from 0.001 to 110 mg/l (Makepeace, 1995). The average oil and grease level in the runoff from residential areas, parking lots, bridge, freeways, terrace houses, and suburbs are 4.1, 15.3, 27, 44, 30, and 47 mg/l, respectively (Stenstrom, *et al.*, 1984; Wakeham, 1977; and Soderlund *et al.*, 1972). Compared to the urban runoff from different land uses, the oil and grease level of the wharf runoff was significantly lower. This is likely due to two reasons: relatively less traffic around the log handling areas compared to the above mentioned urban areas and well maintained vehicles used in the log handling areas.

The typical criteria for the discharge of oil and grease in urban runoff is "no visible discharge" (Environment BOP, 1995, NCASI, 1992). From the results obtained from the present study, it is evident that the storm runoff from the log handling area will meet the discharge criteria set by the local environmental authorities.

6.3.4 Conclusion

Oil and grease should not be a major concern due to its lower concentration (1.0 mg/l) compared to the discharge criteria and the common urban runoff.

6.4 SUMMARY OF STORM RUNOFF WATER QUALITY

A comprehensive investigation was undertaken into optical quality, extractable organic substance, oxygen demand material, nutrients, and oil and grease of 123 runoff samples (only part of the samples were examined for some parameters) collected from the wharf log handling areas and the adjacent urban area during seven significant storm episodes.

The optical quality of the wharf runoff is degraded due to addition of bark and soil-like particles. The black disk visual clarity (0.01-0.02 m) was only 0.5-1.0% of that in the receiving tidal waters. The wharf runoff appears very dark gray to yellowish brown in apparent colour (10YR1/3 to 10YR5/6 Munsell colour chart) and has a soluble yellow substance concentration of about 25 m^{-1}. Power relationships between the traditionally used parameters, for example, suspended solids and turbidity, were identified. The wharf surface pavement types had a significant influence on visual clarity, but little influence on yellow substance concentration.

The potentially toxic resin acids in the wharf runoff has been determined with SIM GC-MS. The average total resin acid level (1,030 ppb) is comparable to that of 1,000 ppb reported at which acute toxicity is likely to be exhibited. A relationship of resin acids against volatile suspended solids was established. Conventional treatment methods of natural sedimentation and flocculation-sedimentation are able to remove the resin acids effectively.

The levels of biological oxygen demand (BOD), total phosphorus and nitrogen in the wharf runoff are considerably higher than those of common

urban runoff. However, the wharf runoff contributes little nitrate nitrogen and oil and grease to the receiving environment.

CHAPTER SEVEN

CONTAMINANT LOAD

CHAPTER SEVEN

CONTAMINANT LOAD

7.1 INTRODUCTION

Chapters 2 to 6 discussed the volume and water quality of storm runoff from the log handling areas at the Mount Maunganui wharves. However, in order to assess the long term environmental impact related to the log operation and the contribution of contaminants from the log handling area to the local ecosystem, it would be helpful to quantify the maximum available source of contaminants from the log handling area, specially particulate substance, and the actual annual contaminant input from the storm runoff. To address this issue, in this chapter we investigate:

i) the maximum available source of particulate substance from the log handling area, and

ii) the annual contaminant loading to the receiving tidal waters associated with the discharge of storm runoff from the log handling areas.

7.2 METHODS

The investigation of maximum available source of particulate substance was undertaken at the Sulphur Point wharf (Figure 7.1) because the wharf surface was well sealed, few potholes existed, and the wharf had been used for log handling only a month before this investigation was undertaken.

For estimating the amount of bark and soil material stripped from the logs after the log stacks were shifted, two areas were selected for sampling (Figure 7.1): A1, which had a log stack with an average height of 4.3 m (3.89 m^3/m^2

of logs), and A2, where the log stack had a mean height of 1.3 m (1.15 m^3/m^2 of logs). 12 squares (0.4x0.4 m) were selected randomly within A1 and A2 and the bark and soil material within each square were collected. Efforts were made to collect all the substance including the very fine particles from each selected square.

In the laboratory, the collected samples were dried at 103ºC, sieved and weighed to determine the amount of bark and soil particles at different sizes. Subsequently, the sieved samples with different sizes were burnt at 550ºC for 3 hour to determine the volatile particulate substance, which can approximately be considered as organic substance.

7.3 RESULTS AND DISCUSSION

7.3.1 Maximum Available Source of Particulate Substance

Table 7.1 presents the average amount of bark and soil material at different size ranges per square metre of wharf surface at A1 and A2 (Figure 7.1) after the log stacks were shifted.

5.00 kg/m^2 and 1.42 kg/m^2 of bark and soil material remained at A1 and A2 after the log stacks were shifted. Dividing these results by the log volumes per square metre of wharf surface at A1 and A2, resulted in 1.29 and 1.23 kg of bark and soil material left per cubic metre of logs shifted from A1 and A2. There was not a significant difference for the results between A1 and A2. On average, 1.26 kg of bark and soil material were left on the wharf surface per cubic metre of logs shifted.

Smaller particles are of greater concern because they can be transported easily by the runoff. On average, the particles with a size <4.0 mm account for 29.4% of the total particles left per cubic metre of logs shifted (0.37 kg/m^3).

Table 7.1 The average amount (g) of bark and soil material left per square metre of wharf surface after the log stacks were shifted from A1 (4 samples, the average height of the log stack was 4.3 m) and A2 (2 samples, the average height of the log stack was 1.3 m). ATP: amount of total particles; AVM: amount of volatile particles.

Size (mm)	A1			A2		
	ATP	AVP	AVP/ATP (%)	ATP	AVP	AVP/ATP (%)
>4.0	3582	*		986	*	
1.0-4.0	369	211	57	164	114	70
0.21-1.0	702	219	31	150	48	32
0.063-0.21	303	52	17	85	13	16
<0.063	44	7.1	16	32	5.4	17
Σ	5001			1417		

* AVP was not determined because almost all the particles larger than 4 mm were bark.

The organic fraction is also of concern due to the potential for depleting dissolved oxygen in the receiving water when the organic substances decompose. From Table 7.1, the organic fraction was basically proportional to the particle sizes. Particles >4.0 mm were comprised mainly of bark. For the particles with a size of 1.0-4.0 mm, the organic fraction accounted for 64%, but only 16.5% for particles <0.063 mm. Overall, the organic substance accounted for 38.2% of the particles with a size <4.0 mm. That results in 0.14 kg of organic substance with a size <4.0 mm being left on the wharf surface per cubic metre of logs shifted.

After the log stacks are shifted, the bark and soil material left on the wharf surface is piled and then loaded onto trucks by graders. A significant amount of bark and soil material is removed by the graders (Table 7.2). The removing efficiency was 95% at A1, but only 57% at A2. It appeared that the more the bark and soil material left on the wharf surface before cleaning (5.00 kg/m^2 at A1 and 1.42 kg/m^2 at A2), the greater the mechanical cleaning efficiency. This result is in accord with that obtained by US Naval Radiological Defence Laboratory (Lee *et al.*, 1959; Clark *et al.*, 1963; cited by Sutherland *et al.*, 1978) and Sartor *et al.* (1974). As the heights of most log stacks are around 4-5 m at the Port of Tauranga, the cleaning efficiency

obtained at A1 was reasonable, namely, 0.26 kg/m^2 of bark and soil material still left on the wharf surface after mechanical cleaning.

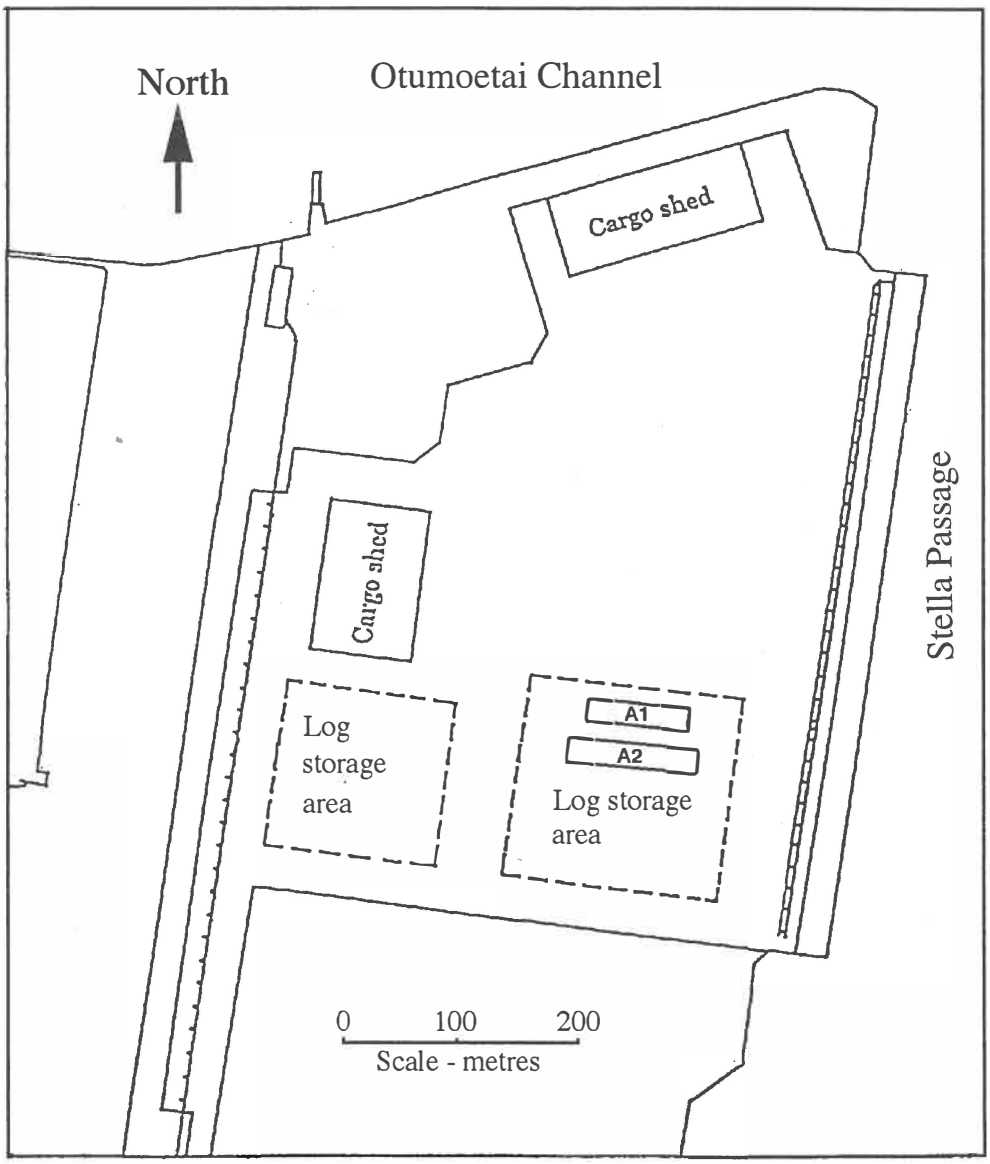

Figure 7.1 The Sulphur Point wharf at the Port of Tauranga, showing the sampling area A1 and A2 when the investigation of maximum available source of particulate substance related log operation was undertaken in September, 1992.

The mechanical cleaning efficiency decreased with reducing particle size (Figure 7.2), from 99.2% for the particles >4.0 mm to 27.3% for the particles <0.063 mm, which are mainly responsible for the deterioration of runoff optical quality. Sartor *et al.* (1974) indicated that a sizeable percentage of the pollution potential of street debris was contained in the very fine silt-like solids fraction (diameter <0.043 mm). These very fine particles, although accounting for only 5.9 % by weight of the total solids, contained approximately a quarter of the total oxygen demand, more than half of the heavy metals, and nearly three quarters of the total pesticides.

Table 7.2 The average amount (g) of bark and soil material per square metre of wharf surface after mechanical cleaning at A1 (3 samples) and A2 (3 samples). The symbols used in Table 7.2 are as the same as those in Table 7.1.

Size (mm)	A1			A2		
	ATP	AVP	AVP/ATP (%)	ATP	AVP	AVP/ATP (%)
>4.0	27	23	86.6	51	46	89.3
1.0-4.0	49	20	41.1	120	60	49.6
0.21-1.0	75	23	30.8	234	73	31.4
0.063-0.21	75	16	20.7	150	48	32.3
<0.063	32	6.4	20.4	52	9.2	17.9
Σ	256	88	34.3	607	236	39.0

As there is a very high cleaning efficiency for large particles, the smaller particles <4.0 mm account for 89.5% of total particles left on ground after cleaning, i.e. 0.23 kg/m^2 of bark and soil material. The average organic fraction of the particles <4.0 mm accounted for 28.4% of total particles <4.0 mm after mechanical cleaning, similar to that before cleaning. That means 0.065 kg/m^2 of organic substance with a size <4.0 mm was still left on the ground after mechanical cleaning.

The calculated maximum available sources of bark and soil material (MASBS) at different sizes at the Port of Tauranga are shown in Table 7.3.

Table 7.3 Calculated maximum annual source of bark and soil material (tonnes) at different sizes from the log handling areas at the Mount Maunganui wharf, before and after mechanical cleaning. Annual log turnover: 2 million tonnes; log density in the field: 0.95 tonne/m^3; MASBS: maximum annual source of bark and soil material; MASBS4: maximum annual source of bark and soil material with a size <4.0 mm; MASOS: maximum annual source of organic substance; MASOS4: maximum annual source of organic substance with a particle size <4.0 mm.

	MASBS	MASBS4	MASOS	MASOS4
Before cleaning	2650	779	*	295
After cleaning	141	124	48	35

* not determined.

As it is practically impossible to reduce the amount of bark and soil material stripping from the logs during log operations, the key to mitigating the available contaminant source is to clean the wharf surface as soon as the log stacks are shifted, and to raise the cleaning efficiency. Based on the initial results in this present study, it is apparent that there is room for improvement in the cleaning efficiency. Sutherland *et al.*, (1978) investigated the effect of different street cleaning operations on the pollutant removal efficiency. Their data suggested that the frequency of street cleaning had the greatest effect on the removal efficiency, and that vacuumised street sweepers are approximately 5 % more efficient than motorised equipment.

7.3.2 Main Contaminant Load

7.3.2.1 Methods

The contaminant loading from the log handling area at the Mount Maunganui wharf, CL (kg), was calculated by:

$$CL = (V_s * C_s + V_g * C_g) * 10^{-3} \qquad (7.1)$$

where, V_s and V_g are the annual runoff volumes from the sealed and gravelled areas (92,300 and 25,300 m^3a^{-1}), C_s and C_g are the average concentrations (g/m^3) of contaminants in the runoff from the sealed and gravel surfaced wharf areas (Table 7.4).

For assessing the contribution of contaminants from unit area of wharf surface, the contaminant load per hectare of sealed and gravelled log handling area per year, $CL_{ha.s}$ and $CL_{ha.s}$ ($kgha^{-1}a^{-1}$), were calculated by the following equations (Table 7.5):

$$CL_{ha.s} = (V_s * C_s / A_s) * 10^{-3} \qquad (7.2)$$

$$CL_{ha.g} = (V_g * C_g / A_g) * 10^{-3} \qquad (7.3)$$

where A_s and A_g are the sealed and gravel surfaced wharf areas (12.4 ha and 6.8 ha).

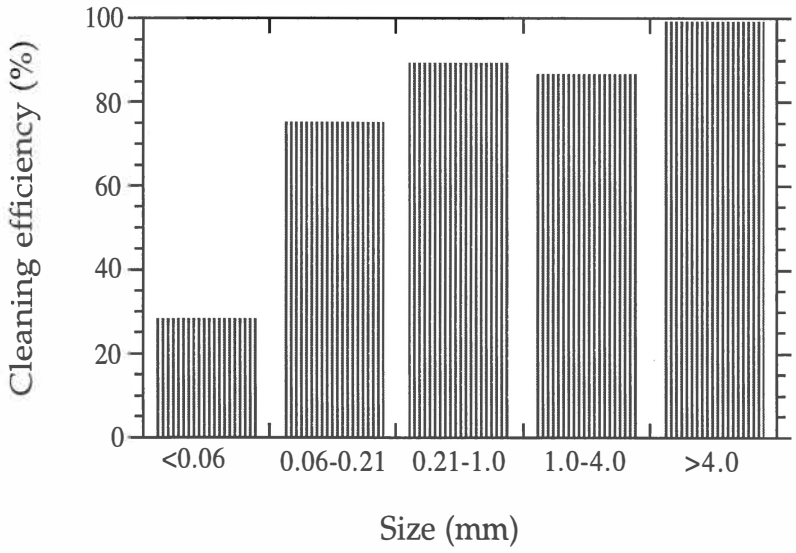

Figure 7.2 Mechanical cleaning efficiencies of the bark and soil material (5.00 kg/m^2 before cleaning) with different particle sizes at the Sulphur Point wharf.

Table 7.4 Average concentrations (g/m^3) of main contaminants in the runoff samples collected from the sealed and gravel covered areas at Mount Maunganui wharf. SS; suspended solids; VSS: volatile suspended solids; BOD: biochemical oxygen demand; OAG: oil and grease; TP: total phosphorus; DRP: dissolved reactive phosphorus; TKN: total Kjeldahl nitrogen; NON: nitrate nitrogen; TRA: total resin acids, sum of nine identified resin acids: pimaric acid, abietic acid, dehydroabietic acid, 7-hydroyx dehydroabietic acid, secodehydroabietic acid-1, secodehydroabietic acid-2, sandaracopimaric acid, isopimaric acid, dehydro-dehydroabietic acid.

Terms	SS	VSS	BOD	OAG	TP	DRP	TKN	NON	TRA
Sample number	110	110	30	30	30	30	30	30	16
Storm events	6	6	3	3	3	3	3	3	2
Sealed area	529	318	104	0.9	3.8	2.1	2.4	0.04	0.81
Gravelled area	1529	549	183	1.1	5.8	2.2	5.9	0.04	1.1

Table 7.5 The main contaminant loading from the storm runoff from the whole log handling areas, and the main contaminant yield rate per hectare of sealed and gravelled areas at the Mount Maunganui wharf. TACL: total annual contaminant load from the entire log handling area at the Mount Maunganui wharf (kga^{-1}); AORB: The number of residents who create the equivalent amount of contaminants through discharging untreated domestic effluent compared to the storm runoff from the wharf log handling areas; AORA: The number of residents who create the equivalent amount of contaminants areas through discharging biologically treated wastewater compared to the storm runoff from the wharf log handling; ACL/HS: annual contaminant load per hectare of sealed wharf surface ($kgha^{-1}a^{-1}$); ACL/HG: annual contaminant load per hectare of gravelled wharf surface ($kgha^{-1}a^{-1}$); the other symbols are as the same as those in Table 7.4.

Terms	SS	VSS	BOD	OAG	TP	DRP	TKN	NON	TRA
TACL	87,500	43,200	14,200	110	500	250	370	4.7	103
AORB	3,300	2,170*	600	9*	520*	--	77*	--	--
AORA	42,700	--	6,940	--	520	--	104*	38	--
ACL/HS	3,940	2,370	770	6.7	28	16	18	0.3	6.0
ACL/HG	5,680	2,040	680	4.1	22	8.2	22	0.2	4.1

* The concentrations of the contaminants in the untreated and treated effluent come from Browne (1990).

-- No data available for the concentration of the terms.

7.3.2.2 Suspended solids and volatile suspended solids

87,500 kg of particulate substance, of which 43,200 kg were volatile, were calculated as entering the receiving tidal water annually from the entire log handling area (19.2 ha).

The average concentration of suspended solids in the runoff from the sealed area was only 36% of that in the runoff from the gravelled area. In other words, future sealing of the gravelled log handling area could significantly reduce the suspended solid concentration. However, the annual suspended solids loading per hectare of sealed area was decreased only 30%. The volatile suspended solids loading rate from the sealed area was even 16% higher than that from the gravelled area, although the volatile suspended solid concentration of the runoff from the sealed area was only 58% of that in the runoff from the gravelled area. This is because the annual storm runoff volume from per hectare of sealed area was doubled due to the decrease of depression storage and infiltration rate (see Chapter 2).

Williamson (1986) investigated the sediment loads from different developing urban areas in New Zealand. The approximate range of sediment yield varied from about 2,500 to 270,000 $kgha^{-1}a^{-1}$ for large catchments with small pockets of construction to small construction sites. However, the suspended solid loads for the developed urban areas were significantly lower. The sediment export rates from residential, commercial and industrial areas ranged from 620-2300, 50-830, and 400-1700 $kgha^{-1}a^{-1}$ (Browne, 1990). Compared to these results, the suspended solids loads from the wharf areas (3,940 and 5,680 $kgha^{-1}a^{-1}$ for sealed and gravelled areas), were approximately equivalent to large urban area with small pockets of construction.

Typical suspended solid concentration of untreated municipal effluent in New Zealand is about 220-250 g/m^3 and the per capita effluent flow is about

330 litres per day (Anon, 1991; Anon, 1994). The annual suspended solids loading to the receiving tidal water from the wharf runoff is equivalent to that of untreated domestic effluent from 2,900 to 3,300 local residents. For the Tauranga region, the water quality of local domestic effluent was improved significantly after secondary treatment (Table 7.6) and the effluent was discharged into the Tauranga Harbour about 1.5 km away from the log handling area. The annual suspended solids load from the wharf log handling area is slightly higher than that from the treated domestic effluent from Tauranga region (85,000 kg).

Table 7.6 Average concentration and annual loads of suspended solid (SS), BOD_5, total phosphorus (TP), and nitrate nitrogen of the effluent from Tauranga District Council Sewage Treatment Plant after secondary treatment. 13,700 m^3 of treated effluent were discharged into the Tauranga Harbour from this Plant daily (Power, 1990).

Terms	SS	BOD_5	TP	NO_3-N
Concentration (g/m^3)	17	17	8	1.16
Annual load (kga^{-1})	85000	85000	400000	8000

7.3.2.3 Oxygen demand substance (BOD_5)

The calculated BOD loading rates from the sealed and gravelled wharf areas are 770 and 680 $kgha^{-1}a^{-1}$. Roesner (1982) investigated the BOD loading rates from 4 cities in the United States and the results were 30.4, 42.6, 34.8, and 113.3 $kgha^{-1}a^{-1}$ for the four cities. Although the BOD loading rates depended on a few factors, such as annual runoff volume and ratio of impervious area to total catchment area, these results can be used as order of magnitude estimates of annual BOD loads. The BOD loading rates obtained from the sealed and gravelled wharf areas were about 6-25 times that of the urban areas.

The BOD values of biologically treated local municipal effluent is about 17 g/m^3 (Anon, 1991). The annual BOD loading to the receiving water from the

entire log handling area at Mount Maunganui wharf (14,200 kg) was equivalent to that from treated local domestic effluent created by 6,940 local residents.

7.3.2.4 Nutrients

The total phosphorus loading rates from the sealed and gravelled wharf areas (28 and 22 $kgha^{-1}a^{-1}$) were substantially higher than those, ranged at 0.4-1.3, 0.1-0.9, and 0.9-4.1 $kgha^{-1}a^{-1}$, from residential, commercial and industrial areas (Browne, 1990).

Compared to the total phosphorus level of Tauranga region domestic effluent after secondary treatment (8 mg/l, Power, 1990), the annual total phosphorus load from the log handling area was equivalent to that of the biologically treated domestic effluent from 520 local residents.

The wharf runoff contributes little nitrate to the receiving tidal waters due to the significantly lower nitrate level in the wharf runoff (0.041 and 0.040 mg/l for the sealed and gravelled areas), compared to those of common urban runoff (0.01 to 12 mg/l, Makepeace, 1995).

Higher total nitrogen load rates were identified from the sealed and gravelled areas (18 and 22 $kgha^{-1}a^{-1}$) compared to those from residential, commercial and industrial areas (5.0-7.3, 1.9-11, and 1.9-14 $kgha^{-1}a^{-1}$,Browne, 1990). However, the annual total nitrogen load from the wharf runoff was only equivalent to that of typical biologically treated domestic effluent (30 mg/l, Browne, 1990) from 104 residents.

7.3.2.5 Oil and grease

As the average oil and grease levels in the wharf (1.0 mg/l) were considerably lower than those in the urban runoff and domestic effluent,

the wharf runoff does not contribute significant amount of oil and grease to the receiving environment.

7.3.2.6 Resin acids

About 103 kg of resin acids were calculated as entering the receiving tidal waters annually from the log handling area.

Although the total resin acid level in the runoff from the sealed wharf area was lower than that from the gravelled area, the resin acid load per hectare of sealed area (6.0 $kgha^{-1}a^{-1}$) is higher than that per hectare of gravelled area (4.1 $kgha^{-1}a^{-1}$), as the annual storm runoff volume per hectare of sealed area was doubled due to the decrease of depression storage and infiltration rate.

No data are available on the presence of resin acids in domestic effluent and urban runoff. However, as mentioned before, the resin acid level in the adjacent urban runoff (1 µg/l) was about only 0.1% of that in the wharf runoff. Accordingly, the wharf runoff would be the main source of resin acids in the harbour sediment adjacent to the wharf log handling areas.

7.4 CONCLUSIONS

Based on investigation of storm runoff water quality and quantity, as well as the bark and soil material left on the wharf surface around the log handling areas at the Port of Tauranga, we can conclude:

1 0.37 kg of bark and soil material with a particle size <4.0 mm, of which 38% was volatile, were stripped per cubic metre of logs shifted. For a timber port with an annual log turnover of 2 million tonnes, the maximum annual available source of bark and soil material with a size <4.0 mm is of order 740 tonnes.

2 There is room for improving mechanical cleaning efficiency to mitigate the available contaminant source related to the log operations because the present mechanical cleaning efficiency was not high, specially for fine particles.

3 The suspended solid load from the log handling area was about 4,500 $kgha^{-1}a^{-1}$. In total 87,500 kg of suspended solids, of which 43,200 kg were volatile, entered the receiving tidal waters from the Mount Maunganui wharf, through which about 2 million tonnes of logs were loaded onto ships annually during the study period. That is equivalent to the suspended solid loading from local domestic effluent created by 2,900 - 3,300 residents annually.

4 Sealing the gravelled wharf surface could significantly decrease the concentration of suspended solids, but the annual suspended solid and volatile suspended solid loading per unit wharf area remained similar due to the increase of annual runoff volume.

5 The annual BOD load from the log handling areas (14,200 kga^{-1}) is equivalent to that from the untreated domestic effluent created by 600 local residents. The BOD yield rate from the wharf areas (680 - 770 $kgha^{-1}a^{-1}$) is 6-25 times that of the urban areas.

6 The yield rates of total phosphorus (26 $kgha^{-1}a^{-1}$) from the wharf log handling areas are 6-260 times higher than those from urban. The total nitrogen loading rate (19 $kgha^{-1}\ a^{-1}$) from the wharf areas is 1.4 - 10 times that of the urban runoff.

7 The contribution of nitrate and oil and grease from the wharf runoff is not appreciable.

8 It seems that the storm runoff from the wharf log handling areas is the main source of resin acids and contributed 103 kg resin acids to the receiving water annually.

CHAPTER EIGHT

ACCUMULATION OF RESIN ACIDS IN THE ADJACENT SEDIMENT

CHAPTER EIGHT

ACCUMULATION OF RESIN ACIDS IN THE ADJACENT SEDIMENTS

8.1 INTRODUCTION

Elevated levels of resin acids may be found in the sediment of a water body near the discharge points of effluent which contains resin acids since one of the mechanisms whereby resin acids are lost from a water column is sedimentation. From Chapter 7, 103 kg of resin acids entered the receiving tidal waters annually with the storm runoff from the log handling area at the Mount Maunganui wharf. It is possible that some of the resin acids are deposited on the sea floor around the effluent discharge points. Many resin acids, for instance, dehydroabietic acid (DHAA), are environmentally persistent, and are known to accumulate in sediment (Brownlee, 1977; Barrick and Hedges, 1981; Simoneit, 1986; Wilkins *et al.*, 1996, 1997).

Resin acids in the sediments and their distribution around the runoff discharge points were investigated. This chapter presents the results of studies undertaken during 1995 - 1996. As mentioned in Chapter 1, the potential impact of resin acids on the benthic biota is beyond the scope of this study and will be investigated separately.

8.2 METHODS

8.2.1 Sampling

Ten sites were chosen at different distances from the two runoff discharge points around the log handling area (Figure 8.1). Sites S0 - S4 are directly opposite to the southern outfall and 1, 15, 50, 120, and 250 m, respectively,

away from the outfall. Sites N0-N4 are directly opposite the northern outfall and 1, 40, 80, 160, 290 m, respectively, away from that outfall. Two sites from the Central Bank, LWC and DW, about 2300 and 2800 m away from the log handling area, were chosen as control sites (Figure 8.1).

Surface sediment samples, typically 0-10 cm, were collected from each site. The samples from the S0 and N0 sites, both are about 1 m away from the outfalls, were collected manually because these two sites were exposed or nearly exposed during low tide. Samples from the N1, N2, S1, S2, S3, and S4 sites were taken using a grab sampler. At the S3, S4, LWC, and DW sites, samplers were collected by SCUBA divers because there was too much shell material for the grab sampler to function. The samples were stored in plastic bags which had been rinsed with 2 M acid (HCl) and base (NaOH) solutions and distilled water. On return from the field, the samples were frozen at -18^{o}C until extraction was undertaken.

The samples were different in texture. Conventional analyses, such as grain size distribution and loss on ignition, of these samples were undertaken. The loss on ignition was determined by weight loss of the dried samples (103^{o}C) after combustion at 550^{o}C for 3 hours. Table 8.1 gives descriptions of these samples.

It is noteworthy that the appearance and texture of the samples from sites S0 and N0 were significantly different. The S0 site is exposed during low tide (Figure 8.2a). The sample from this site consisted of brown coarser sand and pebbles and it had very low loss on ignition (1.6%). However, the N0 site is underneath the wharf and is not exposed during low tide (Figure 8.2b). It is located in a small perched pool beside the northern outfall where a significant amount of bark residue had accumulated. The sample from the N0 site appeared black and included a large amount of bark residue, which could be identified visually.

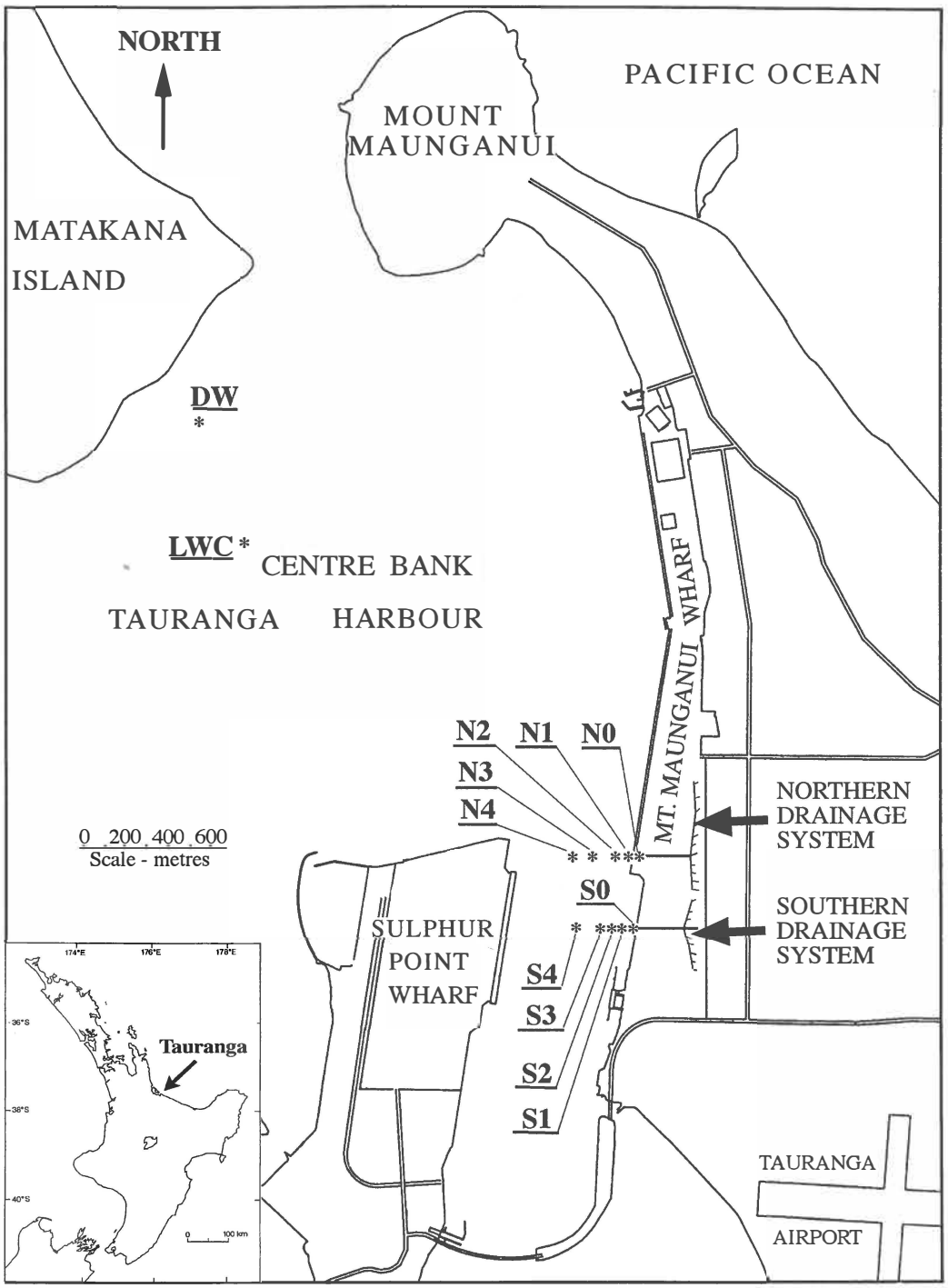

Figure 8.1 Locations of sediment sampling sites adjacent to the log handling areas and the Centre Bank, Tauranga Harbour. Sites N0-N4 are the locations opposite the northern drainage system; S0-S4 are locations opposite the southern drainage system; sites DW and LWC are the two control sites.

8.2.2 Pre-treatment

The sediment samples were homogenised, drained and dried naturally at room temperature (17-23°C). During the drying period, the samples were frequently disturbed using a clean class rod to prevent the samples aggregating together.

The dried sediment samples were sieved to determine the particle size distribution (Figure 8.3). A weighed portion of the < 0.2 mm fraction was extracted for the samples from the N0, N1, N2, N3, N4, S0, S1, S2, S3, and S4 sites. A weighed portion of the < 0.5 mm fraction was extracted for the control site samples DW and LWC because the quantity of the < 0.2 mm fraction of these two samples were not adequate (Figure 8.3).

Since the samples were dried at room temperature (the samples were not dried at 103°C, since it was feared that some resin acids would decompose), the moisture content of each sample might be different. In an attempt to standardise the results for comparability with previous researchers, the final results were expressed in resin acid content per kilogram of dried sediment samples at 103°C, the standard temperature for removing the free water in the sediment (APHA, 1992). Before extraction, each sample was homogenised and divided into two parts. One part was weighed and extracted. Another part was used to determine moisture content immediately. By knowing the moisture content, the actual dry weight (at 103°C) of the samples extracted could be calculated (Table 8.1). All results shown in this chapter are compound content per kilogram of dried sediment at 103°C.

Table 8.1 Description of the 12 sediment samples taken from Tauranga Harbour.

Sample Code	Distance to the outfalls (m)	Water depth (m)	Sediment type	Moisture Content (%)[1]	Loss on ignition (%)[2]	Loss on ignition (%)[3]
S0	1	1.0	coarser sand and pebbles, brown	1.0	1.6	1.9
S1	15	2.0	medium sand, brown, no pebbles	1.1	1.8	2.9
S2	50	7.0	black, silty, anoxic mud	3.6	7.2	8.6
S3	120	14	black, silty, anoxic mud	3.3	6.7	7.2
S4	250	14	fine sand, dark brown	2.7	5.5	6.2
N0	1	1.0	coarser, black, lots of bark residue	10.9	34.7	40.6
N1	40	14	fine sand, dark brown, some anoxic mud	2.4	4.8	5.1
N2	80	14	fine sand, grey brown	3.6	5.3	6.2
N3	160	14	fine-medium sand, shells, grey brown	1.7	3.8	3.8
N4	290	14	fine sand, dark grey brown, some shells	1.6	3.8	3.9
LWC	2300	5	fresh coarser sand, lots of shells	0.4	0.7	0.7
DW	2800	5	fresh coarser sand, a few shells	0.4	0.7	0.7

[1] moisture of the <0.2 mm fraction dried at room temperature (18-23 °C)

[2] loss on ignition of the whole samples

[3] loss on ignition of the < 0.2 mm fraction.

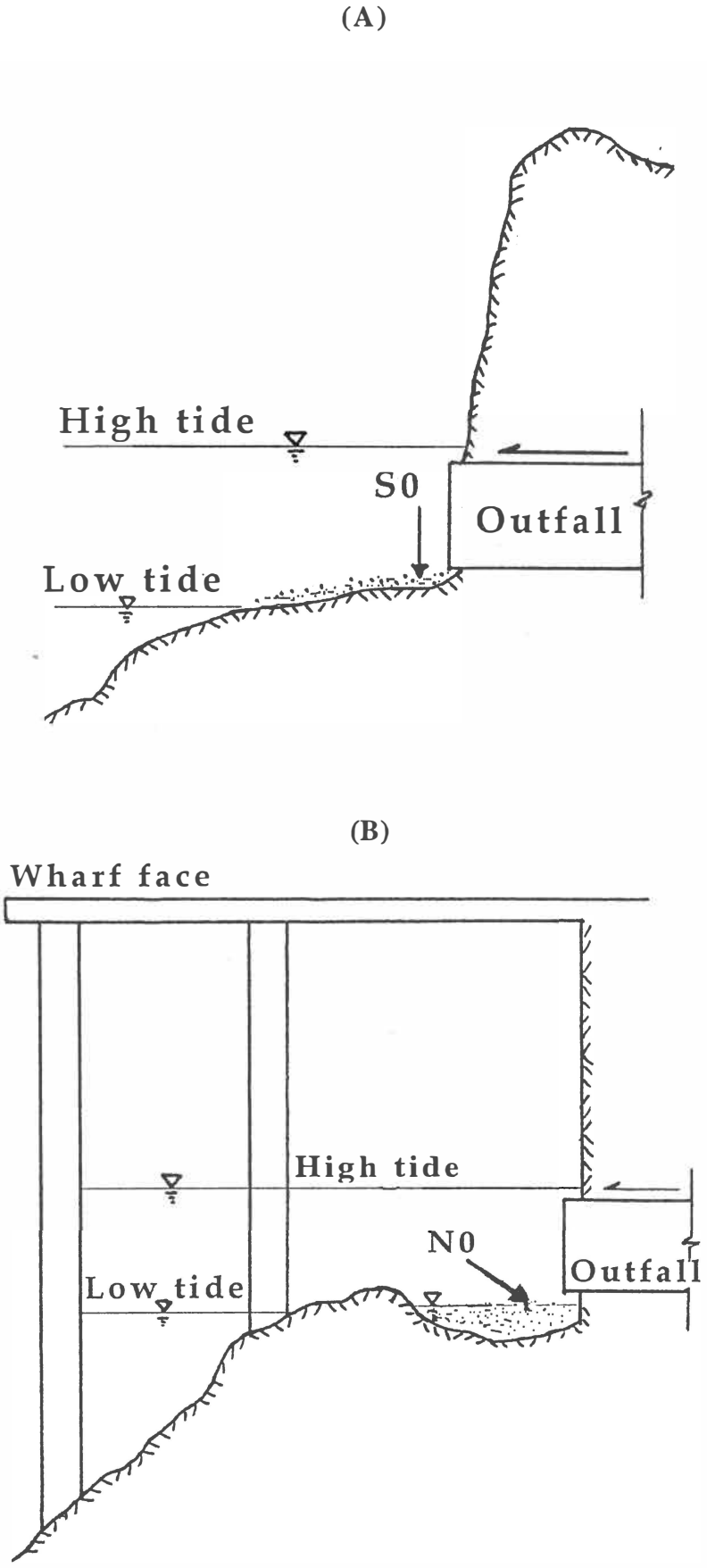

Figure 8.2 Schematic diagram of sampling sites at S0 (A) and N1 (B).

8.2.3 Extraction

A sieved portion of each sediment sample was weighed (the amount depended on the estimated resin acid levels according to the three trial extractions undertaken in advance) and extracted for 16 hours with 1:1 hexane-isopropanol in a Soxhlet extractor. *O*-methylpodocarpic acid (PDA) was added to the sediment samples as surrogate (recovery) standard immediately before extraction commenced. After extraction, *O*-methyl-podocarpic acid ethyl ester (PDA-Et) was added into the hexane-isopropanol extract as internal standard. The extracts were concentrated to 1-2 ml under reduced pressure using a rotary evaporator, and derivatised using an ethereal solution of diazomethane (CH_2N_2) (CARE: diazomethane is explosive and carcinogenic). For fully converting the acids to methyl esters, the concentrated extracts with added diazomethane were allowed to stand at room temperature for 30 minutes and left in a refrigerator (1-3^{o}C) for 24 hours. Excess diazomethane was blown off under a stream of oxygen free nitrogen.

A Unilab (Auburn, Australia) acid washed sand sample was extracted and identified as blank.

8.2.4 Identification and Quantification

Selected ion mode (SIM) GC-MS was used to identify and quantify the resin acids in the sediment samples. The details of the identification and quantification were given in Chapter 5.

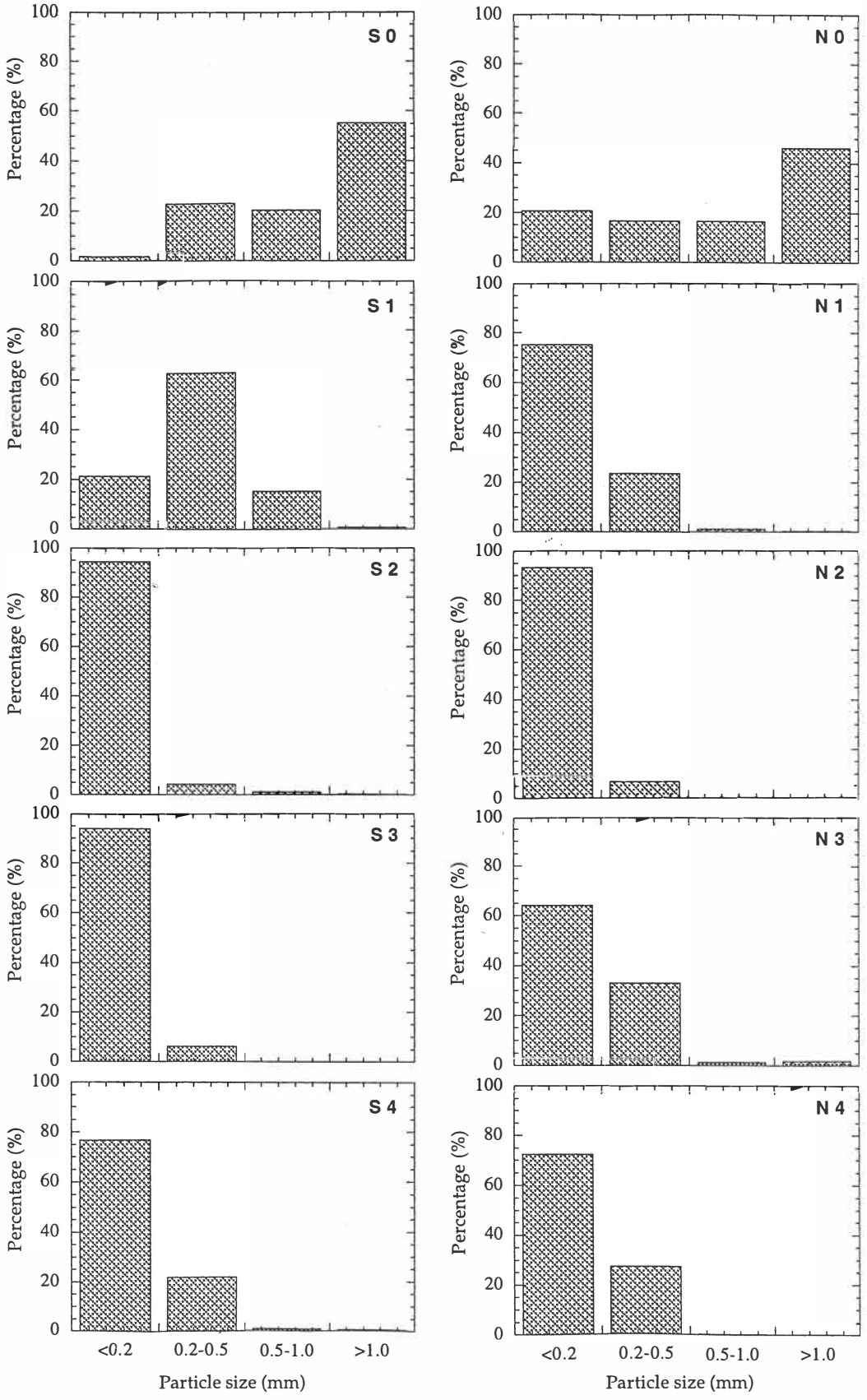

Figure 8.3a Particle size distribution of the sediment samples collected from the Tauranga Harbour adjacent to the log handling areas at Mount Maunganui wharf.

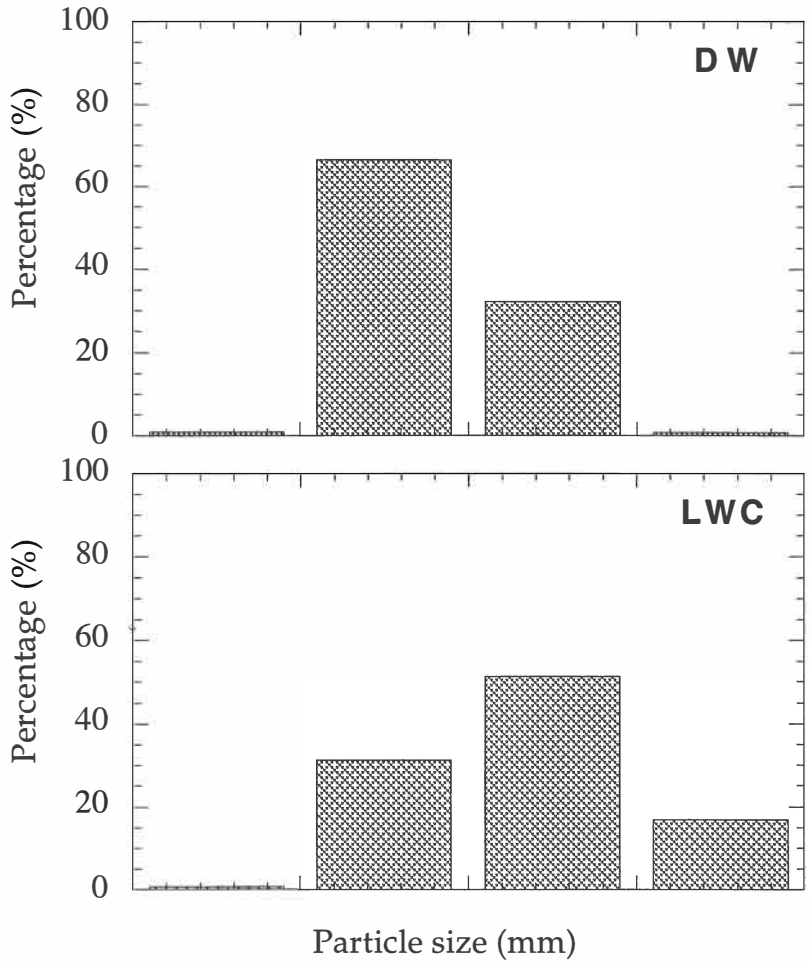

Figure 8.3b Particle size distribution of the sediment samples collected from the control sites (DW and LWC) in the Tauranga Harbour.

8.3 RESULTS AND DISCUSSION

8.3.1 Overall Resin Acid Level

Table 8.2 gives the resin acid levels in the 12 samples identified by selected ion mode (SIM) GC-MS in this study. The chemical structures of these identified compounds are shown in Figure 5.3b.

Compared to the resin acid levels in the storm runoff from the log handling areas (72 - 2300 ppb, mean level 1030 ppb), the total resin acid level of the sediment sample at the N0 site (874,000 ppb) is about 800 times higher. This

result is similar to those obtained for Tarawera river sediment samples (Wilkins *et al.*, 1996, 1997). In river water samples, a concentration of some 20-100 ppb of DHAA can result in a sediment concentration a few orders of magnitude greater (e.g. 100,000 ppb), depending on sediment type, origin and concentration of the pollutant, and the distance to the effluent discharge points (Wilkins *et al.*, 1996, 1997).

As mentioned in Section 8.2.2, the sediment sample from the N0 site was special in texture. It was collected from the small pool beside the northern outfall. Unlike the samples from the other sites, which primarily consist of silt, sand, or pebbles, a substantial amount of bark residue was present in the N0 site sample. The high loss on ignition (34.7%) indicated a high level of the organic contribution, therefore, the detection of an elevated level of resin acids was expected.

The total resin acids of all the other sediment samples (820-3900 ppb) was similar compared to those in the storm runoff from the log handling areas. The low resin acid level in the sediment can be partly attributed to the turbulent depositional environment after the runoff entered the receiving tidal water.

The outfalls of the two drainage systems are located between low and high waters (See Figure 8.2). Due to the difference of density, the fresh runoff floated on the sea surface after it was discharged into the Harbour and moved away within a short period due to the surface tidal or wind driven current (see Chapter 9).

Table 8.2 Resin acids (ppb) identified with selected ion mode (SIM) GC-MS in the sediment samples collected in the Tauranga Harbour. Pim: pimaric acid; Sand: sandaracopimaric acid; Iso: isopimaric acid; de-DHAA: dehydrodehydroabietic acid; DHAA: dehydroabietic acid; Ab: abietic acid; 7-OH: 7-hydroxydehydroabietic acid.

Sample Code	Pim	Sand	Iso	de-DHAA	DHAA	Ab	7-OH	TRA	Re (%)
LWC	300	130	ND	10	760	Nd	ND	1200	87.9
DW	ND	ND	ND	ND	580	ND	ND	580	89.4
S4	82	51	ND	ND	660	ND	31	820	89.5
S3	84	57	ND	21	790	ND	30	980	89.3
S2	180	ND	ND	ND	1710	ND	27	1920	87.6
S1	510	190	ND	34	1440	ND	32	2210	89.6
S0	750	270	ND	56	2770	ND	55	3900	90.7
N4	320	140	ND	30	870	ND	17	1380	86.7
N3	340	130	ND	20	830	ND	ND	1320	87.7
N2	240	120	ND	20	710	ND	ND	1090	90.8
N1	370	180	ND	30	1050	ND	23	1650	89.6
N0	173,000	30,300	116,000	5,980	457,000	43,900	48,100	874,000	87.3

The bark particles discharged into the receiving water with the runoff, which are believed to be the source of resin acids in the runoff, are lighter than water and it is very difficult for them to settle on the sea floor in a turbulent fluid environment.

Another likely reason is that the sediment samples collected in this present study came from the recent deposition due to the extensive dredging program of 1990 - 1992. Extensive dredging and widening of the shipping channels, including the present investigation areas, occurred during the major dredging programme of 1990-1992 when about 5,000,000 m^3 of sediments were dredged. By March, 1992, the Port had the capacity to handle ships with a draft of 11.7 m at all stages of the tide. Thus, when the samples were collected in March, 1995 (S0-S4, N0-N2) or November, 1995 (N3 and N4) the sediments had been exposed to the wharf discharge impacts for only 36 (S0-S4, N0-N2) or 44 months (N3 and N4).

The results obtained in this present study were significantly different to those encountered in the vicinity of the Tarawera River and Matata Lagoon, New Zealand (Wilkins *et al.*, 1996, 1997). The Matata Lagoon was influenced by Tarawera River which contains resin acids due to the discharge of effluent from two pulp and paper mills upstream (about 200,000 m^3 per day). The resin acid level in the sediment collected in the Tarawera River bed and around the lagoon was about a few hundreds of ppm. Even for the control sites, which experienced little impact from the river, but had a natural accumulation of tree branches and twigs (the sediment samples are black, silty, and anoxic mud), the total resin acid level (around 50 ppm) was substantially higher than that of the sediment samples obtained in this present study.

8.3.2 Distribution of Resin Acids with Distance from the Outfalls

Figure 8.4 gives the total resin acid levels of the sediment samples at different distances from the runoff discharge points.

Curve fitting using either a power equation, or a logarithmic equation was applied to model the total resin acid levels in sediment samples collected up to 250 m from the southern stormwater outfall. Storm runoff input from the Sulphur Point wharf, which also contains significant levels of resin acids (Tian *et al.*, 1995), may limit the use of the power equation, $TRA = 4339D^{-0.281}$ ($R^2 = 0.94$, TRA = total resin acid concentration in ppb; D = distance in m from wharf front), to the region 250 m away from the Mount Maunganui wharf. The second equation, $TRA = 3877 - 1299*\log D$ ($R^2 = 0.98$), does however appear to have some validity beyond 250 m, in so much as it tends towards zero (the likely level immediately after dredging) at increasing distance from the Mount Maunganui wharf front.

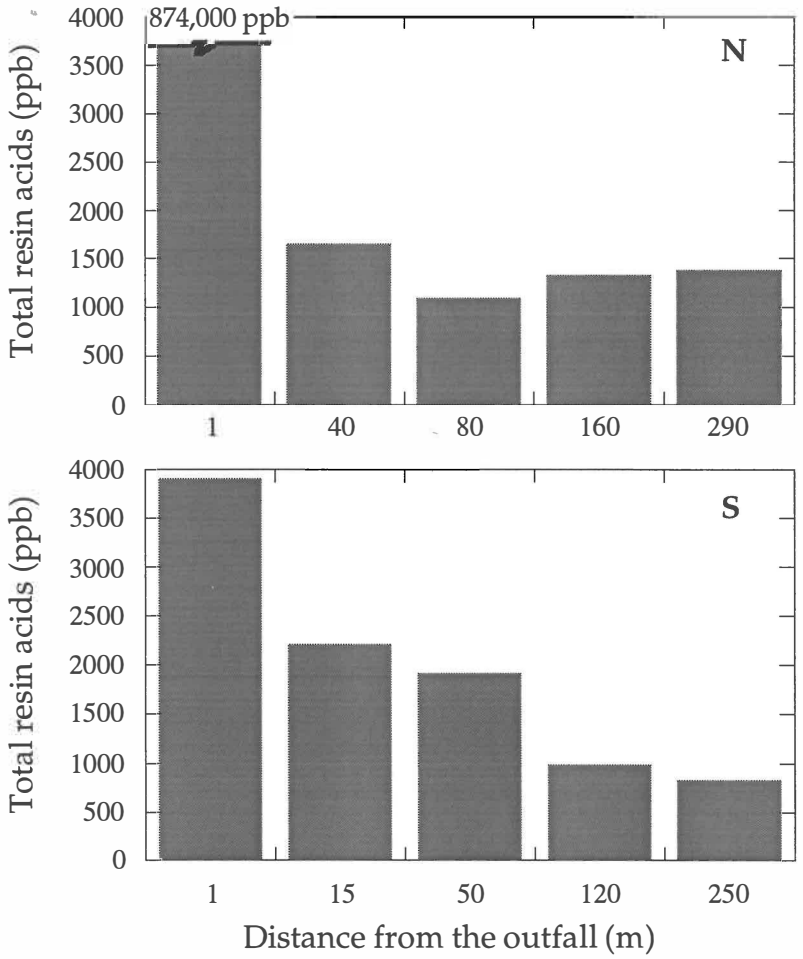

Figure 8.4 Total resin acid concentrations of the sediment samples collected at different distances from the outfalls of the northern drainage system (N) and southern drainage system (S) at the Mount Maunganui wharf.

For the northern drainage system, the resin acid levels of the sediment samples from the N3 and N4 sites were similar (1320 and 1380 ppb), and slightly higher than that from the N2 site (1090 ppb). This was probably due to the different sampling dates. Samples from the S0, S1, S2, S3, S4, N0, N1, and N2 sites were collected on March 10, 1995. As there was too much shell material at the N3 and N4 sites to collect with the grab sampler, the samples at these two sites were collected by SCUBA divers eight months later, i.e., on November 2, 1995. As presented previously, extensive dredging and widening of Tauranga Harbour shipping channels, including the area adjacent to the log handling wharf in the vicinity of Sulphur Point, occurred during 1990-1992. Thus it follows that when the samples were collected in March, or November, 1995, the sea bed sediments had been exposed to the wharf stormwater discharge impacts for a maximum period of 36, or 44 months, respectively.

Based on the mean total resin acid levels determined for the S3 and S4 samples (900 ppb; 36 months accumulation) and N3 and N4 samples (1350 ppb, 44 months accumulation), the net accumulation rate of resin acids in sediment in the shipping channel between the Mount Maunganui and Sulphur Point wharves can be estimated to be currently of the order 300 ppb/year (southern outfall) and 370 ppb/year (northern outfall) respectively, assuming a linear accumulation rate to date.

Although the above method for estimating net resin acid accumulation rate might not be very accurate, the results, 300 - 370 ppb/year, suggest that the present net resin acid accumulation rate in the sediment around the shipping channel between the Mount Maunganui wharf and Sulphur Point wharf is significantly low. Further study is required to accurately quantify the long term balance of resin acid deposition (accumulation) and degradation (removal) in harbour sediments. Also, investigation is required on the potential impact of resin acids in sediments on the benthic biota.

Care must be exercised in comparing the levels of total resin acids identified in the S3, S4, N3 and N4 samples (820-1380 ppb) and the control site LWC and DW samples (580 and 1190 ppb respectively) since the former sediments have only been exposed to resin acid influenced storm runoff for about 3-4 years, while the levels identified in the control site samples can be attributed to the long term (> 30 years) accumulation of low levels of resin acids.

8.3.3 Individual Resin Acids

As for the storm runoff, dehydroabietic acid (DHAA) is the dominant resin acid among the identified individual resin acids in all the sediment samples (Figure 8.5). The average ratio of DHAA to total resin acid, expressed as %, (70%, SD = 10%) is significantly higher than that (45%, SD = 7.8%) in the storm runoff from the log handling areas.

Apart from DHAA, there are some other changes concerning the average percentage contribution of individual resin acid to total resin acids between the storm runoff and the sediment samples (Table 8.3).

Table 8.3 Ratios of individual resin acid to total resin acids, expressed as %, identified in the storm runoff and the sediment samples in this present study. The details of the runoff and sediment sample were given in Table 5.1 and Table 8.1.

Ratios	DHAA	Pim	de-D	Ab	7-OH	Sand	Seco	Iso
Runoff	45	11	8.6	5.5	16	2.3	3.7	7.7
Sediment	70	18	1.3	0	1.4	7.3	0	0

In the sediment samples, the percentage contribution of pimaric and sandaracopimaric acid to total resin acids are higher than those in the runoff samples. However, the percentage contribution of dehydro-DHAA and 7-OH DHAA to total resin acids are lower than those in the runoff samples.

Osborne (1991) and LaFlamme and Hites (1978) proposed the possible degradation pathways for abietic acid. Abietic acid can be metabolised to

dehydroabietic acid by losing two hydrogen under a certain conditions. As expected, no abietic acid was detected in the sediment samples. It is highly possible that the abietic acid was metabolised to dehydroabietic acid as indicated by the significantly higher DHAA ratio in the sediment than that in the runoff.

Isopimaric acid and secodehydroabietic acid were also not detected in the sediment samples. Further investigation is needed to identify the fate of isopimaric and secodehydroabietic acid from the runoff.

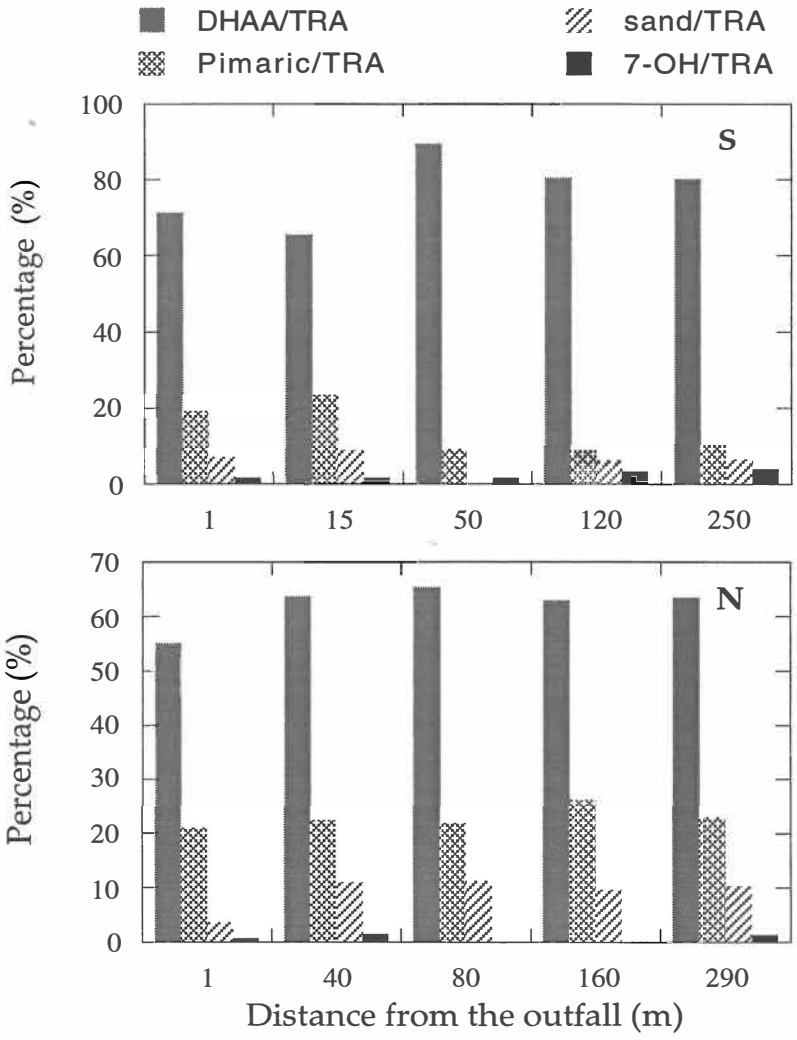

Figure 8.5 Ratios of dehydroabietic acid, pimaric acid, sandaracopimaric acid and 7-OH dehydroabietic acid to total resin acids, expressed as %, identified in the sediment samples collected from the Tauranga Harbour adjacent to the log handling areas at Mount Maunganui wharf.

8.4 CONCLUSIONS

Based on the analyses of resin acids in the sediment samples collected from the Tauranga Harbour adjacent to the log handling areas and the Central Bank, the following points can be concluded:

1. The resin acid levels in the sediment adjacent to the runoff discharge points ranged from 800 to 4,000 ppb.

2. The impact on the sediment from the storm runoff was limited to a distance of about 100 m.

3. The current net accumulation rate of resin acids in the shipping channel west of the log handling areas at the Mount Maunganui wharf (Stella Passage) was estimated to be in range of 300 to 370 ppb per year. Further study is required to accurately quantify the long term balance of resin acid deposition (accumulation) and degradation (removal) in harbour sediments, as well as the potential impact of resin acids on the benthic biota.

CHAPTER NINE

DISPERSION AND DILUTION OF STORM RUNOFF IN THE HARBOUR

CHAPTER NINE

DISPERSION AND DILUTION OF STORM RUNOFF IN THE HARBOUR

9.1 INTRODUCTION

From Chapters 4 and 5, it was demonstrated that the optical quality of the storm runoff from the log handling area at Mount Maunganui wharf was degraded and the runoff possessed high levels of resin acids due to the addition of bark particles. However, whether the storm runoff will induce environmental problems or how serious the environmental impact will be depends not only upon the contaminant level in the runoff, but also the extent of dilution and mixing in the receiving tidal waters. For example, according to the Resource Management Act 1991 (Sections 70 and 107), there shall be no "conspicuous change in the colour or visual clarity" of the receiving water after discharge of any effluent after "reasonable mixing". Accordingly, it is important to understand the dispersion and dilution of the runoff in the receiving tidal waters. No attempt was made to define "reasonable mixing" in this study.

The aims of this chapter therefore are:

- to investigate the dynamics of the plume caused by the wharf runoff in the receiving tidal waters; and

- to apply a numerical model to simulate the mixing and dispersion of the effluent and predict the plume behaviour under certain weather conditions.

It is important to understand the features of the problem to be solved. The main problems confronting this study are: (i) complicated effluent sources, (ii) restrictions of field investigations due to proximity of port operations, and (iii) the difficulty of obtaining data in extreme rainfall events.

The main characteristics of the effluent discharges are as follows:

- There are about 20 storm drains along the wharf, and more from the Sulphur Point wharf and the urban area southwest of the Mount Maunganui wharf; and

- As the wharf surface pavement types, land use and sub-catchment area of each drainage system are different, the runoff flow rates and water quality from these drainage systems may be different during a storm and from storm to storm.

Restraints on field investigation include:

- Difficulties with data collection. The sea area adjacent to Mount Maunganui wharf (Stella Passage) is a busy shipping channel. It is not practical to deploy moored instruments, such as temperature, salinity and turbidity sensors, in the channel to trace the dispersion of the runoff for a relatively long term; and

- Rare and erratic suitable conditions. The opportunities for collecting the field data are rare because of the imprecise nature of the weather forecast and other logistic difficulties in assembling instruments and personnel at short notice.

These features had an influence on determining the methods for field investigation of the plume dynamics.

9.2 DYNAMICS OF BUOYANT PLUMES

The characteristics of buoyant jets or plumes have been well documented although numerical modelling of buoyant jet or plume dynamics has been developed over the past two decades only (Huang and Spaulding, 1995; Wood, 1991).

Many discharges into the environment can be classified as buoyant jets or plumes, which are derived from sources of both momentum and buoyancy. The dynamics of a buoyant jet is determined by two groups of factors: the properties of the jet at the initial stage (near the source) and the environmental conditions after discharge.

The initial conditions include the geometry of the jet, the mean jet exit velocity, initial difference between the discharge and the ambient fluid etc. However, in this present study, the runoff discharge from the outfalls of the two drainage systems around the log handling area did not form a "jet", hence this study did not treat "initial" mixings. Instead, the study was only concerned with medium-far field mixing of the effluent within the harbour after measuring salinity and turbidity away from the outfalls where the initial dilution had finished.

As described in Chapter 1, the outfalls of both drainage systems around the log handling area are located between low and high waters (Figure 1.7). The inside bottom of the outfalls is about RL 0.4 m. When the sea level is lower or slightly higher than the inside bottom of the outfalls (there is about 30-32% of probability that at any point in time the tidal level will be below RL 0.4 m from examination of the tide curves obtained for the Sulphur Point wharf), the runoff enters the harbour and falls freely to the channel side.

The drainage systems around the wharf area were designed to be able to drain runoff formed by a storm with a five year return period at a tidal level of RL 1.5

m. For a rainfall with a lower return period, the momentum of the water flow from the outfalls is not significant. For example, the estimated maximum runoff flow rate from the southern drainage system during the rainfall on October 10, 1995 (see Section 9.6) was 0.72 m^3/s. That equals to a mean velocity of 0.32 m/s in the outfall pipes (The sectional area of the two parallel main pipes with a diameter of 1.2 m is 2.26 m^2).

The northern outfall is located underneath the wharf face (see Figure 8.2b). A few piles are located in front of the outfall and quite often, a big ship berths along the wharf face. The piles and the ship further decrease the momentum of the out-flowing runoff. The lack of measurement of exiting velocity from the outfalls is another reason to study the medium-far field dispersion and dilution only.

Factors affecting the dynamics of a buoyant plume include turbulence eddy size and intensity, cross flow, and density stratification of the receiving water body. As the runoff is surface discharged, the plume remains on the sea surface and becomes advected by cross currents, as well as wind. Accordingly wind stress is also an important environmental factor.

i) The pressure gradient

The buoyancy of a discharge into the ocean may be associated with a higher temperature or a reduced salinity or both. Because of the low density of the discharged water, its free surface is above the level of the surrounding seawater. The resulting pressure gradient causes a lateral spreading of the plume over the ambient seawater, accompanied by a thinning in its vertical thickness.

The pressure gradient, arising from the buoyancy of the low density water, is the main driving force in the equation of motion for water in the plume. The

other forces which may play a significant part are friction at the interface with the lower layer, possibly accompanied by entrainment, vertical turbulent stress, and horizontal turbulent stress.

ii) Exchange processes and mixing

When a plume moves downstream, it entrains some of the underlying and adjacent water. The plume may be regarded as an advective feature, transferring water bodily, but it is understood that some sort of mixing or entrainment takes place between the plume and water adjacent to it.

The most general treatment is to regard the exchange process as a horizontal eddy diffusion, assuming that the flux of any constituent of concentration, C, is proportional to the concentration gradient,

$$F = -N_h \frac{dC}{dx} \qquad (9.1)$$

where N_h is the eddy diffusivity in the X direction. If the properties of the plume can be specified, in a statistical sense, it may be possible to estimate the value of N_h from the concentration gradients. If not, N_h may have to be estimated empirically from field observations of the distribution of the constituent and its rate of input to the system.

iii) Vertical mixing

In the simplest case of a constant-density tidal flow, vertical mixing is caused predominantly by turbulence generated by bottom stress. The logarithmic velocity profile law leads to a parabolic distribution of the vertical eddy viscosity, E_v,

$$E_v = \kappa D u^* \frac{z}{D}\left[1-\frac{z}{D}\right] \qquad (9.2)$$

where, u^* is the shear velocity, D the water depth, κ the von Karman constant (0.4).

If the water column is stratified, the gradient Richardson number, *Ri*, which is a ratio of vertical density gradient to vertical velocity gradient, can be used to estimate the shear instability. *Ri* is defined by,

$$R_i = -g\left(\frac{\partial \rho}{\partial z}\right) / \rho\left(\frac{\partial u}{\partial z}\right)^2 \qquad (9.3)$$

When *Ri* is small, say < 0.25, the vertical density gradient is insufficient to suppress shear instabilities with the result that the turbulent mixing occurs across the halocline. For large values of gradient Richardson number, for example, in excess of about 2, mixing is totally suppressed by the vertical density gradient and the flow remains laminar.

A few formulae have been developed for estimating the vertical mixing coefficient in the case of stably stratified water column, such as, Munk and Anderson (1948), Pritchard (1967), and Perrels and Karelse (1981).

iv) Ambient Crossflows

Generally, the behaviour of a buoyant jet in the environment into which it is discharged will be controlled by a characteristic length scale which is a function of the source flow momentum, flow flux, and the distance from the source. Very close to the source, momentum will usually control the behaviour of the jet. However, there was no significant jet at the outfalls being treated here.

Beyond the initial mixing zone, buoyancy and underlying flow will determine the dynamics of the plume. When the distance from the source is long enough, the buoyancy produced by the density difference between freshwater and saline water becomes very small due to mixing and underlying flow will ultimately be the dominating influence to control the plume.

This present study did not treat "initial" mixings as described previously. For the medium-far field dispersion and dilution, buoyancy, tidal flow and wind stress dominate the plume behaviour. The influence of wind stress on plume behaviour is discussed in Section 9.5.2.

9.3 FIELD MEASUREMENTS

Two groups of data are required to understand the plume dynamics and to simulate the plume behaviour with a numerical model: the data involved in the dispersion and mixing processes of the plume, and the relevant environmental parameters.

9.3.1 Plume Behaviour

Ideally the plume should be monitored with instruments around the mixing zone at different locations and water depths. However, it is difficult to do so at Tauranga Harbour because of the restraints mentioned in section 9.1. Accordingly, the following methods were used for the field investigation.

Video camera method

In order to trace the plume, a programmed video camera controlled by a micro-processor[1] was set up on the top of the 30 m high No.24 light tower at the southern end of the Mount Maunganui wharf (Figure 9.1a). The video camera was programmed to film for 10 seconds every 20 minutes during day time.

[1] Developed at the Joint Centre of Excellence in Coastal Oceanography and Marine Geology.

Measurement using a boat

The 6 metre survey boat (Port of Tauranga Ltd.) was used for measuring salinity and turbidity in the receiving tidal waters during and after a rainfall event. A differential GPS on deck was used to determine the boat locations in the harbour.

A portable Yeo Kal turbidimeter with a pressure sensor and a portable Yeo Kal salinity meter with a temperature sensor were used to measure the salinity and turbidity. They were calibrated before use. Standard seawater used for the calibration of the Yeo Kal salinity meter was the same for the salinity calibration of the S4 current meters (see next section).

9.3.2 Other Related Parameters

Wind

Wind records at Salisbury Wharf (Figure 9.1b) were obtained from the Port of Tauranga and then digitised.

Rainfall

Rainfall records were obtained from the two Lambrecht 1509H raingauges set around the log handling area (see Chapter 2).

Runoff flow rates

Because of the practical difficulties of direct gauging (see Chapter 2), the runoff flow rates from the outfalls of the storm drainage systems were estimated by the method discussed in Chapter 2.

Currents

Two InterOceans S4 current meters were deployed between September 12, 1995 and October 10, 1995, around the outfalls of the southern storm drainage system to measure the currents (Figure 9.1b). Due to restraints of instrument

deployment, the current meters were deployed about 60 metres from the eastern bank. Table 9.1 gives the details of the deployment.

Sub-surface buoys with a lift of 80 kg were used to produce a high lift force on the current meters, so that they would remain relatively upright in spite of wave and current influences. The anchor weights were about 150 kg to counter the buoyancy and ensured that the mooring did not drift. As the standard InterOcean S4 current meters were also used to record the salinity, the salinity sensors of the current meters were calibrated with the same seawater for the calibration of the Yeo Kal portable salinity meter.

Table 9.1 Current meter deployments

Period	Coordinates (BOP)	Location code	Mooring methods	Height above sea bed (m)	Water depth[1] (m)	Terms measured
12/9/95-10/10/95	274793E 710814N	S1	sub-surface buoys	7	8.5	C,S,T[2]
12/9/95-10/10/95	274778E 710684N	S2	sub-surface buoys	7	8.5	C,S,T[2]

[1] The water depths are the distances below the chart datum.

[2] C - current; S - salinity; T - temperature

Tide

Tidal records were obtained from three tidal stations at Moturuki Island, Sulphur Point, and Tug Berth (see Figure 1.5b and Figure 9.1b). All tidal records were adjusted to the same datum used for the Tauranga Harbour bathymetry survey.

9.4 RESULTS AND ANALYSES OF FIELD MEASUREMENTS

9.4.1 Salinity

Measurements of seawater salinity in the harbour under different weather conditions were undertaken at various times between 1993 and 1996, in order to obtain a database for seawater salinity variation with time and vertical distribution around the Stella Passage area.

Long term variation of salinity

Figure 9.2 shows the salinity values recorded by the two S4 current meters at locations S1 and S2 (Figure 9.1b) from September 12 to October 10, 1995. A two day period of salinity at both S1 and S2 as well as water levels recorded at Sulphur Point are shown in Figure 9.3.

As presented in section 9.3.2, the two current meters were deployed 7 m above the sea bed (8.5 m above the chart datum). The salinity values shown in Figures 9.2 and 9.3 were salinity values at varying distances from the water surface at different tidal phases. However, the salinity values recorded at each low and high tide were basically at the similar water depth (1.7 ± 0.2 m for low tide and 3.2 ± 0.2 m for high tide).

At each low tide, salinity variation (Figure 9.2) is probably associated with variation in the freshwater input from the several steams entering the southern end of the Tauranga Harbour, which is up harbour of the timber port. These are the Rocky Stream, Waitao Stream, Ngapeke Stream, Waikite Stream, Kaitemako Stream, and Waimapu Stream. This causes a salinity oscillation with the tidal currents between the streams and the Harbour entrance as seen in Figure 9.3. After a rainfall event, low tide salinity values dropped gradually and reached their lowest point after several tidal cycles. This suggests that the peak freshwater flow from the streams does not reach the Stella Passage

immediently after a storm. After salinity reached its lowest value, it recovers slowly during dry weather.

Ideally investigation of the salinity structure around the wharf area and the overall dynamics of Tauranga Harbour, particularly freshwater input from the above mentioned streams should be undertaken. However, there are no hydrological stations set at any streams entering the southern end of Tauranga Harbour. An attempt was made to estimate the influence of freshwater input on the values of minimum salinity from rainfall records obtained from the raingauges set in this study, but there was no significant correlation between the salinity decrease and the rainfall recorded on the wharf. The lack of significant correlation may be explained by a difference of precipitation at the port, and in the stream catchments which enter the southern end of Tauranga Harbour. According to Quayle (1984), the annual precipitation around the Tauranga region varies from 1,400 mm or less along the coast to around 2,500 mm in the Kaimai and Mamaku Ranges although the horizontal distance from the coast to the Kaimai Range is only 25 - 30 km. This would explain why there was an obvious reduction of low tide salinity after 3.8 mm rainfall recorded at the wharf area on September 19, 1995, when this event did not produce any appreciable runoff from the wharf area.

Vertical distribution of salinity

Two surveys were undertaken on October 28, 1993, and August 8, 1995, to investigate the vertical salinity distribution under different weather conditions.

When the survey was undertaken on October 28, 1993, there had been a relatively long period of fine weather. Between October 12 to October 28, 1993, only 7.3 mm rainfall fell over 6 hours of period on October 19. If the same rainfall was experienced within the catchments of the streams, not much runoff would be expected to enter the harbour. Three sites, shown in Figure 9.1a, were chosen to undertake the survey.

Figure 9.4 shows the vertical distribution of salinity at the 3 locations under different tide conditions. The water levels at Sulphur Point during the survey are shown in Figure 9.5A.

After 16 days of fine weather, the seawater salinity adjacent to the log handling areas (Stella Passage) had the following features. There was 1 ppt salinity difference between the top (32.5 ppt) and bottom (33.5 ppt) of the water column at low tide and this difference was mainly exhibited within the top 4 m of the water column (0.8 ppt). Around the high tide, the salinity difference between the top and bottom was about 0.3 ppt at all the 3 survey sites, which mostly occurred within the top 2 m of the water column (0.2 ppt).

The second survey was undertaken on August 8, 1995, at the northern end of the Oil Tanker Berth (Figure 9.1a). The water levels at Sulphur Point during the survey are presented in Figure 9.5B. Before the survey, three rainfall episodes were experienced at the port area on August 3 (42.4 mm), August 5 (13.2 mm), and August 6 (10.0 mm). It was expected that the streams would bring a large amount of freshwater into the southern harbour.

Results of this survey are given in Figure 9.6. During low tide, the surface water salinity (0.2 m from water surface) was 26.0 ppt and increased to 31.2 ppt at 4.5 m of water depth. Below 4.5 m, the salinity gradient was significantly lower. This phenomenon may be explained by the local bathymetric features. Figure 9.7 shows the bathymetric change along the centre Stella Passage. The currents shown in the figure are at peak ebb tide, obtained by model simulation (see later sections). The shipping channel was dredged only to the southern end of the Oil Tanker Berth. The average water depth during low tide is less than 5 m south of the Oil Tanker Berth. During ebb tide, the freshwater from the streams flows from south to north. As the water with lower salinity is lighter, it remains within the top 5 m of the water column after it passes from the southern end of the shipping channel into the Stella Passage. It is

noteworthy that the downwelling currents shown in Figure 9.7 are relatively small, but they bring some water from 4.5 m down to about 6 m, which is the maximum depth before salinity is nearly gradient constant (Figure 9.6).

The salinity increase from low to high tide at a given water depth for a given location depends on freshwater input, tidal currents, local morphology etc. During the second survey on August 8, 1995, the seawater salinity at different water depths increased approximately linearly from the low to high tide (Figure 9.8).

Strongest vertical salinity gradient at high tide also mainly appeared near the top layer, but was more restricted, being predominantly in the top 2 m rather than in the top 5 m as recorded at low tide. The salinity difference (1.1 ppt) was still higher than that (0.3 ppt) observed after 16 days of fine weather.

A survey was undertaken immediately after the rainfall event on November 10, 1995. The rain commenced from 00:30 and stopped at 07:10. When the survey was undertaken after 09:00, some runoff was still entering the harbour although the rain had stopped 2 hours earlier (Surface flooding was formed around the log handling area in the early morning due to the blockage of the cesspits around the wharf. These cesspits were cleaned up manually after 08:00. This is why some runoff was still entering the harbour around 09:00). Figure 9.9 shows the rainfall and water levels recorded at Sulphur Point and Tug Berth (shown in Figure 1.5b and Figure 9.1b) on November 10, 1995.

Vertical salinity profiles were recorded at six sites (Figure 9.10). When the survey was undertaken, these sites were within the plume. The vertical salinity profiles (Figure 9.11a-b) exhibited strong vertical salinity stratification, both at the plume head (sites L7, L8, and L9) and the plume tail (sites L13, L14, and L15). The plume was well defined and restricted in the top 2 metres, suggesting weak vertical mixing.

Unfortunately, not all data for model calibration were obtained during the survey. Therefore, this rainfall event was not undertaken for model calibration.

In summary, based on the field measurements in this study, the seawater salinity around the Stella Passage exhibited the following features:

i) the seawater salinity varied with tidal levels, reaching its minimum value at low tide and maximum value one hour after high tide;

ii) there was an obvious salinity stratification around Stella Passage in the Tauranga Harbour. The extent of the stratification depends greatly on the rainfall and weather conditions. At low tide, $\frac{\partial S}{\partial z}$=1.15 ppt/m within the top 4.5 m of the water column 3 days after a 42 mm of rainfall, and $\frac{\partial S}{\partial z}$=0.25 ppt/m after 16 days of fine weather.

9.4.2 Results from the Video Camera

From September 28 to October 5, 1995, 3 appreciable rainfall events were recorded by the video camera.

The first rainfall event (September 29)

The first appreciable rainfall (8.5 mm) fell on September 29, 1995. The plume shapes which were digitised from the video images are shown in Figure 9.25. The rainfall intensity, cumulative rainfall, wind, and tidal levels are shown in Figure 9.12.

Although the rain began at 03:08, from the video camera images, no runoff was produced until 06:28 because the rainfall intensity was 0.9 mm/hour only. The rainfall intensity increased to 8.3 mm/hour at 06:22. From the picture at 06:48,

the visible plume had moved about 150 m across the channel and was 50-70 m wide (Figure 9.25a).

The plume tip rotated to the south, due to the flood tide current (Figure 9.25b). The 15 m/s northeasterly winds helped the plume to spread toward the southwest side of the channel, about 150-200 m (Figure 9.25c). About 1.5 hours after the rainfall turned to drizzle at 07:00, visual evidence of the plume soon disappeared.

The second rainfall event (October 1)

The second appreciable rainfall occurred on October 1, 1995. It was a short heavy shower which lasted only 40 minutes, resulting in a cumulative rainfall of 8.5 mm. The plume time series digitised from the video images are shown in Figure 9.26. The rainfall intensity, cumulative rainfall, wind, and tidal levels are shown in Figure 9.13.

The wharf runoff which started to enter the harbour at 09:28 coincided with mid flood tide. Therefore, the plume travelled to the south (Figure 9.26b-d).

The rain stopped at 09:45, but the urban runoff from the adjacent urban area, which takes longer to reach the harbour outfall, caused the discharge to continue, although the flow rates decreased. By 11:30, the plume was no longer visible in the video picture.

The third rainfall event (October 5)

The third rainfall came on October 5, 1995. In total, 22.4 mm of rainfall fell on the log handling areas. The rainfall intensity, cumulative rainfall, wind, and water levels are shown in Figure 9.14.

It started drizzling at 11:37 and became heavier at 15:45 (6.3 mm/hour). Appreciable runoff was seen in the harbour at 16:08. Figure 9.27 shows the

plume time series. High tide was around 16:45 and so tidal currents were slack. Thus, the plume crossed the channel and moved slightly to the south under the influence of the weak flood tide currents and moderate north-easterly wind (around 10 m/s, 30°T). After 17:00, the ebb currents commenced and at 17:48, the plume turned to the north, moved by the ebb currents. The wind direction changed to westerly at 18:00 and southwesterly later (12-15 m/s) and a narrow plume band along the east bank of Stella Passage formed. Unfortunately, it was too dark to trace the plume after 18:28. The results, however, showed that the very strong dependence of plume movement on wind direction and strength as well as the tidal currents.

9.5 NUMERICAL MODELLING

9.5.1 Model Selection

The dynamics of the plume in the receiving tidal waters in this study is affected by a number of factors, such as wind, tide, waves, buoyancy, volume of effluent etc. To model the plume in such a dynamic system, an advanced 3-dimensional numerical model is needed. This level of modelling should be able to simulate the shear through the vertical, the Richardson number across the density interfaces, the forcing phenomena (wind, buoyancy, density, tides etc.), and the input from the outfalls.

In this study, a fully coupled 3-dimensional circulation and transport hydrodynamic numerical model 3DD (Black, 1983 and 1992) was chosen. The code is general and has been applied to vertically-stratified and homogeneous ocean, continental shelf and shallow coastal water environment (Black, 1987, 1995, and 1996). It contains a Eulerian scheme hydrodynamic model coupled with both Eulerian and Lagrangian advection/diffusion scheme.

It was planned to use the Lagrangian plume model within model 3DD (Black, 1996) rather than the Eulerian scheme as applied in this thesis. The Lagrangian model treats sharp density gradients and was developed for cases such as those studied by Black (1996). By using the Eulerian scheme some information is lost particularly at the leading edge of the plume where density discontinuity effectively represents a shock front.

However, using the Eulerian scheme and the video observations it was found that the plume spread over large distances and that advection due to wind and tidal currents had a very strong influence on plume movement. This meant that the main aim of the chapter could be satisfied, i.e. the mapping of plume excursion and average dilutions within the study region. It is recommended, however, that further work could be undertaken to investigate plume mixing around the outfall, particularly now that it has been shown that the estuary is stratified and that the plume is entrained within a salinity structure which is more complex than has been assumed in past studies.

9.5.2 Model Description

Like any other hydrodynamic numerical model, model 3DD is based on the momentum and mass conservation equations. The momentum equation describes the acceleration/retardation of the water body when forces/friction are applied. The equation derives from Newton's 2nd law of motion, which states that the rate of change of motion (acceleration) of a body is directly proportional to the resultant force acting upon it, and is in the direction of that force, and inversely proportional to the body mass. The conservation equation keeps a check on the total mass entering/leaving model cells and ensures that mass is conserved in these cells.

Momentum equation

$$\frac{\partial u}{\partial t}+\frac{u\partial u}{\partial x}+\frac{v\partial u}{\partial y}+\frac{w\partial u}{\partial z}-fv=-\frac{g\partial \varsigma}{\partial x}-\frac{1\partial P}{\rho\partial x}+A_H\left(\frac{\partial^2 u}{\partial x^2}+\frac{\partial^2 u}{\partial y^2}\right)+\frac{\partial}{\partial z}\left(N_z\frac{\partial u}{\partial z}\right) \tag{9.4}$$

$$\frac{\partial v}{\partial t}+\frac{u\partial v}{\partial x}+\frac{v\partial v}{\partial y}+\frac{w\partial v}{\partial z}+fu=-\frac{g\partial \varsigma}{\partial y}-\frac{1\partial P}{\rho\partial y}+A_H\left(\frac{\partial^2 v}{\partial x^2}+\frac{\partial^2 v}{\partial y^2}\right)+\frac{\partial}{\partial z}\left(N_z\frac{\partial v}{\partial z}\right) \tag{9.5}$$

Mass conservation

$$w=-\frac{\partial}{\partial x}\int_{-h}^{z} u\,dz-\frac{\partial}{\partial y}\int_{-h}^{z} v\,dz \tag{9.6}$$

where, t is the time, u and v are horizontal velocities in the x and y directions respectively, $\dot{w}$ the vertical velocity in the z direction (positive upward), h the total water depth, ξ the sea level above a horizontal datum, g the gravity acceleration, f the Coriolis parameter, P the pressure, A_H the horizontal eddy viscosity coefficient, and N_z the vertical eddy viscosity coefficient.

The pressure at water depth z is given:

$$P=P_{atm}+g\int_{z}^{o}\rho\,dz \tag{9.7}$$

where P_{atm} is the atmospheric pressure.

For temperature and salinity, the conservation equations can be written as:

$$\frac{\partial T}{\partial t}+\frac{u\,\partial T}{\partial x}+\frac{v\partial T}{\partial y}+\frac{w\partial T}{\partial z}=\frac{\partial}{\partial z}\left(K_z\frac{\partial T}{\partial z}\right)+K_H\left(\frac{\partial^2 T}{\partial x^2}+\frac{\partial^2 T}{\partial y^2}\right) \tag{9.8}$$

$$\frac{\partial S}{\partial t}+\frac{u\,\partial S}{\partial x}+\frac{v\partial S}{\partial y}+\frac{w\partial S}{\partial z}=\frac{\partial}{\partial z}\left(K_z\frac{\partial S}{\partial z}\right)+K_H\left(\frac{\partial^2 S}{\partial x^2}+\frac{\partial^2 S}{\partial y^2}\right) \tag{9.9}$$

where T is temperature, S is salinity, K_H and K_z are the horizontal and vertical coefficients of eddy diffusivity.

Using the temperature and salinity, the density can be computed according to an equation of state of the form:

$$\rho = \rho(T, S, z) \tag{9.10}$$

Surface boundary conditions at $z = 0$ are:

$$\begin{aligned} &\rho N_z \frac{\partial u}{\partial z} = \tau_x^s \\ &\rho N_z \frac{\partial v}{\partial z} = \tau_y^s \\ &\frac{\partial \varsigma}{\partial t} + u\frac{\partial \varsigma}{\partial x} + v\frac{\partial \varsigma}{\partial y} = w^s \end{aligned} \tag{9.11}$$

where τ_x^s and τ_y^s denotes the components of wind stress and

$$\begin{aligned} \tau_x^s &= \frac{\rho_a}{\rho}\gamma\,|W|\;W_x \\ \tau_y^s &= \frac{\rho_a}{\rho}\gamma\,|W|\;W_y \end{aligned} \tag{9.12}$$

ρ is the water density, W the wind speed at 10 m above sea level, W_x and W_y are the x and y components, γ is the wind drag coefficient, ρ_a the density of air.

Surface boundary condition for salinity is:

$$\rho N_z \frac{\partial S}{\partial z} = S_l \tag{9.13}$$

where

$$S_l = S(0)\,(E_l - P_l)/\rho \tag{9.14}$$

$S(0)$ is the surface salinity, E_l is the evaporation rate per unit sea surface, P_l is the precipitation rate per unit sea surface area.

At sea bed, $z = -h$, we obtain

$$\rho N_z \frac{\partial u}{\partial z} = \tau_x^h \qquad (9.15)$$
$$\rho N_z \frac{\partial v}{\partial z} = \tau_y^h$$

where τ_x^h and τ_y^h are the components of bottom stress. Applying a quadratic law at the sea bed, we get,

$$\tau_x^h = g u_h (u_h^2 + v_h^2)^{1/2} / C^2 \qquad (9.16)$$
$$\tau_y^h = g v_h (u_h^2 + v_h^2)^{1/2} / C^2$$

where, u_h and v_h are the bottom current and C is Chezy's Coefficient. For a logarithmic profile,

$$C = 18 \log_{10}(0.37\, h/z_0) \qquad (9.17)$$

where z_0 is the sea bed roughness length.

Also

$$\frac{\partial S}{\partial z} = 0 \qquad (9.18)$$

The equation of state in a salinity stratified condition can be approximated as

$$\rho = \rho_0 + \alpha S \qquad (9.19)$$

where α is of order 0.74 at 20 ^oC and ρ_0 is the density of fresh water (1000 kg m^{-3}).

The equation of state in a salinity and temperature stratified condition can be approximate as

$$\rho = 1000\,(1 - 3.7\text{x}10^{-6}T'^2 + 8.13*10^{-4}S) \qquad (9.20)$$

where $T' = T + 2.7$ (°C). T is the temperature in °C and S is the salinity (typically 35 ppt).

To evaluate the vertical mixing, five options are given in model 3DD, depending on the characteristics of the problems facing in different studies. A common approach is to use a parabolic mixing length formulation with Richardson number scaled reduction in stratified conditions. The mixing length is given as

$$l_m = \kappa\, z(1-z/h) \qquad (9.21)$$

$$N_z = l_m^2\left[\left(\frac{\partial u}{\partial z}\right)^2 + \left(\frac{\partial v}{\partial z}\right)^2\right]^{\frac{1}{2}} \qquad (9.22)$$

where l_m is the mixing length, κ =0.4, z is the distance from the sea bed, h is the water depth, u and v the orthogonal velocities. Equation 9.22 shows that the vertical eddy viscosity is parabolic in the z direction. It goes to zero at both water surface and sea floor.

A more detailed description about model 3DD and its support software is presented by Black (1996).

9.5.3 Establishment of the Hydrodynamic Model

9.5.3.1 Model grids

Previous modelling experiences (Black *et al.*, 1995) showed that three rules should be followed for determining model grid size:

- A model should resolve the local morphology, and therefore, the grid size should be determined by the scale of the smallest features which appreciably influence the water flow;

- The grid should be aligned with the dominant flow direction at the location of highest speed; and

- The open boundary should be placed as far as practicable from the regions or areas with rapid change of water depth or speed and direction of the water flow.

In addition, the availability of boundary conditions must also be considered.

In this study, the plume varied greatly under different wind, rain, and tide conditions. A suitable grid size and model area should be able to meet the need of simulating the plume dynamics under a variety of conditions, as well as using reasonable CPU time. From these considerations, a 75 m grid was chosen to meet such needs.

A 75 m (Tauranga Port model) and a 300 m (Tauranga Harbour model) grid (Figures 9.15 and 9.16) had been established previously during the Tauranga Harbour Model Study (Barnett, 1985; Black, 1985). Both of these grids were suitable for developing boundary conditions for the present study.

As boundary conditions were not available for the 75 m grid model, the 300 m coarser grid model was used to derive the required boundary conditions for the 75 m grid model. The 75 m grid model was then used to specify boundaries for a local 3-dimensional model.

The hydrodynamics around the runoff discharge points in the Stella Passage are complicated. Furthermore, according to the field measurements, the advection and dispersion of the plume occurred mainly at the sea surface. Therefore, only a 3-dimensional model can simulate such complicated plume dynamics. However, to run a 3-dimensional mode over the entire 75 m grid (which has 102x103 = 10506 cells) would require a very long CPU time for each simulation. Accordingly, a sub-grid model (Stella Passage model) was extracted from the 75 m Tauranga Port model (Figure 9.17). This still retained the 75 m spacing but had 11 vertical layers.

The two model grids are aligned with True North. The model cells are referred to by their I and J cell numbers. I is the number of model grid along the East-West direction and J is the number of cells in the North-South direction.

The Bay of Plenty coordinates of the origins of each model grid (I=1, J=1) are presented in Table 9.2.

Table 9.2 Bay of Plenty coordinates of the origins (I=1, J=1)of each model grid.

	300 m grid	full 75 m gird	75 m grid
Coordinates	251244E	269319E	273819E
(BOP)	703022N	706847N	709247N

9.5.3.2 Bathymetry

The latest bathymetry survey undertaken by Port of Tauranga in 1994 was used for all the three model grids.

9.5.3.3 Boundary conditions

There are two open boundaries in the 300 m Tauranga Harbour model: the northern and eastern boundary (Figure 9.16). Tide records from Moturiki Island (cell 82, 37 in the 300 m grid) were used as the open boundary water levels for both northern and eastern boundaries, under the assumption that sea surface gradients are not significant. Moreover, model predictions on the ebb delta were not used in this study.

9.5.4 Calibration and Verification of the 300 m Tauranga Harbour Model (2-dimensional only)

Eddy viscosity is a parameter which reflects the momentum transfer across the shear zone by diffusion between adjacent parcels of water with different moving velocities. It acts as a velocity smoothing algorithm. The typical value of eddy viscosity is between 1 and 10 m^2s^{-1} (Black, 1995). In this study, eddy viscosity coefficient of 5 m^2s^{-1} was used for model calibration.

Sea floor roughness length was adjusted during the calibration. Four simulations with roughness lengths (z_0) of 0.002 m, 0.001 m, 0.0009 m, and 0.0007 m were carried out for the 300 m grid model. The simulation period was from 22:00:00, September 27 to 24:00:00, October 6, 1995 (spring tide is around September 29, the tidal range is 1.86 m). Wind records during the same period were used as the wind boundary file.

It was found that a roughness length of 0.0009 m produced best model results compared to the measured water levels at Sulphur Point (I=77, j=26 in Figure 9.16; the location is also shown in Figures 1.5b and 9.1b) and the Tug Berth (i=78, j=34 in Figure 9.16; the location is also shown in Figures 1.5b and 9.1b) (Figure 9.18). Measured and model predicted water levels at Tug Berth are exceptionally close.

9.5.5 Calibration and Verification of the 75 m Tauranga Port Model (2-dimensional only)

Water level time series at the corresponding positions for the 75 m model grid were extracted from the 300 m grid simulation as the boundary files for running the 75 m model.

Roughness lengths of 0.002 m, 0.0009 m, and 0.0007 m were used to calibrate the model. Once again, the roughness length of 0.0009 m produced best model results. Figure 9.19 shows comparisons of the water levels at Sulphur Point and Tug Berth.

The predicted water levels at Tug Berth are well matched with those measured. At Sulphur Point, while the results are much better than with the low resolution 300 m grid, there are still minor differences between the measured and predicted water levels around high tide. There are probably some local factors influencing the water levels which are still not resolved at 75 m grid. The measured water levels at Sulphur Point are 5-8 cm higher than those at Tug Berth around high tide (Figure 9.20). The agreement between model and data shows that this 5-8 cm rise is mostly being accounted for by the model.

A survey of currents around the wharf area was undertaken by Environment BOP on March 18, 1992. There has been no significant bathymetry change since the completion of the capital dredging program by March, 1992. And so, the results obtained from this survey can be used as a reference for comparison with the currents predicted by the model. Ten locations were chosen in that survey (Figure 9.21). Figure 9.22 gives the predicted and measured current velocity at selected locations (similar tide and wind conditions were used in the model simulation). The current velocity and pattern of change at these locations predicted by the 2-dimensional 75 grid model are basically well matched with those measured.

However, the measured currents with the two current meters deployed at locations S1 and S2 cannot be reproduced in the 2-dimensional 75 m grid model (Figure 9.23) . This was probably due to the following reasons:

- There is a great variation of bathymetry from the eastern side of Stella Passage to the edge of the shipping channel (water depth varied from 0.5 m to 14 m within 60 m). This variation cannot be presented in a 75 m grid model;

- The southern outfall is located in a small bay. The northern side of this outfall is the southern end of the present wharf and its southern side is the Oil Tanker Berth. This feature could not be well represented in a 75 m grid model;

- The data obtained from the two current meters show an irregular variation which is hardly matched to the water levels recorded during the same period 100 m away from the location S2. There appears to be no correlation between offshore currents in the channel and those in the sheltered zone; and

- The current meter deployment sites were only 200-300 m south of the wharf, and large vessels frequently berthed, turned, and departed during the current meter deployment times. The movement of these vessels possibly had an influence on the currents around the current meter deployment sites, although this is likely to be a secondary effect.

9.6 CALIBRATION OF THE SUB-GRID 75 M STELLA PASSAGE MODEL (3-DIMENSIONAL)

9.6.1 Introduction

From field observation, the freshwater runoff remained primarily at the sea surface after it entered the harbour. Accordingly, the top layer of the model was given a thickness of 0.3 m. Layers 2-5 were assigned a thickness of 1 m, and layers 6-11 a thickness of 2 m. This meant that best resolution was at the surface where the plume resided.

The 75 m Stella Passage model has open boundaries on all four sides (Figure 9.17). For the 3-dimensional model, three groups of basic boundary files are required: sea level or currents, salinity input, and freshwater volume.

Boundary sea levels or currents were extracted from the calibrated 75 m Tauranga Port model and applied without modification. Due to difficulties of direct gauging of runoff flow rates, the runoff input was estimated based on the method discussed in Chapter 2.

9.6.2 Establishment of Boundary Salinity Files

The boundary salinity is not available in the present study because of the restraints on instrument deployment in the harbour and other logistic difficulties affecting manual field measurements. The following method was used to derive boundary salinity based on values recorded with the current meters at the S1 and S2 locations.

For salinity, the mass conservation equation 9.6 can be written as:

$$\frac{\partial S}{\partial t}+\frac{u\partial S}{\partial x}+\frac{v\partial S}{\partial y}+\frac{w\partial S}{\partial z}=\frac{\partial}{\partial z}\left(K_z\frac{\partial S}{\partial z}\right)+K_H\left(\frac{\partial^2 S}{\partial x^2}+\frac{\partial^2 S}{\partial y^2}\right) \quad (9.23)$$

During flood or ebb tide, current velocities along y and z directions are small compared to the current velocity along x direction. Accordingly, the above equation can be simplified as:

$$\frac{\partial S}{\partial t}+\frac{u\partial S}{\partial x}=\frac{\partial}{\partial z}\left(K_z\frac{\partial S}{\partial z}\right)+K_H\left(\frac{\partial^2 S}{\partial x^2}+\frac{\partial^2 S}{\partial y^2}\right) \quad (9.24)$$

For a given layer in the water column, if horizontal and vertical eddy diffusivities are neglected, we have:

$$\frac{\partial S}{\partial t}+\frac{u\partial S}{\partial x}=0 \quad (9.25)$$

For a given layer in the water column at a given location, spatial salinity variation along x direction, $\frac{\partial S}{\partial x}$, can be calculated if current velocity, u, and temporal salinity variation, $\frac{\partial S}{\partial t}$, are known at the site. In this study, the location S2 where a current meter was deployed (Figure 9.1b) was chosen as a reference point. $\frac{\partial S}{\partial t}$ was calculated from the salinity time series recorded by the current meter. However, a weighted-average current along Stella Passage (predicted by the 2-dimensinal 75 m Tauranga Port model) was used as current velocity, u, instead of using current velocity recorded at S2 by the current meter. The reason for doing so was because the currents along Stella Passage are variable. According to the current pattern predicted by the model, four sections were chosen between the southern and northern boundary (two sections were located south of the location S2, 2 sections north of the location S2). The weighted-average current from the southern boundary to northern boundary u_a, was calculated as:

$$u_a = \sum u_i L_i \Big/ \sum L_i \qquad (9.26)$$

where u_i is the current velocity of section i (i = 1,4), L_i the length of section *i*.

With known $\frac{\partial S}{\partial t}$ and u_a for a given time, $\frac{\partial S}{\partial x}$ at S2 was calculated. The salinity at southern (S_s) and northern boundary (S_n) were calculated by:

$$S_s = S - \frac{\partial S}{\partial x}(L1 + L2) \qquad (9.27)$$

$$S_n = S + \frac{\partial S}{\partial x}(L3 + L4) \qquad (9.28)$$

where, S is the salinity at location S2, $(L1+L2)$ is the distance from the site S2 to the southern boundary, $(L3+L4)$ is the distance from the location S2 to the northern boundary.

The western boundary (Figure 9.17) was divided into 2 segments. The four cells immediately next to the northern boundary on Centre Bank were assumed to have the same salinity as the northern boundary cells. For the other cells along the western boundary, the salinity was assumed to be the same as those measured at the S2 site. The eastern boundary (Figure 9.17) is not far from the southern boundary, and so the southern boundary salinity time series was used.

9.6.3 Model Calibration

The model was calibrated by comparison to the video images of plume behaviour and examination of vertical mixing. With the calibration of the 2-dimensional 75 m Tauranga Port model, the sea bed roughness length of 0.0009 m was retained in the 3-dimensional 75 m grid Stella Passage model.

Because local stratification data were not available, the above-mentioned parabolic mixing length formula was used in this study (equation 9.21). Black (1990) using long-term field data from a stratified channel tested 6 different formulae for the eddy viscosity and 4 for the eddy diffusivity in a numerical model. He found that the following formula developed by Perrels and Karelse (1981) was most applicable,

$$N_{zR} = N_z \, e^{-CR_i} \qquad (9.29)$$

where C=4 for the eddy viscosity and 12 for the eddy diffusivity. With exponential form, the eddy viscosity and diffusivity decrease quickly with increasing Richardson number.

Because a Eulerian scheme was used in the model, a uniform eddy diffusivity value was applied in both the x and y grid directions as flow streamlines were not computed. Longitudinal eddy diffusivity values of 0.005, 0.0005, and 0.0001 were tested in the calibrations. Results (Figure 9.24) showed that the plume behaviour was not strongly affected by the chosen eddy diffusivity values because the high Richardson number significantly reduces its value in stratified conditions (equation 9.29).

The three rainfall events on September 29, October 1, and October 5, 1995 were calibrated. Figures 9.25, 9.26, and 9.27 show the plume time series digitised from the video images and predicted by the 3-dimensional Stella Passage model for the three rainfall events.

It is noteworthy that the model results are expressed as salinity reduction (negative values). For a given rainfall event, when the calibration or simulation had been completed, an extra run was undertaken with all parameters remaining the same but without runoff added. The salinity reduction is the salinity difference between each pair of simulations. As discussed in the

previous section, the boundary salinity values were estimated based on the salinity recorded by the current meter at location S2 using equation 9.25, instead of directly measured ones from the field. While any salinity errors affect the results between the two simulations, by subtracting the two cases, the error is greatly reduced.

From Figures 9.25, 9.26 and 9.27, the predicted plumes are well matched with those captured with the video camera. Minor differences between the actual plume shapes and the simulated ones occurred at the plume head. In reality, the plume started at a single point and in spite of the lateral mixing, the plume remained narrow around the outfall. However, the plume started within a whole cell, which is 75 m wide, in the Eulerian scheme simulation.

From the simulations, vertical thickness of plume around the outfall in the model retains less than 1.5 m for all three rainfall events (Figure 9.28). This is comparable to the results recorded 20 m away from the southern outfall on April 5, 1995 immediately after a rainfall event of 16 mm (Figure 9.29).

9.6.4 Plume Dynamics under Different Weather Combinations

The purpose of this model study is to predict the plume dynamics under different weather conditions, particularly what will happen during flood tide and under strong northerly and easterly winds. Four simulations were carried out under different tidal and wind conditions. The common assumptions for all four simulations were:

i) spring tide (tidal range = 1.86 m); and
ii) a storm with 5 year return period, constant rainfall on the port area lasting 6 hours, which is 104 mm/6 hours in the Tauranga Region (Quayle, 1984).

Simulation 1 (2 hours of 40 knot easterly winds turning to 40 knot northerly winds)

Apart from the above-mentioned common assumptions, other assumptions for simulation 1 are as follows:

i) the storm hit the port area 1.5 hours before low tide and the runoff starts to enter the harbour 1 hour before the low tide; and

ii) winds of 40 knots from the easterly direction start upon the arrival of the storm and turn to northerly 2 hours later. In reality, there is 8 degree difference between the eastern bank of Stella Passage and the True north (the V direction of the model grid), and so the wind direction of the "northerly" was set to 10°T. To allow for the "cold start" in the model, the model start time is 5 hours earlier than the starting time of the runoff.

Current Pattern and Plume Dynamics

Figure 9.30a shows the surface currents and plume at low tide which is 1 hour after the runoff starts to enter the harbour (t = 6 hours in the figure). The strong surface currents across the channel, especially the area opposite the outfalls, are characterised by wind stress (τ_x=1.14 Nm^{-2}, equation 9.12) and pressure gradient caused by the addition of freshwater. Due to the low density of the plume water, its free surface is above the level of the surrounding seawater. The resulting pressure gradient causes a lateral spreading of the plume over the ambient seawater. This explains why the plume spreads to its left and right.

Downwelling currents are present at the western boundary of the Stella Passage when the surface water meets the western boundary (Figure 9.30b). This downwelling induces a cross-sectional circulation by pushing the water mass under the top two layers, and creating a return current of low intensity to the east. At water depth of around 2 m (the interface of the plume and

seawater), part of the water rises due to entrainment in the surface layer. For the water mass at layers 6 and 7, the flow bifurcates at the eastern bank.

With continuing addition of runoff, the plume spreads further to the west (Figure 9.30c, t = 7 hours). At this stage, the flood tide current starts and the plume spreads toward the south due to the southwestwards surface currents.

Strongest downwelling and thickening of the plume appears at the western boundary at this time due to the downwelling currents (Figure 9.30d) with the maximum thickness of 4.5 m. However, upwelling at the eastern side constricts the plume to a thinner surface feature. Overall, the plume is much thicker than 1 hour previously.

After the wind direction changed to northerly, the currents and plume shapes varied greatly. Figure 9.30e-j shows the surface current pattern and plume shape transitions under the strong northerly winds.

Under the strong northerly winds, the southwards moving surface currents (around 0.5 m/s) are driven by the flood tide, the surface wind stress, and the pressure gradient due to the addition of runoff. Because of the fast surface currents, the residual freshwater at the western side of the channel essentially disappeared one hour after the wind direction changed. The disappearance of the freshwater occurred because (i) there was no further freshwater supply, (ii) vertical mixing, and (iii) advection south (out of the area of interest).

There is not a great change of current pattern and plume shapes between peak flood and high tide (t = 9-12 hours in the figures). During this period, wind and the runoff flow rates remain constant. The only change during this period is the reduction in tidal current. The currents around the Stella Passage are nearly southward and the plume remains in the eastern half of the Stella Passage.

The plume mainly remains in the top 2-3 layers around the peak flood tide period (Figure 9.30k-m). The vertical mixing around this period was not as strong as that in the previous simulation at the western boundary during low tide under the easterly winds (Figure 9.30d). There was no appreciable presence of fresh water deeper than 3 m. This is probably due to the following reasons:

i) Around peak flood tide, the current vertical shear was small (Figure 9.30n). According to equation 9.22, a lower vertical velocity gradient would lead to lower vertical mixing.

ii) The water depth shallows rapidly (from 14 m to 4-5 m) after passing the southern end of Stella Passage which causes strong upwelling currents (Figure 9.30n). The upwelling currents prevent downwelling carrying freshwater into the deeper layers. Actually, the plume becomes thinner after it passes the southern end of Stella Passage; and

iii) The strong currents mean that the plume moved more quickly to the model boundary.

The plume moved out of the model area quickly due to the fast flood currents after the runoff ceased from the wharf discharge point (Figure 9.30o-p). In reality, the runoff flow rate would decrease gradually after the storm stopped.

Although the fate of the plume was not simulated after it moved out of the southern boundary of this 75 m Stella Passage model, the behaviour can be deduced based on the following:

Strong southwards currents are predicted along the Town Reach (Figure 9.31, obtained from the 75 m grid Tauranga Port model under the same 40 knot northerly winds). Eastward currents only occur after passing the Harbour

Bridge and were rather weak. Accordingly, the plume would mainly advect further south along the Town Reach, instead of turning to Waipu Bay (Figure 9.31).

Dilution Rate

Dilution usually is defined as a ratio of total volume of a sample to effluent volume contained in the sample (Fischer *et al.*, 1979). For an unit volume of mixture (seawater and effluent), the dilution rate will be the reciprocal of effluent volume. Based on the definition, the dilution rate for any layer of a given model grid can be calculated from the following formula:

$$D = C_o /(C_o - C) = C_o/SD \qquad (9\text{-}30)$$

where, D is dilution rate, C_o ambient salinity (ppt) without the addition of wharf runoff. It was obtained from the simulation without runoff added, under the same weather conditions. C salinity (ppt) with the addition of wharf runoff. $SD = C_o - C$ (ppt).

One concern is whether the plume remains as a coherent body and impinges on the Whareroa Marae (Figure 9.1b) area through the channel underneath the small causeway bridge at Whareroa Point (Figure 9.1b, cell number: 13, 3). At cell 12, 3 (next to the causeway bridge), the surface water salinity reduction is 0.75 ppt during peak flood flow and dilution rate is 44 times. From Chapter 4, the arithmetic average turbidity of the runoff samples obtained from the outfalls of the northern and southern storm drainage systems are 542 and 304 NTU, respectively. After 44 times of dilution, the turbidity at the cell 12, 3 would be 7.0-12.3 NTU. This is considerably higher than the background turbidity level of < 2.0 NTU (Mathew, personal communication), suggesting that the effect of the plume is evident at this site in these conditions. This is comparable to measurements of 7.1-8.5 NTU taken under similar conditions (6-18 m/s northwesterly) but less heavy rainfall (43 mm)

Simulation 2 (30 knot northeasterly winds)

For this scenario, all the assumptions from the previous case were retained, except for the wind conditions. A 30 knot northeasterly (45°T) wind was assumed during the entire storm episode. Figure 9.32a-f shows the time series of plume shapes from low to high tide.

During low tide (t = 6 hours), the surface southwestwards currents were associated with the wind stress and pressure gradient due to the addition of the runoff, resulting in stronger surface currents in plume than adjacent regions. After low tide, the flood currents accelerated causing the currents to be higher than at low tide.

The plume reached cell 12, 3 by 7 and 8 hours. The dilution rate at this cell was again 44 times. Later in the simulation, the plume remained relatively stable in the channel and did not reach cell 12, 3.

Due to similar reasons explained in simulation 1, the plume remained within the top three layers (Figures 9.32g-h and 9.32i) because of the weak vertical mixing. As previously shown in simulation 1, when the plume passed the southern end of the Stella Passage, it became thinner because of the upwelling currents from the underneath layers.

In summary, under consistent 30 knot northeasterly winds, the plume advected towards to the southwest. The plume (defined by minimum salinity reduction of 0.5-1.0 ppt) was shaped as a parallelogram about 1000 m along the south-north direction and 700 m along the south-west direction. The salinity drop at cell 12, 3 was only around 0.2 ppt, which indicated a dilution of 167 times.

Simulation 3 (consistent 30 knot easterly winds)

All the assumptions remained the same as in simulation 1 except for the wind conditions. 30 knot easterly winds (90°T) were assumed during the entire rainfall event. Figure 9.33a-f shows the time series of plume shapes from low to high tide.

For the first 2 hours (t=6, 7 hours), the plume behaviour is similar to simulation 1, but with shorter plume dimensions from east to west due to the weaker easterly (in simulation 1, it was 40 knot easterly winds for the first 2 hours, instead of 30 knot easterly in this simulation).

When the flood tidal currents become stronger 2 hours after the low tide (t = 8, 9, 10 hours in the figures), the surface currents become more complicated. The forces acting on the surface water include: wind stress, tidal water surface gradient, and pressure gradient caused by the addition of the runoff.

At the western boundary, the water mass downwelled and moved southwards. Because of the downwelling currents, the plume at the western boundary was twice as thick as that at the eastern side. At the eastern side, the upwelling currents led to a thinner plume (Figure 9.33g). The plume shapes at different layers of the peak flood tide (t = 9 hours) are shown in Figure 9.33h-j.

In summary, under consistent 30 knot easterly winds, the plume advects towards the west and then turned to the south. The plume thickness along the eastern bank is about an half long as at the western bank. The salinity reduction at cell 12, 3 is 0.1 ppt, which results in a dilution rate of 330 times.

Simulation 4 (30 knot easterly turning to 30 knot southerly winds)

Simulation 4 was designed to model the plume behaviour under an ebb tide. The assumptions were:

i) the storm commenced on the port area one hour earlier and the runoff started to enter the harbour half an hour earlier than the high tide; and

ii) 30 knot easterly winds started with the runoff, and then turned to 30 knot southerly winds 1.5 hours later. Because of the 8 degree difference between the eastern bank of the Stella Passage and True north (the V direction of the model grid), the wind direction of the "southerly" was set to 190°T.

The model start time was 13 hours earlier than the starting time of the runoff, to avoid "cold start" effects.

For the first 1.5 hours (around high tide), the movement and shape of the plume are similar to those during low tide conditions under 30 knot easterly winds in simulation 3 (see Figure 9.33a, b). When the wind direction changes to southerly, the plume turns to the north quickly (Figure 9.34a-e).

The plume is not as wide as during the flood tide shown in the previous simulations, although the same longitudinal and lateral horizontal eddy diffusivities are used for all the simulations. The narrower plume is probably a result of the following:

i) During ebb tide, the currents are faster than those under flood tide and the current speed and direction are uniform along the eastern boundary. This lead to only minor lateral velocity gradients, and thus weaker lateral mixing and advection; and

ii) Currents from the Otumoetai Channel (Figure 9.1b) prevents the lateral advection of the freshwater to the west.

The vertical mixing is also weaker (Figure 9.34f). The plume is mostly within the top 3 layers (2 m). This may be related to upwelling beneath the plume. Figure 9.34f shows this occurring with downwelling on the opposite of the channel.

Because of the faster currents and weaker horizontal and vertical mixing, the plume remains coherent over a much longer distance than during the flood tide. As such, the dilution rate at cell 14, 38 was only 6 times.

9.6.5 Discussion

To date, no acute toxic events, which have resulted in dead fish or other marine life adjacent to the log handling area, have been reported after a storm, although the wharf runoff contains significantly high levels of resin acids (1035 ppt, equals to 96 hours LD50 of resin acids). A scientific explanation is required.

As mentioned in previous chapters, there are two main drainage systems around the log handling area: the southern and northern systems (Figure 3.1). The southern drainage system receives storm runoff not only from the wharf area, but also the adjacent urban area. Due to the addition of the adjacent urban runoff which contain little resin acids (1.3 and 4.1 ppb for the two samples examined in this study, see Chapter 5), the resin acid level of the runoff exiting the southern outfall has been mitigated. The ratio of adjacent urban runoff and wharf runoff is estimated to be 3-4:1 at the southern outfall, and so the average resin acid level of the runoff from the southern outfall is about 200-250 ppb. Consequently, the runoff from the southern outfall would not lead to an acute toxic event to local marine life.

The northern drainage system collects wharf runoff only. From the model simulations, the minimum salinity always occurred around slack water several hours after commencement of runoff. The minimum salinity values at this specific time were more than 12 ppt for all four simulations, resulting in a dilution rate of 1.6 times. For the other simulation times, the dilution rate was always more than 2 times. It is noteworthy that the minimum dilution rate occurred only within the cell next to the northern outfall and was restricted in the top layer (0.3 m). For the other sea area, including the layers beneath this top layer, the dilution rises.

In summary, the short duration and restricted region of the low dilution pulse of effluent around slack water may explain why there have been no reports of acute toxic events. Furthermore, pelagic fish may not like to swim within the water column with very low salinity which may be another possible reason. In this case explanation is given for why no acute toxic events, like dead fish, have been reported. This does not mean there is no chronic impact on marine life. However, as stated in Chapter 1, the investigation of chronic impact, particularly on benthic biota, is beyond the scope of this study and is being investigated separately from this study.

From the model simulation results, the plumes retained a thickness less than 4 m, mostly 2-3 m, under different weather conditions. Upwelling currents occurred underneath the eastern boundary of Stella Passage under easterly and northeasterly winds. The upwelling currents prevent sedimentation of particles in the wharf runoff. Furthermore, the bark particles, the source of the resin acids, are lighter than water. They can hardly settle even in still waters. This explains why the resin acid levels in the adjacent sediments were of the same order compared to that in the storm runoff (see Chapter 8). This differs from those in the sediment samples from Matata Lagoon, Tarawera River bed, and the bark dumping area in the Tauranga Harbour (Healy *at al.*, 1997; Wilkins, *et al.*, 1996, 1997) because of the different hydrodynamic circumstances.

9.7 CONCLUSIONS

Based on the field measurements and numerical model simulations, the following conclusions can be deduced:

1. Obvious natural salinity stratification excluding the timber wharf runoff is mainly restricted on top 4.5 m of water column at low tide and 2 m at high tide. The extent of the stratification depends greatly on the rainfall and weather conditions (at low tide, $\frac{\partial S}{\partial z}$=1.15 ppt/m within the top 4.5 m of water column 3 days after a 44 mm rainfall and $\frac{\partial S}{\partial z}$=0.25 ppt/m after 16 days of fine weather).

2. The model simulations show that wind stress and the pressure gradient caused by the addition of runoff have the greatest influence on the plume dynamics during the flood tide. However, ebb tidal currents have a strong influence on plume dynamics during the ebb.

3. The plumes from the timber port were mostly retained within the top 2-3 m of water column, except at the western side of Stella Passage where the thickness of the plume was 4-5 m under 30-40 knot easterly and northeasterly winds.

4. For storm rainfall with a 5-year return period falling consistently over the port area for 6 hours, the plume behaviour varies with wind conditions. Under 40 knot northerly winds, the plume is constricted to the eastern side of the Stella Passage. The dilution rate at the cell next to the Whareroa Point causeway bridge was 44 times. Under 30 knot easterly (90°T) or northeasterly (45°T) winds, the plume covers nearly the whole of Stella Passage in the surface waters. However, there is hardly any influence at

depth and near the Whareroa Point causeway bridge (dilution rate >165 times).

5. If the same storm hit the port area during the ebb tide (30 knot southerly winds), the plume remains more coherent than during flood tide, because of faster currents, upwelling beneath the plume and constriction by currents entering from the Otumoetai Channel.

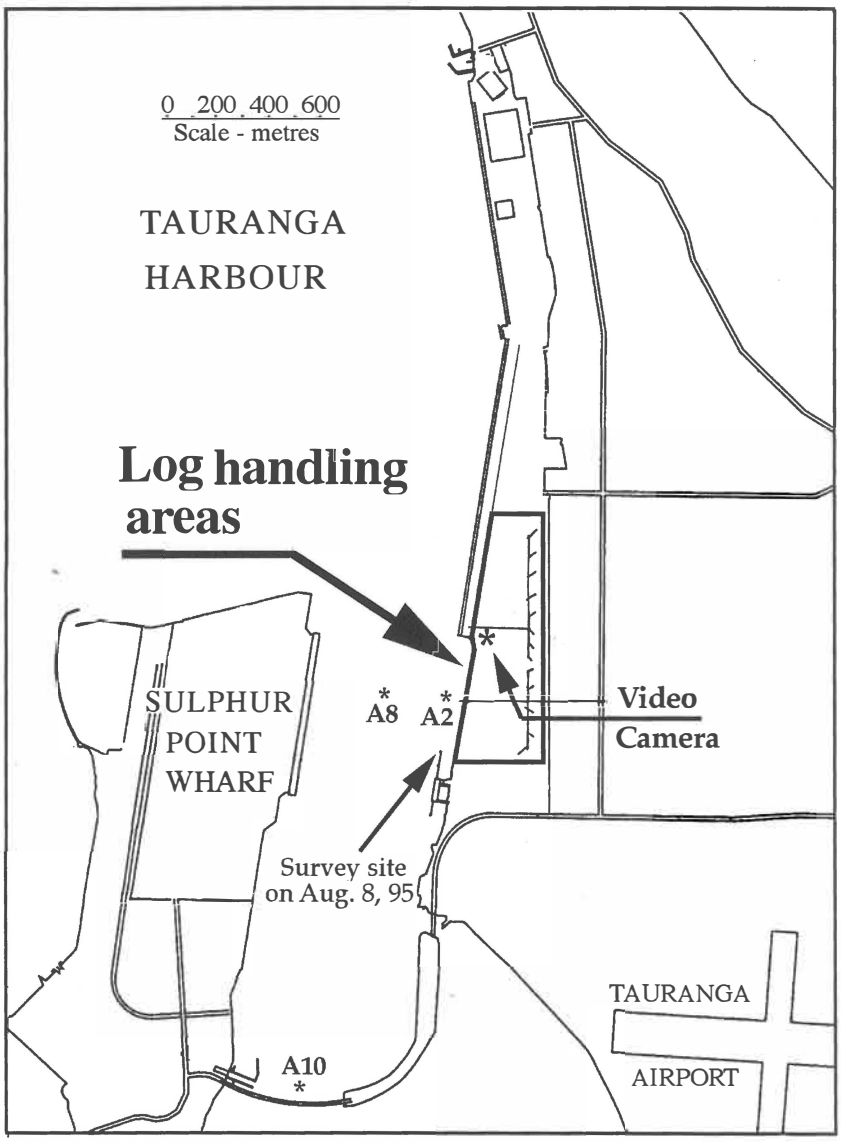

Figure 9.1a Tauranga Harbour and Mt. Maunganui wharf, showing the location where a video camera was deployed to monitor the plumes, the locations of background salinity survey undertaken on October 28, 1993 (A2, A8, and A10), and the location of background salinity survey on August 8, 1995.

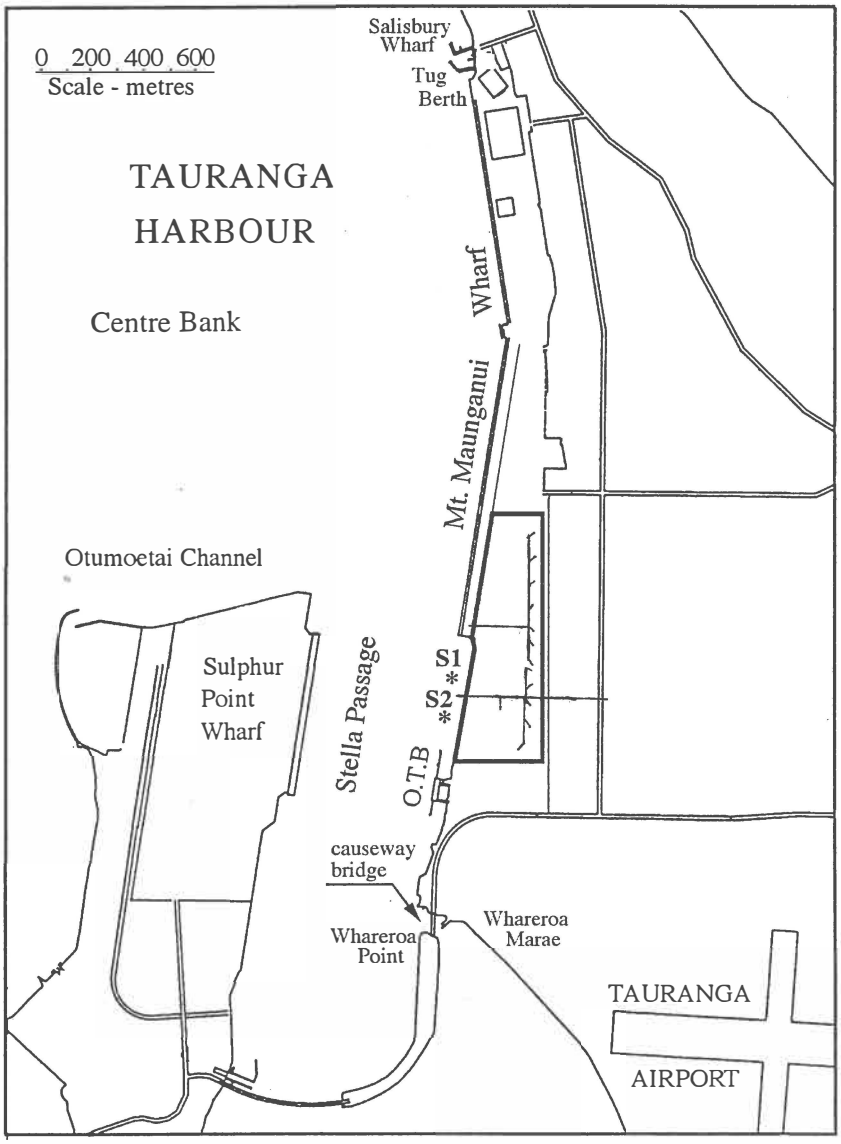

Figure 9.1b Tauranga Harbour and Mt. Maunganui wharf, showing the locations of the current meter deployment (S1 and S2) and other places around the log handling area mentioned in the text. O.T.B: Oil Tanker Berth.

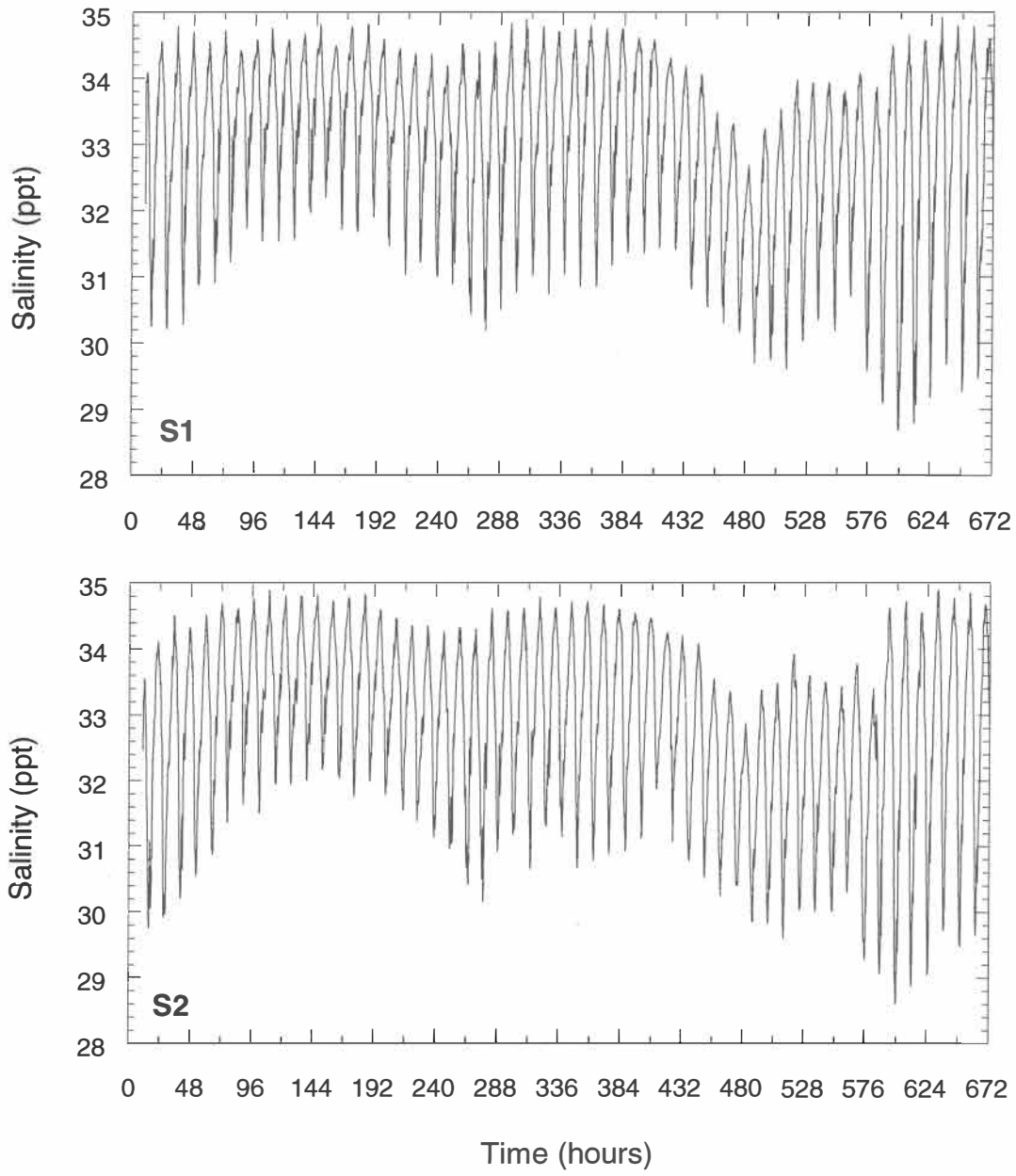

Figure 9.2 Salinity at locations S1 and S2 from 00:00:00, September 12 to 00:00:00, October 10, 1995. The two current meters were both 7.0 m above the sea bed.

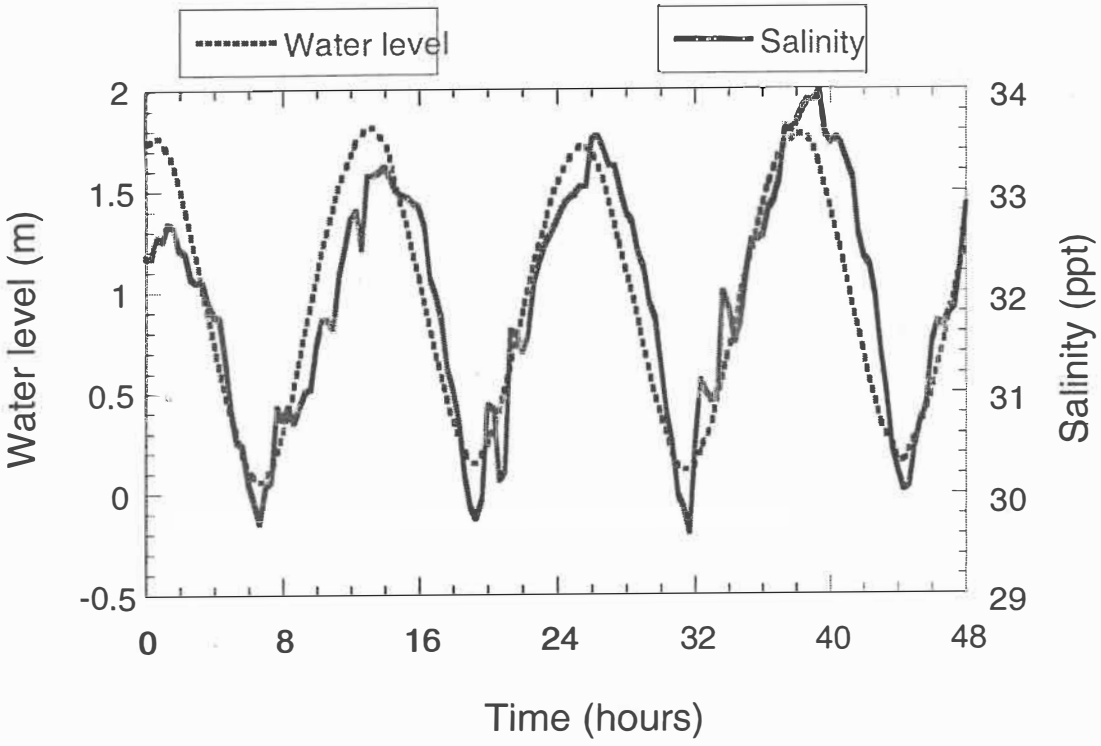

Figure 9.3 Salinity at location S1 and water levels recorded at Sulphur Point from 00:00:00, September 29, to 00:00:00, October 1, 1995.

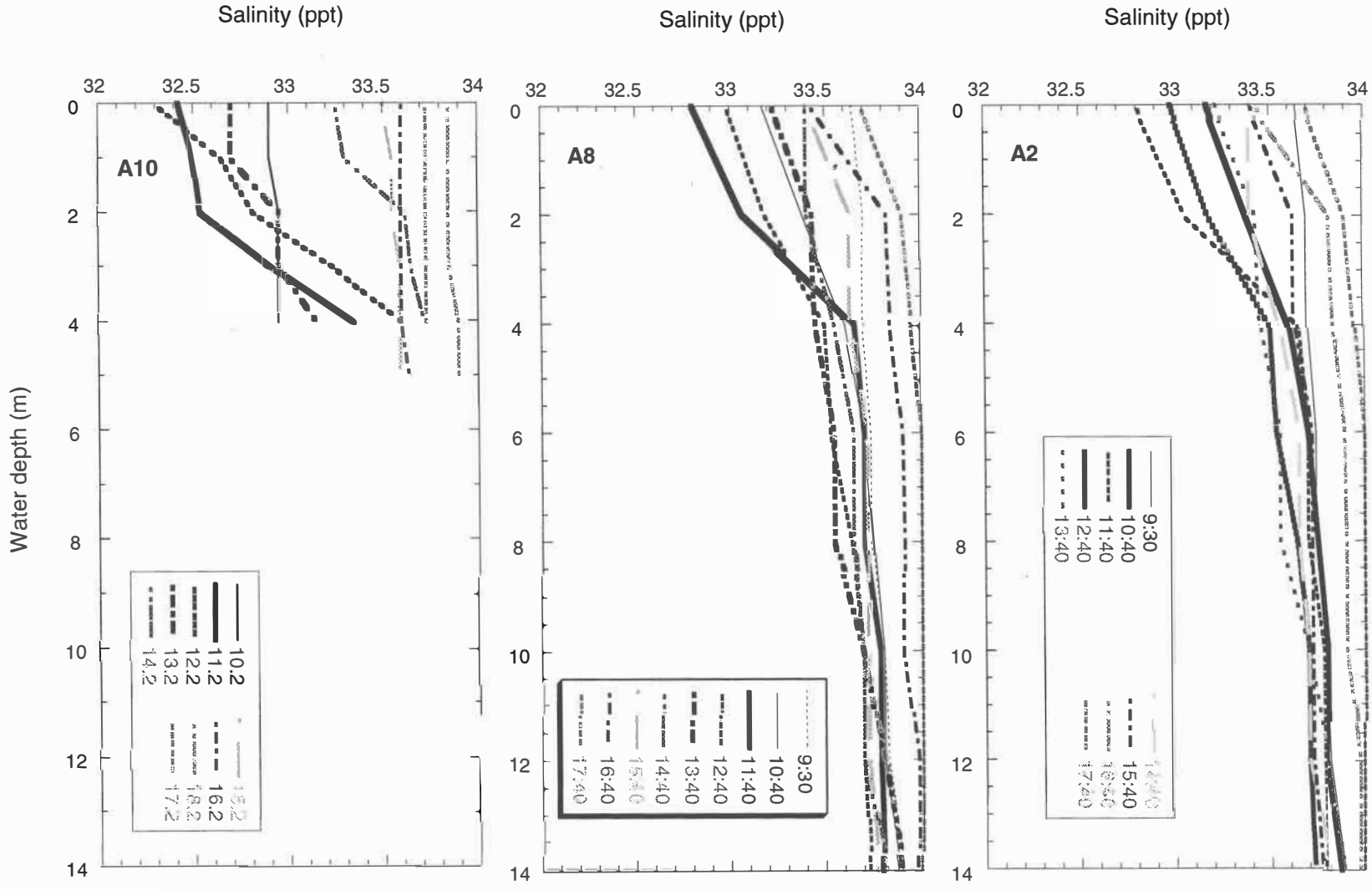

Figure 9.4 Vertical distribution of salinity for different tide conditions measured at sites A2, A8 and A10 on October 28, 1993. Site locations were shown in figure 9.1a. There had been no significant rainfall since October 12, 1993.

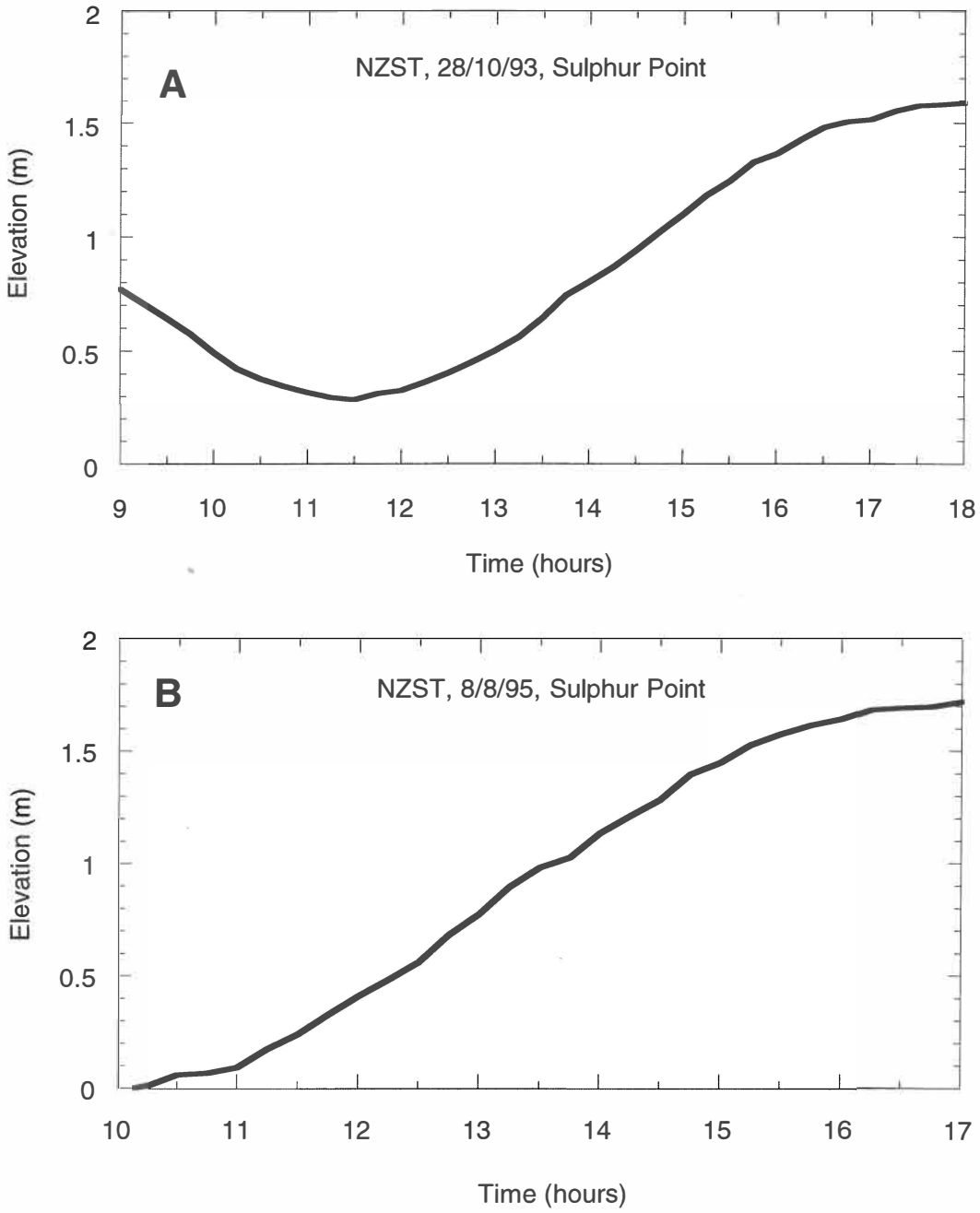

Figure 9.5 Water levels recorded at Sulphur Point on October 28, 1993 (A) and August 8, 1995 (B).

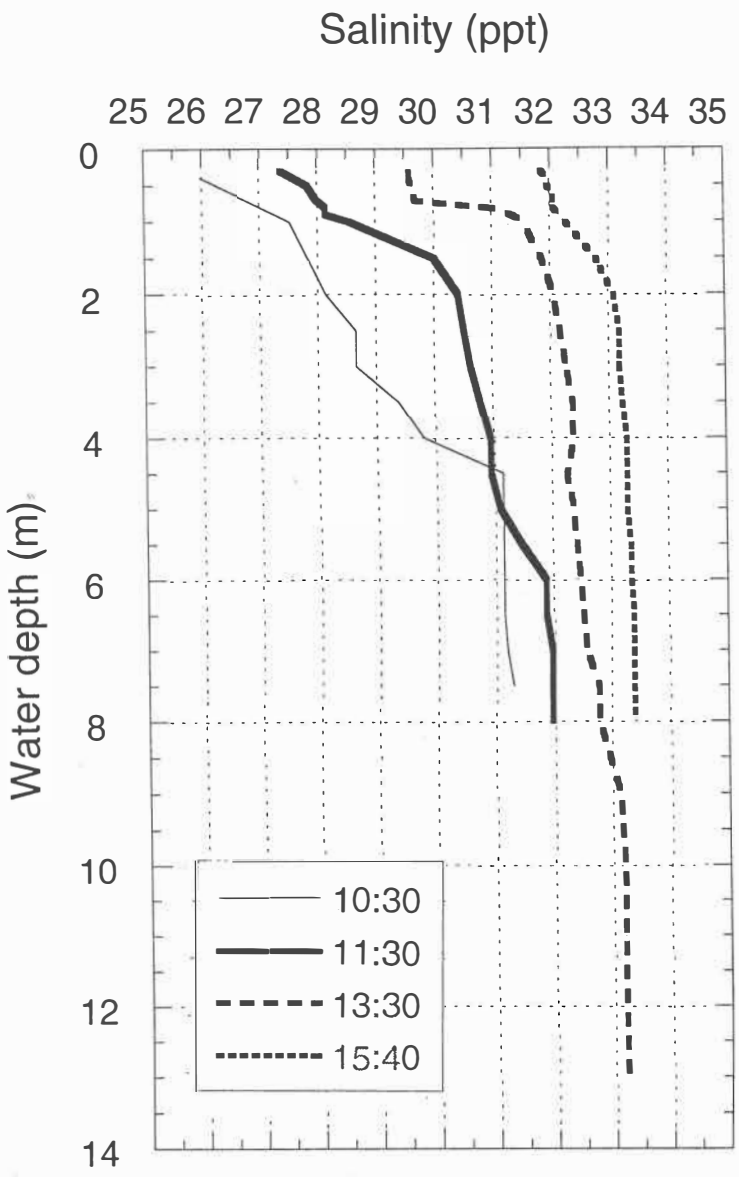

Figure 9.6 Vertical distribution of salinity for different tidal conditions at the northern end of the Oil Tanker Berth measured on August 8, 1995. Three rainfall events were experinced in the Tauranga region on August 3 (42.3 mm), August 5 (14.2 mm) and August 6 (10.0 mm).

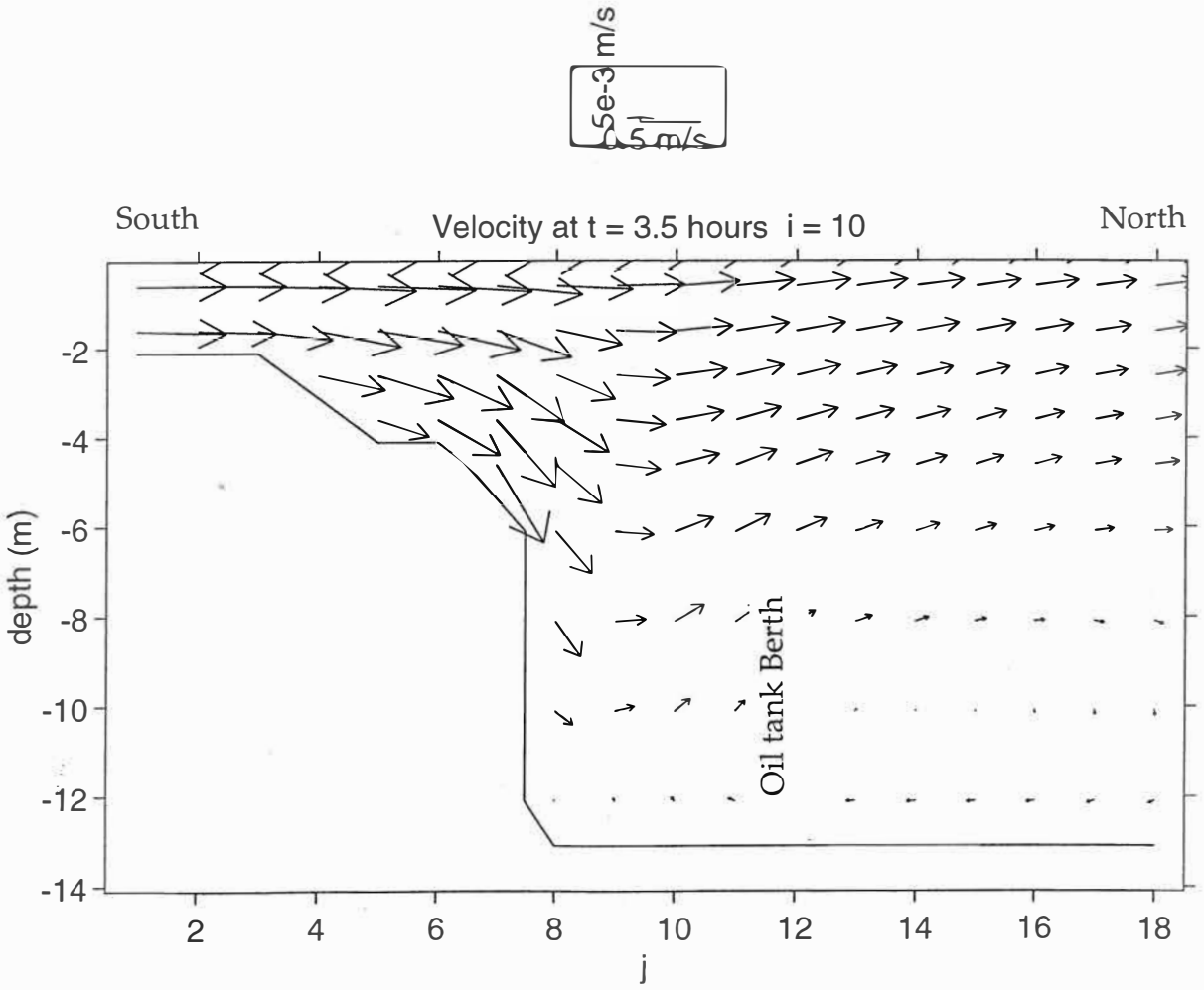

Figure 9.7 Side-view of the current pattern along the centre of Stella Passage during peak ebb tide obtained through model simulation. The natural and dredged bathymetry of the channel is shown.

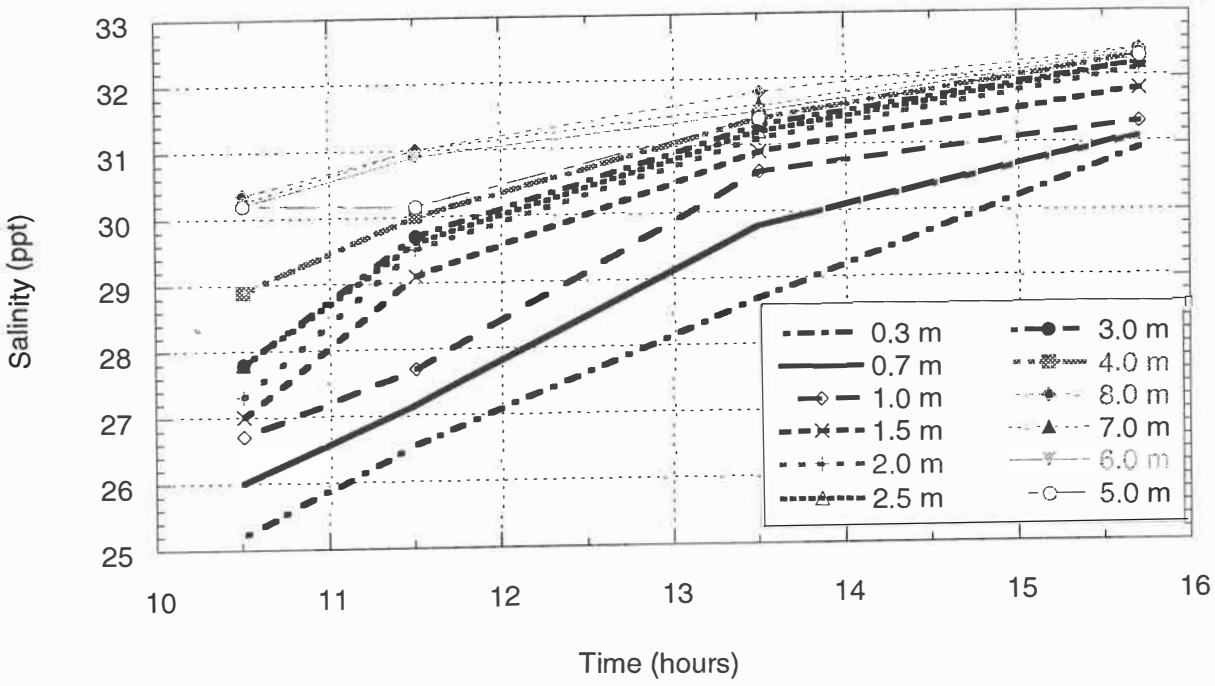

Figure 9.8 Salinity variation with time at different water depths at the northern end of the Oil Tanker Berth measured on August 8, 1995. Three rainfall events were experienced in the Tauranga region on August 3 (42.3 mm), August 5 (14.2 mm) and August 6 (10.0 mm), 1995.

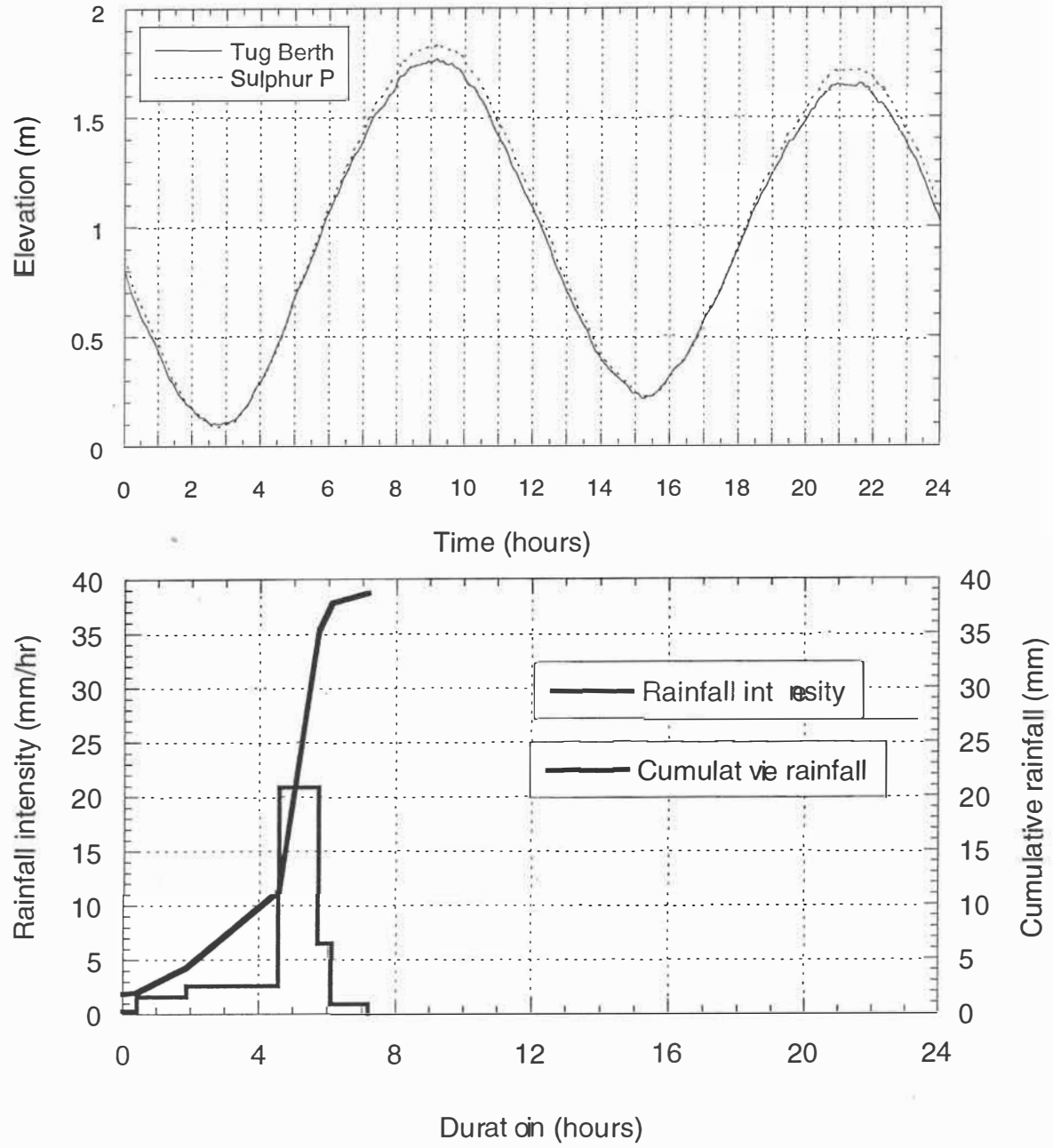

Figure 9.9 The rainfall and water levels from 0:00:00 to 24:00:00 on November 10, 1995.

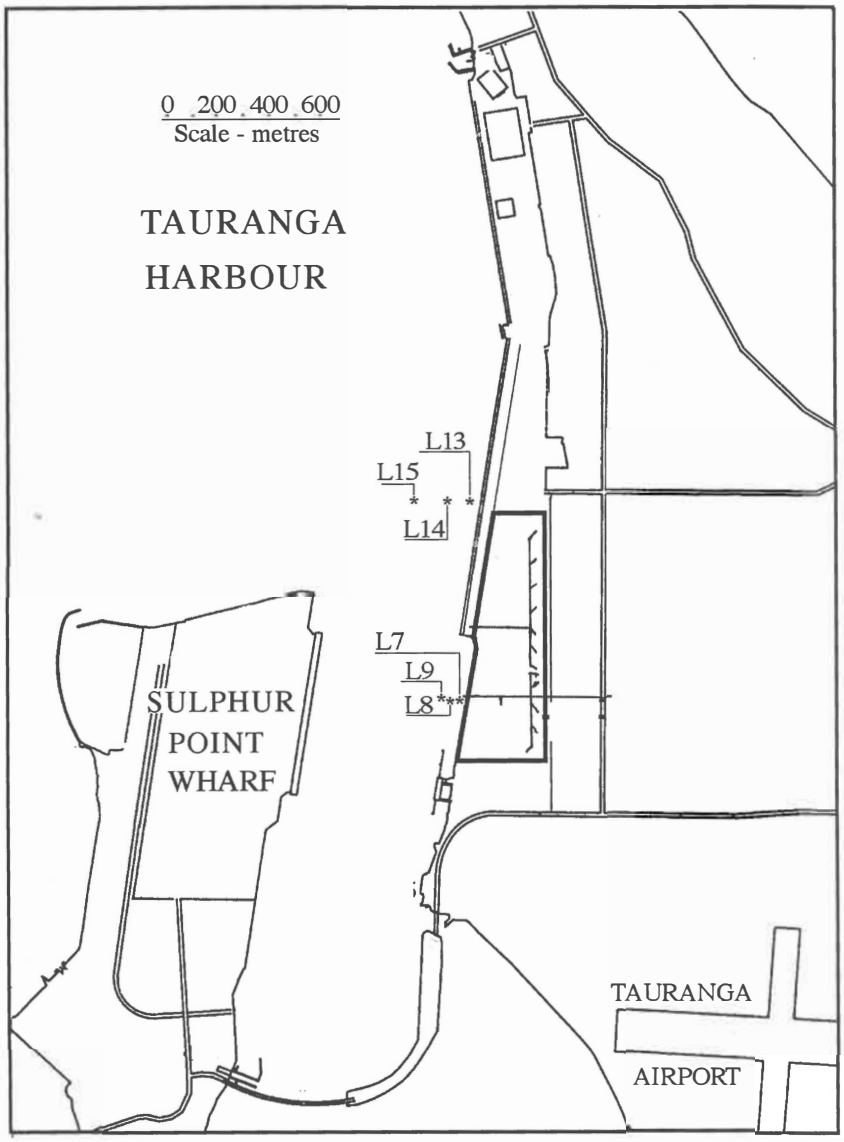

Figure 9.10 Locations where vertical salinity profiles were measured immediately after the rainfall on November 10, 1995.

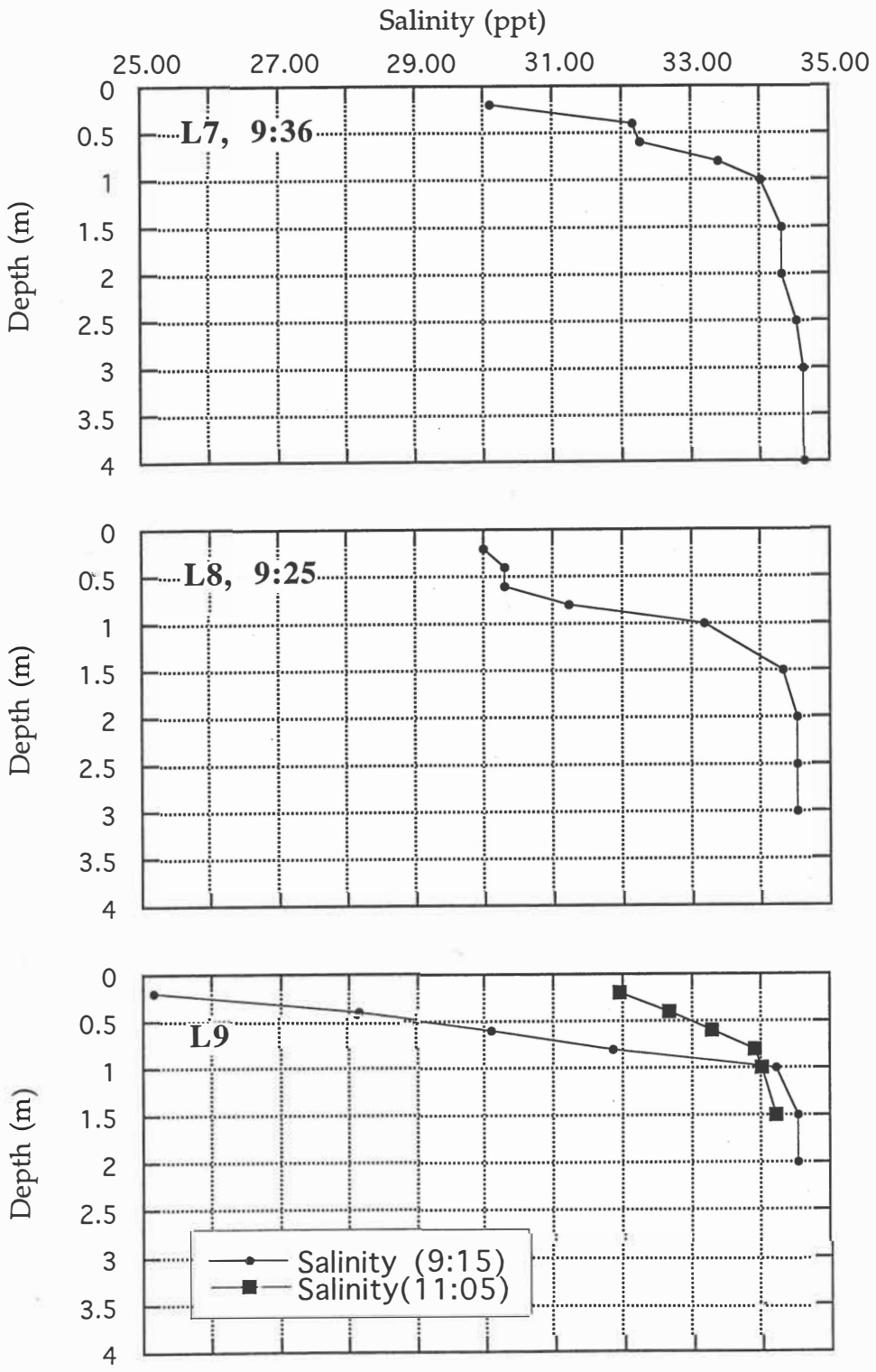

Figure 9.11a Vertical profiles of salinity at the plume head (L7, L8, and L9) immediately after the rainfall on November 10, 1995.

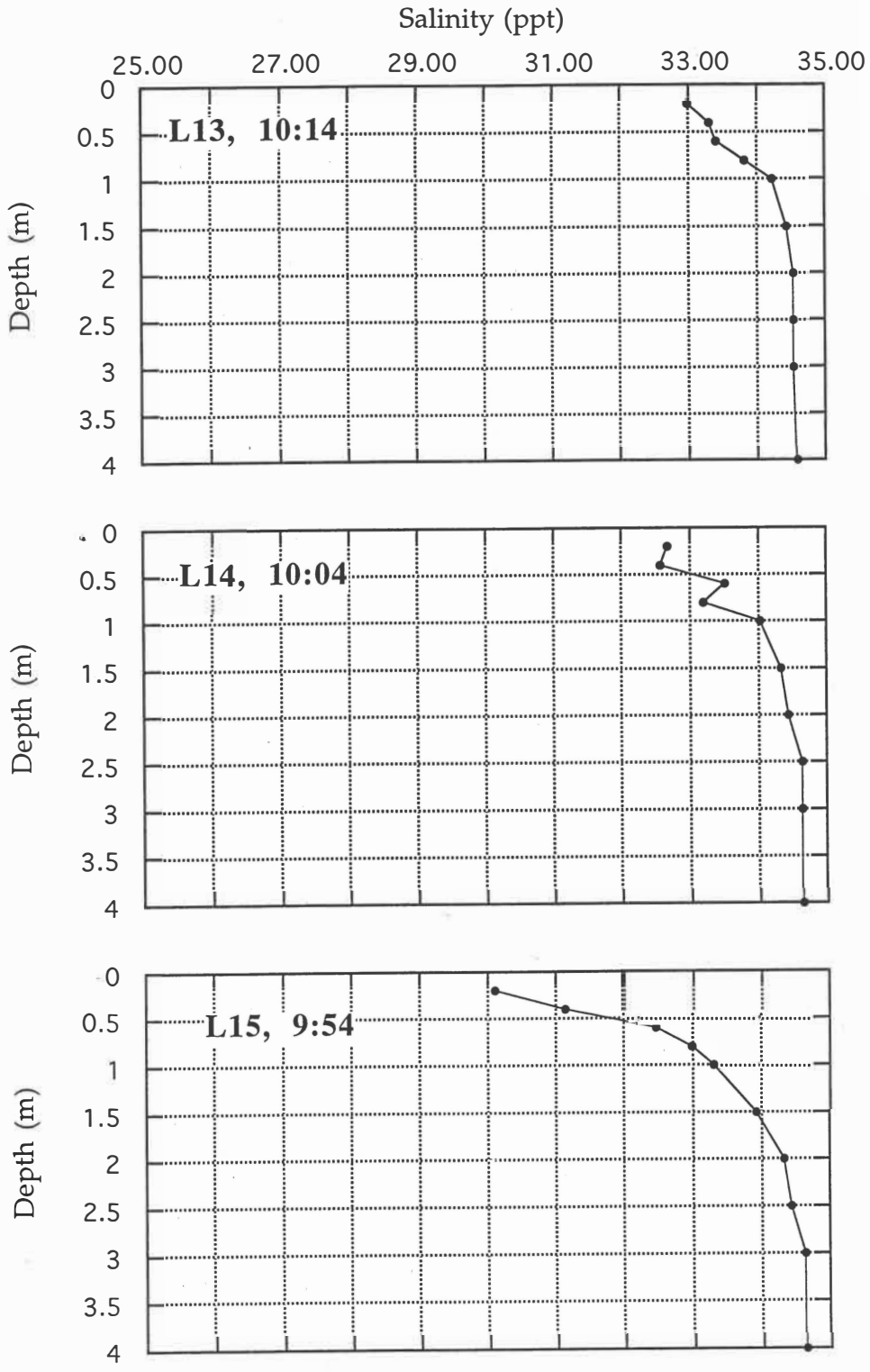

Figure 9.11b Vertical profiles of salinity at the plume tail (L13, L14, and L15) immediately after the rainfall on November 10, 1995.

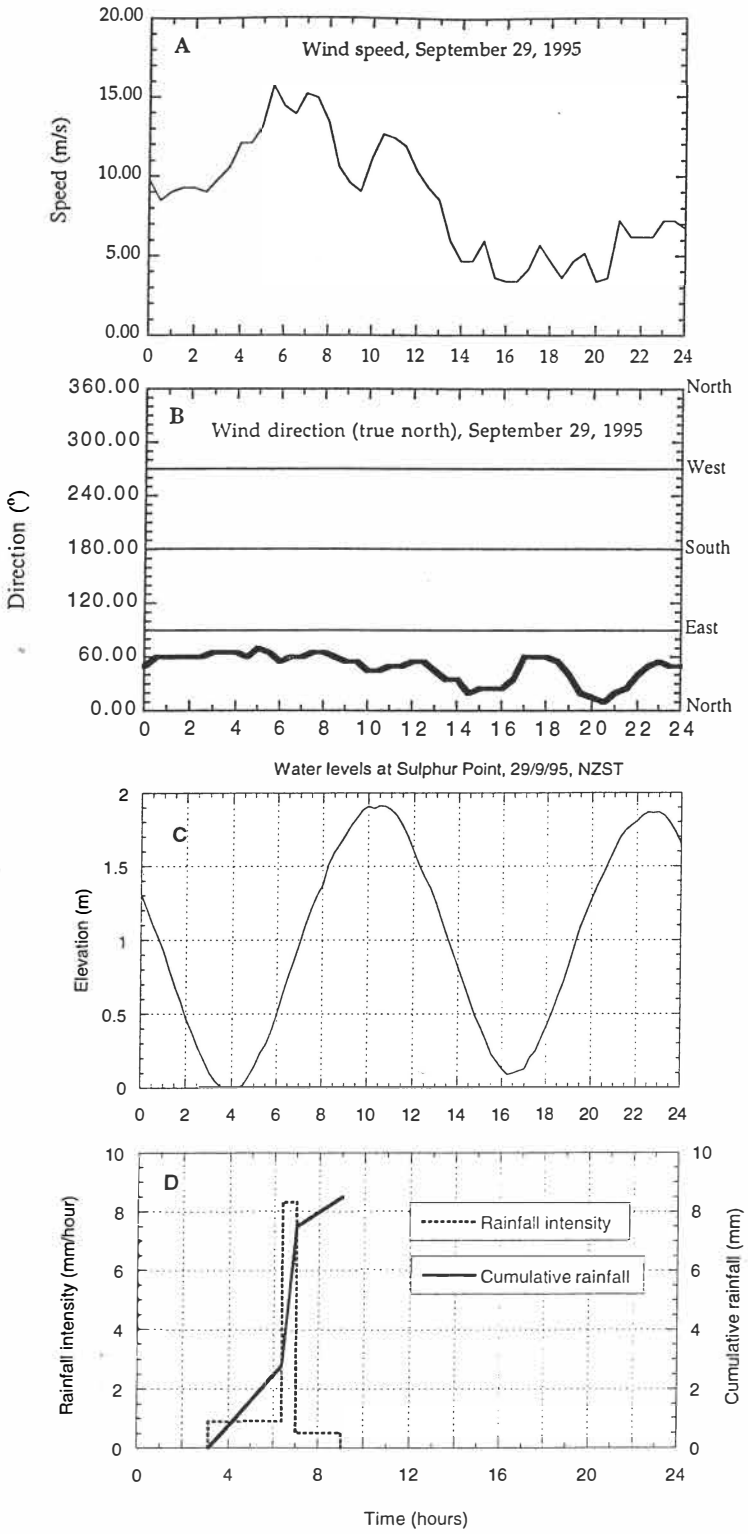

Figure 9.12 Wind (A, B), water levels (C), rainfall intensity and cumulative rainfall (D) on September 29, 1995.

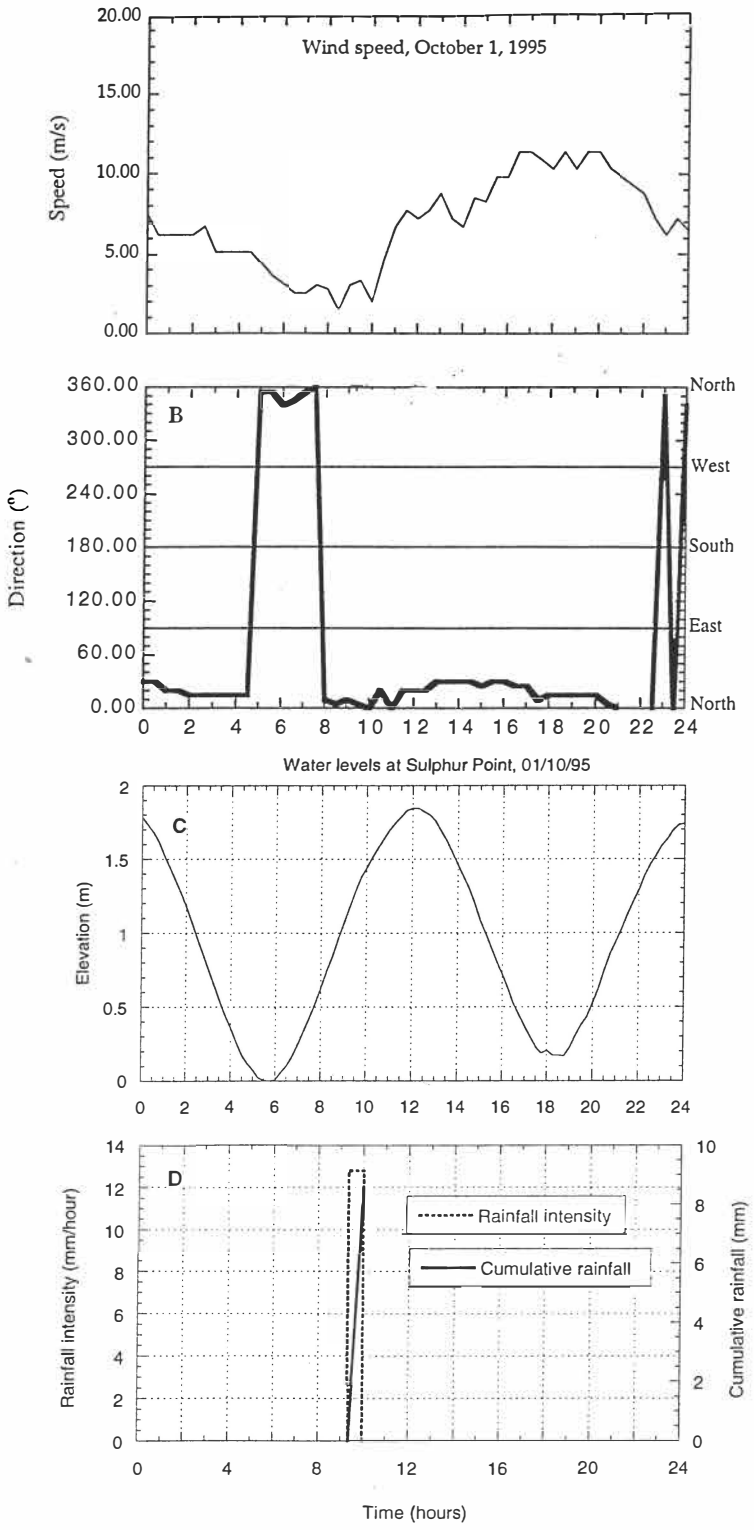

Figure 9.13 Wind (A, B), water levels (C), rainfall intensity and cumulative rainfall (D) on October 1, 1995.

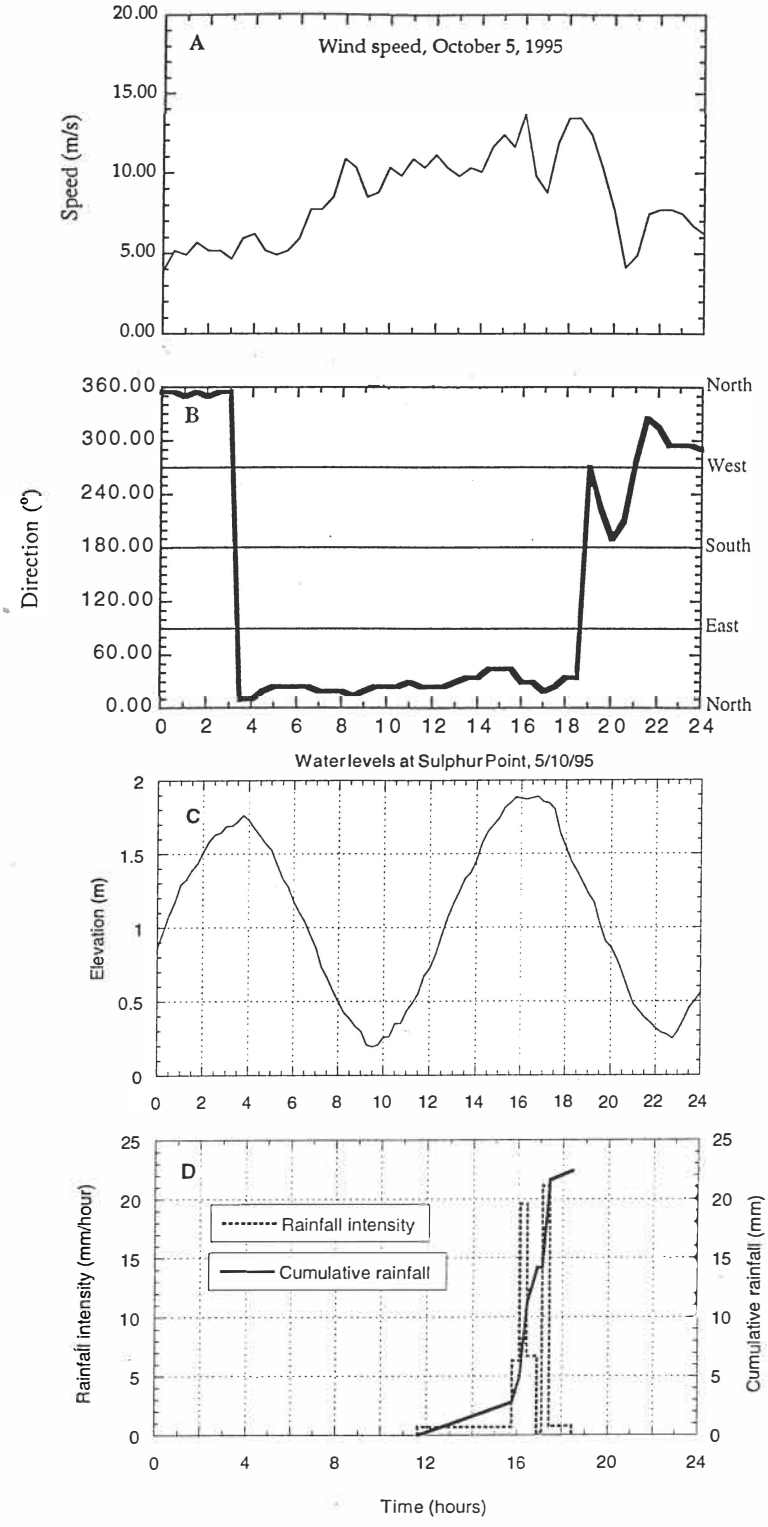

Figure 9.14 Wind (A, B), water levels (C), rainfall intensity and cumulative rainfall (D) on October 5, 1995.

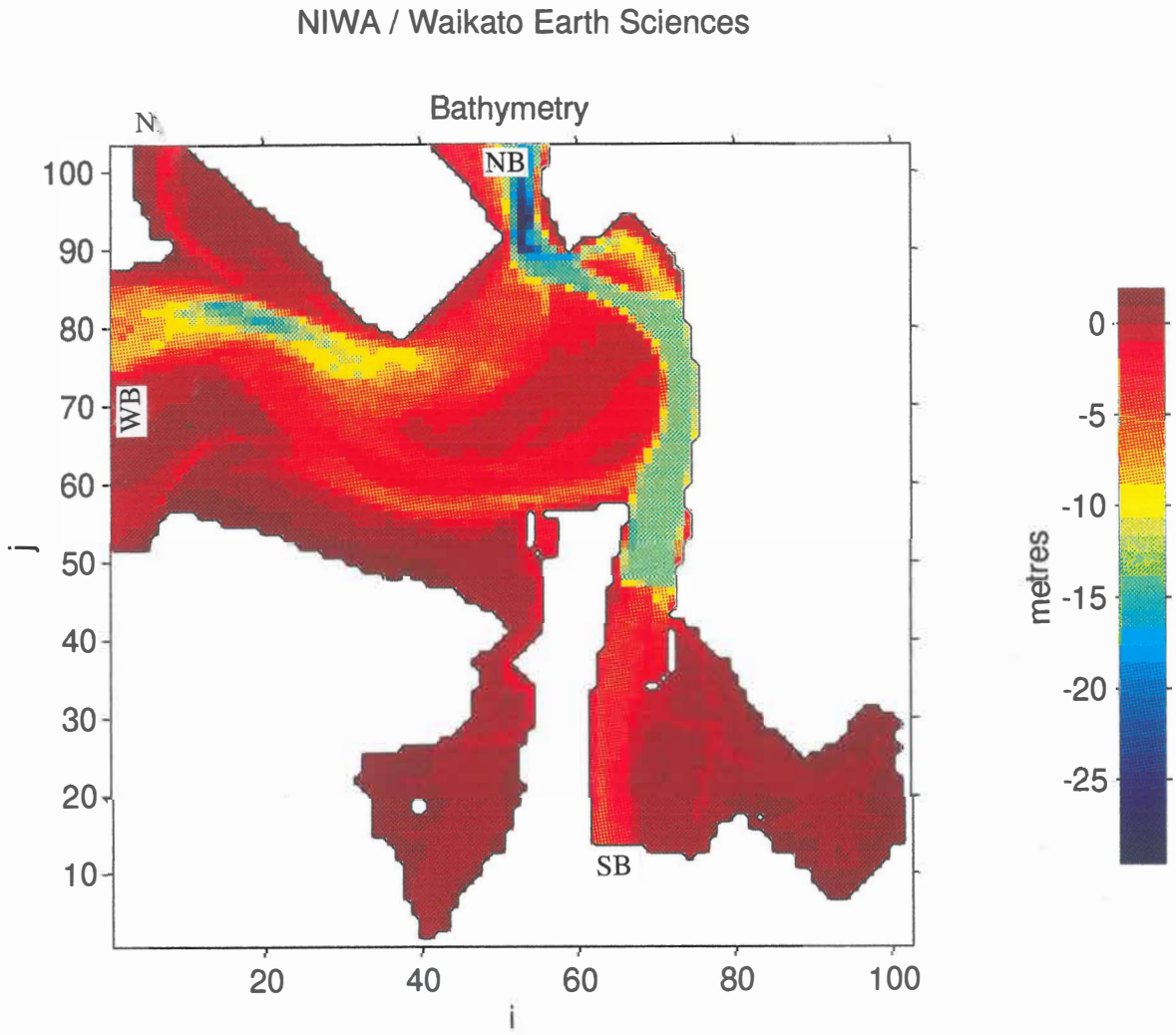

Figure 9.15 The 75-m Tauranga Port Model, showing bathymetry and the open boundaries (NB: northern boundary; SB: southern boundary; WB: western boundary).

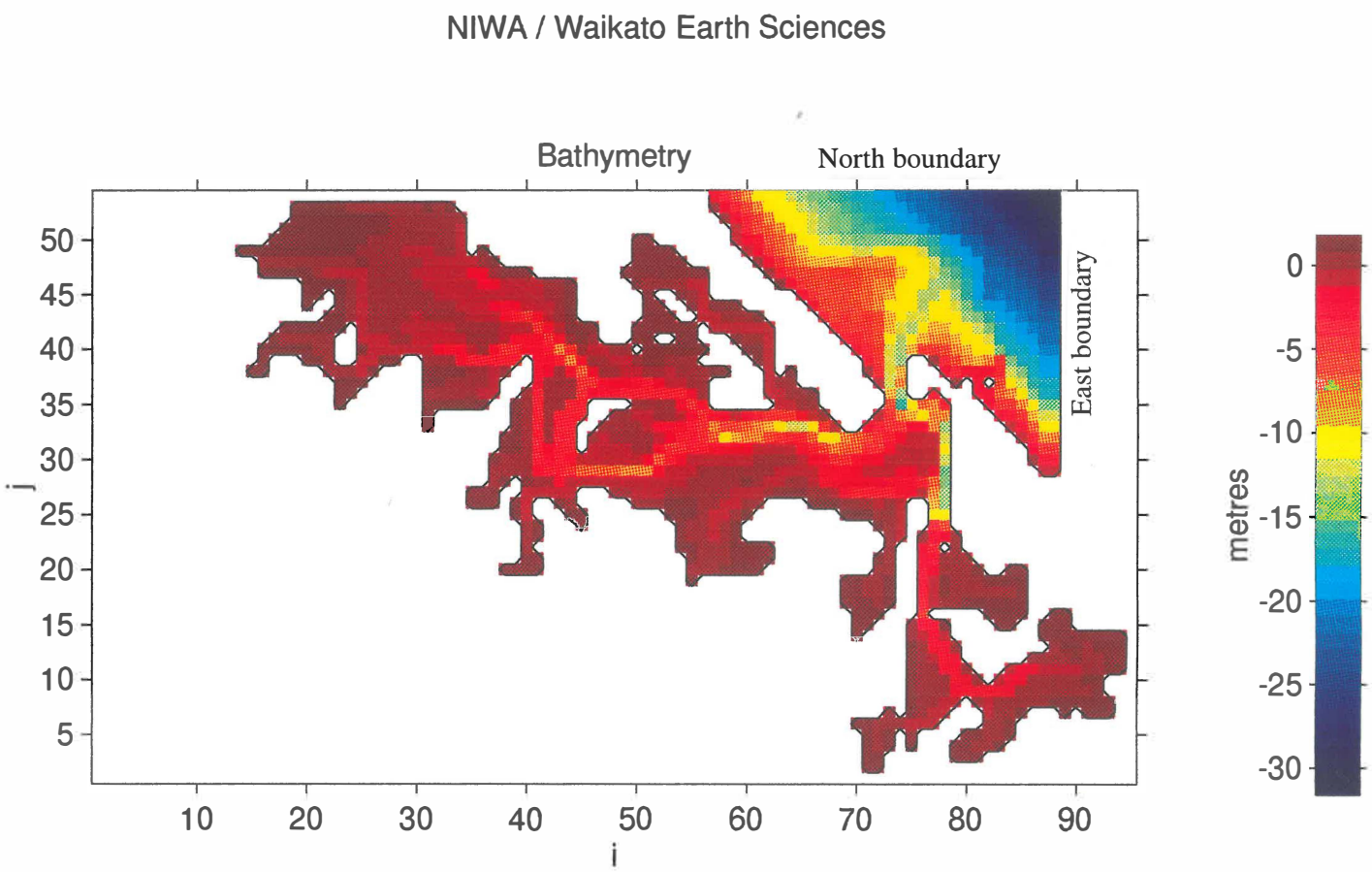

Figure 9.16 The 300-m Tauranga Harbour Model, showing the bathymetry and the open boundaries.

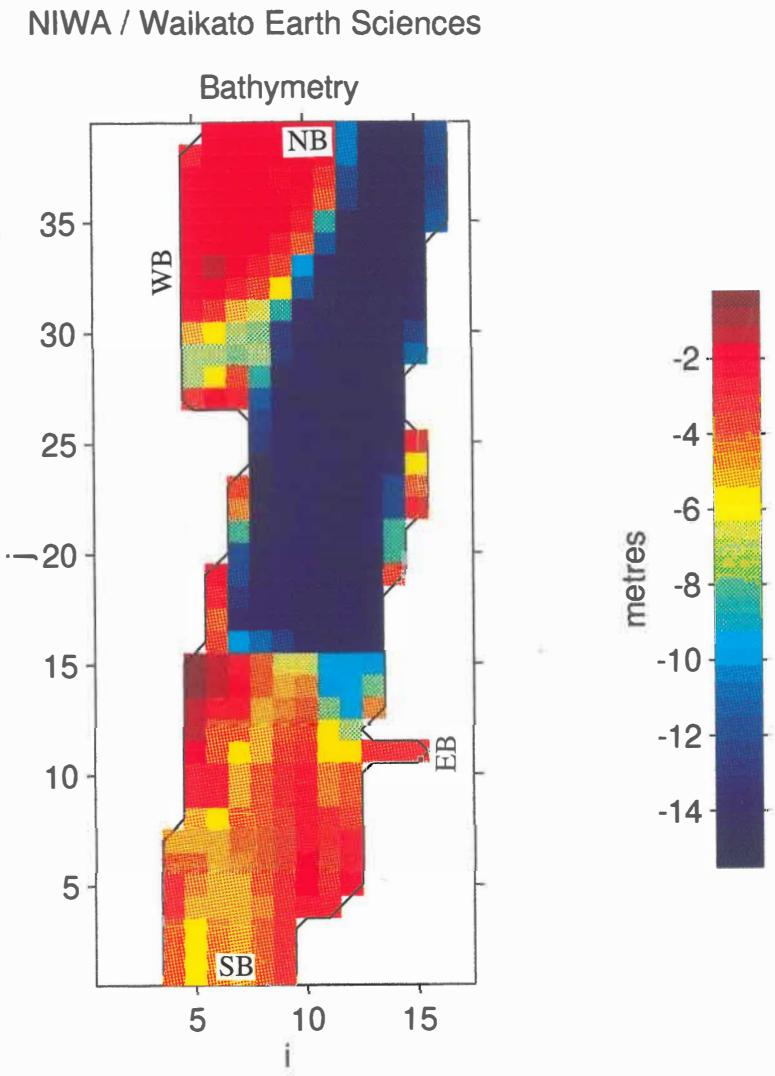

Figure 9.17 The 75-m Stella Passage Model extracted from the full 75-m Tauranga Port Model. SB: southern boundary; EB: eastern boundary; NB: northern boundary; WB: western boundary.

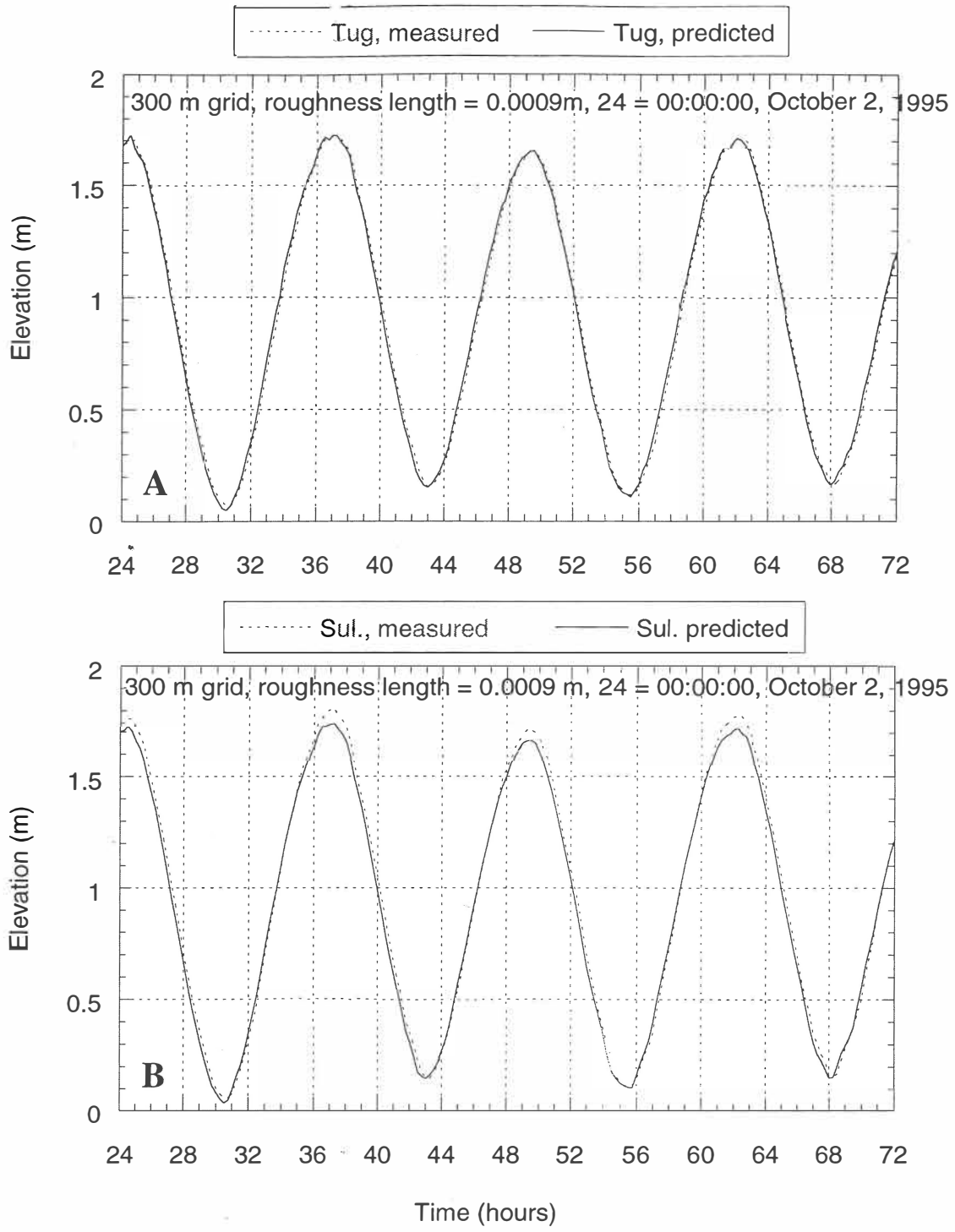

Figure 9.18 Measured and predicted water level time series from 00:00:00, October 2, 1995 to 00:00:00, October 4, 1995, with the 300-m Tauranga Harbour Model (2-dimensional only) at Tug Berth (A) and Sulphur Point (B).

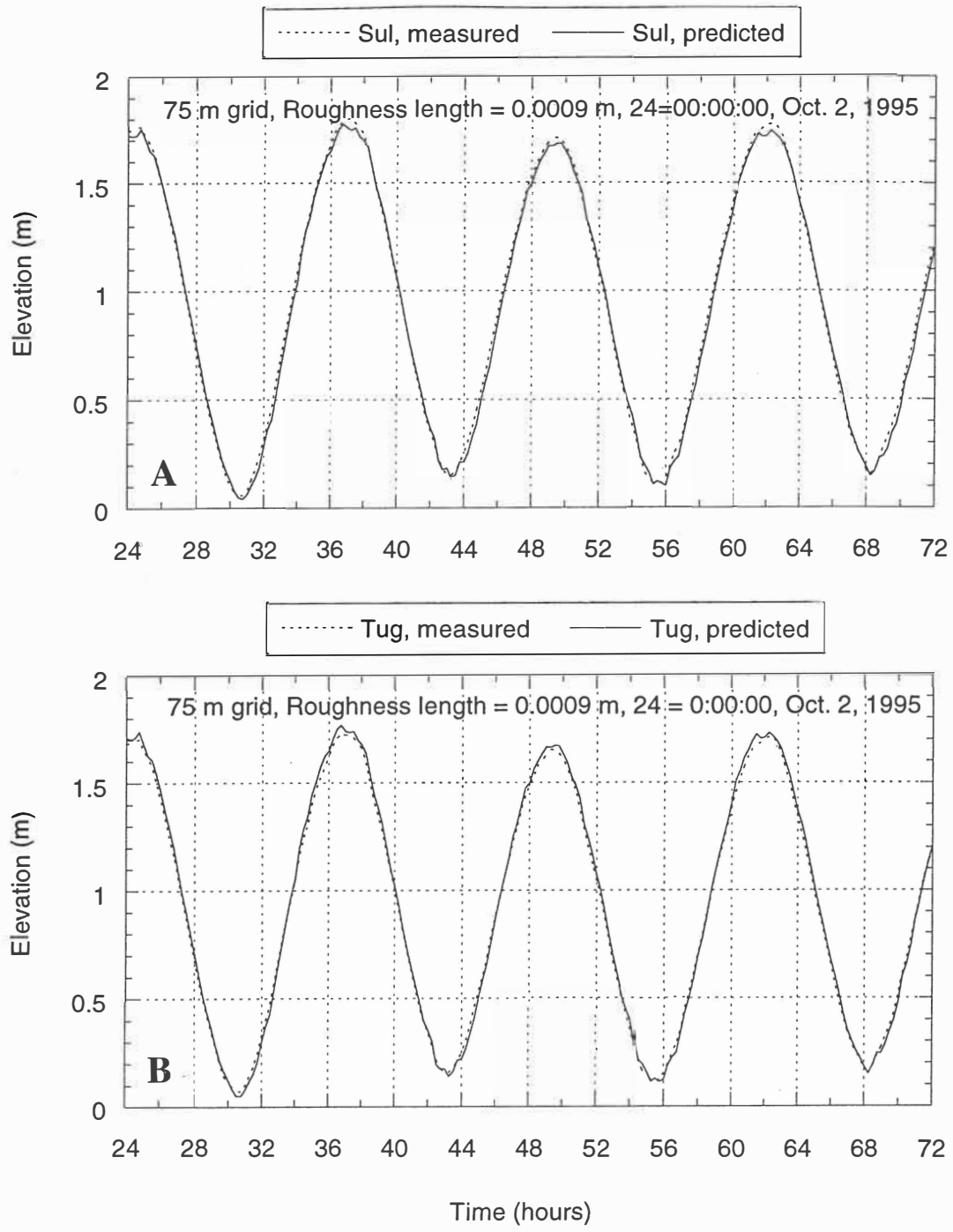

Figure 9.19 Water level time series from 00:00:00, October 2, 1995 to 00:00:00, October 4, 1995, measured and predicted with the 75-m Tauranga Port Model (2-dimensional only) at Sulphur Point (A) and Tug Berth (B).

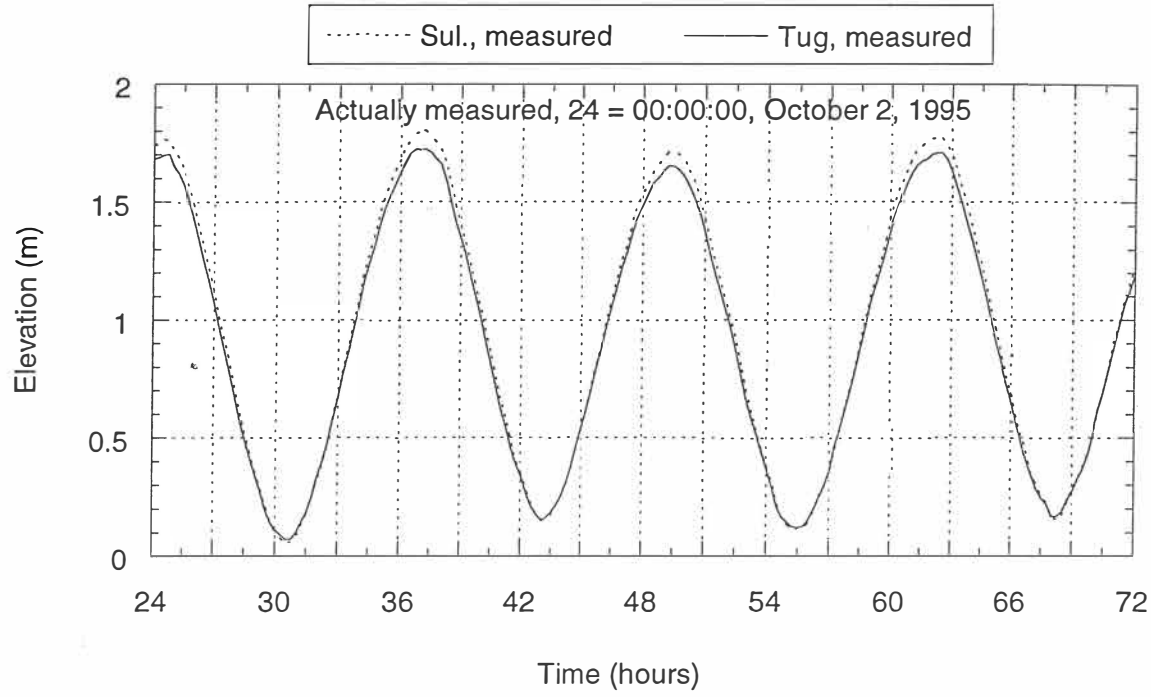

Figure 9.20 Measured water level time series at Sulphur Point and Tug Berth from 00:00:00, October 2, 1995 to 00:00:00, October 4, 1995.

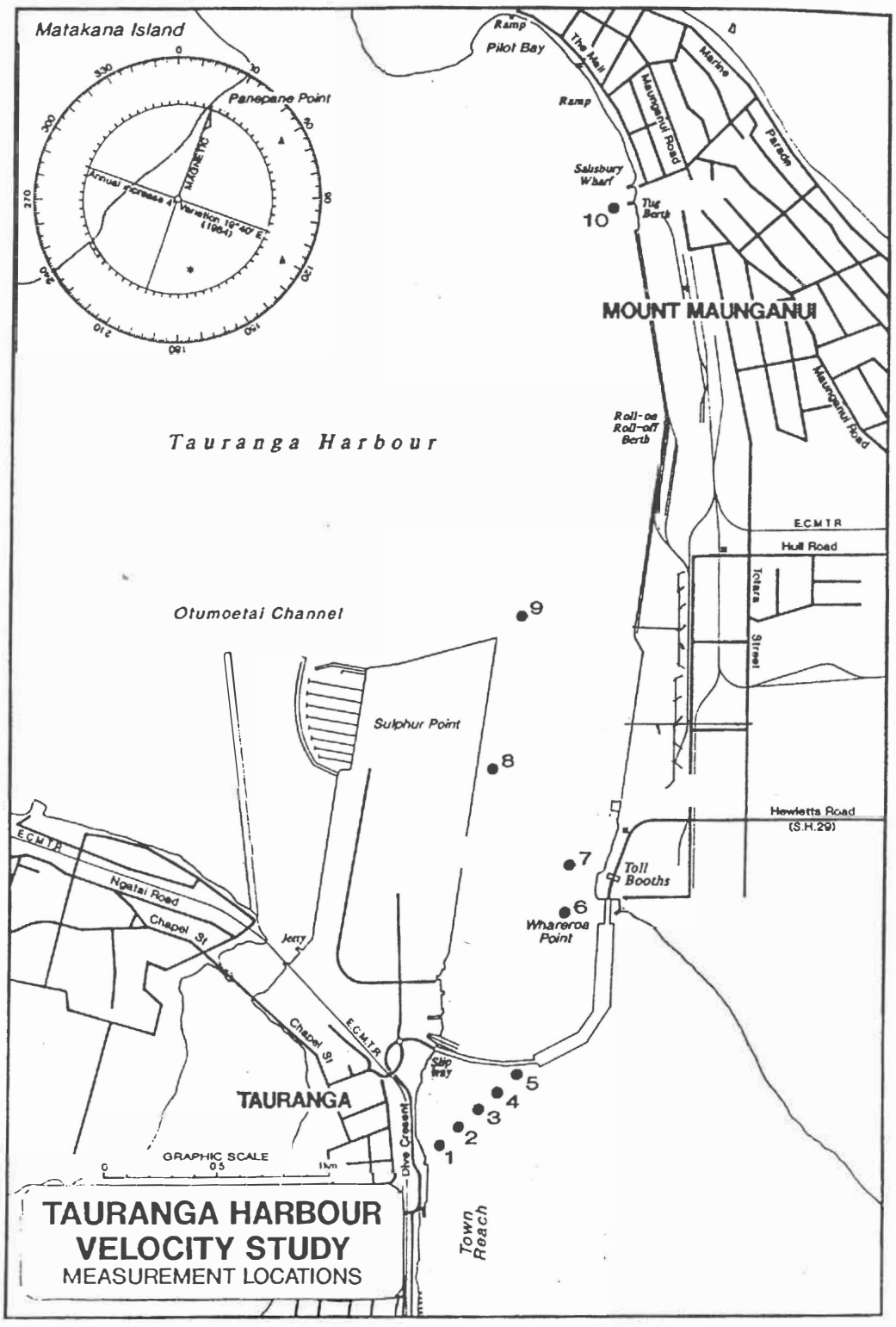

Figure 9.21 The locations for current measurements in Tauranga Harbour undertaken by the Environment Bay of Plenty on March 18, 1992 (after O'Shaughnessy and Stringfellow, 1992).

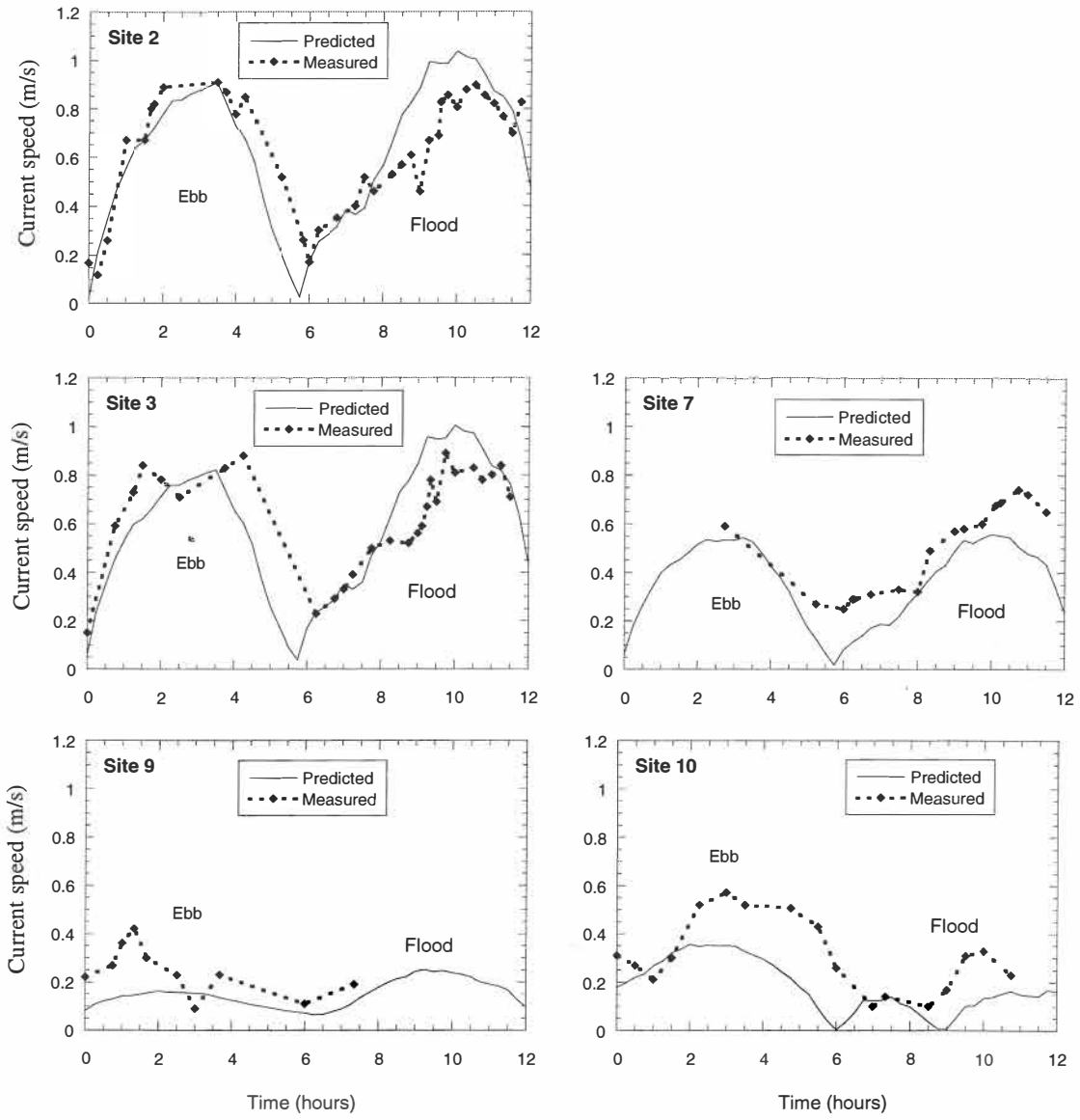

Figure 9.22 Currents predicted by the 75-m Tauranga Port Model (2 dimensional) and currents measured at selected locations by the Environment Bay of Plenty on March 18, 1992. The measured currents are recorded at 0.6 of the water depth from the water surface.

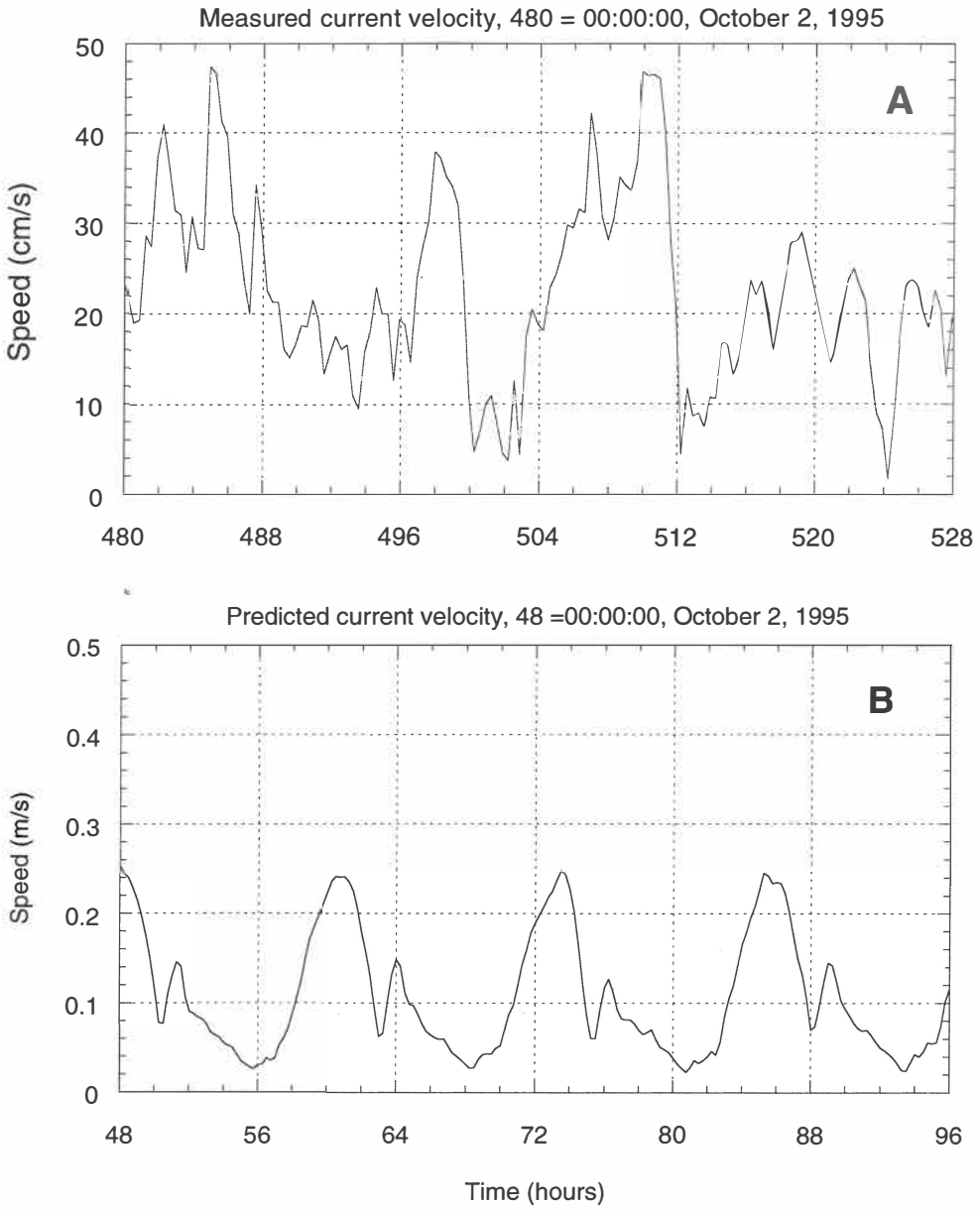

Figure 9.23 Measured currents (A) and currents predicted by the 75 m 2-dimensional Tauranga Port Model (B) at location S1 from 00:00:00, October 2 to 00:00:00, October 4, 1995.

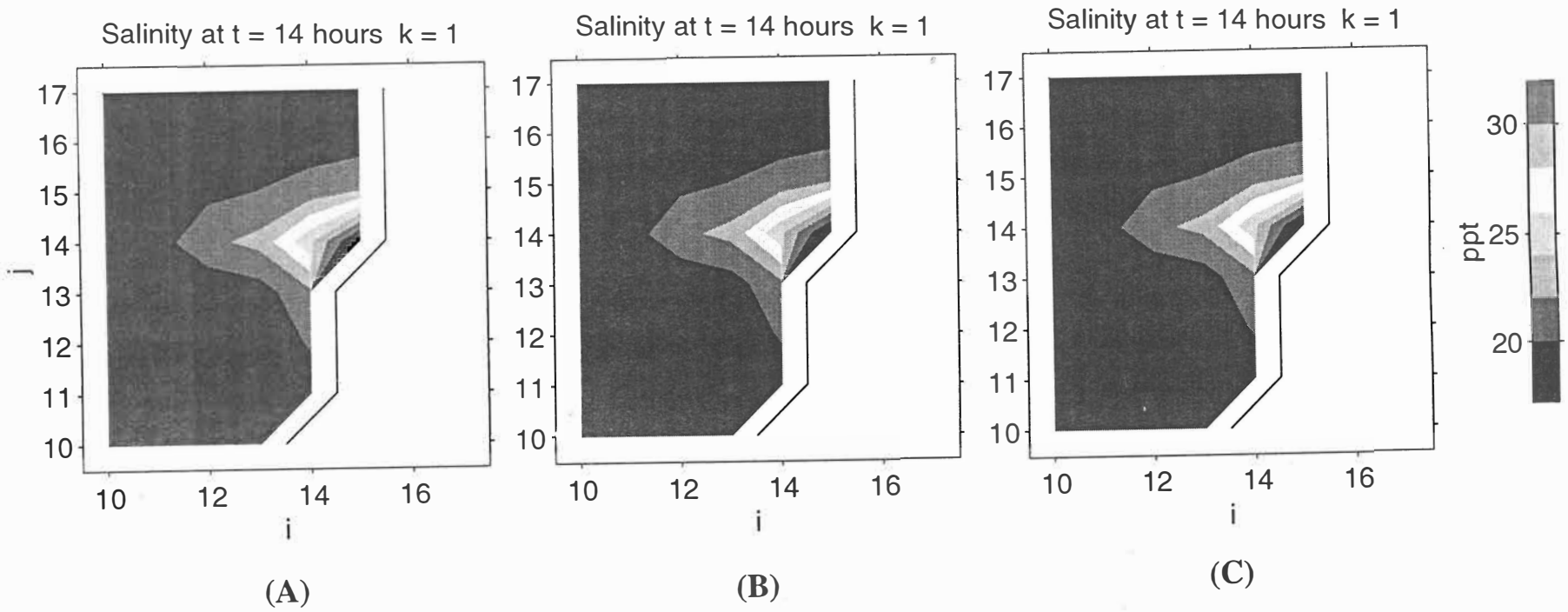

Figure 9.24 Predicted surface plumes at 18:00 hours (t = 14 hours in the figures), October 5, 1995, for longitudinal eddy diffusivity values of 0.005 (A), 0.0005 (B), and 0.0001 (C).

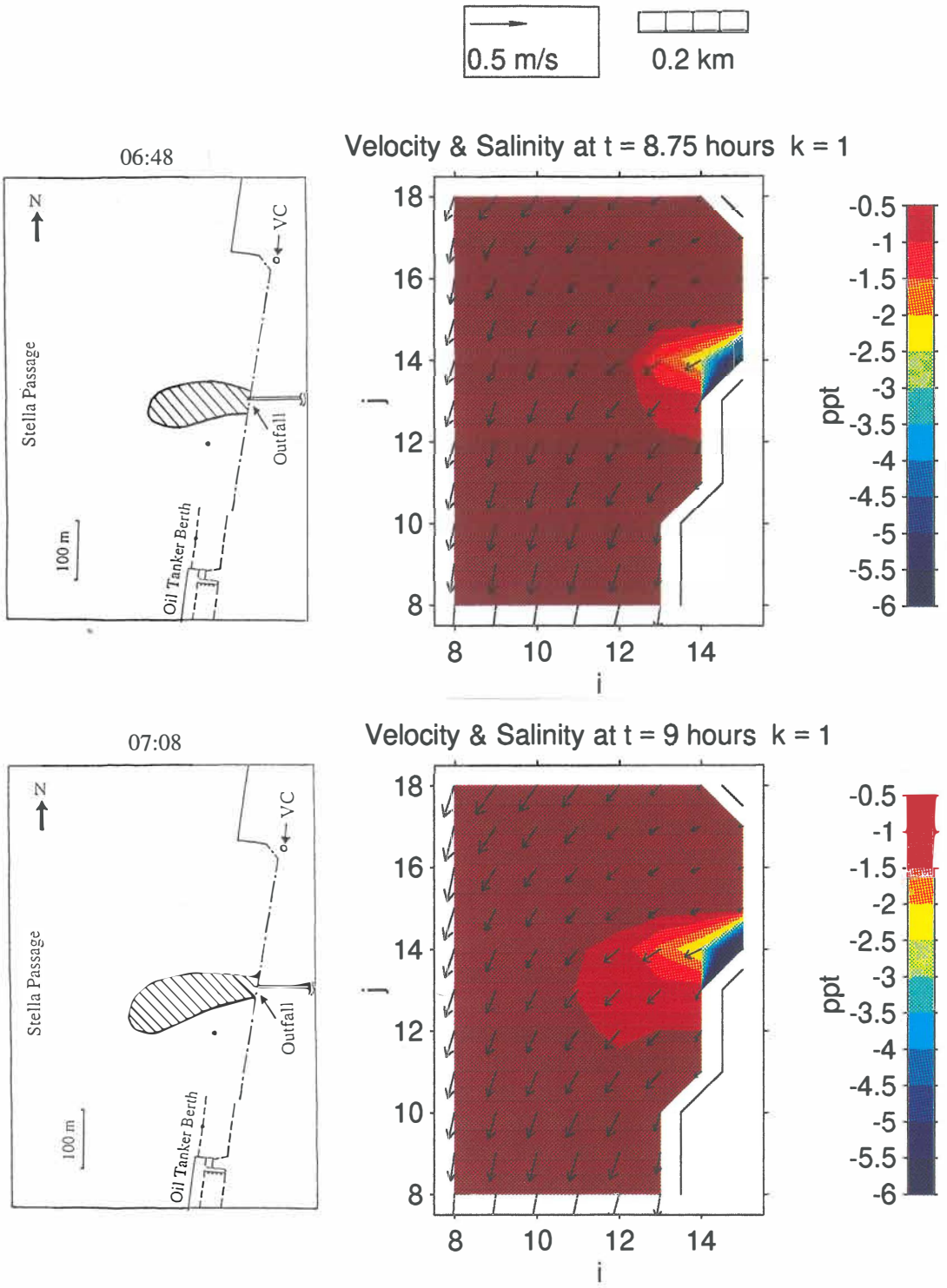

Figure 9.25 Measured (digitised video camera images) plumes at the surface layer (with a thickness of 0.3 m) during the rainfall on September 29, 1995, compared to predictions of the 75 m 3-dimmensional Stella Passage model. The model starting time is 22:00, September 28, 1995.

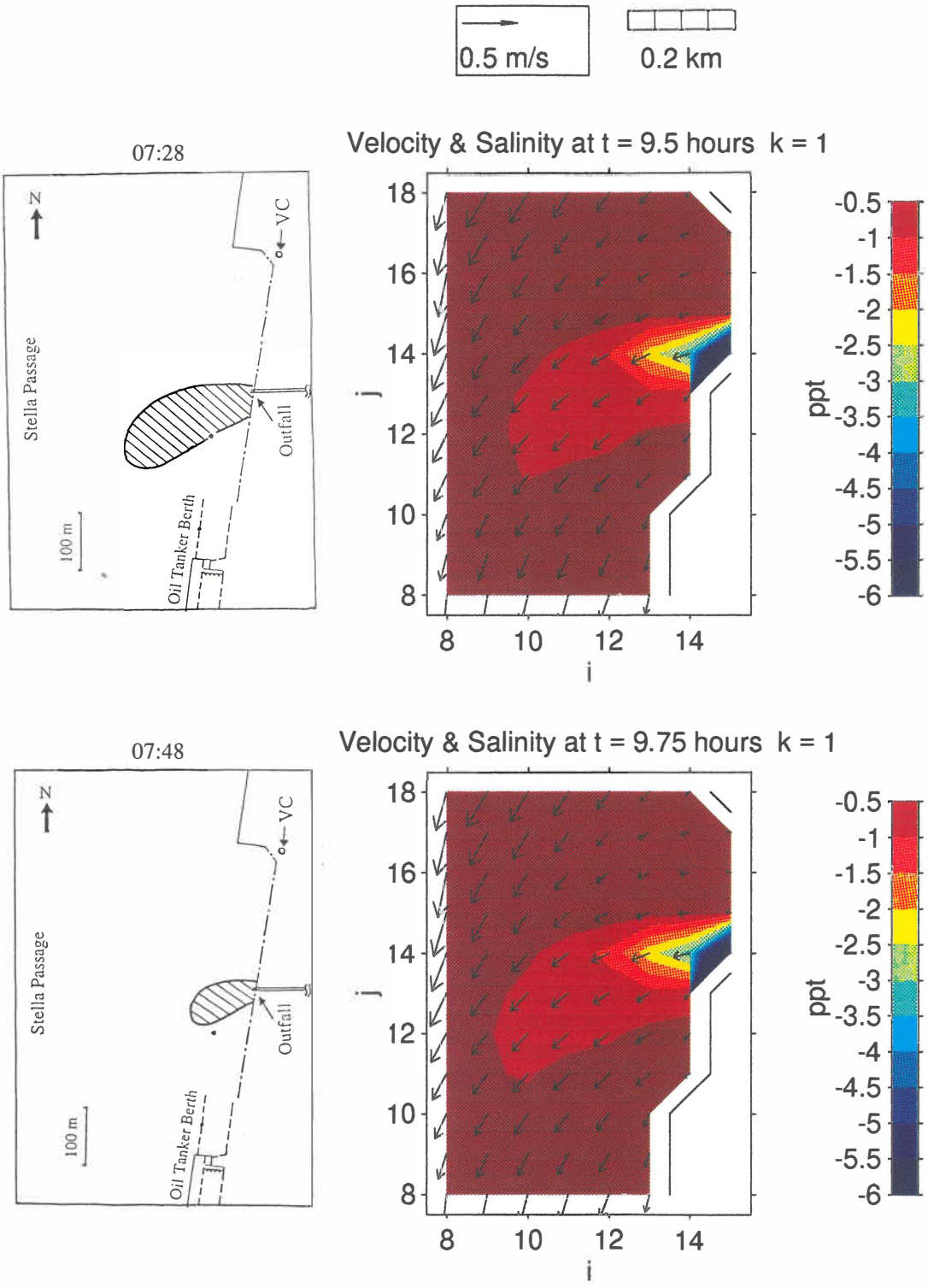

Figure 9.25 (Cont.)

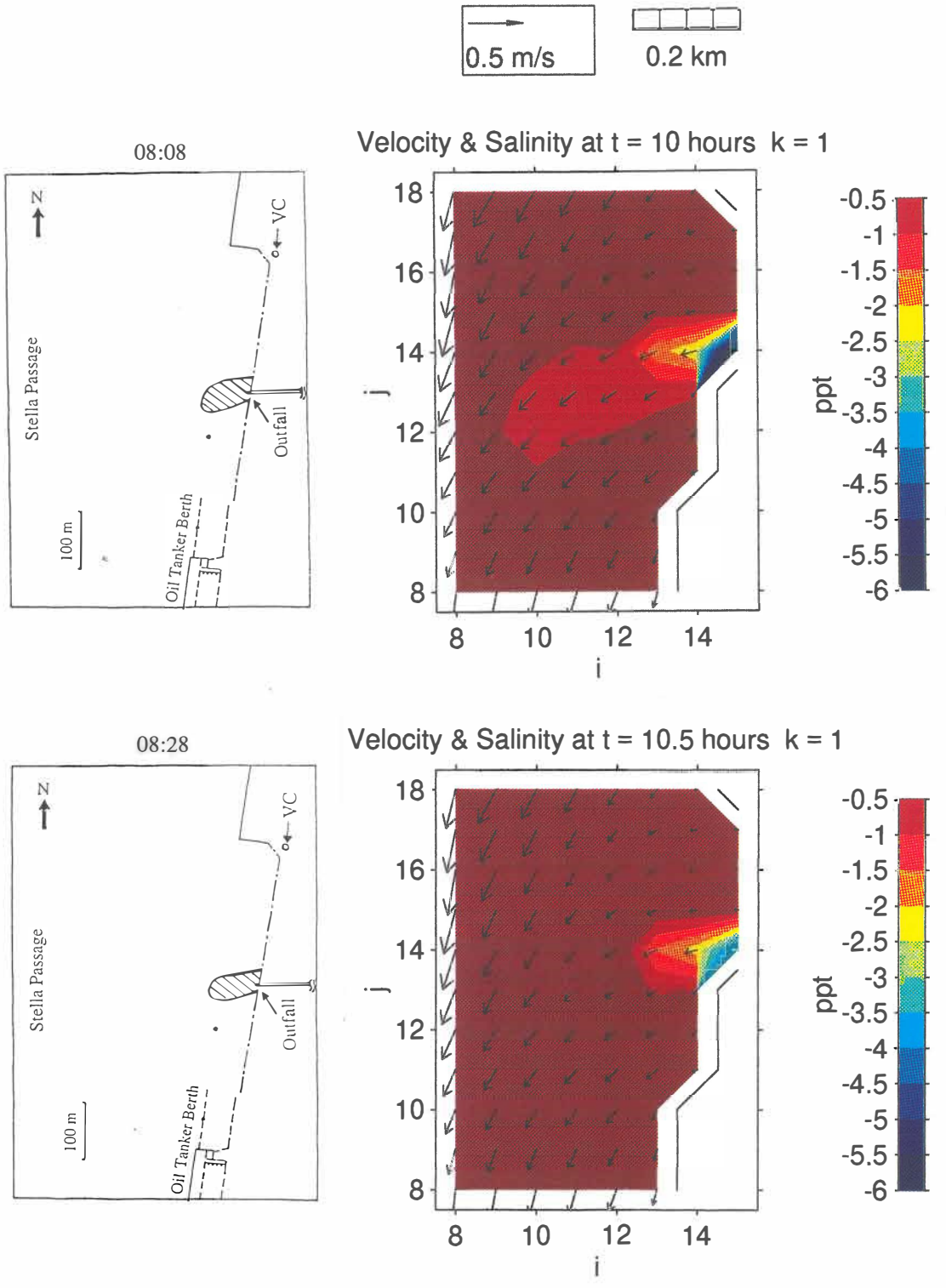

Figure 9.25 (Cont.)

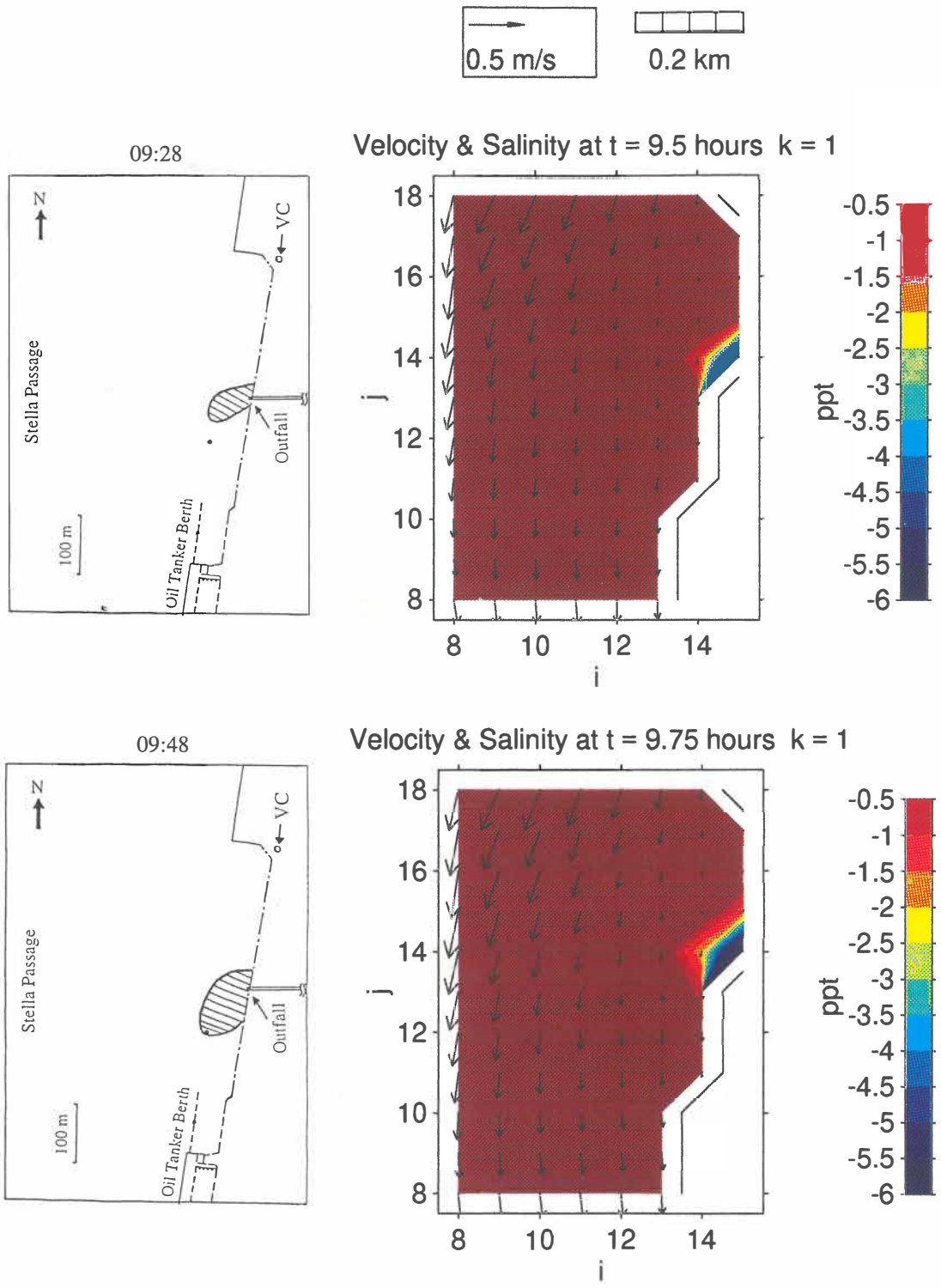

Figure 9.26 Measured (digitised video camera images) plumes at the surface layer (with a thickness of 0.3 m) during the rainfall on October 1, 1995, compared to predictions of the 75 m 3-dimmensional Stella Passage model. The model starting time is 00:00, October 1, 1995.

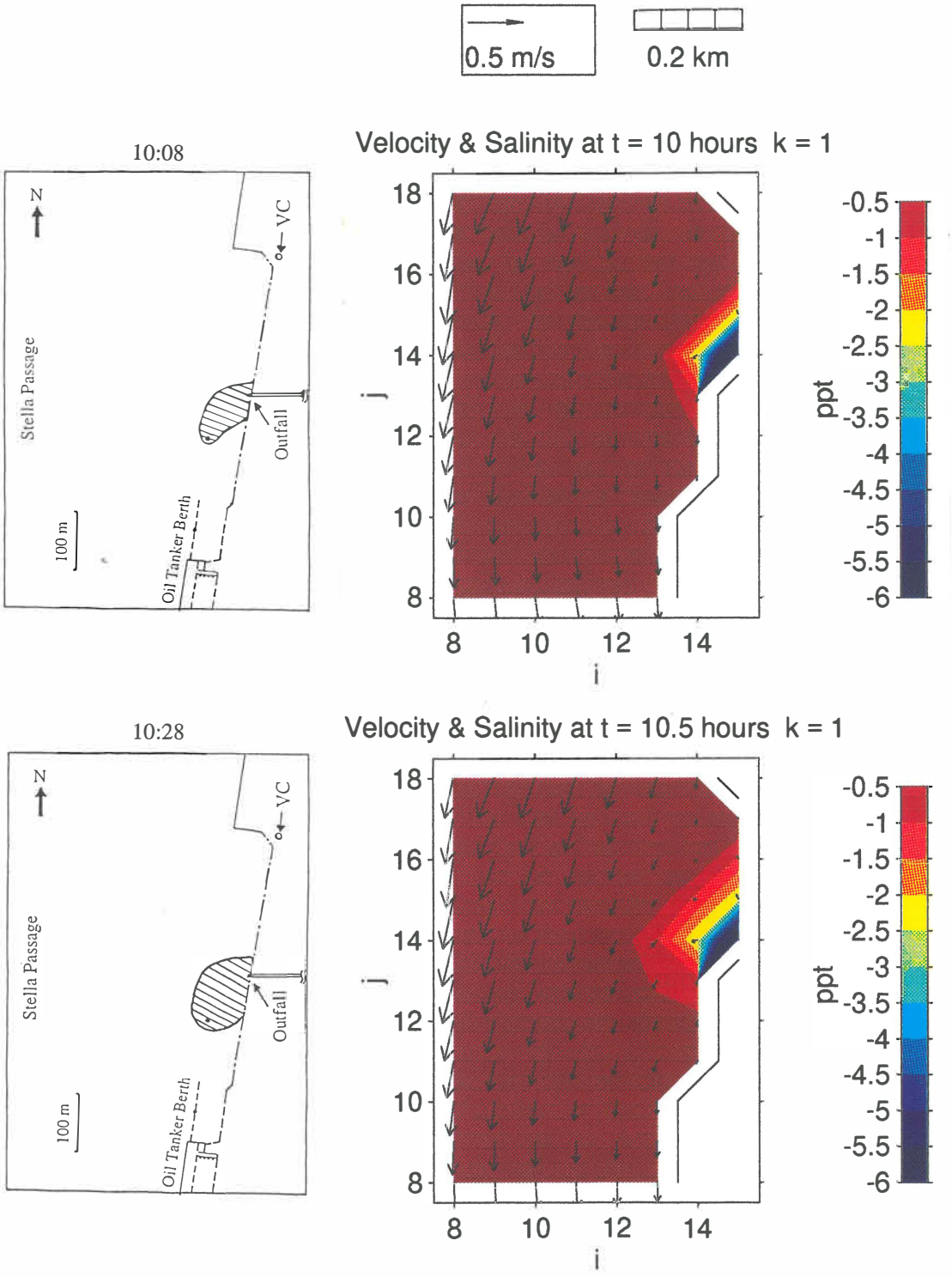

Figure 9.26 (Cont.)

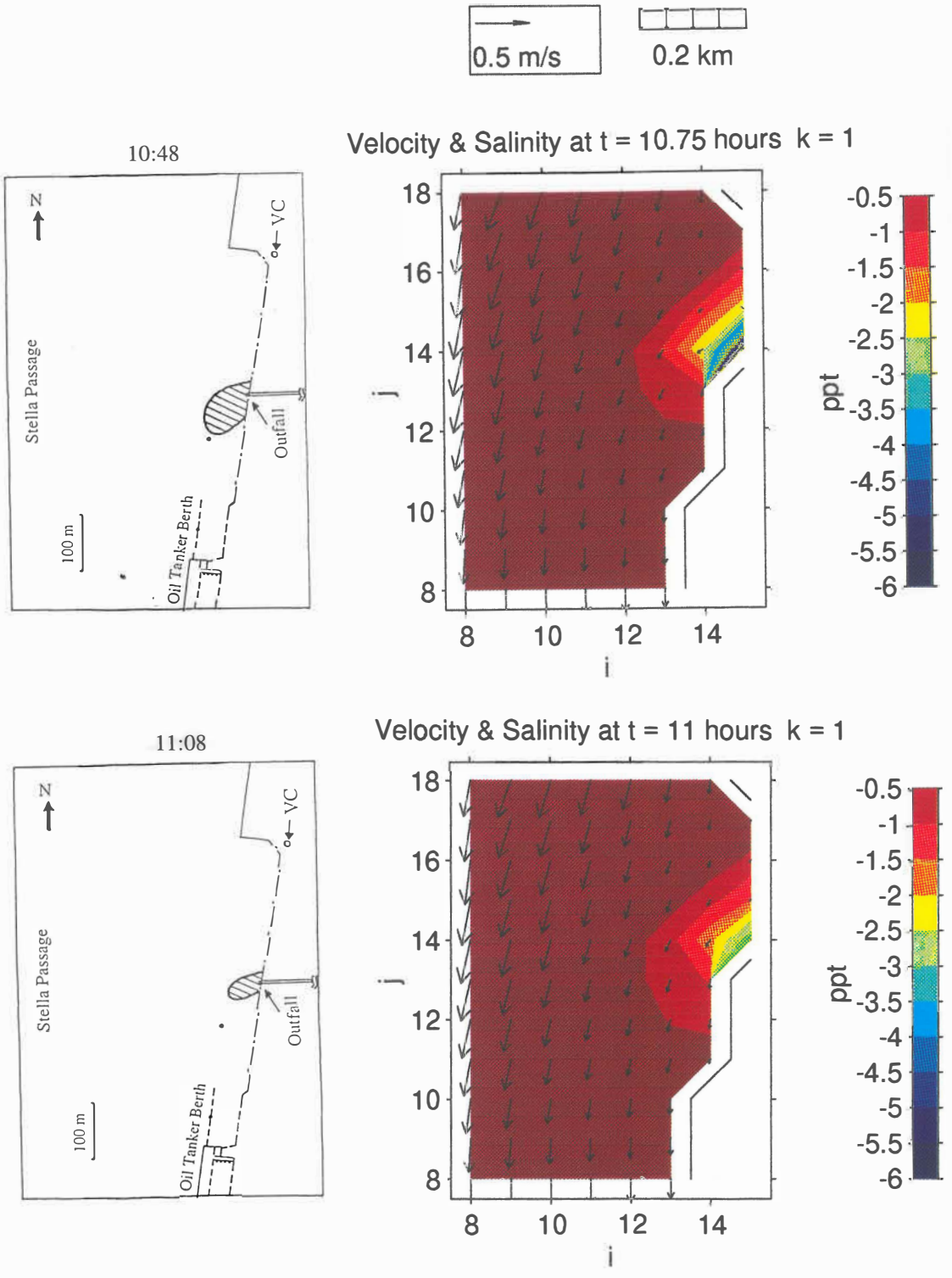

Figure 9.26 (Cont.)

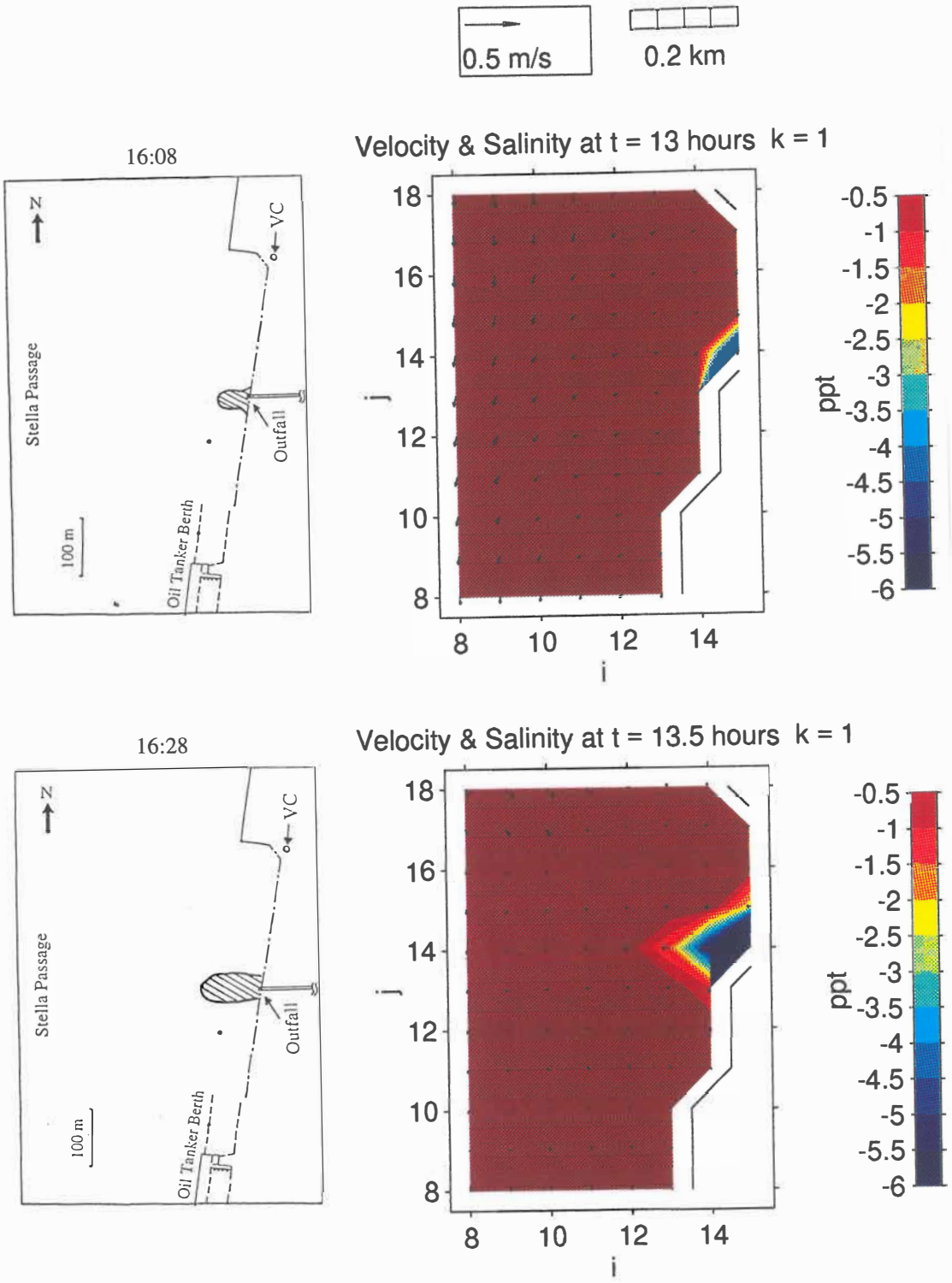

Figure 9.27 Measured (digitised video camera images) plumes at the surface layer (with a thickness of 0.3 m) during the rainfall on October 5, 1995, compared to predictions of the 75 m 3-dimmensional Stella Passage model. The model starting time is 03:00, October 5, 1995.

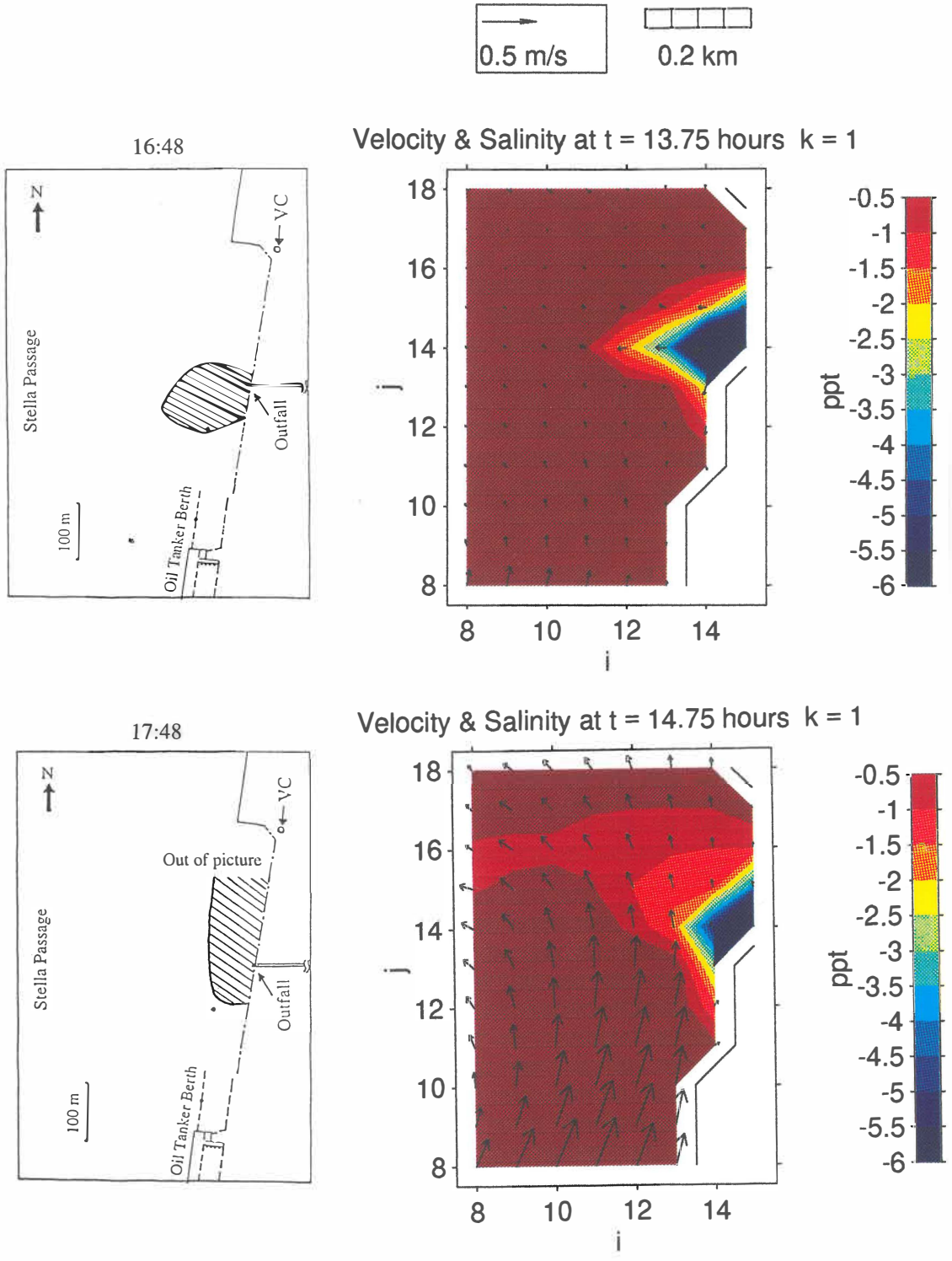

Figure 9.27 (Cont.)

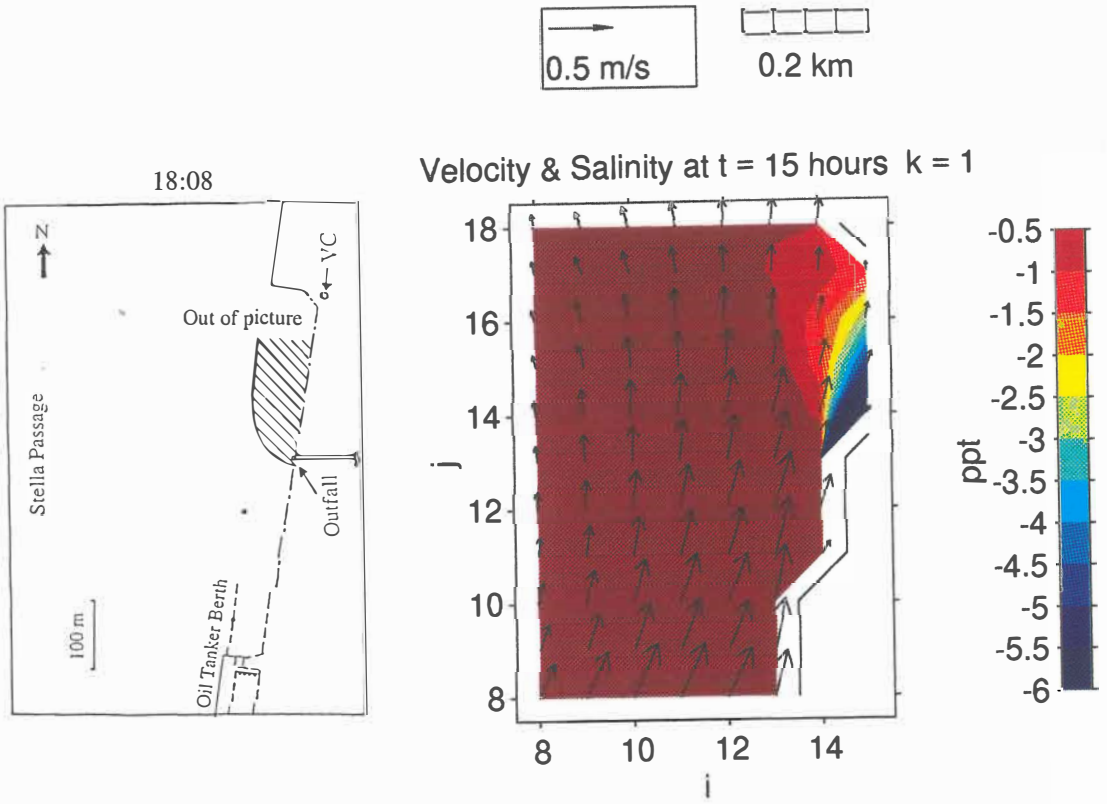

Figure 9.27 (Cont.)

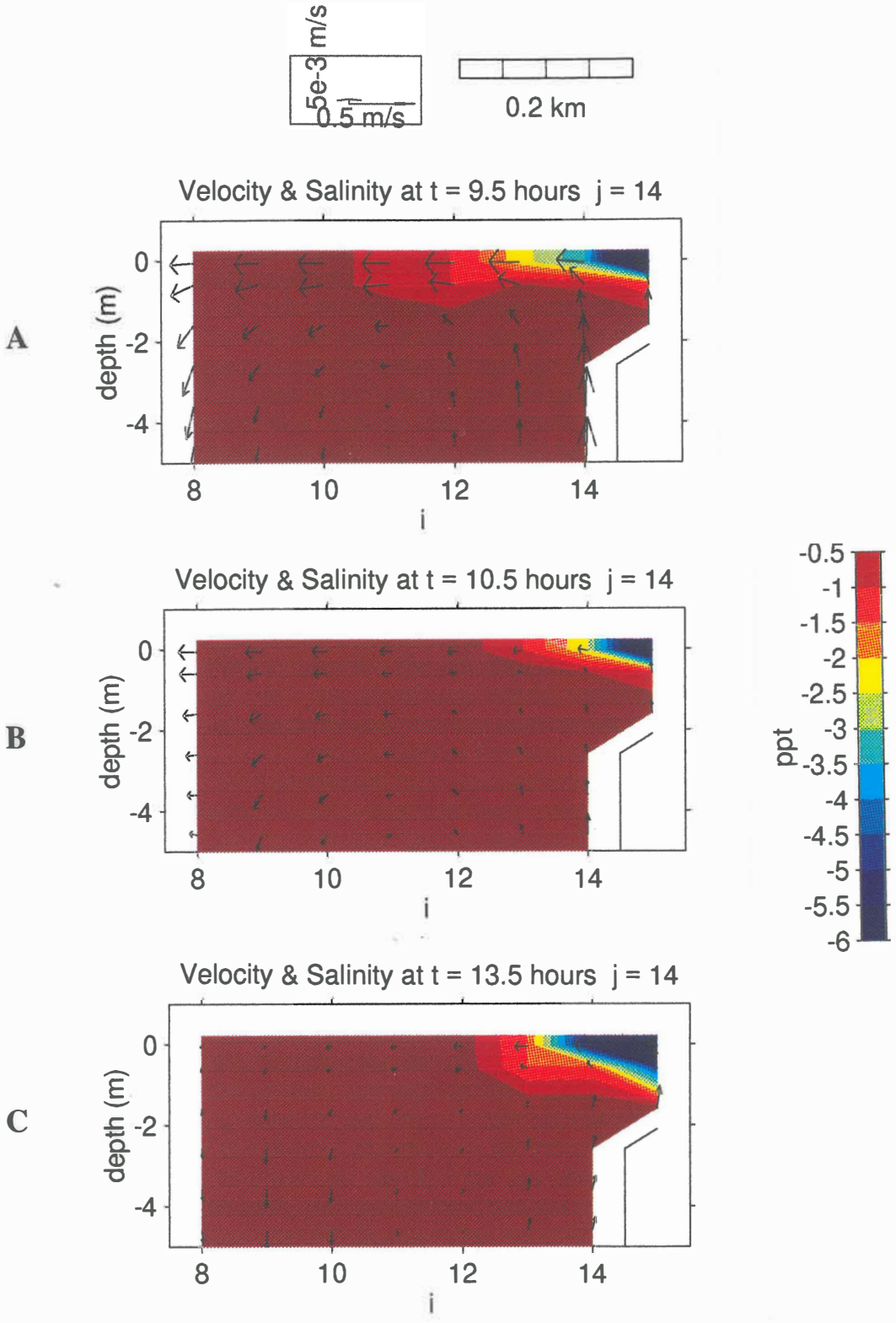

Figure 9.28 Predicted plume and currents in the cross-section at J=14 for the rainfall events on September 29 (A), October 1 (B), and October 5 (C), 1995.

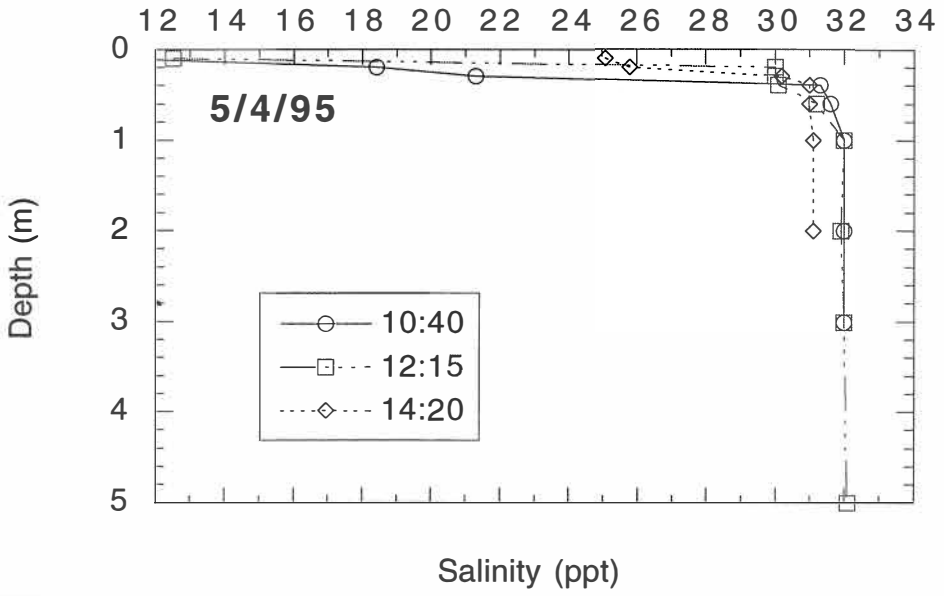

Figure 9.29 Vertical salinity distribution at the S0 site (20 m away from the southern outfall 1 hour after 16 mm of rainfall on April 5, 1995.

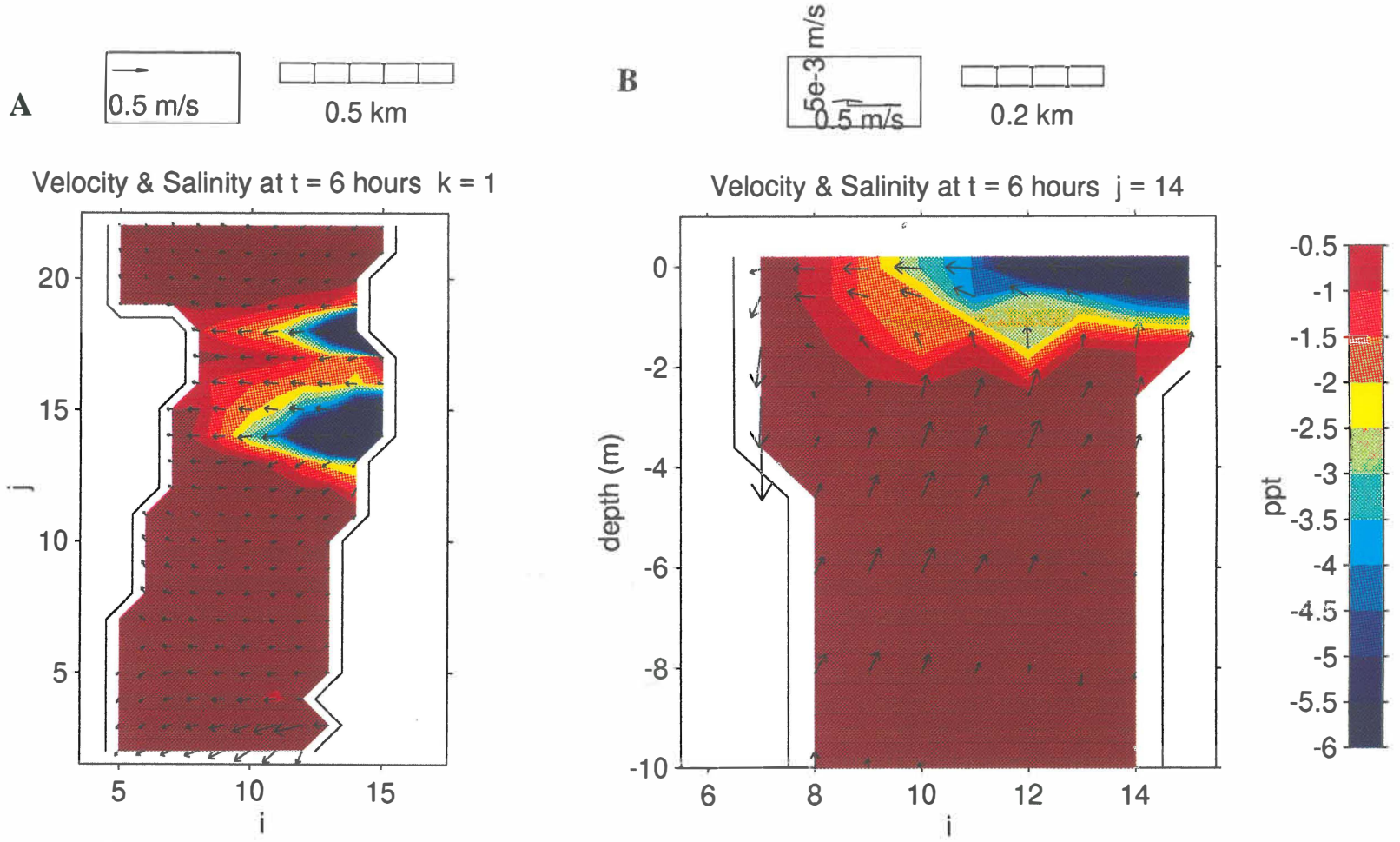

Figure 9.30a-b Predicted plume and currents in the surface layer (a) and the cross-section at J=14 (b) during low tide (t = 6 hours in the figures) under 40 knot northerly winds.

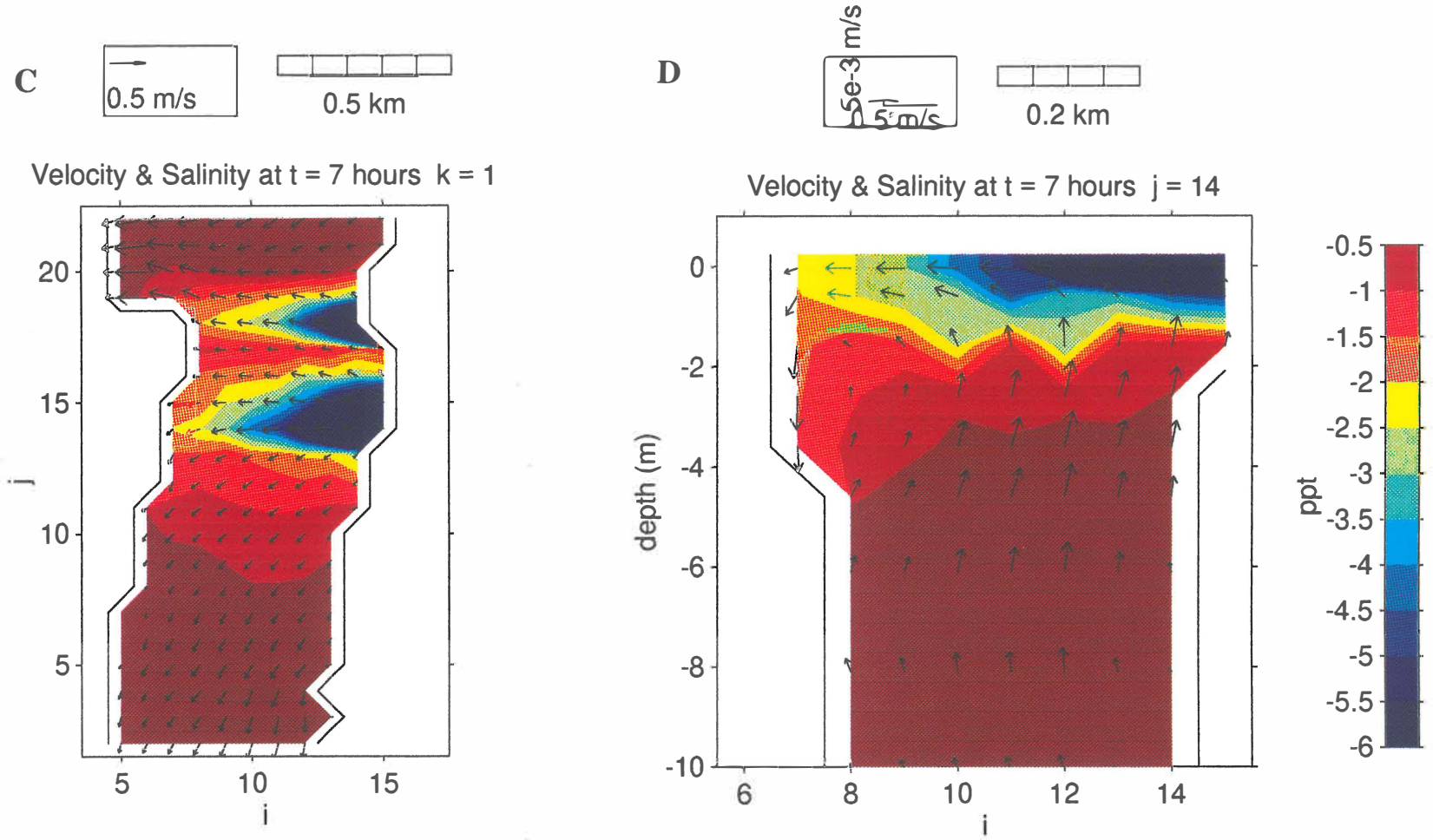

Figure 9.30c-d Predicted plume and currents in the surface layer (c) and the cross-section at J=14 (d) 1 hour after the low tide (t = 7 hours,) under 40 knot easterly winds.

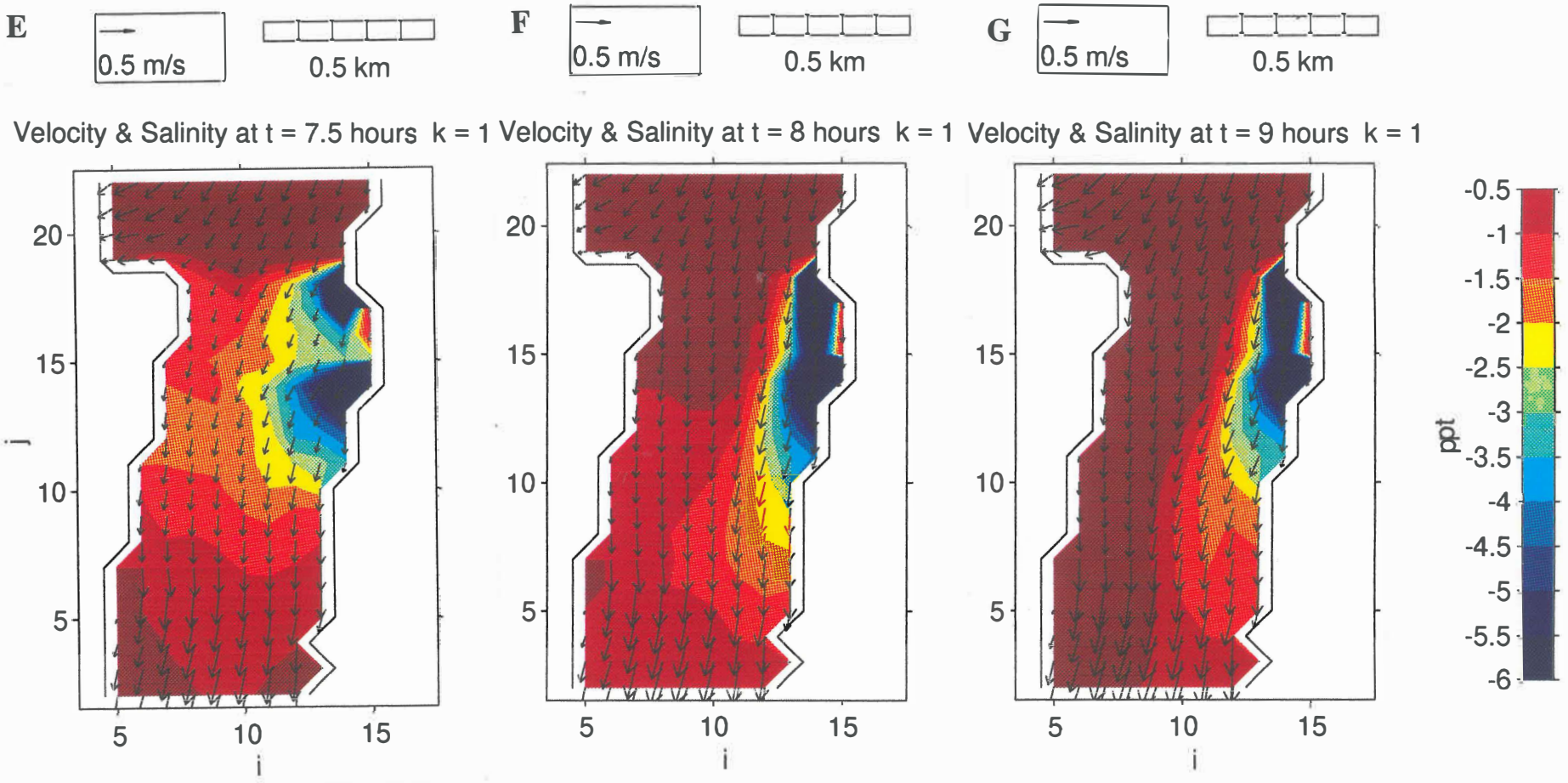

Figure 9.30e-j Predicted plumes and currents in the surface layer 1.5 - 6 hours after the low tide (*t* = 7.5-12 hours) under 40 knot northerly winds.

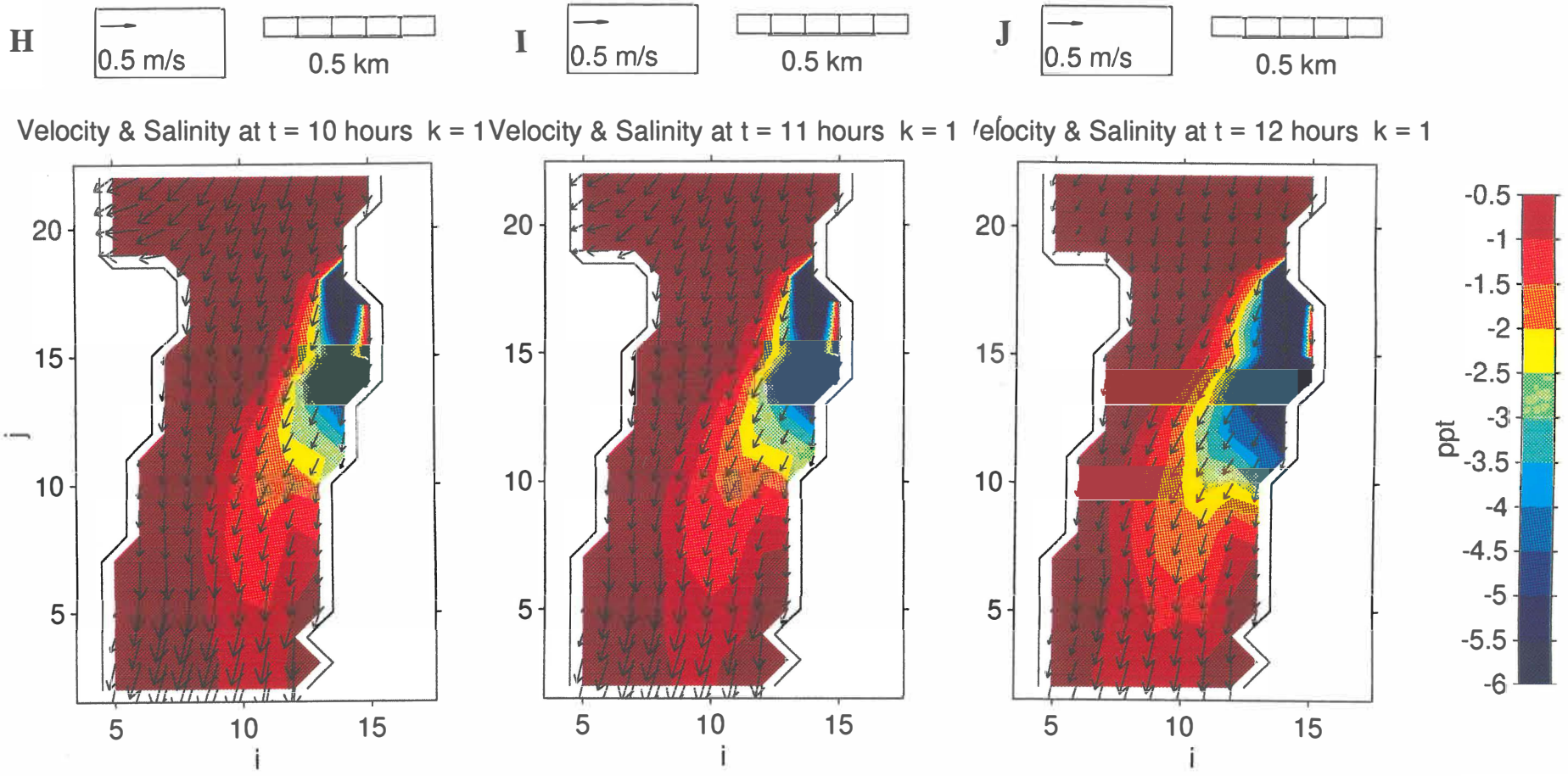

Figure 9.30e-j Predicted plumes and currents in the surface layer 1.5 - 6 hours after the low tide (t = 7.5-12 hours) under 40 knot northerly winds.

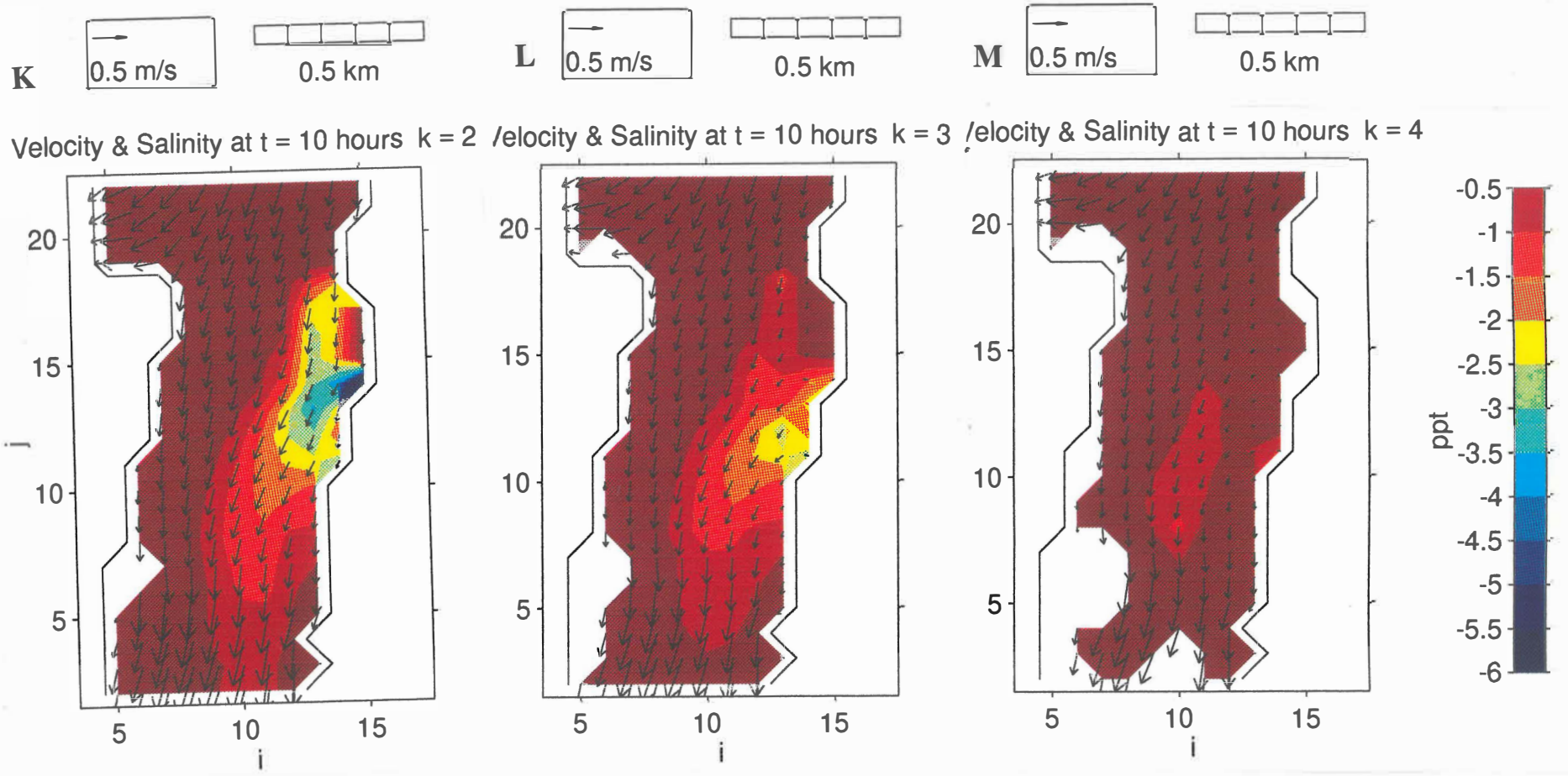

Figure 9.30k-m Predicted surface currents and plume shapes at layers 2 (k), 3 (l), and 4 (m) at 4 hours after the low tide (t = 10 hours) under 40 knot northerly.

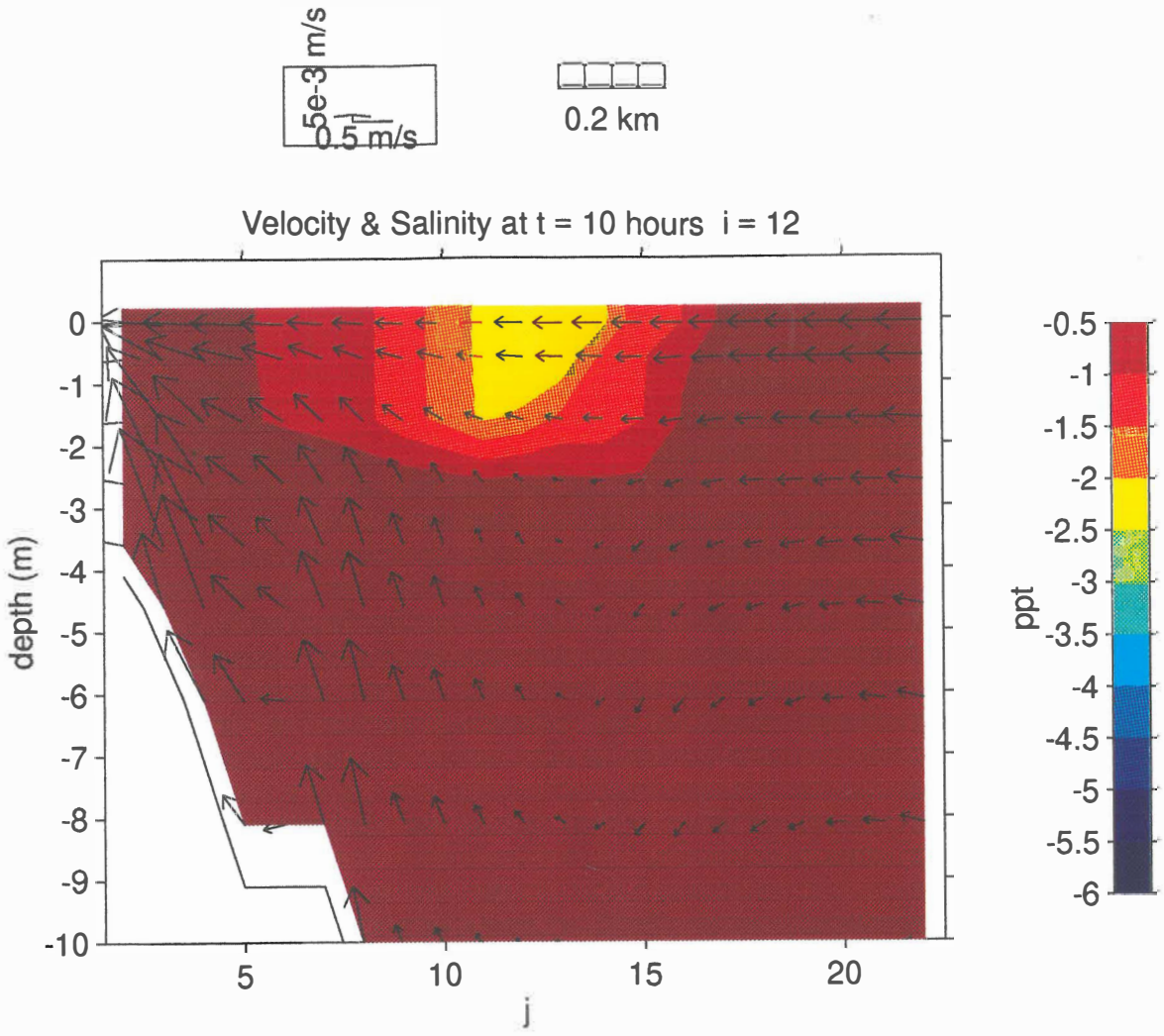

Figure 9.30n Plume shape and current pattern in cross-section I=12 at 4 hours after the low tide (t = 10 hours) under 40 knot northerly.

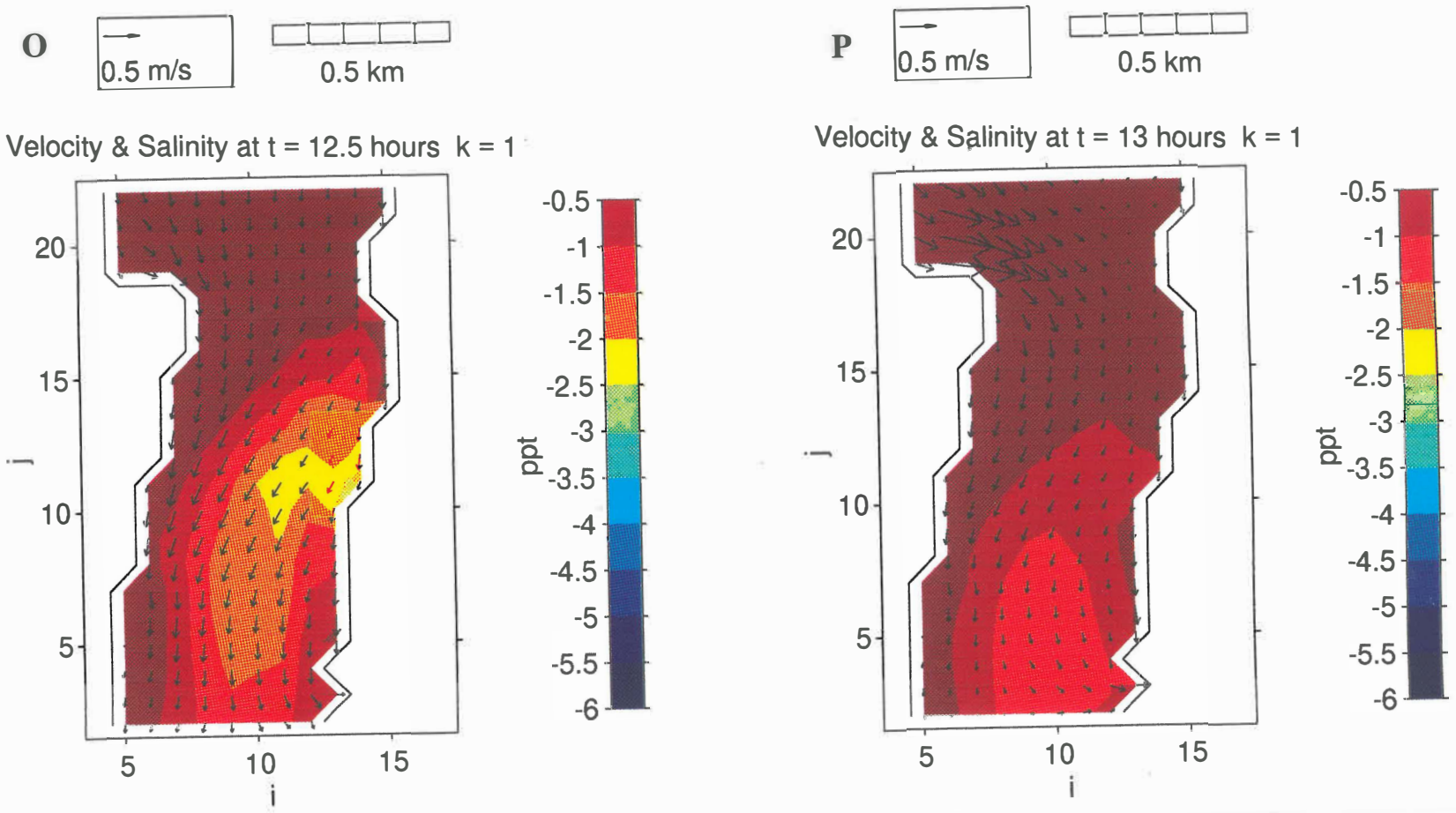

Figure 9.30o-p Predicted plumes and currents in the surface layer at 0.5 hour (o) and 1.0 hour (p) after the runoff stopped entering the harbour under 40 knot northerly winds.

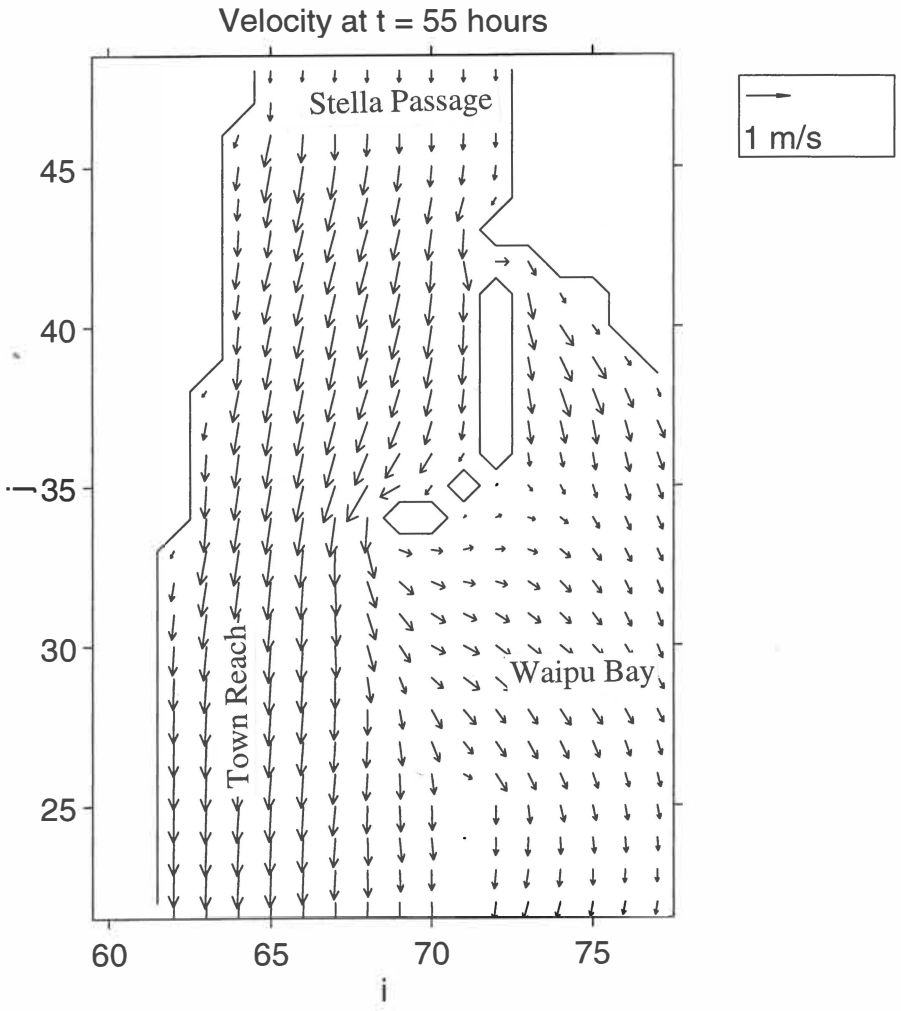

Figure 9.31 Predicted current pattern around the Stella Passage, Town Reach, and Waipu Bay region from the 75 m Tauranga Port model (2-dimensional) under 40 knot northerly winds.

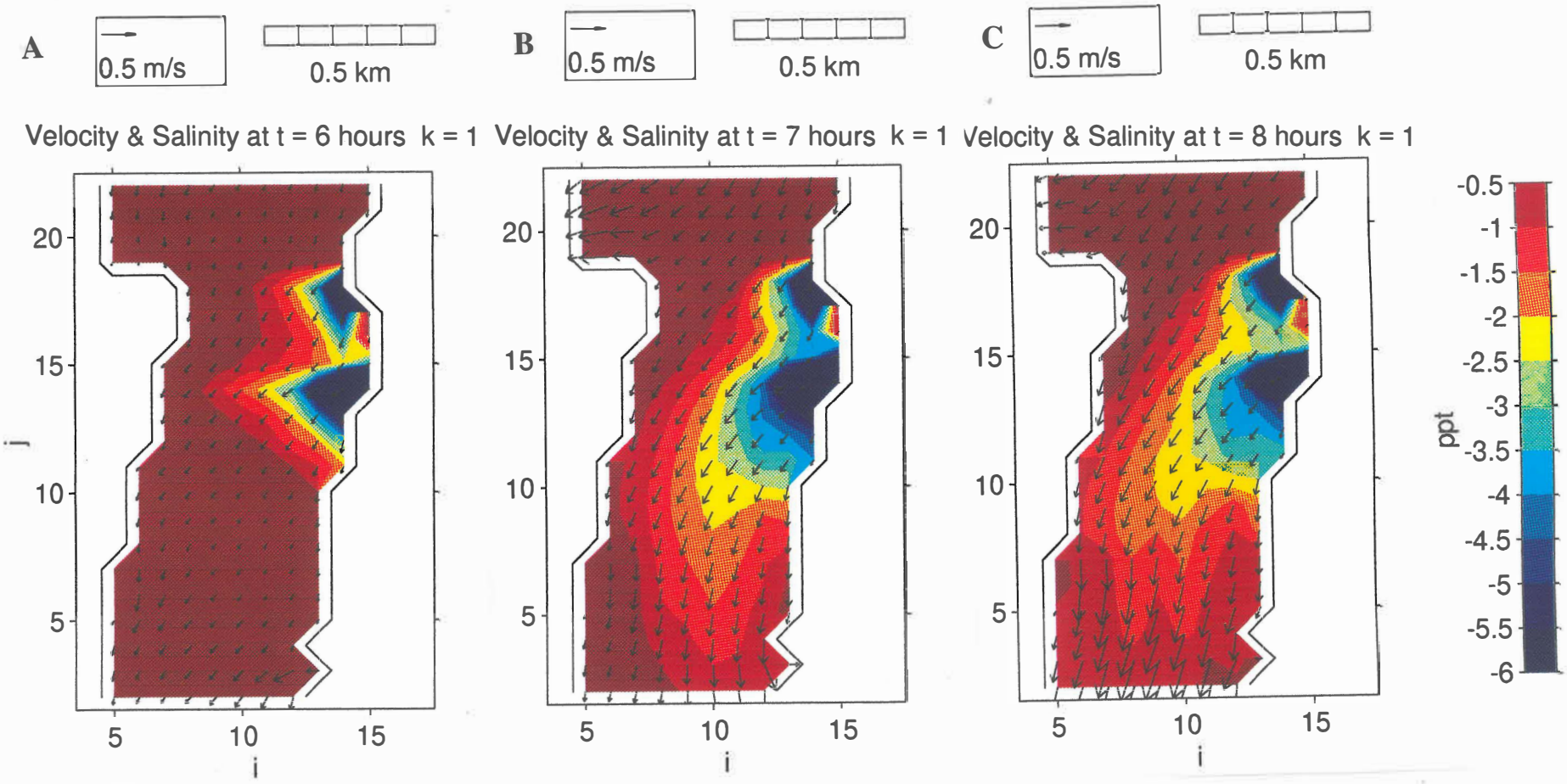

Figure 9.32a-f Predicted plumes and currents in the surface layer from low to high tide (t = 6-12 hours) under 30 knot northeasterly winds.

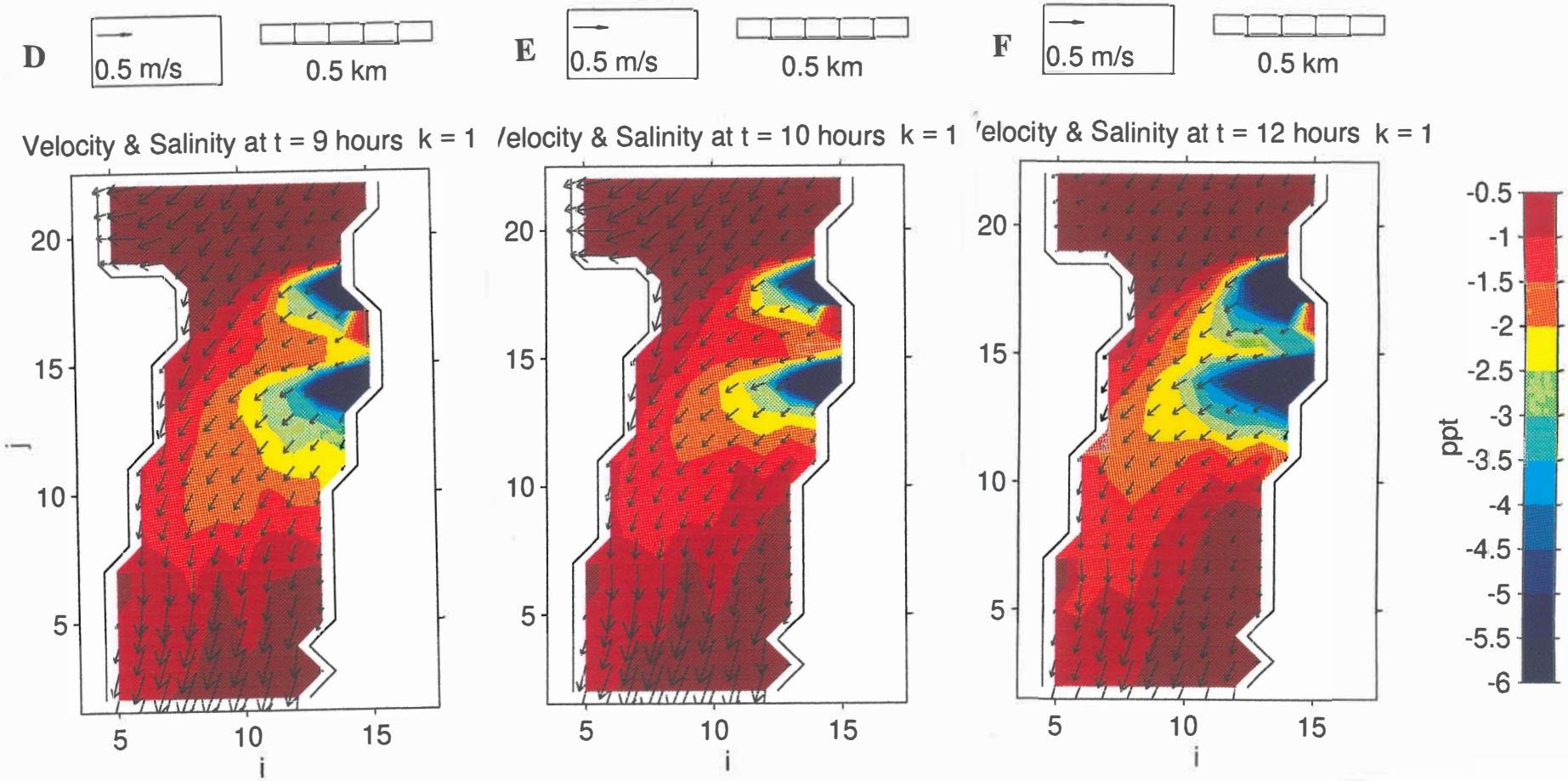

Figure 9.32a-f Predicted plumes and currents in the surface layer from low to high tide (t = 6-12 hours) under 30 knot northeasterly winds.

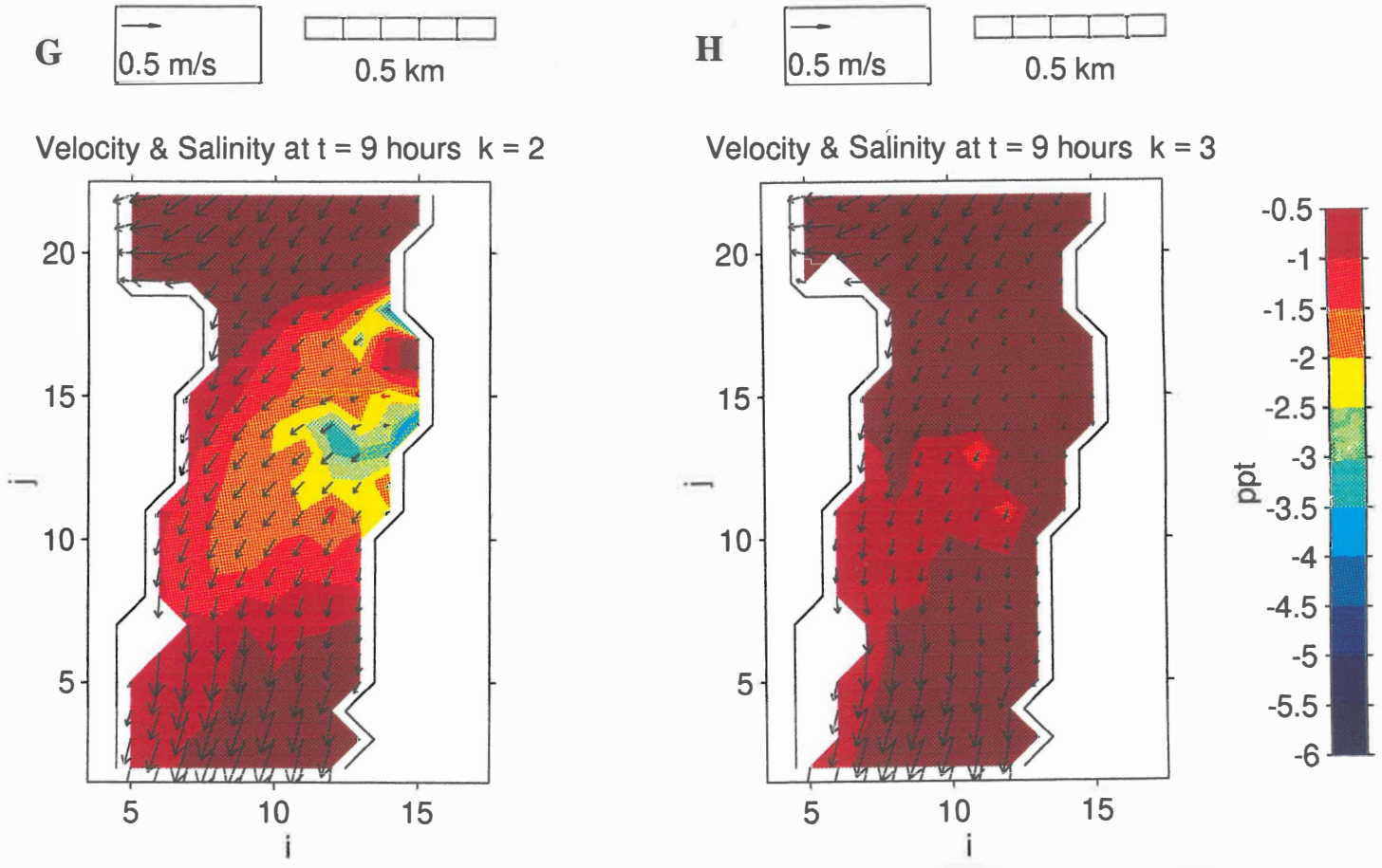

Figure 9.32g-h Predicted currents and plume in layers 2 (g) and 3 (h) during peak flood tide (t = 9 hours) under 30 knot northeasterly winds.

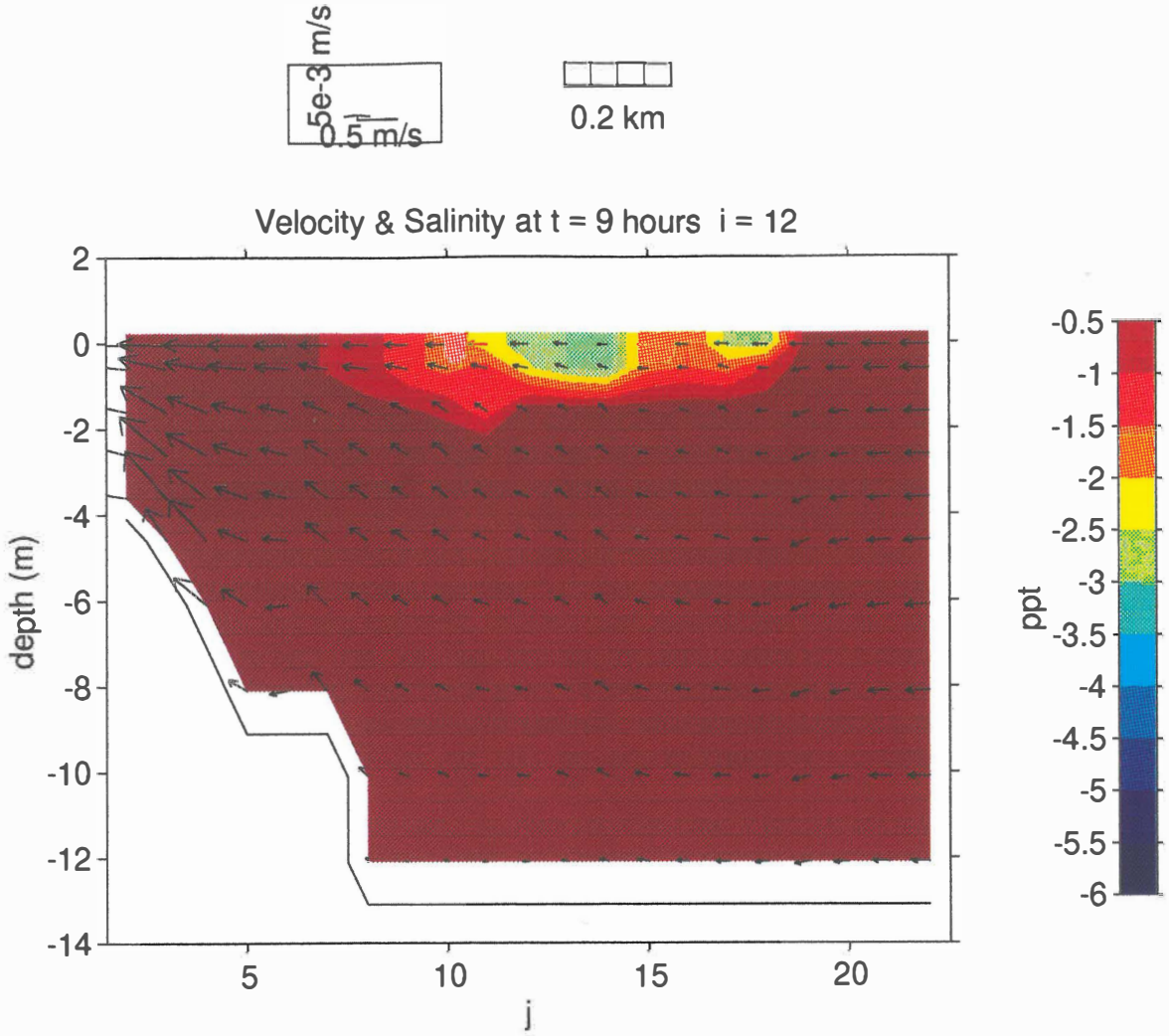

Figure 9.32i Plume shape and current pattern in cross-section I=12 during peak flood tide (t = 9 hours) under 30 knot northeasterly winds.

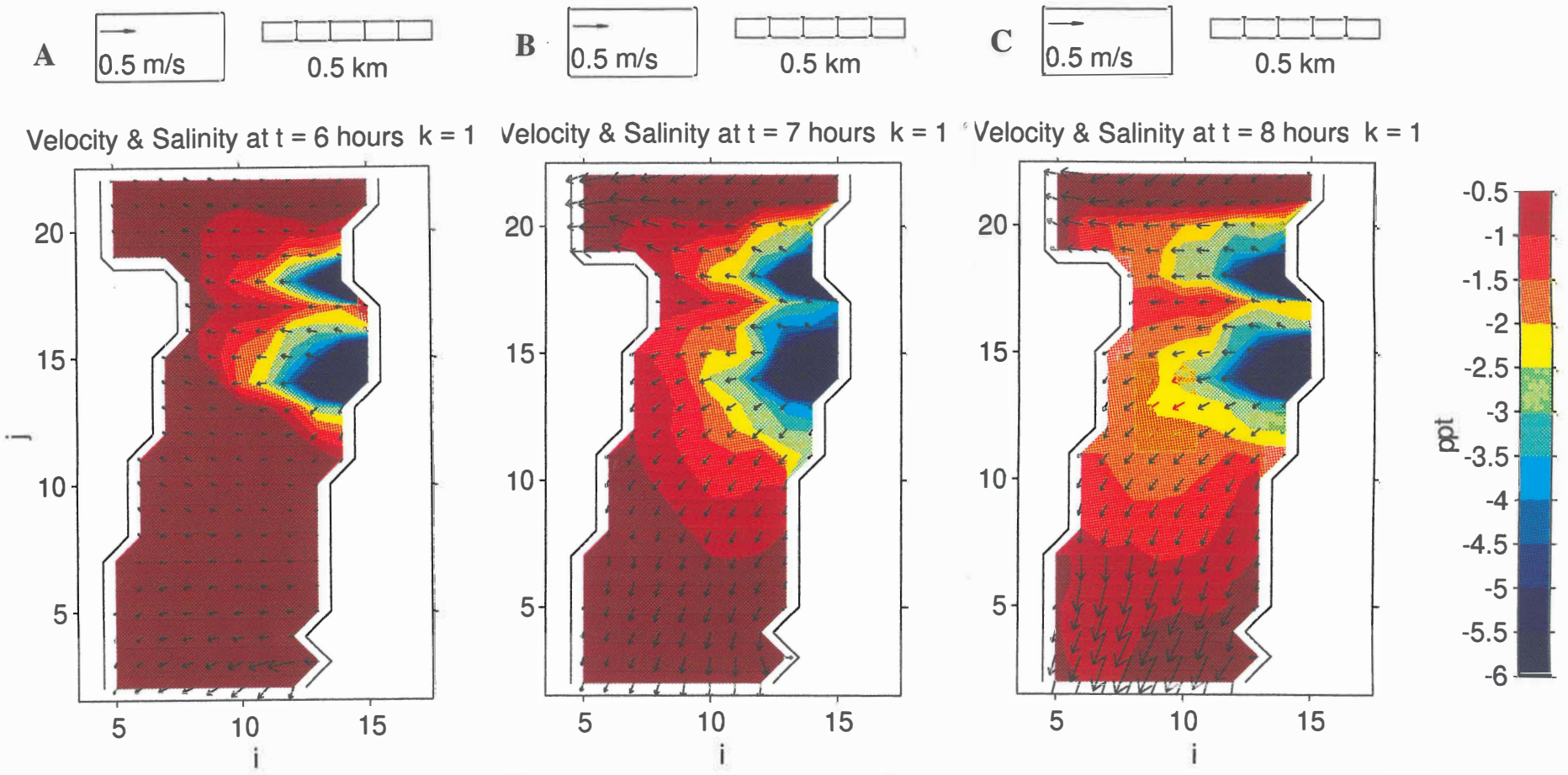

Figure 9.33a-f Predicted plume and currents in the surface layer from low to high tide (t = 6-12 hours) under 30 knot easterly winds.

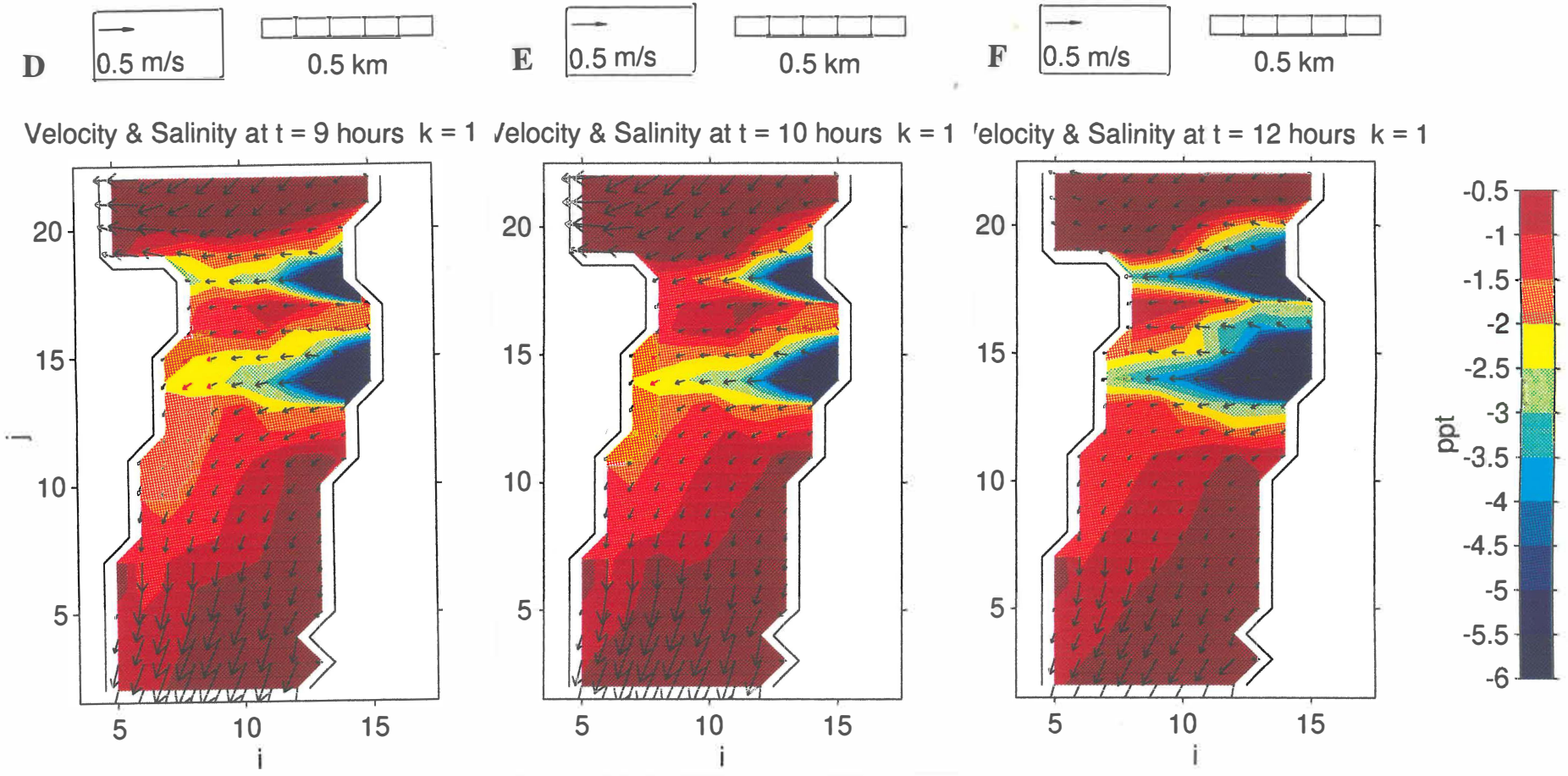

Figure 9.33a-f Predicted plume and currents in the surface layer from low to high tide (t = 6-12 hours) under 30 knot easterly winds.

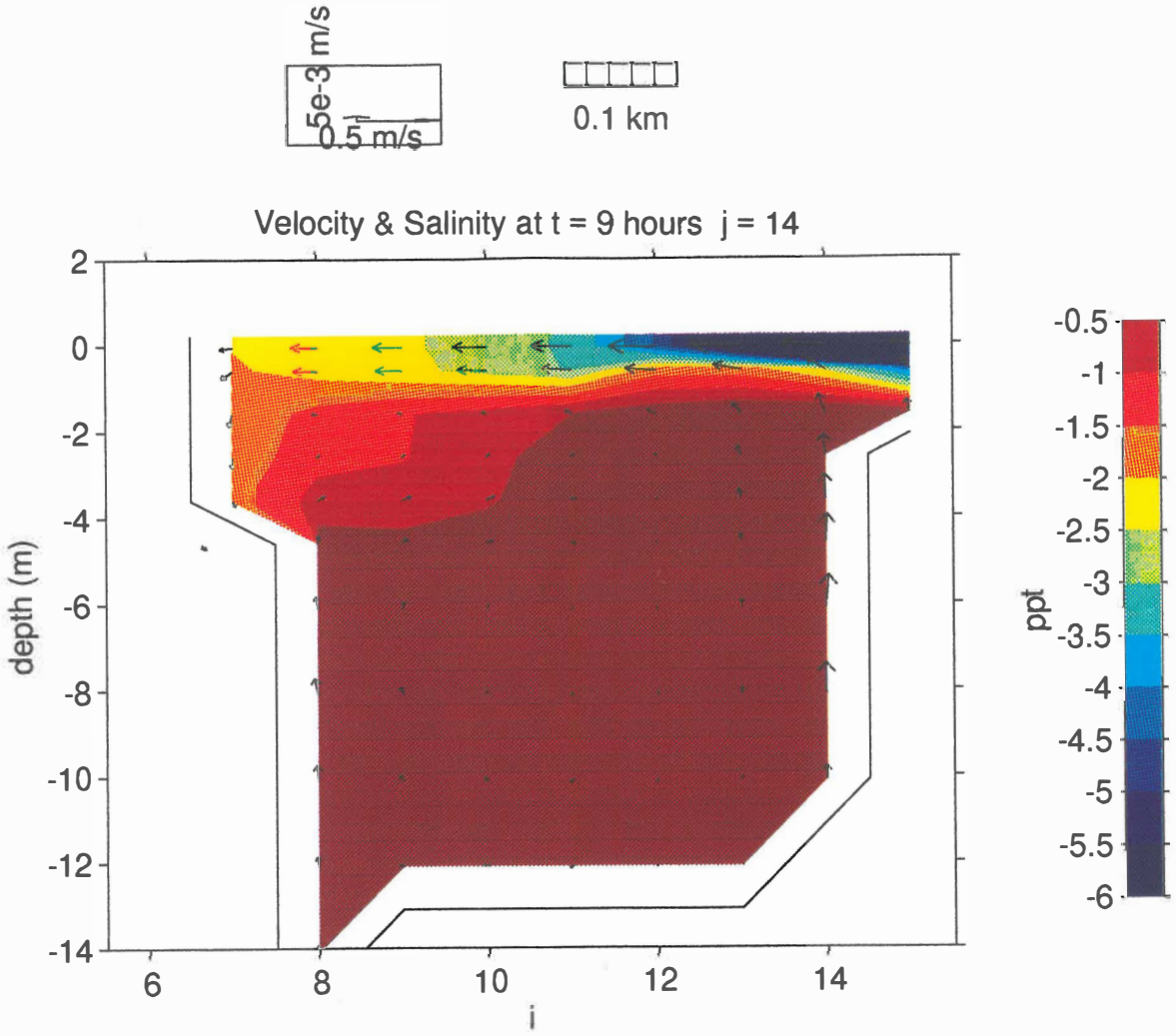

Figure 9.33g Predicted plume and currents at cross-section J=14 during peak flood tide (t = 9 hours) under 30 knot northeasterly winds.

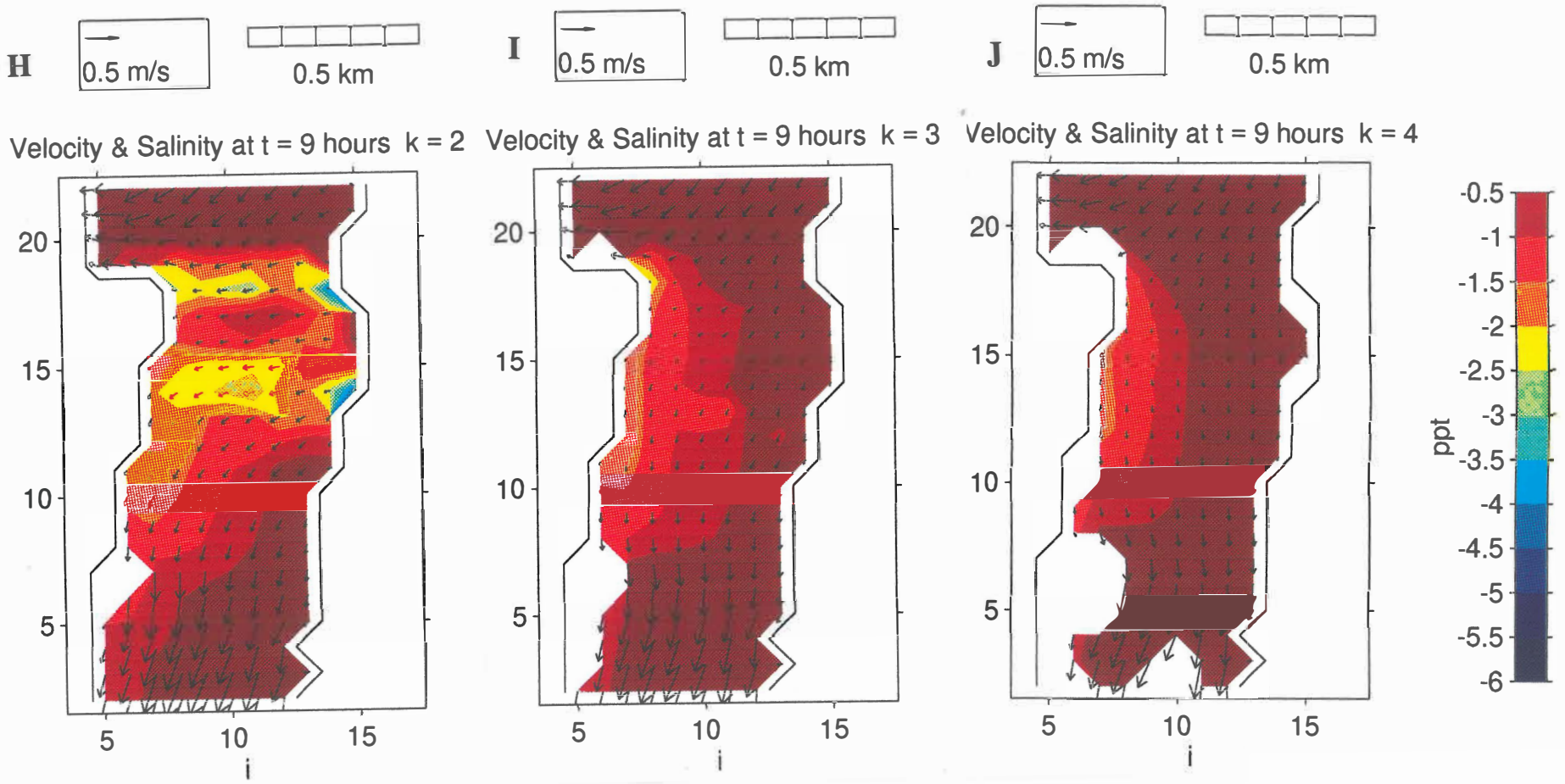

Figure 9.33h-j Predicted plume and currents in layer 2 (h), 3 (i), and 4 (j) during peak flood tide (t = 9 hours) under 30 knot northeasterly winds..

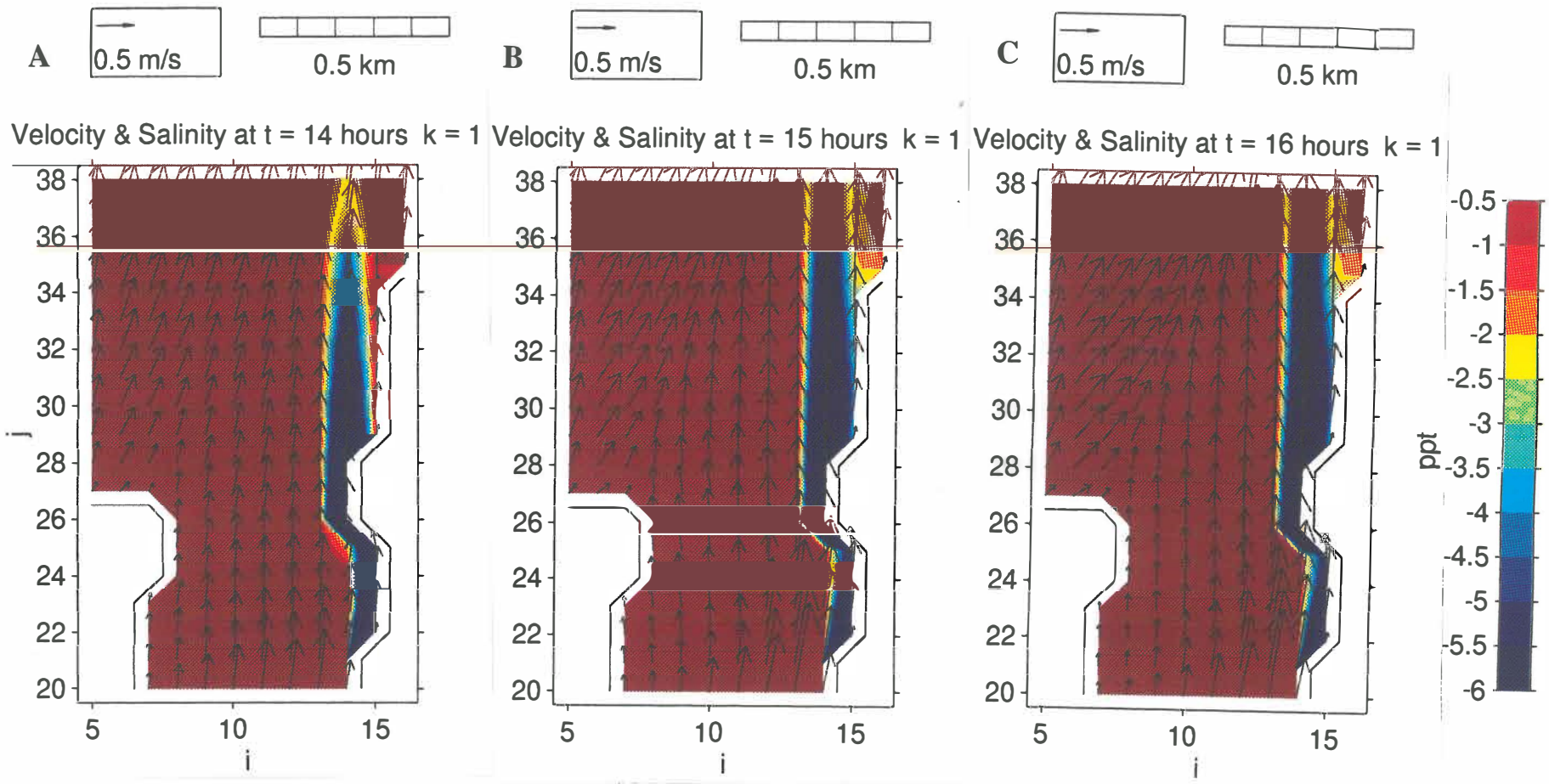

Figure 9.34a-e Predicted plume and currents in the surface layer at 2-6 hours after high tide (t = 14-18 hours) under 30 knot southerly winds.

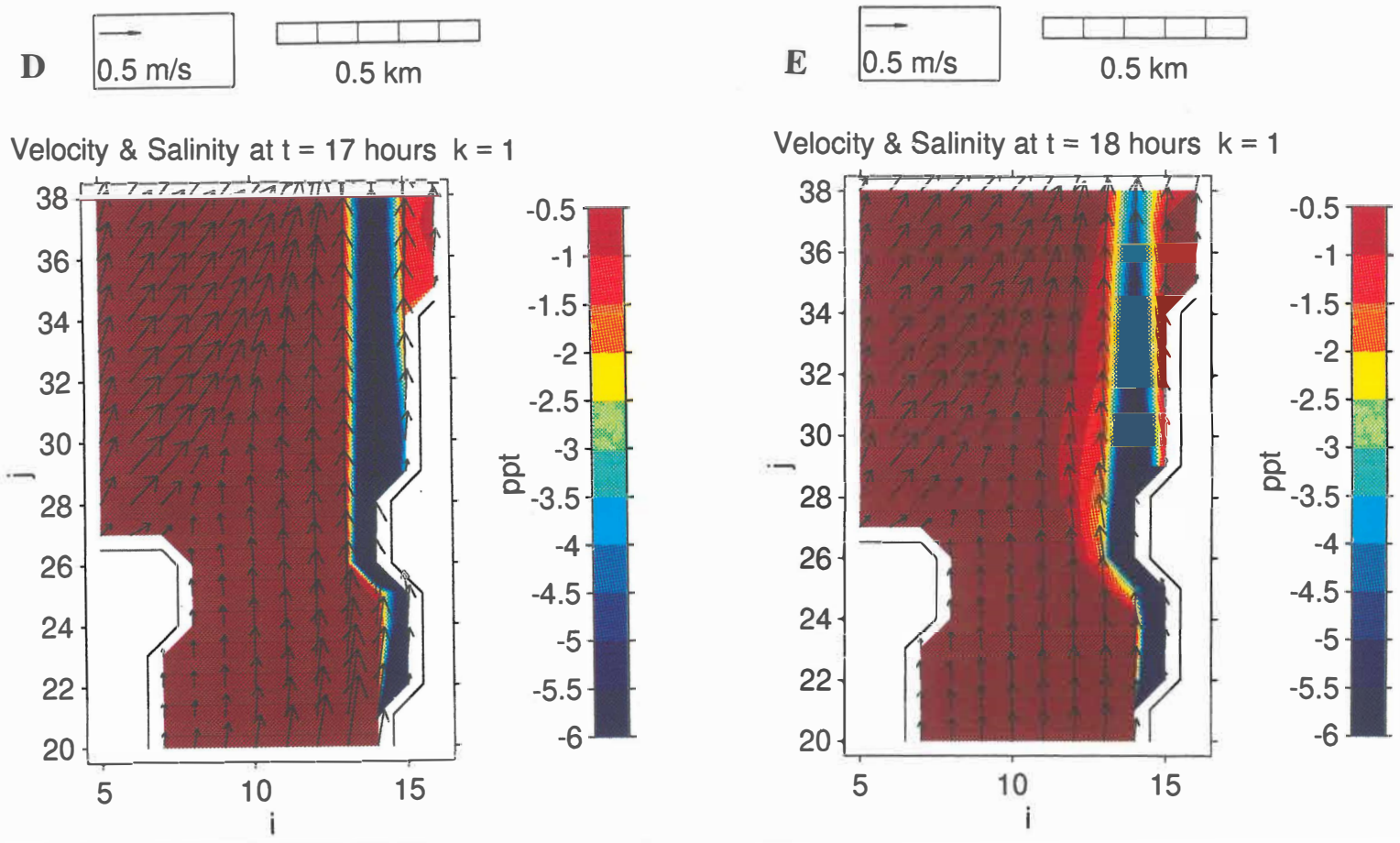

Figure 9.34a-e Predicted plume and currents in the surface layer at 2-6 hours after high tide (t = 14-18 hours) under 30 knot southerly winds.

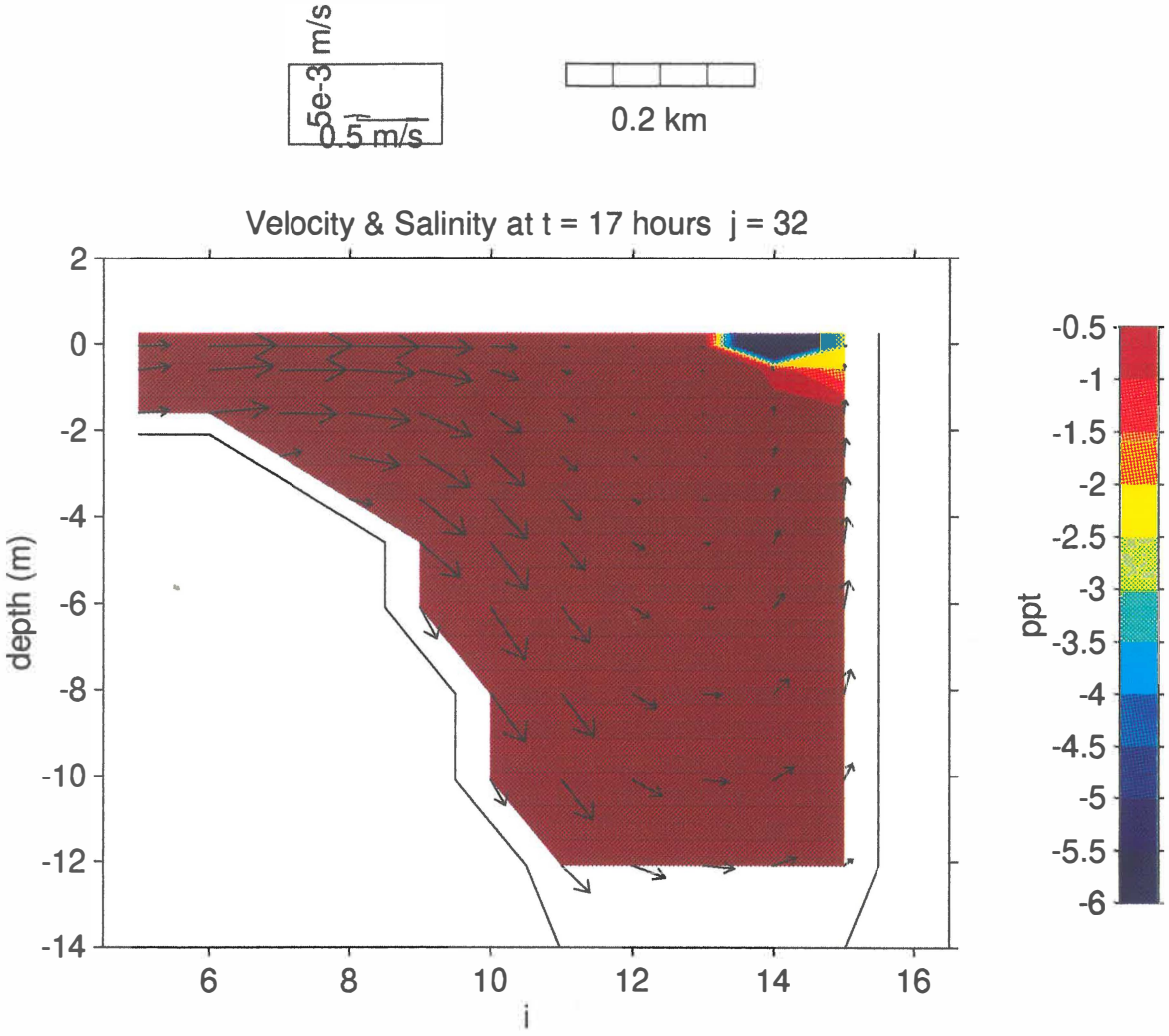

Figure 9.34f Predicted plume and currents in at cross-section J=32 at 5 hours after high tide (t = 17 hours) under 30 knot southerly winds.

CHAPTER TEN

CONCLUSIONS AND RECOMMENDATIONS

CHAPTER TEN

CONCLUSIONS AND RECOMMENDATIONS

This study involves storm runoff water quantity and quality, contaminant input to the local ecosystem from the Mt. Maunganui wharf, accumulation of potentially toxic resin acids in adjacent sediments, and the dilution of the wharf runoff in the receiving tidal waters. It was undertaken to estimate possible adverse environmental impact associated with the log operation at the Port of Tauranga Ltd. This chapter provides a brief summary of the main findings, discusses the implications of these findings for the wharf runoff management at the Port of Tauranga, and gives suggestions for further study.

10.1 SUMMARY OF THE MAIN FINDINGS

1. Based on field data and rainfall records, about a half of the annual precipitation falling over the log handling areas is converted to surface runoff (117,000 m^3a^{-1}). Annual runoff volume per hectare of wharf surface is estimated as 7,500 $m^3ha^{-1}a^{-1}$ for the sealed area and 3,700 $m^3ha^{-1}a^{-1}$ for the gravelled area.

2. The optical quality of the wharf runoff is degraded due to addition of bark and soil-like particles. The black disk visual clarity (0.01-0.02 m) was only 0.5-1.0% of that in the receiving tidal waters. The wharf runoff appears very dark gray to yellowish brown in apparent colour (10YR1/3 to 10YR5/6 Munsel colour chart) and has a soluble yellow substance concentration of about 25 m^{-1} Power relationships between the traditionally used parameters, for example, suspended solids and turbidity, were identified. The wharf surface pavement types had a significant influence on visual clarity, but little influence on yellow substance concentration.

3. The potentially toxic resin acids in the wharf runoff has been determined with SIM GC-MS. The average total resin acid level (1,030 ppb) is comparable to that of 1,000 ppb reported at which acute toxicity is likely to be exhibited. A relationship of resin acids against volatile suspended solids was established. Conventional treatment methods of natural sedimentation and flocculation-sedimentation are able to remove the resin acids effectively.

4. The levels of biological oxygen demand (BOD), total phosphorus and nitrogen in the wharf runoff are considerably higher than those of common urban runoff. However, the wharf runoff contributes little nitrate nitrogen and oil and grease to the receiving environment.

5. About 87,500 kg of suspended solids, 43,000 kg of volatile suspended solids, 14,200 kg of BOD, 500 kg of phosphorus, and 103 kg of resin acids are discharged to the Tauranga Harbour annually from runoff from the Mt. Maunganui wharf. The input of nitrogen and oil and grease are not significant

6. Analyses show that the impact on adjacent sediments from the storm runoff is limited to a distance of about 100 m from the discharge points and the resin acid levels in the sediments within this distance was not significantly higher compared to that of the storm runoff. The net resin acid accumulation rate in the shipping channel (Stella Passage) beside the log handling areas was estimated to be in the range of 300 to 370 ppb per year.

7. Based on field investigation and numerical simulations, the findings on dispersion and dilution of the wharf runoff in the receiving tidal waters are as follows: (i) the sea water around Stella Passage experienced an obvious natural salinity stratification, the extent of which depends greatly on the weather conditions; (ii) the wind drag stress and the pressure gradient caused by the addition of runoff had the greatest influence on the plume dynamics during flood tide. The plumes basically remain within the top 2-3 m of the water

column under different winds; (iii) the plume is unlikely to advect to the Whareroa Marae under strong (30-40 knots) easterly or northeasterly winds for a storm with a 5-year return period. However, there is an obvious influence on the Whareroa Marae under 30-40 knot northerly winds; and (iv) the short duration and restricted region of the low dilution pulse of effluent around slack water may explain why there has been no reports of acute toxic events.

In summary, the objectives set in this study have been achieved. The findings obtained in this study provide a rational basis for the management of runoff from the timber wharf for the Port of Tauranga, and will also have potential application for the other timber ports around New Zealand, because to date, no comprehensive study has been undertaken on runoff water quality and quantity, annual contaminant input to the local ecosystem, accumulation of environmentally resistant and toxic resin acids, and dispersion and dilution of the wharf runoff in the receiving tidal waters.

10.2 IMPLICATIONS FOR WHARF RUNOFF MANAGEMENT

There are two potential concerns for the immediate environmental impact of the wharf runoff: an acute toxic event, and a conspicuous change of optical quality of the receiving tidal waters. As the minimum initial dilution rate is above 1.6 for a storm with a 5-year return period (see Section 9.6.5) and the duration of a plume existence in the harbour is relatively short, there has been no reported acute toxic event in the Stella Passage. This does not mean there is no chronic impact on marine life (which is beyond the scope of this study). Secondly, the wharf runoff does change the optical quality of the receiving tidal water conspicuously. The plume can nearly cover the entire Stella Passage area under strong easterly or northeasterly winds for a heavy storm, although the chance is rare.

Briefly, the most serious concern of the wharf runoff is that it will deteriorate the optical quality of the receiving tidal waters.

For an existing timber port like the Port of Tauranga, it may not be practical to consider a huge treatment facility due to space restraint. The following potential options at present are suggested:

i) *Sealing of the gravelled wharf surface and improvement of the surface sweeping efficiency*. The runoff water optical quality from the sealed area is significantly higher compared to that of the gravelled area; however the annual contaminant input to the harbour will not be improved significantly, due to the increase of runoff volume.

ii) Extension of the present outfall to the sea floor at 14 m depth. From understanding of the mixing, advection, and dispersion processes which result in diffusion of effluent when injected at a point source, it would seem advantageous to inject the runoff wastewater from the wharves as deep as possible in the adjacent channel. The less dense runoff will rise through the tidal water column at the same time as being acted upon by the ambient tidal currents and undergoing turbulent diffusion, and thus dilution of the effluent. This will to a greater or lesser degree improve the optical condition of the receiving tidal waters.

10.3 RECOMMENDATIONS TO FURTHER STUDY

Time and funding have been limited in this project as in all other similar projects. This meant that some aspects related to the wharf runoff discharge have not been investigated. The following further studies are suggested:

1. Establish a long term monitoring program to monitor possible long term accumulation of typical contaminants, such as resin acids in the adjacent

sediments and long term impact on marine biota in Tauranga Harbour, particularly the benthic biota.

2. Further work should be undertaken to investigate salinity structure and the complex plume mixing around the outfalls.

3. Determine the feasibility of extending the present outfalls to the sea floor at 14 m depth and using a numerical model predict the initial dilution rate of the wharf runoff after the extension.

4. Investigate the possible release of chemicals sprayed onto the debarked logs for preventing the growth of microorganisms on the logs. If there is no significant release of the chemicals to the environment, the export of debarked logs should be encouraged. This would likely improve the optical quality of the wharf runoff.

REFERENCES

Amendola, G.A., Handy, R.E., Jr., and Bodien, D.G., 1989. Bench-scale study of dioxins and furan (2,3,7,8-TCDD and 2,3,7,8-TCDF) treatability in pulp and paper mill wastewater. *Tappi,* 72(12), 189-195.

American Public Health Association, 1992. *Standard methods for the examination of water and wastewater*. 18th edition, APHA Publication Office, pp.2.53 - 2.58.

American Society for Testing and Materials (ASTM), 1987. *Annual Book of ASTM Standards. Section II: Water and Environmental Technology*, Volume 11.02, Philadelphia, USA, pp. 869-873.

Anon, 1966. *The science of colour*. The Committee on Colorimetry of the Optical Society of America, Optical society of America, Washington, D.C.

Anon, 1991. *Tauranga area sewerage: receiving waters study-Mount Maunganui outfall*. A report prepared for Tauranga District Council by BECA Steven Consulting Environmental Engineers. 38 pp.

Anon, 1994. *Wastewater treatment and disposal for Hamilton City; Hamilton sewage and the Waikato River*. Report W51/1, Hamilton, New Zealand, 41 pp.

Anon. 1954. *Munsell book of colour.* Munsell colour Co. Baltimore, Maryland, U.S.A.

Anon. 1986. Meeting the challenge of nonpoint source control. *Journal of Water Pollution Control Federation* 58(7), 730-740.

Auckland Regional Council (ARC), 1992a. *An Assessment of stormwater quality and the implications for treatment of stormwater in the Auckland Region*. Environment and Planning Division Technical Publication No.5.

Auckland Regional Council (ARC), 1992b. *Design guideline manual for stormwater treatment devices*. Environment and Planning Division Technical Publication No.10.

Auckland Regional Water Board (ARWB), 1988. *Assessment of urban and industrial stormwater inflows to the Manukau Harbour*. Prepared by Kingett Mitchell and Associates Ltd, ARWB technical Publication No.74.

Barnett, A.G., 1985. *Tauranga Harbour Study, Part III: Hydrodynamics*. A report for the Bay of Plenty Harbour Board, pp. 10-11.

Bell, R.G.,1991. *Port of Tauranga model study: (Deepened shipping channel proposal)*. Consultancy Report No. 6127/1, NIWA, Hamilton, New Zealand, 22 pp.

Bell, R.G.,1994. *Port of Tauranga model study: Sulphur Point Wharf extensions*. Consultancy Report No. POT 002/1, NIWA, Hamilton, New Zealand, 21 pp.

Benzie, W.J. and Courchaine, R.J., 1966. Discharges from separate storm sewers and combined sewers. *Journal of Water Pollution Control Federation,* 38(3), 410-418.

Black, K.P., 1983. *Sediment transport and tidal inlet hydraulics*. Doctor of Philosophy thesis, University of Waikato, New Zealand, Volume 1, test, 331 pp. Volume 2, Figures and Tables.

Black, K.P., 1987. Eddy formation in unsteady flows. *Journal of geophysical research*, 92(C9), 9514-9522.

Black, K.P., 1992. Evidence of the importance of deposition and winnowing of surficial sediments at a continental shelf scale. *Journal of Coastal Research*, 8(2), 319-331.

Black, K.P., 1995. *Numerical modelling of physical marine processes*. Lecture notes, Waikato University, New Zealand, 19 pp.

Black, K.P., 1996. *The hydrodynamic model 3DD and support software*. Occasional Report No.19, Waikato University, Hamilton, New Zealand, 53 pp.

Black, P.E. 1980. Water quality patterns during a storm on a mall parking lot. *Water Resources Bulletin*, 16(4), 615 - 620.

Blackwell, H.R., 1946. Contrast thresholds of the human eye. *Journal of the Optical Society of American*, 36, 624-643.

Brady, B.E. and Humiston, G.E., 1986. *General chemistry: principles and structure* John Wiley and Sons, 390 pp.

Bricaud, A., Morel, A. and Prieur, L. 1981. Absorption by dissolved organic matter of the sea (yellow substance) in the UV and visible domains. *Limnology and Oceanography*, 26(1), 43 - 53.

Brown, G.W. and Krygier, J.T., 1971. Clear-cut logging and sediment production in the Oregon Coast Range. *Water Resources Research,* 7(5), 1189-1198.

Brown, G.W., Gahler, A.R. and Marston, R. B., 1973. Nutrient losses after clear-cut logging and slash burning in the Orgon Coast Range. *Water Resources Research,* 9(5), 1450-1453.

Brown, T.C., Brown, D. and Binkley, D., 1993. Laws and programs for controlling nonpoint source pollution in forest areas. *Water Resources Bulletin,* 29(1), 1-13.

Browne, F.X., 1990. *Stormwater management*. In *Standard handbook of Environmental Engineering*. Edited by Corbitt, R.A., McGraw-Hill Publishing Company, New York, pp. 7.1 - 7.135.

Burm, R.J., Krawczyk, D.F. and Harlow, G.L., 1968. Chemical and physical comparison of combined and separate sewer discharge. *Journal of Water Pollution Control Federation,* 40(1), 400-407.

Chung, L.T.K., Meier, H.P. and Leach, J.M., 1979. Can pulp mill effluent toxicity be estimated from chemical analyses? *Tappi,* 62: 71-73.

Cordery, I. 1977. Quality characteristics of urban storm water in Sydney, Australia. *Water Resources Research*, 13(1), 197 - 202.

Coulter, J.D. and Hessell, J.W.D., 1980. *The frequency of high intensity rainfalls in New Zealand. Part II, Point estimates*. New Zealand Met. S. Misc. Pub. 162, 23 pp.

Davies-Colley, R.J. 1992. Yellow substance in coastal and marine waters around the South Island, New Zealand. *New Zealand Journal of Marine and Freshwater Research*, 26, 311 - 322.

Davies-Colley, R.J. and Close, M.E., 1990. Water colour and clarity of New Zealand rivers under baseflow conditions. *New Zealand Journal of Marine and Freshwater Research*, 24, 357 - 365.

Davies-Colley, R.J. and Smith, D.G., 1992. Offsite measurement of the visual clarity of waters. *Water Resources Bulletin,* 28(5), 951-957.

Davies-Colley, R.J. and Vant, W.N., 1987. Absorption of light by yellow substance in freshwater lakes. *Limnology and oceanography*, 32(2), 416-425.

Davies-Colley, R.J., 1988. Measurement of water clarity using a black disk. *Limnology and Oceanography,* 33, 616 - 623.

Davies-Colley, R.J., 1990. Frequency distributions of visual water clarity in 12 New Zealand rivers. *New Zealand journal of marine and freshwater research,* 24(3): 453-460.

Davies-Colley, R.J., 1990. Secchi disc transparency and turbidity. Discussion, *Journal of Environmental Engineering Division*, ASCE, 116(4), 796 - 798.

Davies-Colley, R.J., Vant, W.N. and Smith, R.J., 1993. *Colour and clarity of natural waters*. Ellis-Horwood, Chichester, U.K. 310 pp.

Davies-Colley, R.J., Vant. W.N., and Wilcock., R.J., 1988. Lake water colour: comparison of direct observations with underwater spectral irradiance. *Water Resources Bulletin*, 24(1), 11-18.

Davies-Colley, R.J. and Close, M.E., 1990. Water colour and clarity of New Zealand rivers under baseflow conditions. *New Zealand journal of marine and freshwater research,* 24(3), 357-365.

Day, H.R. and Felbeck, G.J., 1974. Production and analysis of a humic-acid-like exudate from the aquatic fungus. *Journal of American Water Works Association,* 66, 484-488.

Dell, P.M., 1993. *Pulp and Paper industry study tour*. Environmental Report 93-4 of Environment BOP, 73 pp.

Eganhouse, R.P., and Kaphan, I.R., 1981. Extractable organic matter in urban stormwater runoff. 1. Transport dynamics and mass emission rates. *Environmental Science and Technology*, 15, 310-315.

Eganhouse, R.P., Simoneit, B.R.T.,and Kaphan, I.R., 1981. Extractable organic matter in urban stormwater runoff. 2. Molecular characterization. *Environmental Science and Technology*, 15, 315-326.

Environment BOP, 1995. *Proposed Regional Coastal Environment Plan.*, Whakatane, New Zealand, 74 pp.

Field, R., and Struzeski, E.J., Jr., 1972. Management and control of combined sewer overflow. *J. Water Pollution Control Federation,* 44(7), 1393-1415.

Firth, B.K. and Backman, C.J., 1990. Comparison of Microtox testing with rainbow trout (acute) and *Ceriodaphnia* (chronic) bioassays in mill wastewaters. *Tappi,* 73(12), 169-174.

Fischer, H.B., List, E.J., Koh, R.C.Y., Imberger, J., and Brooks, N.H., 1979. *Mixing in inland and coastal waters*. Academic Press, New York.

Goettle, A. and Krauth, K., 1981. Total pollution loads considering urban storm runoff. *Water Science and Technology,* 13(3), 155-173.

Grace, R.V., 1993. *Effects on benthic biota of pine bark waste in stormwater*. A consultant report to the Port of Tauranga. 21 pp.

Grieve, I.C., 1985. Determination of dissolved organic matter in streamwater using visible spectrophotometry. *Earth surface processes and landform*, 10(1): 75-78.

Harman, L. and Weenick, R.O., 1967. A note on the fatty acid composition of the liopids from the bark of *pinus radiata*. *New Zealand Journal of Sciences,* 10, 636-638.

Harr, R.D. and Fredriksen, R.L., 1988. Water quality after logging small watersheds within the Bull Run Watershed, Oregon. *Water Resources Bulletin,* 24(5), 1103-1111.

Healy, T.R., Wilkins, A.L., and Leipe, T., 1997. Extractives from a coniferous bark dump in coastal estuarine sediments. *Journal of Coastal Research*, 13(2), 293-296.

Hornbeck, J.W., Pierce, R. S. and Federer, C.A., 1970. Streamflow changes after forest clearing in New Zealand. *Water Resources Research,* 6(4), 1124-1132.

Huang, W., and Spaulding, M, 1995. 3D model of estuarine circulation and water quality induced by surface discharges. *Journal of Hydraulic Engineering*, 121(4): 300-311.

Hunter, J.V., 1979. Contribution of urban runoff to hydrocarbon pollution. *Journal of Water Pollution Control Federation*, 51(8), 2129-2138.

Ishaq, A.M. and Khararjian, H.A. 1988. Stormwater harvesting in the urban watersheds of arid zones. *Water Resources Bulletin*, 24(6), 1227 - 1235.

Jerlov, N.G., (1976). *Marine optics.*. Elsevier oceanography series 14. 231 pp.

Jewson, D.H., and Taylor, J.A. 1978. The influence of turbidity on net phytoplankton photosynthesis in some Irish lakes *Freshwater Biology*, 8, 573-584.

Junna, J. and Ruonala, S., 1991. Treads and guidelines in water pollution control in the Finnish pulp and paper industry. *Tappi*, 74(7), 105-111.

Kinae, N, Hashizume, T., Makita, T.,Tomita, I., Kimura, I., and Kanamori, H., 1981. Studies on the toxicity of pulp and paper mill effluents-I. mutagenicity of the sediment samples derived from kraft paper mills. *Water research,* 15(1), 17-24.

Kingett Mitchell and Associates, 1993. *Stormwater management plan for Port Shakespeare*. Consulting report prepared for Port Marlborough New Zealand Ltd, 66 pp.

Kirk, J.T.O. 1976. Yellow substance (Gelbstoff) and its contribution to the attenuation of photosynthetically active radiation in some inland and coastal South-Eastern Australia waters. *Australian Journal of Marine and Freshwater Research*, 27(1), 61-71.

Kirk, J.T.O., 1980. Spectral absorption properties of natural waters: Contribution of soluble and particulate fractions to light absorption in some inland waters of south-eastern Australia. *Australia Journal of Marine and Freshwater Research,* 31, 287-296.

Kirk, J.T.O., 1983. *Light and photosynthesis in aquatic ecosystems*. Cambridge University Press, Cambridge, 401 pp.

Kirk, J.T.O., 1988. Optical water quality -- what is it and how should we measure it? *Journal of Water Pollution Control Federation*, 60, 194-197.

Leach, J.M., Mueller, J.C. and Walden, C.C. (1978). Biological detoxification of pulp mill effluents. *Process Biochemistry*, 13(1),18 - 21.

Leersnyder, H., 1992. Urban stormwater quality control: the performance of settling ponds. In *Proceeding of New Zealand hydrological Society 1992 symposium*.

Li, J.Y., and Adams, B.J., 1993. *Comprehensive urban runoff quantity/quality management modelling*. In *New techniques for modelling the management of stormwater quality impacts* (Editor: James W.), Lewis Publishers, Florida, USA, p151 -p176.

Lindholm, O. and Balmer, P., 1978. Pollution in storm runoff and combined sewer overflows. In *Urban Storm Drainage*. Pentech Press pp.575-585.

Lloyd, J.A., 1978. Distribution of extractives in *Pinus radiata* earlywood and latewood. *New Zealand Journal of Forestry Sciences,* 2, 288-294.

Lythgoe, J.N., 1979. *The ecology of vision*. Oxford University Press, 244 pp.

MacKenzie,M.J., and Huntr, J.V., 1979. Sources and fates of aromatic compounds in urban storm runoff. *Environmental Science and Technology*, 13(2), 179-183.
Makepeace, D.K., Smith, D.W., and Stanley, S.J., 1995. Urban stormwater quality: summary of contaminant data. *Critical Reviews in Environmental Science and technology*, 25(2), 93-139.

Mance, G. and Harman, M.M.I., 1978. *The quality of urban stormwater runoff*. In *Urban Storm Drainage*. Pentech Press, pp. 603-617.

McCabe, B., 1991. *Storm water treatment investigation and design report*. Report to the Environment BOP for obtaining Water Right for stormwater discharge at Sulphur Point. 25 pp.

McCarthy, P.J., Kennedy, K.J., and Droste, R.L., 1990. Role of resin acids in the anaerobic toxicity of chemithermomechanical pulp waste water. *Water Research*, 24(11), 1401-1405.

McCluney, W.R., 1975. Radiometry of water turbidity measurements. J*ournal of Water Pollution Control Federation,* 47, 252-266.

McDonald, I.R.C. and Porter, L.J., 1969. The resin and fatty acid composition of *Pinus radiata* and its relation to the yield and composition of New Zealand tail oil. *New Zealand Journal of Sciences,* 12, 352-362.

McIntosh, J., 1994. *Tauranga Harbour Regional Plan: Water and sediment quality of Tauranga Harbour*. Environmental Report 94/10, Environment Bay of Plenty, Whakatane, New Zealand, 290 pp.

Mealanen, M.J. and Laukkanen, R.H., 1981. Urban runoff quality in Finland and its dependence on some hydrological parameters. *Water Science and Technology,* 13(2), 1073-1083.

Ministry for the Environment of New Zealand, 1994. *Water Quality Guidelines No. 2: Guidelines for the Management of Water Colour and Clarity*. Wellington, New Zealand, 77 pp.

Moore, T.R., 1985. The spectrophotometric determination of dissolved organic carbon in peat waters. 49, 1590-1592.

Morales, A., Birkholz, D.A. and Hrudey, S.E. (1992). Analysis of pulp mill effluent contaminations in water, sediment, fish bile - fatty and resin acids. *Water Environmental Research*, 64(4), 660-668.

Morales, A., Birkholz, D.A. and Hrudey, S.E., 1992. Analysis of pulp mill effluent contaminants in water, sediment, and fish bile--fatty and resin acids. *Water environment research,* 64, 660-667.

Munk, W., and Anderson, E.R., 1948. Notes on the theory of the thermocline. *Journal of Marine Research*, 7, 276-295.

Naohide, K., Takashi, H., Toshio, M., Isao, T., Ikuo, K., and Hisayuki, K. 1981. Studies on the toxicity of pulp and paper mill effluents — I. Mutagenicity of the sediment samples derived from kraft paper mills. *Water Research*, 15, 17 - 24.

National Council of the Paper Industry for Air and Stream Improvement (NCASI), 1992. *Storm water from log storage site: a literature review and case study*. Technical Bulletin No. 637, New York, U.S.A., 30 pp.

Nix, S.J., 1994. *Urban stormwater modelling and simulation*. Lewis Publishers, Florida, USA, p 27 - p28.

O'Shaughnessy, B. and Stringfellow, M., 1992. *Velocity measurements for oil boom design, Tauranga*. Technical report No.19, Bay of Plenty Regional Council, Whakatane, New Zealand. 20 pp.

Oikari, A. and Nittyla, J., 1985. Subacute physiological effects of the bleached kraft mill effluent (BKME) on the liver of trout, *Salmo gairdneri*. *Safety of Ecotoxicological Environment*, 10, 159-172.

Oikari, A., Holmbom, B., Anas, E. and Bister, H. 1980. Distribution in a recipient lake and bioaccumulation in fish of resin acids from kraft pulp mill waste waters. *Paperi ji Puu*, 62, 195 - 197.

Oikari, A., Holmbom, B., Anas, E., Miilunpalo, M., Kruzynski, G., and Castren, M., 1985. Ecotoxicological aspects of pulp and paper mill effluent discharge to an inland water system: distribution in water, and toxicant residues and physiological effects in caged fish (*Salmo gaidneri*). *Auqatic Toxicology*, 6, 219-239.

Overton, D.E. and Meadows, M.E., 1976. *Stormwater modeling*. Academic Press 358 pp.

Owe, M., Craul, P.J. and Halverson, H.G. 1982. Contaminant levels in precipitation and urban surface runoff. *Water Resources Bulletin*, 18(5), 863 - 868.

Owens, J.W., 1991. The hazard assessment of pulp and paper effluent in the aquatic environment: a review. *Environment Toxicology and Chemistry*, 10, 1511-1540.

Patric, J.H. and Reinhart, K.G., 1971. Hydrologic effects of deforesting two mountain watersheds in West Virginia. *Water Resources Bulletin,* 7(5), 1182-1187.

Perrels, P.A.J., and Karelse, M., 1981. *A two dimensional laterally averaged model for salt intrusion in estuaries*. Delft Hydraulic Laboratory, No 262, pp. 483-535.

Porter, L.J., 1969. The resin and fatty acid content of living *pinus radiata* wood. *New Zealand journal of science,* 12, 687-693.

Power, F.M., 1990. *Compliance/impact monitoring report of Tauranga District Council Wastewater Treatment Plant*. Report to Bay of Plenty Regional Council, Technical report No. 2, Whakatane, New Zealand, 111 pp.

Pritchard, D.W., 1967. *Observations of circulation in coastal plain estuaries*. In *Estuaries*, Editor: Lauff, G.H., AAAS Publication, No.83, Washington D.C., pp. 37-44.

Quayle, A.M., 1984. *The climate and weather of the Bay of Plenty Region*. New Zealand Meteorological Service Misc. Publication 115(1), 56 pp.

Reckhow, K.H., Butcher, J.B. and Marin, C.M. 1985. Pollutant runoff models: selection and use in decision making. *Water Resources Bulletin*, 21(2), 185 - 195.

Roesner, L.A., 1982. *Quality of urban runoff*. In *Water resources monograph series, No.7: Urban storm hydrology*. Edited by Kibler, D.F., American geophysical union, Washington, D.C., pp. 176-177.

Rogers, P. and Rosenthal, A., 1988. The imperatives of nonpoint source pollution policies. *Journal of Water Pollution Control Federation,* 60(11), 1912-1921.

Sandstrom, O., Neuman, E. and karas, P., 1988. Effects of a bleached pulp mill effluent on growth and gonad function in Baltic coastal fish. *Water science and technology,* 20(2), 107-118.

Sartor, J.D., Boyd, G.B. and Agardy, F.J., 1974. Water pollution aspects of street surface contamination. *J. Water Pollution Control Federation,* 46(3), 458-467.

Simoneit, B. R. T., 1986. *Cyclic terpenoids of the geoshere*. In Johns, R. B. (ed.) *Biological markers in the sedimentary record*. Methods in Geochemistry and Geophysics, No.24, Amsterdam, Elservier, 364 pp.

Singh-Thandi Makhan, 1993. *Some aspects of the organic chemistry of the Tarawera River*. M.Sc Thesis, Department of Chemistry, The University of Waikato, pp. 97.

Smith, D.G., Cragg, A.M. and Croker, G.F., 1991. Water clarity criteria for bathing waters based on user perception. *Journal of Environmental management,* 33(3), 285-299.

Soderlund G. and Lehtinen H., 1972. *Comparison of discharges from urban stormwater runoff, mixed storm overflow and treated sewage.* Advances in Water Pollution Research - Proceedings of the Sixth International Conference, edited by Jenkins, S.H. Pergamon Press, London, 1972, pp. 309-318.

Stenstrom, M.K., Silverman, G.S., and Bursztynsky, T.A., 1984. Oil and grease in urban stormwaters. *Journal of Environmental Engineering*, 110(1), 58-72.

Streibl, M. and Herout, V., 1969. *Terpenoids - especially oxygenated mono-, sesqui-, di-, and triterpenes.* In Eglinton, G. and Murphy, M.T.J. (eds.), *Organic geochemistry - methods and results*, Berlin, Springer Verlag, 828 pp.

Sutherlandd, R.C. and McGuen, R.H., 1978. Simulation of urban nonpoint source pollution. *Water Resources Bulletin*, 14, 409-427.

Tan, S.T., 1988. Extractives from New Zealand Honeys I: White Clover, Manuka and Kanuka Unifloral Honeys. *Journal of Agricultural and Food Chemistry,* 4, 1807.

Tana, J.J. 1988. Sublethal effects of chlorinated phenols and resin acids on Rainbow Trout (Salmo Gairdneri). *Water Science and Technology*, 20(2), 77 - 79.

Tavendale, M.H., 1994. *Characterisation and fate of pulp mill derived resin acids in a New Zealand receiving environment.* Ph.D thesis, University of waikato, Hamilton, New Zealand. 200 pp.

The Ministry for the Environment of New Zealand, 1994. *Water quality guidelines No. 2: Guidelines for the management of water colour and clarity.* Wellington, New Zealand, 75 pp.

Thurman, E.M., 1985. Organic geochemistry of natural waters. Amsterdam, Martinus Nijhoff, 273 pp.

Tian, F., 1993. *Disposal of hopper washings and aspects of runoff contamination from the log handling areas at the Port of Tauranga.* M.Phil. thesis, Department of Earth Science, University of Waikato. 171 pp.

Tian, F., Healy, T.R., and Davies-Colley, R.J., 1994. Light absorption by yellow substance in storm runoff from log handling areas at a timber export port, Tauranga, New Zealand. *Journal of Coastal Research*, 10(4), 803-808.

Tian, F., Healy, T.R., and Wilkins, A.L., 1995. Aspects of runoff pollution from the log handling areas at a timber export Port, Tauranga, New Zealand. *Journal of Marine Environmental Engineering*, 1, 231-246

Vant, W.N. and Davies-Colley, R.J., 1984. Factors affecting clarity of New Zealand lakes. *New Zealand Journal of Marine and Freshwater Research*, 18, 367 - 377.

Wakeham, S.G., 1977. A characterization of the source of petroleum hydrocarbons in Lake washington. *Journal of Water Pollution Control Federation*, 49(7), 1680-1687.

Weibel, S.R. and Anderson, R.J. 1964. Urban land runoff as a factor in stream pollution. *Journal of Water Pollution Control Federation*, 36(7), 914 - 924.

Whipple, W., Hunter, J.V. and Yu, S.L., 1974. Unrecorded pollution from urban runoff. *Journal of Water Pollution Control Federation,* 46(5), 873-885.
Wilcock, R.J. and Davies-Colley, R.J., 1983. Here is looking at you. The murky field of water clarity. *Soil and water,* 29(1), 29-33.

Wilkins, A.L. and Panadam, S., 1987. Extractable organic substances from the discharges of a New Zealand pulp and paper mill. *Appita,* 40(3), 208-212.

Wilkins, A.L., Davidson, J.A.C., Langdon, A.G., and Hendy, C.H., 1996. Sodium, calcium, and resin acid levels in ground water and sediments from two sites adjacent to the Tarawera River, New Zealand. *Bulletin of Environment Contamination and Toxicology*, 4,575-581.

Wilkins, A.L., Healy, T.R., and Leipe, T., 1997. Pulp mill-sourced substances in sediments from a coastal wetland. *Journal of Coastal Research*, 13(2), 341-348.

Williamson, R.B., 1985. Urban stormwater quality l: Hillcrest, Hamilton, New Zealand. *New Zealand Journal of marine and freshwater research*, 19, 413-427.

Williamson, R.B., 1986. Urban stormwater quality ll: Comparison of three New Zealand catchments. *New Zealand Journal of marine and freshwater research*, 20, 315-328.

Wood, I.R., 1991. *The behaviour of an outfall plume in a flow - A general program.* In Coastal Engineering - Climate for change. Proceedings of the 10th Australasian Conference on Coastal and Ocean Engineering, Auckland, New Zealand, 2-6 December, 1991, pp. 9-18.

Wu, J.S. and Ahlert, R.C., 1978. Assessment of methods for computing storm runoff loads. *Water Resources Bulletin*, 14(2), 429 - 439.